nature portfolio

https://doi.org/10.1038/s41586-023-06021-8

Supplementary information

General access to cubanes as benzene bioisosteres

In the format provided by the authors and unedited

Supplementary Information

General Access to Cubanes: Ideal Bioisosteres of *ortho*-, *meta*-, and *para*-Substituted Benzenes

Mario P. Wiesenfeldt[1,4], James A. Rossi-Ashton[1,4], Ian B. Perry[1,4], Johannes Diesel[1], Olivia L. Garry[1], Florian Bartels[1], Susannah C. Coote[2], Xiaoshen Ma[3], Charles S. Yeung[3], David J. Bennett[3] & David W. C. MacMillan[1]*

[1]Merck Center for Catalysis at Princeton University, Princeton, NJ, USA. [2]Lancaster University, Bailrigg, Lancaster, LA1 4YB, United Kingdom. [3]Department of Discovery Chemistry, Merck & Co., Inc., Boston, MA, USA. [4]These authors contributed equally: Mario P. Wiesenfeldt, James Rossi-Ashton, Ian B. Perry. *e-mail: dmacmill@princeton.edu

1. Materials and methods

Commercial reagents were purchased from standard commercial suppliers such as Sigma-Aldrich, TCI, Acros, or Combi-Blocks, and used as received unless otherwise indicated. Dimethyl cubane-1,4-dicarboxylate (**8**) and 4-methoxycarbonylcubanecarboxylic acid (**16**) were purchased from Boron Molecular and used as received. Dichloromethane and toluene were purified by passage through columns of activated alumina according to a method published by the Grubbs group[51]. All other dry solvents were purchased in sure-seal bottles from Sigma-Aldrich or Acros and used without further purification.

Organic solutions were concentrated under reduced pressure on a Büchi rotary evaporator. Filtrations of heterogeneous mixtures were performed using ChemRus 6 mL, 20 mL or 60 mL disposable filters unless otherwise indicated. Chromatographic purification of products was accomplished on an automated Teledyne Isco CombiFlash™ NextGen 300+ system with attached ELS detector or on a Biotage Isolera™ Spektra System, using Isco RediSep Rf, Isco RediSep Rf gold, Silicycle Silia*Sep*™, or Biotage Sfär™ high-capacity silica cartridges. Reverse phase HPLC purification was conducted on a Teledyne ISCO ACCQPrep HP150 system. Thin-layer chromatography (TLC) was performed on Analtech 250-micron silica gel plates. Visualization was accomplished by fluorescence quenching at 254 or 365 nm, or by reaction with $KMnO_4$ stain. Reversed-phase high-performance liquid chromatography was carried out using an Agilent 1100 HPLC-MSD system consisting of a 6130B single quadrupole mass-selective detector (MSD), G1315B diode array detector, G2258A autosampler, two G1361A preparative pumps, one G1379A quaternary pump with degasser, one G1312A binary pump, and three G1364B fraction collectors from Agilent Technologies. System control and data analysis was performed using Agilent's ChemStation software, revision B.03.01-SR.1. A Waters XBridge C18 OBD Prep Column, 100 Å, 5 μm, 19 mm × 150 mm column was used as the stationary phase (Waters Corporation). Gradient elution was carried out using water and acetonitrile as the mobile phase. An aqueous 10% trifluoroacetic acid or 10% ammonium hydroxide solution was added into the mobile phase as a modifier using a static mixer prior to the column, pumped at 1% of the total mobile phase flow rate

^{1}H and ^{13}C NMR spectra were recorded on a Bruker NanoBay Avance III HD NMR 400 MHz instrument or on a Bruker Avance III NMR 500 MHz instrument, and are internally referenced to the residual solvent signals ($CDCl_3$: 7.26 ppm (^{1}H) and 77.16 ppm (^{13}C), d_6-acetone: 2.05 ppm (^{1}H) and 206.26 ppm (^{13}C), CD_2Cl_2: 5.32 ppm (^{1}H) and 53.84 ppm (^{13}C), and d_6-DMSO: 2.50 ppm (^{1}H) and 39.52 ppm (^{13}C). ^{19}F NMR spectra were recorded on a Bruker NanoBay Avance III HD NMR 400 MHz and are reported unreferenced. The multiplicity is denoted as follows: s = singlet, d = doublet, t = triplet, q = quartet, p = pentet, h = hextet, hept = heptet, m = multiplet, br = broad. High-resolution mass spectra were obtained at Princeton University mass spectrometry facilities. IR spectra were recorded on a Perkin Elmer Paragon 1000 spectrometer or on a Perkin Elmer Spectrum 100 FTIR spectrometer and are reported in wavenumbers (cm^{-1}). No melting points were obtained for cubanes due to their (often violent) decomposition at high temperature.

All light-mediated reactions were performed in the PennOC Integrated Photoreactor[52] using an LED module with the indicated wavelength, 100% light intensity, 5200 rpm fans, and 500 rpm stirring unless otherwise indicated. All reactions at a < 0.2 mmol scale were conducted in a multi-

vial holder for five 4 mL screw-cap vials. All reactions at a $\geq$ 0.2 mmol scale were conducted using a standard single-vial holder unless otherwise indicated.

2. De novo synthesis of dimethyl cubane-1,3-dicarboxylate

Synthesis of dihydropyridazine 1

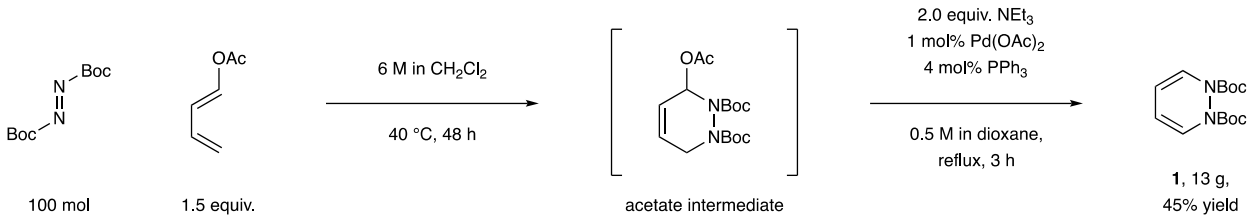

The reaction was conducted according to a modified literature procedure[38]. No attempts were made to optimize the yield. Note that the literature yield is 75%.

Preparation of the acetate intermediate: Di-*tert*-butyl azodicarboxylate (23.03 g, 100 mmol, Combi-Blocks), dry CH_2Cl_2 (16.8 mL, 6 M), and 1-acetoxybutadiene (17.8 mL, 16.8 g, 1.5 equiv., mixture of *cis* and *trans* isomers, Sigma-Aldrich) were heated to 40 °C for 48 h under an N_2 atmosphere. Reaction progress was monitored by consumption of the azodicarboxylate by TLC. Old batches of 1-acetoxybutadiene contained some polymeric species, which led to incomplete conversion even upon extended reaction times. The mixture was allowed to cool to room temperature, transferred to a 1 L round-bottom flask using CH_2Cl_2, and concentrated to a semi-solid using a rotary evaporator inside a fume hood, as an extra precaution due to the toxicity of acetoxybutadiene (most excess butadiene should have polymerized by this point). The crude material was dissolved in EtOAc (ca. 200 mL), and a brownish oil (polyacetoxybutadiene) was triturated by the addition of hexane (ca. 100 mL). The amount of hexane needed depends on the individual batch. Too much hexane will lead to precipitation of the desired product alongside the polymer. The liquid phase was concentrated to ca. 150 mL upon which crystallization began. Crystallization was completed by storing in a freezer (ca. 4 h). The solid precipitate was isolated by filtration yielding 17.7 g of the acetate intermediate as a slightly impure white solid (see Fig. S1). The filtrate was concentrated to ca. 100 mL. As before, additional polyacetoxybutadiene was removed by trituration with hexane leading to the isolation of additional acetate intermediate upon crystallization. Yield: additional 5.12 g as an (impure) white solid.

Comments:

1) The acetoxy group is somewhat labile to hydrolysis. Chromatography or even filtration over silica gel were unsuitable for purification.

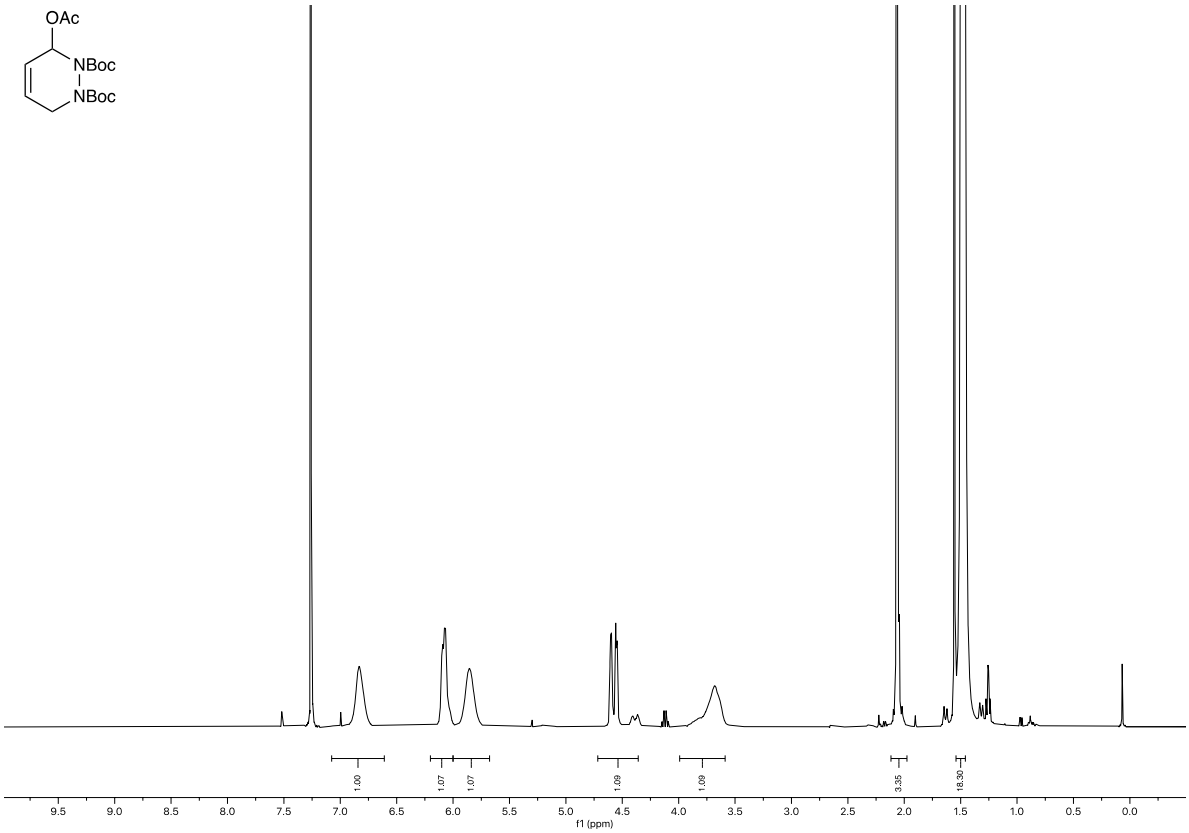

Figure S1 | ^{1}H NMR spectrum of the triturated acetate intermediate.

Elimination to form the dihydropyridazine 1: The acetate intermediate (22.8 g, slightly impure), $Pd(OAc)_2$ (149.5 mg, 1 mol%), PPh_3 (698.7 mg, 4 mol%), 1,4-dioxane (133 mL, 0.5 M), and subsequently triethylamine (18.6 mL, 2.0 equiv.) were added to a flame-dried 250 mL three-neck flask equipped with a stir bar and a reflux condenser under an N_2 atmosphere and refluxed for 3 h. The reaction was monitored by the consumption of the unstable acetate intermediate by TLC. The reaction mixture was allowed to cool to room temperature, concentrated, and purified by automatic column chromatography (Biotage, 330 g column, 0–7% EtOAc for 10 column volumes (CVs), 7–10% for 7 CVs, 10–20% for 5 CVs, 20–50% for 5 CVs; loading with CH_2Cl_2). One batch of the product eluted immediately alongside several impurities presumably due to the high solubility of the dihydropyridazine in CH_2Cl_2. A second batch of the product eluted as pure compound as the amount of EtOAc was increased. Both batches were combined, concentrated, and recrystallized from EtOAc/heptane to deliver the dihydropyridazine product. Yield: 12.6 g, 44.6 mmol, 45% as a white solid.

The obtained analytical data were in good agreement with the literature (Fig. S2)[38].

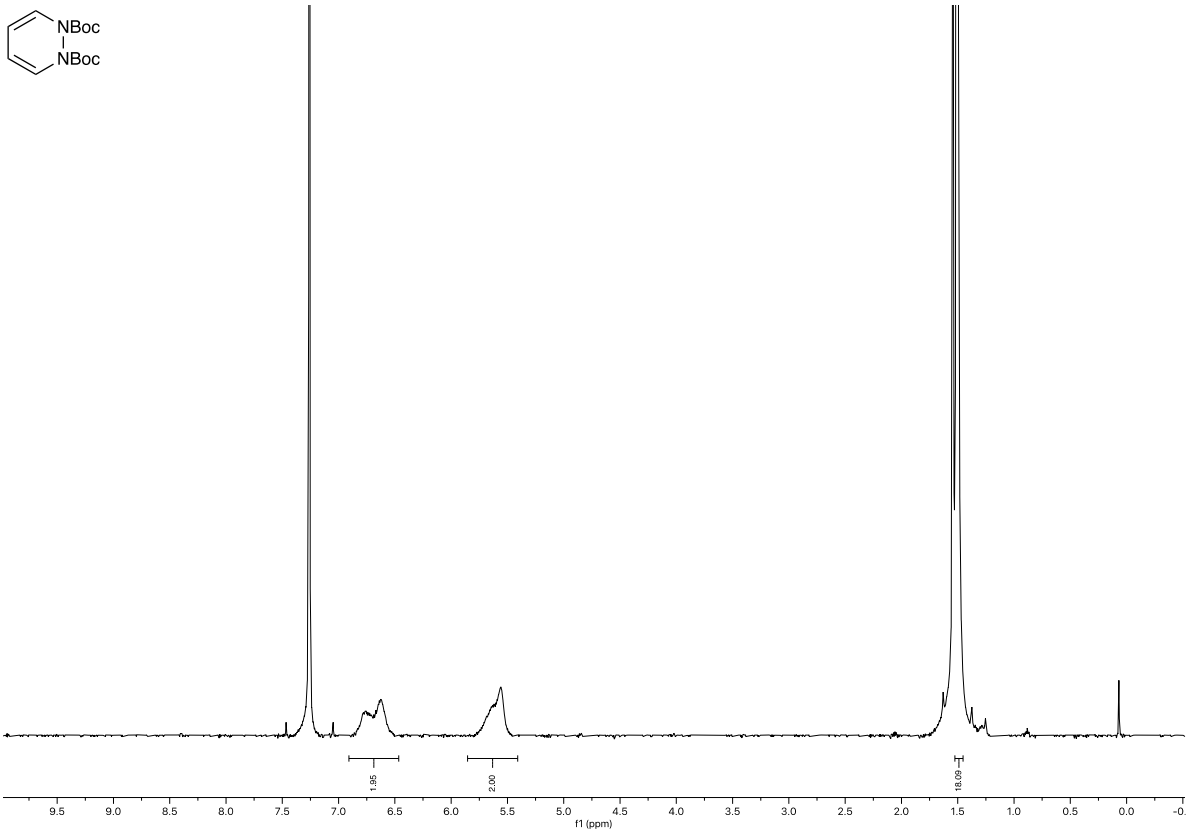

Figure S2 | ^{1}H NMR spectrum of the dihydropyridazine 1.

Comments:

1) The dihydropyridazine is stable for at least 6 months in pure form at –20 °C but decomposes when stored for longer than 1 month in solution at 25 °C.

Synthesis of 2,5-dibromo-1,4-benzoquinone

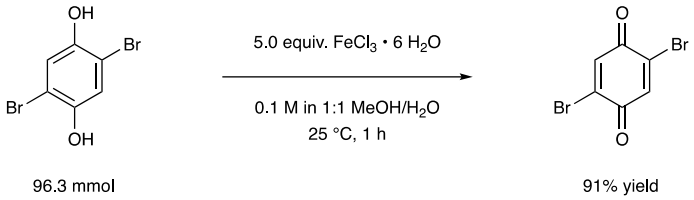

96.3 mmol 91% yield

The reaction was conducted according to a modified literature procedure[53].

Caution: benzoquinones are sensitizers.

A solution of iron(III) chloride hexahydrate (5.0 equiv., 130.1 g, 481.5 mmol) in water (480 mL) was added, as a single portion, to a stirred solution of 2,5-dibromo-1,4-hydroquinone (25.8 g, 96.3 mmol) in MeOH (480 mL) in a 5 L Erlenmeyer flask. The resulting mixture was covered with a glass plate and stirred at room temperature for 1 h. The precipitate was collected by filtration, washed with water (3 x 30 mL) and MeOH (3 x 30 mL). The residue was recrystallized from heptane/ CH_2Cl_2. Recrystallization procedure: 100 mL of both heptane and CH_2Cl_2 were added, and the mixture was heated to reflux. Further CH_2Cl_2 was added until all precipitate was dissolved. The solution was allowed to cool to room temperature at which point crystallization occurred. Crystallization was completed by storing in a freezer (ca. 8 h) and the 2,5-dibromo-1,4-benzoquinone was collected by filtration. Yield: 23.3 g, 87.6 mmol, 91% of yellow crystals.

The obtained analytical data were in good agreement with the literature (Fig. S3)[53].

Comments:

1) 2,5-Dibromo-1,4-benzoquinone is commercially available at a reasonable price (1 g: $118) at BLDpharm. However, it can easily be prepared by oxidation of the corresponding hydroquinone, which is significantly more affordable (1g: $6 at BLDpharm).
2) It is unlikely that stirring for 1 h is required since precipitation occurs after only 5 min and since no visual change is observed after this time.
3) Occasionally, washing with MeOH was not sufficient for complete removal of water leading to iron salts being present in the product even after recrystallization (visually detectable as black dots). In these cases, residual water was removed from a solution of the product in CH_2Cl_2 using a drying agent ($MgSO_4$) prior to recrystallization.

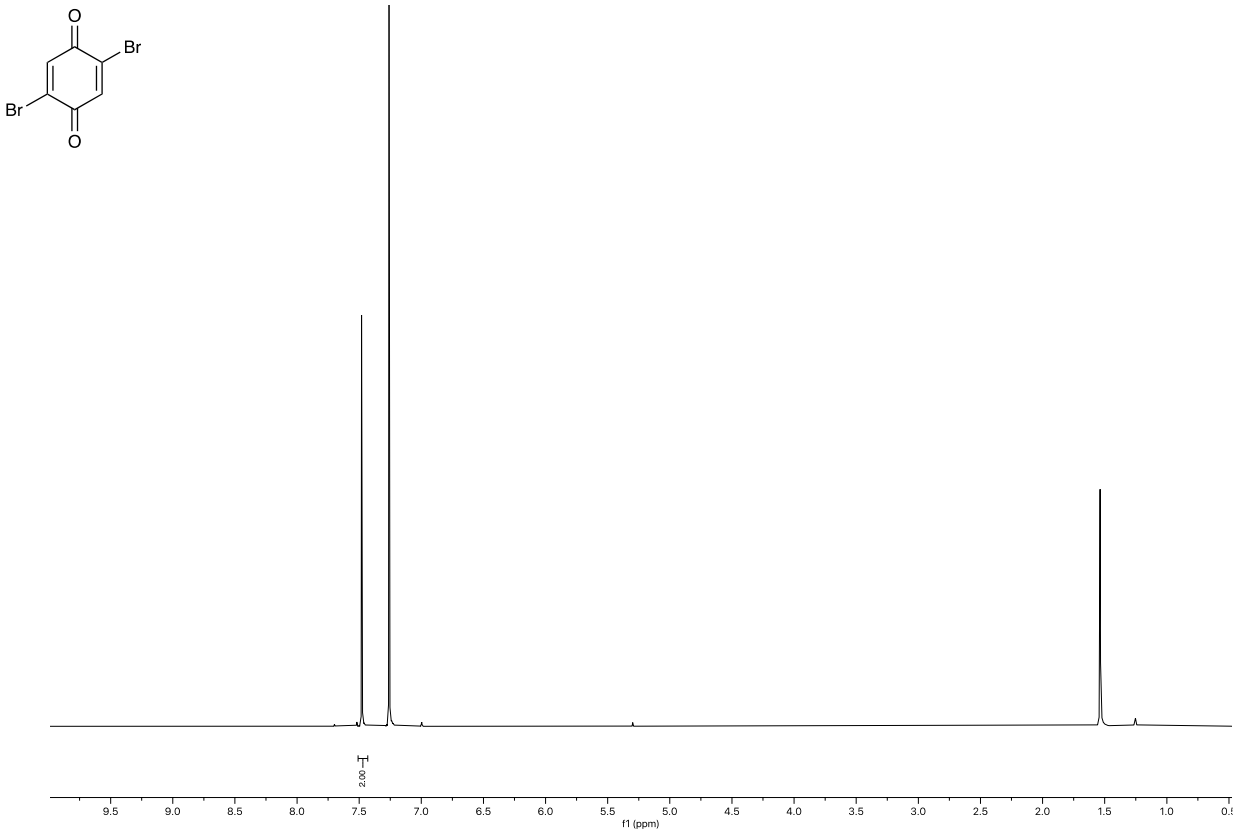

Figure S3 | ^{1}H NMR spectrum of 2,5-dibromoquinone.

Synthetic sequence of step 1: synthesis of tricyclic bisalkene intermediate 2

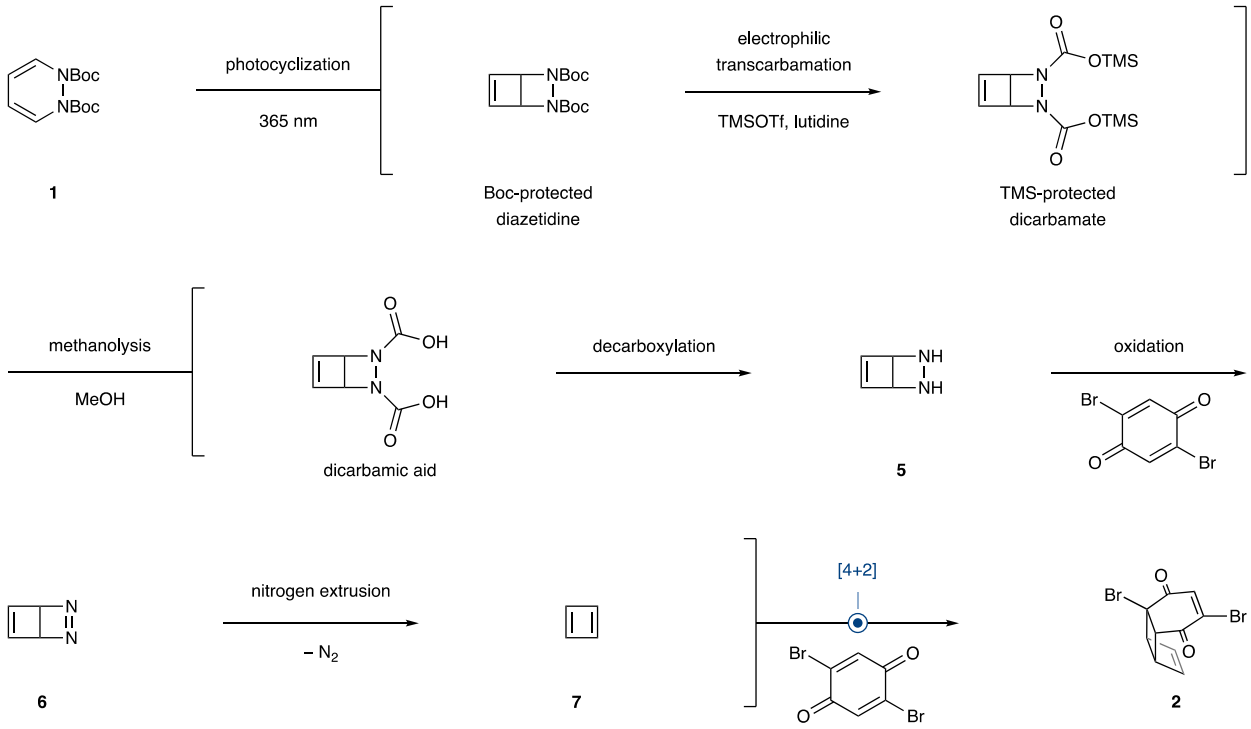

Figure S4 | Synthetic sequence towards the tricyclic bisalkene intermediate 2.

The synthetic sequence to bisalkene **2** starts by light-irradiation of dihydropyridazine **1**, which enables 4-π-cyclization to form the Boc-protected diazetidine (Fig. S4)[39,40]. Addition of TMSOTf in presence of a lutidine buffer forms a TMS-protected dicarbamate by electrophilic transcarbamation[54]. Then, formation of a highly labile dicarbamic acid is immediately followed by decarboxylation to form the equally labile free diazetidine (**5**). **5** is oxidized by one equivalent of the dibromobenzoquinone to form diazine **6**[37]. Extrusion of N_2 then acts as driving force for the formation of the antiaromatic cyclobutadiene (**7**). Finally, the antiaromatic cyclobutadiene (**7**) is highly activated to undergo an *endo*-selective Diels-Alder reaction with an electron-poor alkene such as benzoquinone. As a key design principle, the cyclobutadiene is generated in an oxidative pathway rather than under reducing conditions thus enabling it to be generated in presence of a benzoquinone, which is an oxidant.

In situ-preparation of the TMS-protected dicarbamate

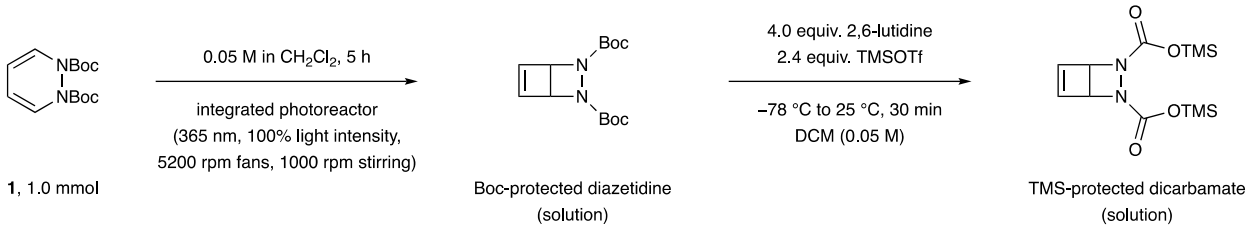

1, 1.0 mmol

Boc-protected diazetidine (solution)

TMS-protected dicarbamate (solution)

Caution: TMSOTf forms triflic acid vapors upon exposure to air. Exposure of the skin to these vapors should be avoided.

Di-*tert*-butyl pyridazine-1,2-dicarboxylate (**1**, 282.3 mg, 1.0 mmol) was added to an oven-dried 40 mL vial equipped with a large cross-shaped stir bar (cooled under an N_2 flow). Dry CH_2Cl_2 (20 mL, 0.05 M) was added, and the colorless solution was degassed by sparging with N_2 for 10 min while cooling with an ice bath. The reaction vessel was thoroughly sealed with molten parafilm and electrical tape and irradiated in an integrated photoreactor (365 nm, 100% light intensity, 5200 rpm fan speed, 1000 rpm stirring, 5 h).

The vial was removed from irradiation and the septum was pierced with a thick needle under N_2 pressure without completely removing the molten parafilm. 2,6-Lutidine (464 µL, 428 mg, 4.0 mmol, 4.0 equiv.) was added via a 1 mL syringe in one go. The vessel was cooled to –78 °C and TMSOTf (434 µL, 533.4 mg, 2.4 mmol, 2.4 equiv.) was added dropwise over ca. 30 s also using a 1 mL syringe. Both 2,6-lutidine and TMSOTf were distilled under an N_2 atmosphere prior to use and stored in a Schlenk flask under an N_2 atmosphere. The vessel was allowed to warm to room temperature over 30 mins by removal of the dry ice bath affording a solution of the TMS-protected dicarbamate.

Comments:

1) A high light intensity is helpful for the internal [2+2] reaction since it facilitates quantitative formation of the Boc-protected diazetidine in a short time. Extended reaction times allow for the thermal formation a 2-aminopyrrole side product[40]. While the diazetidine can safely and easily be isolated by column chromatography (the thermal stability has been verified by differential scanning calorimetry[40], the quantitative yield observed with the use of an integrated photoreactor enables in situ generation of the Boc-protected diazetidine thus improving operational efficiency.

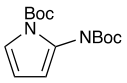

2-amino pyrrol side product

2) Although the TMSOTf turned brown over time, no loss in yield was observed even after storage of either TMSOTf or 2,6-lutidine over several months.
3) The CH_2Cl_2 was dried by storage over activated 4 Å molecular sieves. Water had a detrimental influence on the obtained yield.
4) Our attempts to conduct Boc-deprotection under acidic, basic, thermal, or Lewis-acidic conditions were thwarted by the instability of the free diazetidine intermediate **5** and the tricyclic bisalkene **2**.
5) Prolonged storage of the TMS-protected dicarbamate solution should be avoided.

Deprotection/ Diels-Alder reaction to bisalkene 2

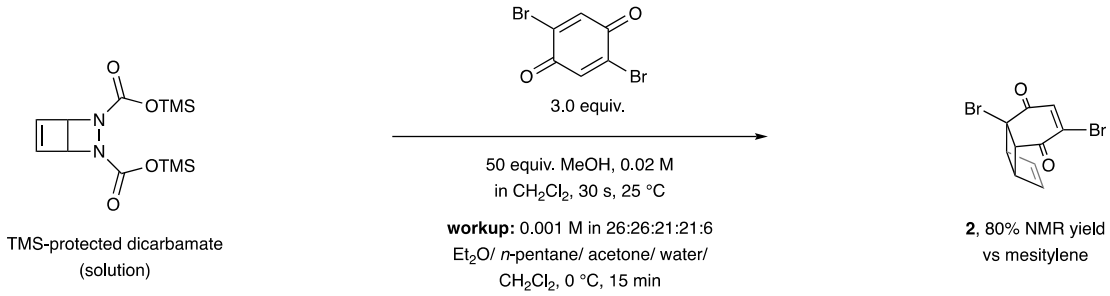

2,5-dibromobenzoquinone (797.7 mg, 3.0 mmol, 3.0 equiv.), dry CH_2Cl_2 (30 mL, 0.1 M with respect to the quinone), and MeOH (2 mL, 50 mmol, 50 equiv.) were added to a 100 mL round-bottom flask. The reaction mixture was stirred rapidly (750 rpm or faster, good stirring is important) as the solution of the TMS-protected dicarbamate, taken up in a 20 mL syringe, was added over exactly 30 s. Yield: 80% of the bisalkene intermediate **2**.

Comments:

1) The yield was measured by ^{1}H NMR spectroscopy using mesitylene as internal standard (140 µL, 1.0 mmol, 1.0 equiv.). The characteristic alkene protons were used for integration (Fig. S5).

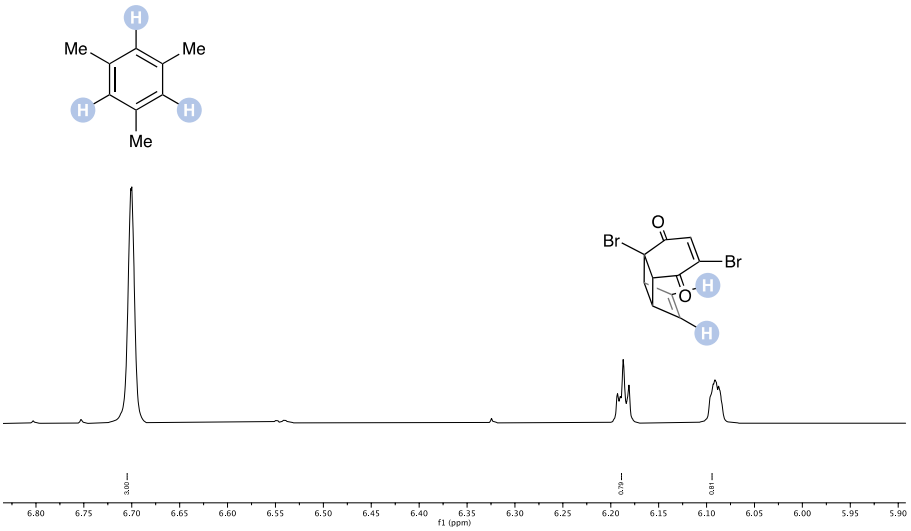

Figure S5 | Crude ^{1}H NMR spectrum of the [4+2] reaction in presence of mesitylene. 1.0 equiv. of mesitylene was used.

2) We noticed that the bisalkene intermediate **2** is unstable to heat, acids, bases, and somewhat unstable to water and methanol. We detected the formation of 2-bromonaphthaquinone, and we assume that this species is formed by strain-releasing ring opening followed by

aromatization via elimination of HBr (Fig. S6). Hence, we believe that the decomposition is autocatalytic due to the concomitant formation of a strong acid.

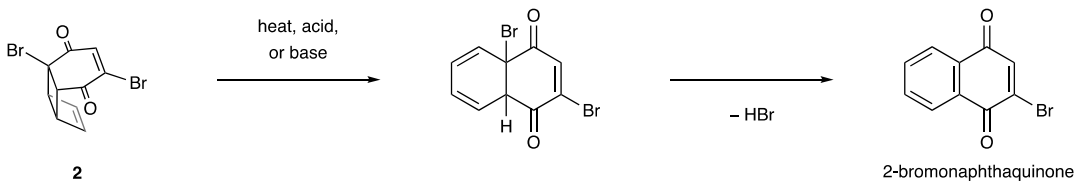

Figure S6 | Formation of 2-bromonapthaquinone.

3) An excess of the quinone is needed to suppress the undesired Diels-Alder reaction between two molecules of the cyclobutadiene formed *in situ*. However, the excess 2,6-dibromobenzoquinone and the 2-bromonaphthaquinone decomposition product could act as a sensitizer during the subsequent [2+2] reaction (vide infra) thus requiring it to be separated from the highly labile tricyclic bisalkene **2**. We attempted rapid purification by column chromatography and various filtration techniques but could only detect the naphthaquinone decomposition product, even when using buffered silica gel, florisil or alumina. To solve this most challenging problem, we elected to conduct a rapid reductive workup under dilute conditions, which converts the problematic quinones into the corresponding hydroquinones (see below).
4) Faster addition (in one go) resulted in a small reduction in yield (<10% difference) while longer addition rates (>1 min) resulted in a roughly 20% reduction in yield presumably due to the instability of the obtained bisalkene to methanol.

Reductive workup (*to remove excess quinone*)**:** The mixture was immediately transferred into a 2 L Erlenmeyer flask containing 240 mL Et_2O, 240 mL pentane, 190 mL acetone, 190 mL water, and ascorbic acid (2.2 g, 12.5 mmol, 12.5 equiv.) in an ice/water bath. The mixture was stirred rapidly (ca. 1250 rpm using a large stir bar (ca. 7 cm length) – rapid stirring of this heterogeneous reaction is required) until the deep green color faded to a light yellowish/green color (ca. 15 min, depending on the stir bar size and the speed of stirring; stirring for longer than 20 min leads to decomposition). The biphasic suspension was washed with water (3 x 250 mL). The combined aqueous phases were back extracted with ether (1 x 250 mL), and the combined organic phases were washed with brine (1 x 250 mL), dried over Na_2SO_4 (large excess), filtered over a fritted glass funnel, and concentrated using a rotary evaporator with the water bath temperature set to 22 °C (max.). During solvent evaporation, the water bath of the rotary evaporator and the flask were covered with aluminum foil to extrude light (together, covering the flask individually prolonged the time required and thus led to decomposition). Et_2O (5 mL) was added, and the solvent was evaporated to ensure crystallization of the hydroquinone byproduct. Pentane (5 mL) was added and evaporated for the same reason. Following evaporation of both solvents, dry toluene (10 mL) was added followed by activated charcoal (50 mg, both more and less charcoal reduce the yield). The mixture was shaken for 1 min before being rapidly filtered through a celite plug (diameter: ca 1.5 cm, height of celite: ca. 2 cm high, slurry with toluene) into an oven-dried 40 mL vial. The flask was washed further with dry toluene (3 x 5 mL), which was also rapidly filtered through the celite plug, to extract the celite. The brownish solution collected, containing 1,8-dibromotricyclo[4.4.0.02,5]deca-3,8-diene-7,10-dione (**2**), was used in the following step with no purification.

Comments:

1) The yield of the bisalkene **5** can be verified by ^{1}H NMR using CH_2Br_2 (34.5 µL) as internal standard. We generally observe < 2% decomposition during the workup.

Step 2: internal [2+2] cycloaddition towards diketone 3

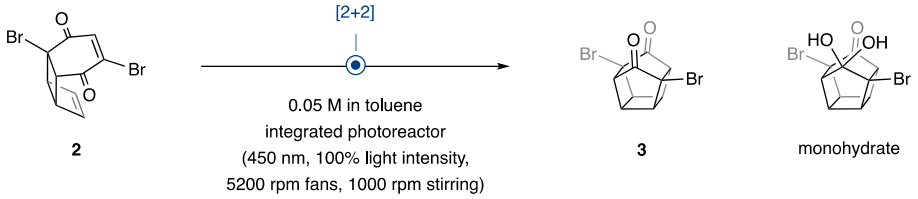

The brownish solution collected in the vial was degassed by sparging with N_2 for 10 min (a big needle is needed to prevent clogging). Then the vial was placed inside an integrated photoreactor (450 nm, 100% light intensity, 5200 rpm fans, 1000 rpm stirring, 16 h). A black suspension of the caged diketone and the monohydrate was obtained after this step. The vial was concentrated using a rotary evaporator.

Comments:

1) The monohydrate results from hydrolysis of the diketone. Vigorous exclusion of water and air will likely result in exclusive formation of the diketone. However, both compounds are stable and productive in the subsequent Favorskii reaction.
2) Both diketone **3** and its monohydrate are poorly soluble in both polar and non-polar solvents and challenging to analyze by ^{1}H NMR spectroscopy due to peaks overlapping. Hence, no reaction control was conducted at this stage.
3) It is challenging to transfer the diketone and monohydrate mixture to a different flask due to their low solubility. Hence the Favorskii reaction was conducted in the same vial.

Step 3: Favorskii ring contraction

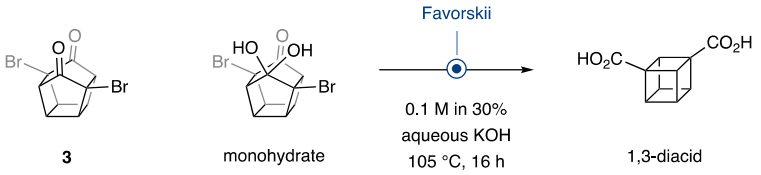

30% aqueous KOH (10 mL) was added to the same vial. This vial was heated to 105 °C in a metal heating block whilst ensuring that the entire liquid phase was covered by the heating block and stirred for ca. 16 h. The yield at this stage was roughly 45%. The aqueous solution was transferred to a 250 mL separating funnel with water (ca. 10–20 mL), washed with Et_2O (ca. 30 mL), and acidified with 1 M HCl. Cubane-1,4-diacid is known to be unstable to concentrated acid[55]. However, we did not observe decomposition during the workup. NaCl (ca. 10 g) was added, and the aqueous solution was extracted with EtOAc (5 x 100 mL). Following drying over Na_2SO_4, 1.5 g activated charcoal was added, and the mixture was filtered over a celite plug with EtOAc. The somewhat volatile diacid was then dry-loaded onto silica gel: silica gel (2 g) was added, and the solvent was removed by evaporation using a rotary evaporator. A water bath temperature of 40 °C was used and the vacuum was no lower than 40 torr to avoid evaporation of the product. The product adsorbed onto silica gel was added to a column (diameter: ca. 7 cm, height: ca. 10–15 cm of a silica gel slurry in CH_2Cl_2). Dry loading was repeated five times by the addition of a small amount of CH_2Cl_2 and 1 g silica gel each time, to ensure that all cubane was transferred to the column. The hydroquinone was eluted with 300 mL CH_2Cl_2. Then the solvent was switched to 0.5% HCO_2H in 9:1 CH_2Cl_2/MeOH (ca. 500 mL) providing a dark brown solution, which was partially concentrated using a rotary evaporator again using caution. To avoid losing the somewhat volatile cubane-1,3-diacid, following evaporation of the CH_2Cl_2/MeOH solvent, the residual formic acid was removed via azeotropic evaporation with pentane (ca. 7 x 5 mL) using a rotary evaporator. Afterwards, the mixture was transferred to an oven-dried 40 mL vial with MeOH, concentrated again, and briefly (for ca. 30 s) submitted to a high vacuum (ca. 0.5 torr). The brown solid or oil was then taken on to the esterification step with no purification.

Comments:

1) After this step, the yield of the dicarboxylate anion in the black solution was determined following addition of 1.0 equiv. of HCO_2K in D_2O (Fig. S7). Occasionally, we observed failure of the NMR measurement due to the strongly ionic character of the sample. Switching off the tuning (with an increased number of scans) ensured the success of the NMR measurement in all cases.

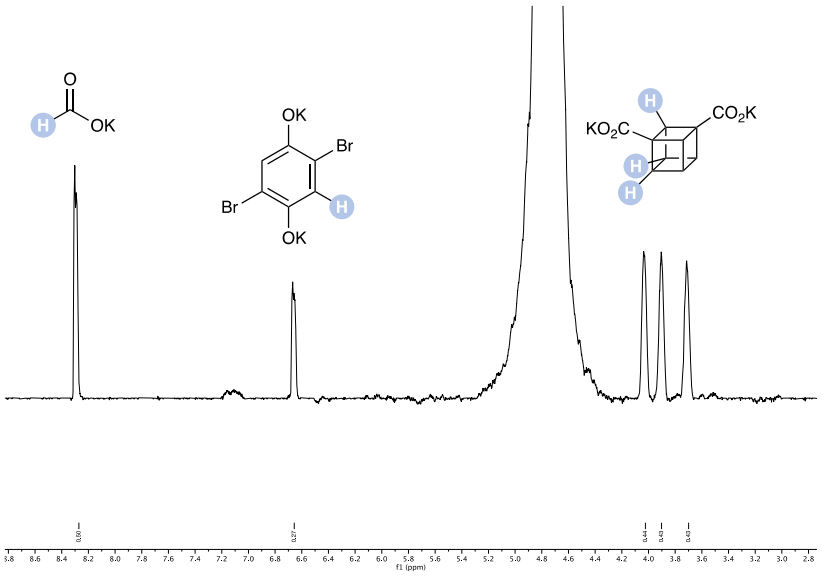

Figure S7 | Crude ^{1}H NMR spectrum of the Favorskii ring contraction in presence of potassium formate. 1.0 equiv. of the formate was used.

Step 4: synthesis of dimethyl cubane-1,3-dicarboxylate (4)

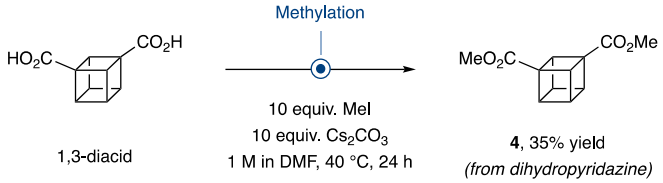

The crude cubane-1,3-diacid and cesium carbonate (1.43 g, 4.4 mmol, 10 equiv.) were suspended in dry DMF (4.4 mL, 1 M) and degassed for 10 min before methyl iodide (274 µL) was added and the reaction was stirred at 40 °C for 24 h. The solution was transferred into a separating funnel with Et_2O (30 mL). 10% aqueous LiCl was added (25 mL). The phases were separated, and the aqueous phase was extracted with Et_2O (5 x 25 mL). The combined organic phases were back extracted with 10% aqueous LiCl (1 x 20 mL), dried over Na_2SO_4, and concentrated. The crude product adsorbed on silica gel was purified by automatic column chromatography (gradient 100% hexane to 100% EtOAc, ISCO, visualization of the products by an ELS detector or 210 nm light) yielding dimethyl cubane-1,3-dicarboxylate (**4**), as a white solid, in 35% over the previous 4 steps (starting from the dihydropyridazine).

Comments:

1) We were unable to detect the dimethyl cubane-1,3-dicarboxylate (**4**) by TLC since it does not absorb UV light at 254 nm and 365 nm and since staining with standard solutions failed.
2) Column chromatography usually provided the product as a pure white solid. However, in some cases a slightly yellowish impurity was still present. This impurity can be removed using purification by preparative reverse-phase HPLC using light-absorption at 210 nm for detection.

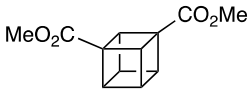

4, ^{1}H NMR (400 MHz, $CDCl_3$) δ 4.46 (ddd, *J* = 6.0, 3.0, 1.8 Hz, 2H), 4.22 (tt, *J* = 4.9, 2.4 Hz, 2H), 4.08–3.92 (m, 2H), 3.71 (s, 6H); ^{13}C NMR (126 MHz, $CDCl_3$) δ 171.78, 53.39, 51.82, 51.23, 49.99, 42.97. ESI-MS: calculated $[C_{12}H_{12}O_4+Na]^+$: 243.0628, found: 243.0629. IR ν = 3000.1, 2984.3, 2952.5, 1716.7, 1435.6, 1309.2, 1206.9, 1171.1, 1157.3, 1086.6, 1043.9, 1015.8, 907.2, 884.9, 854.0, 841.1, 802.2, 709.6.

3. Synthesis of 1-*tert*-butyl-2-methyl cubane-1,2-dicarboxylate

Haller-Bauer cleavage vs Favorskii ring contraction

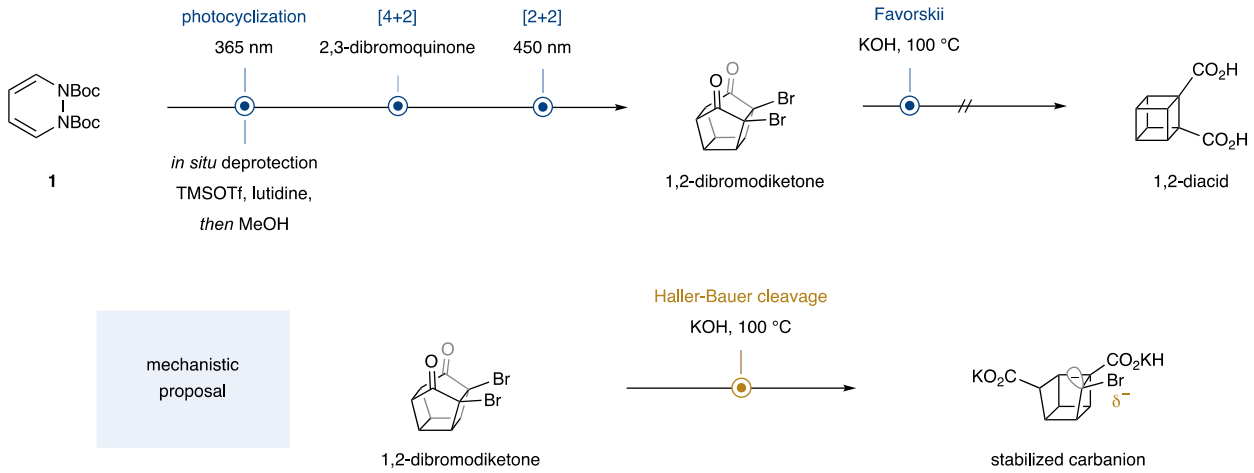

Figure S8 | Failed Favorskii ring contraction towards the 1,2-diacid.

We initially attempted to adapt our protocol for the de novo synthesis of dimethyl cubane-1,3-dicarboxylate (**4**) to the synthesis of dimethyl cubane-1,2-dicarboxylate using 2,3-dibromoquinone (Fig. S8). However, we were unable to observe the corresponding 1,2-diacid even after extensive variation of the reaction conditions. Based on literature precedence[56], we allocate this observation to a Haller-Bauer cleavage, which takes place from the same intermediate as the Favorskii ring contraction and competes with the second, cubane-forming Favorskii reaction. In the Haller-Bauer cleavage, a carbanion is formed at the halide-carrying carbon atom. Presumably, this anion is favored by the electron-withdrawing carboxylate in β-position. Notably, in the pathway towards the 1,3-diacid, that carboxylate would be in γ-position to the bromide thus stabilizing the anion formation at the opposite side, leading to the Favorskii reaction. We attempted to overcome this intrinsic bias utilizing the corresponding diiodo and dichloro diketone substrates, by starting from the dialcohol, which enables Favorskii reaction with milder, non-nucleophilic bases, and by introducing further electron-withdrawing groups onto the cubane. Nevertheless, we have never observed more than traces of the 1,2-diacid. Note that silver salts can violently decompose cubane.

Synthesis of the cubane triester 9 by C–H carboxylation

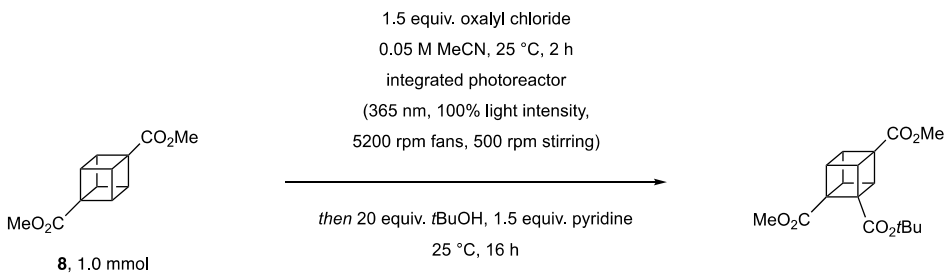

Twenty batches of dimethyl cubane-1,4-dicarboxylate (**8**, 220 mg, 1.0 mmol, 1.0 equiv.) and MeCN (20 mL, 0.05 M) were added to twenty 40 mL vials. The vials were degassed with N_2 for 10 min, before degassed oxalyl chloride (0.12 mL, 1.5 equiv.) was added. The resulting vials were irradiated in the integrated photoreactor (365 nm, 100% light intensity, 5200 rpm fans, 500 rpm stirring) for 2 h. Pyridine (0.12 mL, 1.5 equiv.) and *tert*-butanol (1.9 mL, 20 equiv.) were added to each vial, and the resulting mixtures were stirred for 16 h. The reaction vials were then combined, before being diluted with H_2O, and extracted with CH_2Cl_2. The organics were dried ($MgSO_4$), concentrated, and purified by automatic column chromatography using a 40 g Isco RediSep Rf gold column (eluent: gradient from 0 to 40% Et_2O in hexane).

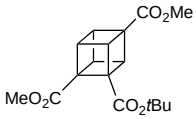

9, 51% yield, white solid. ^{1}H NMR (500 MHz, $CDCl_3$) δ 4.40 (dt, J = 4.4, 1.9 Hz, 2H), 4.30–3.94 (m, 3H), 3.71 (s, 6H), 1.45 (s, 9H); ^{13}C NMR (126 MHz, $CDCl_3$) δ 171.20, 169.87, 168.30, 81.41, 58.08, 56.31, 53.45, 51.93, 51.76, 49.23, 47.71, 45.05, 28.19. EI-MS: calculated $[C_{17}H_{20}O_6]^+$: 320.1254 found: 320.1242. IR ν = 2980, 2953, 1720, 1435, 1393, 1368, 1323, 1216, 1154, 1119, 1090, 1011, 918, 842, 792, 730, 648, 457.

Regioselective deprotection towards monoacid 10

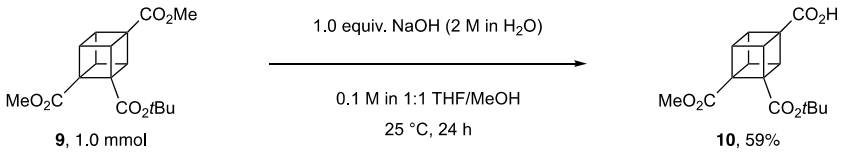

2-(*tert*-Butyl)-1,4-dimethyl cubane-1,2,4-tricarboxylate (**9**, 320 mg, 1.0 mmol, 1.0 equiv.) was added to six 40 mL vials and placed under an N_2 atmosphere. THF and MeOH (1:1, 10 mL, 0.1 M) were added, followed by NaOH (1.0 equiv., 0.5 mL, 2 M in H_2O) dropwise at 0 °C. The reactions were allowed to warm up to room temperature and stirred for 24 h, before the vials were combined, diluted with water, carefully acidified with 1 M aqueous $KHSO_4$, and then extracted with EtOAc. The combined organics were dried ($NaSO_4$), concentrated, and purified by automatic column chromatography using a 40 g Isco RediSep Rf gold column (eluent: gradient from 0 to 10% methanol in dichloromethane + 1% AcOH).

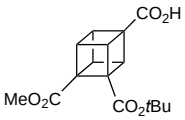

10, 59%, white solid. ^{1}H NMR (500 MHz, $CDCl_3$) δ 4.47 (dd, *J* = 4.5, 2.4 Hz, 2H), 4.30–4.18 (m, 3H), 3.74 (s, 3H), 1.47 (s, 9H); ^{13}C NMR (126 MHz, $CDCl_3$) δ 175.21, 169.78, 168.28, 81.63, 58.08, 56.32, 53.05, 51.83, 49.20, 47.73, 45.10, 28.18. ESI-MS: calculated $[C_{16}H_{18}O_6+Na]^+$: 329.0996 found: 329.1008. IR ν = 2991, 2954, 2927, 2850, 1713, 1677, 1632, 1510, 1478, 1459, 1428, 1410, 1367, 1321, 1301, 1260, 1225, 1184, 1154, 1123, 1087, 1069, 1042, 997, 940, 873, 843, 783, 766, 751, 709, 664, 642, 565, 492, 483, 468.

Decarboxylation towards the 1,2-dicarboxylate 11

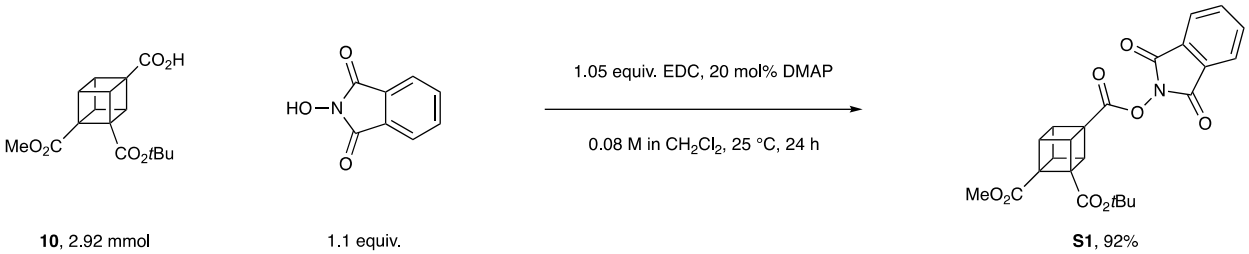

10, 2.92 mmol 1.1 equiv. **S1**, 92%

The cubane monoacid **10** (894 mg, 2.92 mmol, 1.0 equiv.), EDC (558 mg, 1.1 equiv.), *N*-hydroxyphthalimide (573 mg, 1.1 equiv.), and DMAP (70.0 mg, 0.573 mmol, ca. 20 mol%) were taken up in dry CH_2Cl_2 (37 mL, 0.08 M) in a 40 mL oven-dried vial under an N_2 atmosphere at room temperature. The reaction was stirred for 16 h, before being diluted with CH_2Cl_2, washed with water, and subsequently saturated aqueous $NaHCO_3$. The organics were dried ($MgSO_4$), concentrated, and purified by automatic column chromatography using a 40 g Isco RediSep Rf gold column (eluent: gradient from 0 to 20% EtOAc in hexane).

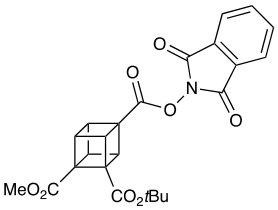

S1, 92% yield, white solid. ^{1}H NMR (500 MHz, $CDCl_3$) δ 7.89 (dd, *J* = 5.4, 3.1 Hz, 2H), 7.80 (dd, *J* = 5.4, 3.1 Hz, 2H), 4.65 (dd, *J* = 4.9, 2.6 Hz, 2H), 4.43 (dq, *J* = 4.9, 2.6 Hz, 1H), 4.33 (t, *J* = 4.9 Hz, 2H), 3.73 (s, 3H), 1.47 (s, 9H); ^{13}C NMR (126 MHz, $CDCl_3$) δ 169.42, 167.59, 166.34, 162.02, 134.96, 129.06, 124.17, 81.81, 58.03, 56.86, 51.89, 50.78, 49.65, 48.28, 45.69, 28.20. ESI-MS: calculated $[C_{24}H_{21}NO_8+Na]^+$: 474.1159 found: 474.1187. IR ν = 3004, 1806, 1781, 1745, 1467, 1436, 1369, 1323, 1213, 1185, 1149, 978, 878, 842, 696.

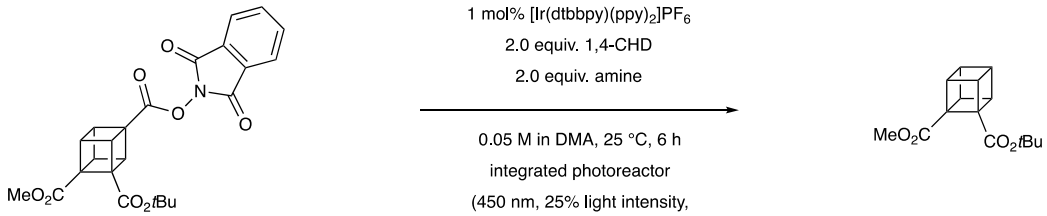

S1, 1.3 mmol **11**, 75%

The redox-active ester **S1** (589 mg, 1.3 mmol, 1.0 equiv.) and $[Ir(ppy)_2(dtbbpy)]PF_6$ (11.9 mg, 1 mol%) were added to an oven-dried 40 mL vial equipped with a stir bar and placed under an N_2 atmosphere. Dry, degassed DMA (26 mL, 0.05 M) was added, followed by triethylamine (0.359 mL, 2.0 equiv.) and then 1,4-cyclohexadiene (0.244 mL, 2.0 equiv.). The vial was sealed with parafilm and placed inside the integrated photoreactor (450 nm, 25% light intensity, 5200 rpm fans, 500 rpm stirring). The reaction was stirred for 6 h, before being diluted with water, and extracted with Et_2O. The organics were dried ($MgSO_4$), concentrated onto silica, and purified by automatic column chromatography using a 40 g Isco RediSep Rf gold column (eluent: gradient from 0 to 100% EtOAc in hexane).

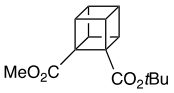

11, 75% yield, white solid. ^{1}H NMR (500 MHz, $CDCl_3$) δ 4.25–4.15 (m, 4H), 4.05–3.85 (m, 2H), 3.70 (s, 3H), 1.43 (s, 9H); ^{13}C NMR (126 MHz, $CDCl_3$) δ 170.69, 169.62, 80.76, 58.64, 57.75, 51.58, 47.45, 47.23, 45.55, 45.38, 28.22. EI-MS: calculated $[C_{15}H_{18}O_4]^+$: 262.1200 found: 262.1213. IR ν = 2997, 2950, 2932, 1709, 1478, 1451, 1428, 1429, 1391, 1367, 1308, 1257, 1220, 1202, 1190, 1156, 1086, 1038, 1015, 988, 951, 909, 866, 844, 806, 757, 723, 688, 633, 470, 427.

4. Amination of cubanes

Scope

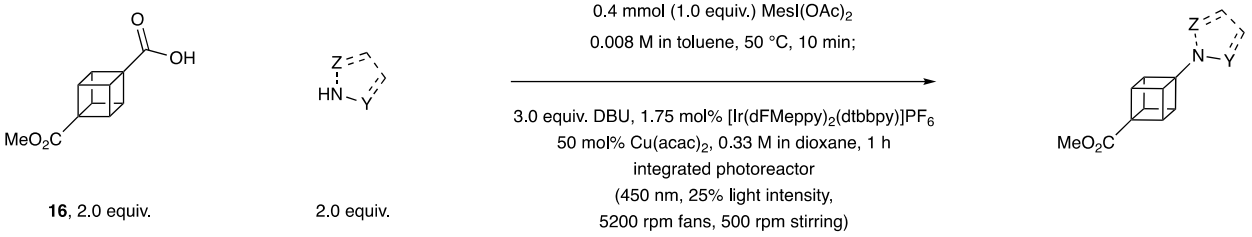

General procedure (GP) 1: A 250 mL round-bottom flask was charged with iodomesitylene diacetate (0.146 mg, 0.4 mmol), 4-(methoxycarbonyl)cubane-1-carboxylic acid (**16**, 0.164 mg, 0.8 mmol, 2.0 equiv.), and 50 mL toluene. The flask was attached to a rotary evaporator with the water bath heated to 50 ºC and the solvent (and the generated acetic acid) was removed over ca. 10 min. A second 50 mL aliquot of toluene was added to the flask and the evaporation was repeated. The evaporation was repeated two more times. After further removal of residual toluene under high vacuum, Iodomesitylene bis(4-(methoxycarbonyl)cubane-1-carboxylate) can be directly used in the following amination reactions.

Iodomesitylene bis(4-(methoxycarbonyl)cubane-1-carboxylate) (263 mg, 0.4 mmol, 1.0 equiv.), the nitrogen nucleophile (0.8 mmol, 2.0 equiv.), $[Ir(dFMeppy)_2(dtbbpy)]PF_6$ (7.1 mg, 1.75 mol%), and $Cu(acac)_2$ (52.4 mg, 50 mol%), were added to an oven-dried 40 mL vial equipped with a stir bar and placed under an N_2 atmosphere. Degassed 1,4-dioxane (12 mL, 0.33 M) was added followed by DBU (0.180 mL, 3.0 equiv.) and the vial was placed inside the integrated photoreactor (450 nm, 25% light intensity, 5200 rpm fans, 500 rpm stirring, single vial holder, 60 min). The reactions were concentrated and purified via automatic column chromatography using a 40 g Isco RediSep Rf gold column (eluent: gradient from 0 to 100% EtOAc in hexane).

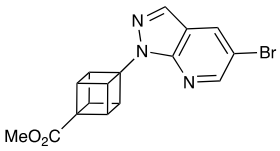

18, 68% yield, off-white solid. ^{1}H NMR (500 MHz, $CDCl_3$) δ 8.54 (d, *J* = 2.1 Hz, 1H), 8.18 (d, *J* = 2.2 Hz, 1H), 8.01 (s, 1H), 4.75–4.68 (m, 3H), 4.41–4.34 (m, 3H), 3.75 (s, 3H); ^{13}C NMR (126 MHz, $CDCl_3$) δ 172.56, 149.75, 148.77, 132.20, 131.87, 117.80, 113.09, 70.56, 56.25, 51.83, 50.97, 45.62. ESI-MS: calculated $[C_{16}H_{12}BrN_3O_2+H]^+$: 358.0186, found: 358.0187. IR ν = 2999, 2355, 1717, 1441, 1321, 1090, 779.

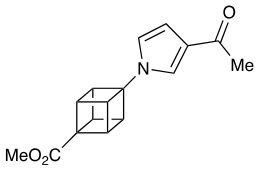

19, 75% yield, white solid. ^{1}H NMR (500 MHz, $CDCl_3$) δ 7.31 (t, *J* = 2.0 Hz, 1H), 6.68 (dt, *J* = 4.6, 2.5 Hz, 2H), 4.38–4.31 (m, 3H), 4.29–4.22 (m, 3H), 3.74 (s, 3H), 2.41 (s, 3H); ^{13}C NMR (126 MHz, $CDCl_3$) δ 193.64, 172.07, 126.69, 122.98, 119.40, 110.28, 70.59, 56.59, 51.90, 50.79, 44.62, 27.33. ESI-MS: calculated $[C_{16}H_{15}NO_3+H]^+$: 270.1125, found: 270.1142. IR ν = 2996, 2357, 1718, 1685, 1576, 1283, 768.

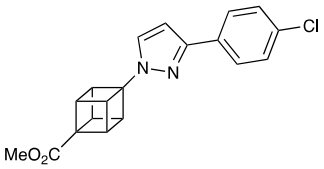

20, 62% yield, off-white solid. ^{1}H NMR (500 MHz, $CDCl_3$) δ 7.79–7.70 (m, 2H), 7.48 (d, *J* = 2.4 Hz, 1H), 7.40–7.32 (m, 2H), 6.60 (d, *J* = 2.4 Hz, 1H), 4.47 (dd, *J* = 5.8, 4.6 Hz, 3H), 4.29 (dd, *J* = 5.8, 4.4 Hz, 3H), 3.75 (s, 3H); ^{13}C NMR (126 MHz, $CDCl_3$) δ 172.24, 151.64, 133.48, 132.01, 128.82, 128.78, 127.13, 103.28, 71.70, 56.36, 51.77, 50.81, 44.82. ESI-MS: calculated $[C_{19}H_{15}ClN_2O_2+H]^+$: 339.0895, found: 339.0914. IR ν = 3005, 1714, 1457, 1113, 1100, 761.

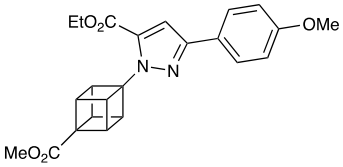

21, 85% yield, white solid. ^{1}H NMR (500 MHz, $CDCl_3$) δ 7.75 (d, *J* = 8.8 Hz, 2H), 7.15 (s, 1H), 6.94 (d, *J* = 8.8 Hz, 2H), 4.52 (dd, *J* = 5.8, 4.5 Hz, 3H), 4.37 (q, *J* = 7.1 Hz, 2H), 4.27 (dd, *J* = 5.7, 4.5 Hz, 3H), 3.84 (s, 3H), 3.74 (s, 3H), 1.40 (t, *J* = 7.1 Hz, 3H); ^{13}C NMR (126 MHz, $CDCl_3$) δ 172.87, 159.74, 159.47, 149.98, 133.42, 126.94, 125.35, 114.23, 108.65, 73.19, 61.27, 55.45, 55.31, 51.76, 51.43, 45.10, 14.48. ESI-MS: calculated $[C_{23}H_{22}N_2O_5+H]^+$: 407.1601, found: 407.1615. IR ν = 2997, 2357, 1713, 1463, 1243, 1108, 837.

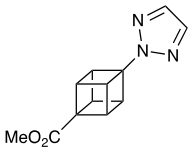

22, 68% yield, white solid. ^{1}H NMR (500 MHz, $CDCl_3$) δ 7.70 (s, 2H), 4.62–4.49 (m, 3H), 4.38 – 4.26 (m, 3H), 3.74 (s, 3H); ^{13}C NMR (126 MHz, $CDCl_3$) δ 172.19, 134.91, 73.16, 56.41, 51.86, 50.97, 45.17. ESI-MS: calculated $[C_{12}H_{11}N_3O_2+H]^+$: 230.0924, found: 230.0937. IR ν = 3005, 2355, 1711, 1447, 1261, 957, 835.

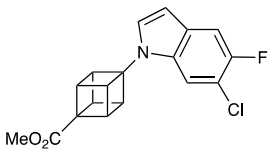

23, 80% yield, white solid. Two subsequent chromatographic separations were required to yield a pure product. ^{1}H NMR (400 MHz, $CDCl_3$) δ 7.36 (d, *J* = 9.6 Hz, 1H), 7.18–7.11 (m, 2H), 6.48 (dd, *J* = 3.1, 0.9 Hz, 1H), 4.54–4.48 (m, 3H), 4.39–4.32 (m, 3H), 3.77 (s, 3H); ^{13}C NMR (126 MHz, $CDCl_3$) δ 172.23, 153.41 (d, *J* = 238.3 Hz), 131.16, 128.47 (d, *J* = 9.0 Hz), 127.00, 115.57 (d, *J* = 21.3 Hz), 111.73, 107.35 (d, *J* = 23.3 Hz), 102.00 (d, *J* = 4.5 Hz), 70.26, 56.15, 51.92, 50.28, 44.77; ^{19}F NMR (376 MHz, $CDCl_3$) δ −126.41 (dd, *J* = 9.7, 6.1 Hz). ESI-MS: calculated $[C_{18}H_{13}ClFNO_2+H]^+$: 330.0692, found: 330.0711. IR ν = 3005, 2355, 1709, 1469, 1212, 1130, 726.

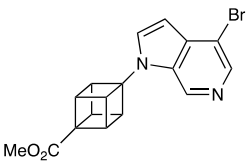

24, 84% yield, white solid. ^{1}H NMR (500 MHz, $CDCl_3$) δ 7.39 (s, 1H), 6.59 (d, *J* = 3.0 Hz, 1H), 4.53 (t, *J* = 4.8 Hz, 3H), 4.38 (t, *J* = 4.6 Hz, 3H), 3.76 (s, 3H), 2 aromatic peaks missing due to line-broadening; ^{13}C NMR (126 MHz, $CDCl_3$) δ 171.94, 139.81, 134.73, 129.38, 101.85, 70.27, 56.21, 51.94, 50.53, 44.89. 3 C missing. ESI-MS: calculated $[C_{17}H_{13}BrN_2O_2+H]^+$: 357.0233, found: 357.0255. IR ν = 2997, 1720, 1471, 1439, 1326, 1211, 894.

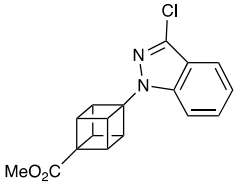

25, 80% yield, off-white solid. δ ^{1}H NMR (400 MHz, $CDCl_3$) δ 7.69 (dt, *J* = 8.1, 1.0 Hz, 1H), 7.42 (ddd, *J* = 8.1, 6.9, 1.1 Hz, 1H), 7.32 (dt, *J* = 8.6, 0.9 Hz, 1H), 7.26–7.20 (m, 1H), 4.71–4.55 (m, 3H), 4.41–4.27 (m, 3H), 3.75 (s, 3H); ^{13}C NMR (101 MHz, $CDCl_3$) δ 172.27, 139.86, 133.94, 127.69, 122.16, 121.86, 120.25, 110.28, 71.58, 56.25, 51.84, 50.72, 45.18. ESI-MS: calculated $[C_{17}H_{13}ClN_2O_2+H]^+$: 313.0738, found: 313.0753. IR ν = 2997, 2355, 1723, 1466, 1334, 1243, 743.

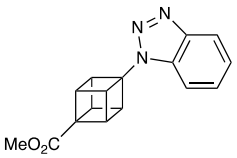

26, 72% yield, white solid. ^{1}H NMR (500 MHz, $CDCl_3$) δ 8.32 (brs, 1H), 7.76 (brs, 1H), 7.54–7.34 (m, 2H), 4.80 (t, *J* = 5.0 Hz, 3H), 4.46 (t, *J* = 4.7 Hz, 3H), 3.77 (s, 3H); ^{13}C NMR (126 MHz, $CDCl_3$) δ 172.01, 127.86, 124.10, 120.31, 109.96, 70.22, 56.46, 51.95, 50.84, 45.68, 2 C missing. ESI-MS: calculated $[C_{16}H_{13}N_3O_2+H]^+$: 280.1081, found: 280.1095. IR ν = 2999, 2355, 1724, 1325, 1124, 1119, 768.

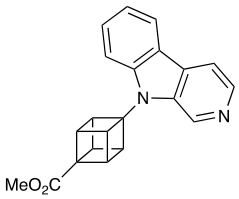

27, 70% yield, off-white solid. ^{1}H NMR (500 MHz, $CDCl_3$) δ 8.95 (s, 1H), 8.46 (d, *J* = 5.2 Hz, 1H), 8.14 (d, *J* = 7.8 Hz, 1H), 7.96 (d, *J* = 5.2 Hz, 1H), 7.56 (ddd, *J* = 8.4, 7.0, 1.3 Hz, 1H), 7.46 (d, *J* = 8.3 Hz, 1H), 7.31 (t, *J* = 7.5 Hz, 1H), 4.88 (t, *J* = 5.2 Hz, 3H), 4.48 (dd, *J* = 6.0, 4.5 Hz, 3H), 3.78 (s, 3H); ^{13}C NMR (126 MHz, $CDCl_3$) δ 172.21, 140.72, 139.07, 136.37, 132.98, 129.69, 128.66, 122.16, 122.03, 120.39, 114.93, 111.37, 71.48, 55.70, 51.92, 51.53, 45.21. ESI-MS: calculated $[C_{21}H_{16}N_2O_2+H]^+$: 329.1285, found: 329.1315. IR ν = 2996, 1725, 1461, 1452, 1435, 1323, 1280, 1231, 1201, 1137, 1090.

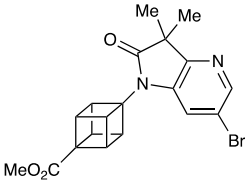

28, 51% yield, white solid. ^{1}H NMR (500 MHz, $CDCl_3$) δ 8.26 (d, *J* = 1.9 Hz, 1H), 6.96 (d, *J* = 1.9 Hz, 1H), 4.69 (dd, *J* = 6.0, 4.4 Hz, 3H), 4.35 (dd, *J* = 6.0, 4.4 Hz, 3H), 3.72 (s, 3H), 1.39 (s, 6H); ^{13}C NMR (126 MHz, $CDCl_3$) δ 179.01, 172.01, 154.83, 143.62, 136.73, 119.12, 118.35, 67.78, 55.49, 51.77, 49.91, 45.49, 45.07, 22.60. ESI-MS: calculated $[C_{19}H_{17}BrN_2O_3+H]^+$: 401.0495, found: 401.0502. IR ν = 2988, 2355, 1720, 1585, 1459, 1156, 727.

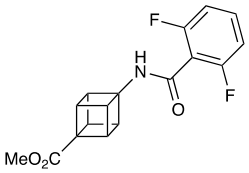

29, 59% yield, white solid. The reaction was run at 0.1 M concentration. ^{1}H NMR (400 MHz, $CDCl_3$) δ 7.38 (tt, *J* = 8.4, 6.3 Hz, 1H), 6.95 (t, *J* = 8.3 Hz, 2H), 6.58 (s, 1H), 4.24 (q, *J* = 4.2 Hz, 6H), 3.72 (s, 3H); ^{1}H NMR (500 MHz, $CDCl_3$) δ 7.31 (tt, *J* = 8.4, 6.3 Hz, 1H), 6.89 (t, *J* = 8.3 Hz, 2H), 6.52 (s, 1H), 4.17 (q, *J* = 4.2 Hz, 6H), 3.65 (s, 3H); ^{13}C NMR (126 MHz, $CDCl_3$) δ 172.79, 160.25 (dd, *J* = 252.9, 6.7 Hz), 159.50, 131.99 (t, *J* = 10.4 Hz), 113.54 (t, *J* = 19.2 Hz), 112.11 (dd, *J* = 25.9, 21.5 Hz), 66.79, 55.77, 51.64, 50.38, 45.24; ^{19}F NMR (376 MHz, $CDCl_3$) δ −111.60–−111.66 (m). ESI-MS: calculated $[C_{17}H_{13}F_2NO_3+H]^+$: 318.0936, found: 318.0956. IR ν = 3261, 2998, 2356, 1701, 1623, 1362, 767.

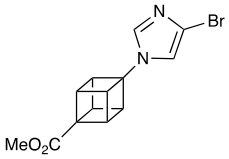

S2, 51% NMR yield. The compound decomposed on silica gel during purification.

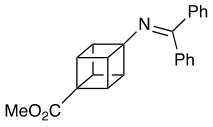

S3, 79% NMR yield. The compound decomposed on silica gel purification.

Comments:

1) Compounds **S2** and **S3** were sufficiently stable to attain NMR yields based on the characteristic, symmetrical cubyl–H signal, both in the reaction mixture and in mildly acidic $CDCl_3$. However, no product was collected upon submission to purification by silica gel. A 2D TLC confirmed their Instability to silica gel.
2) The light intensity had little influence on the amination reaction under our optimized conditions. However, it is known that a switching to a light source with a lower light intensity may require extended reaction times[13].
3) Under the optimized conditions we observe a product containing alkene signals (3% yield) suggesting a ring-opened cubane side product (Fig. S9). This species is the only observable cubyl side product alongside the desired product (68% yield). The crude NMR spectrum does not contain other major side products except for the expected degradation product of the hypervalent iodide starting material, iodomesitylene and remaining amine starting material. We believe that the majority of the remaining balance of cubane-derived products (29%) is taken up by the formation of copper-cubane dimers and resulting decomposition products. Such complexes would not undergo cross-coupling and lead to a dead-end in the catalytic cycle.

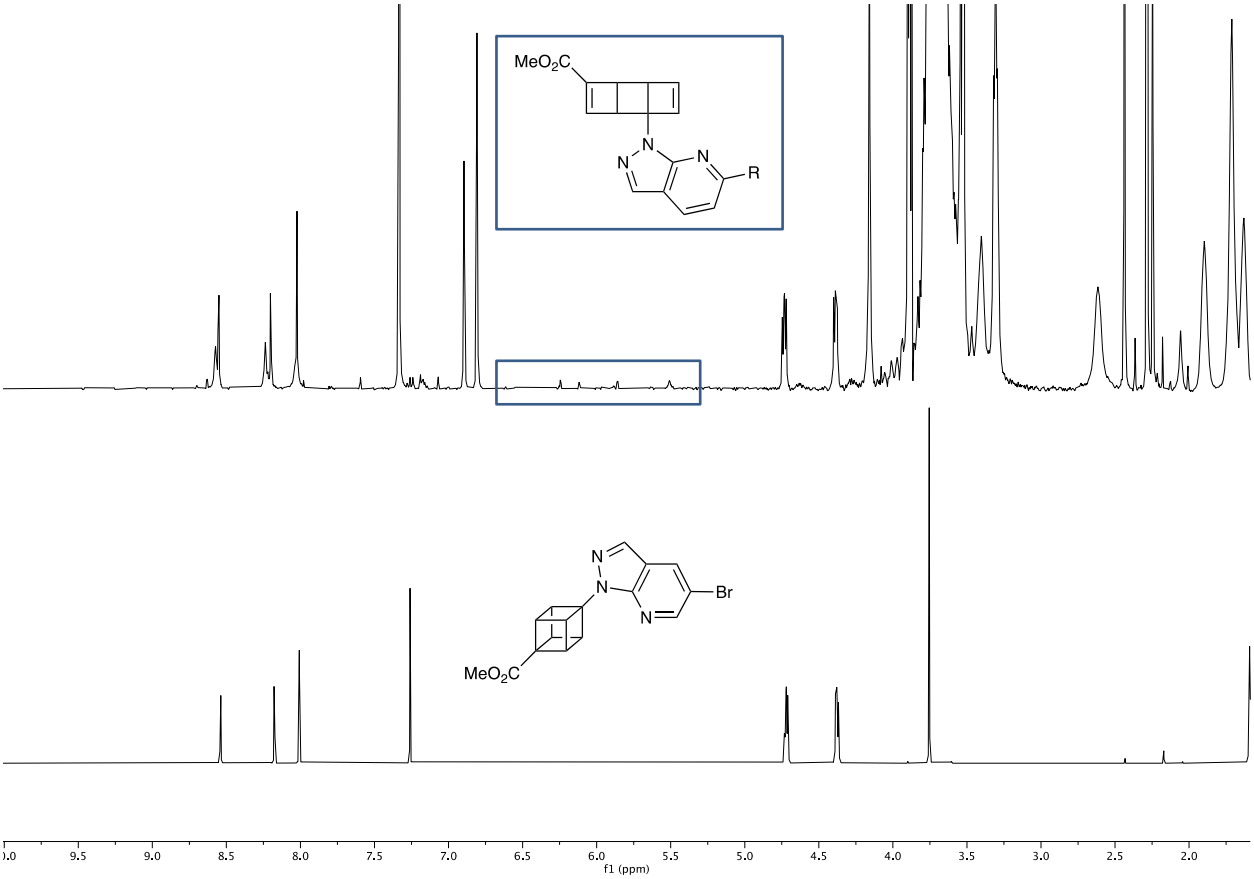

Figure S9 | Crude ^{1}H NMR spectrum of the amination reaction mixture.

5. Alkylation of cubanes

Design plan for the alkylation and arylation of cubanes

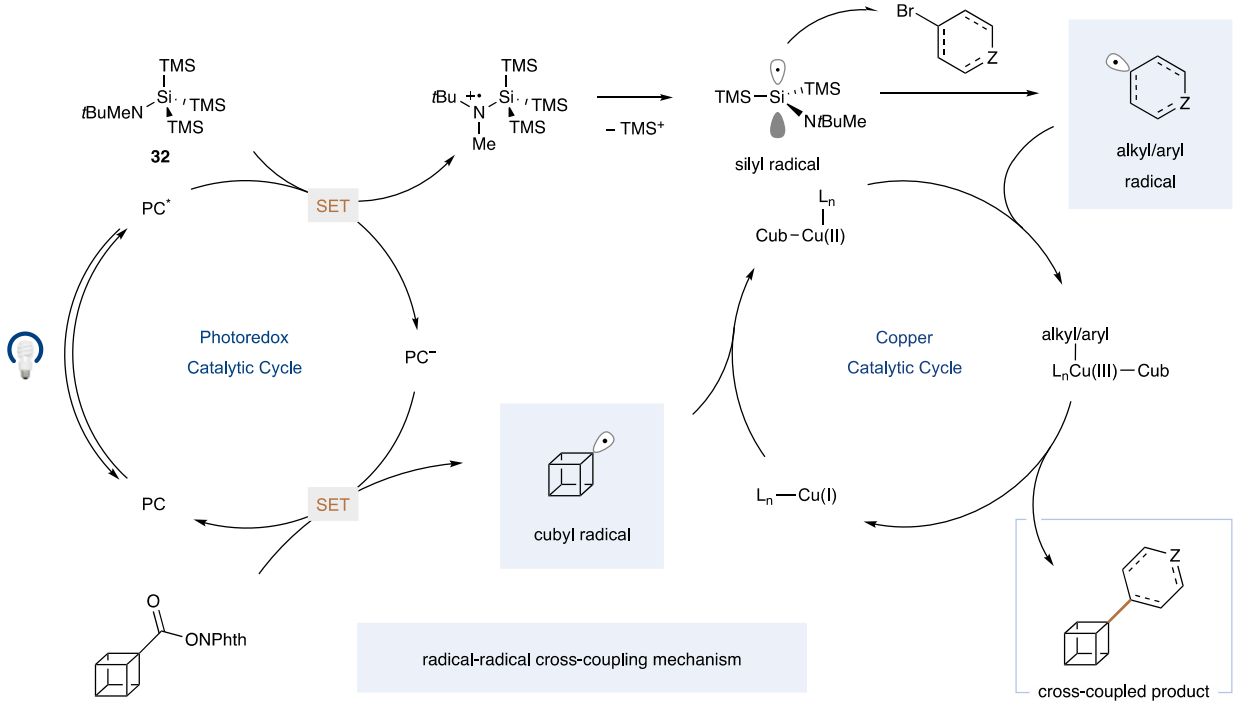

Figure S10 | Design plan for the alkylation and arylation of cubanes.

We envisioned that a copper-mediated C–C cross-coupling could be developed using a radical mechanism (Fig. S10). Reductive quenching of an excited photocatalyst by aminosilane **32** could provide a silyl radical after loss of trimethylsilyl cation. Silyl radicals are well-precedented to undergo facile halogen atom abstraction from both aryl and alkyl halides to afford the corresponding carbon-centered radical intermediates[12,50]. Simultaneously, the reduced photocatalyst could engage with a cubane redox active ester in a single electron transfer (SET) process, affording a cubyl radical after loss of phthalimide anion and carbon dioxide. Both radicals would add subsequently into a copper complex. Productive bond formation could occur via outer- or inner sphere (depicted) reductive elimination, forging the desired cross-coupled product and concomitantly regenerating a catalytically active copper(I) complex.

Synthesis of the *tert*-butyl-methyl aminosilane 32

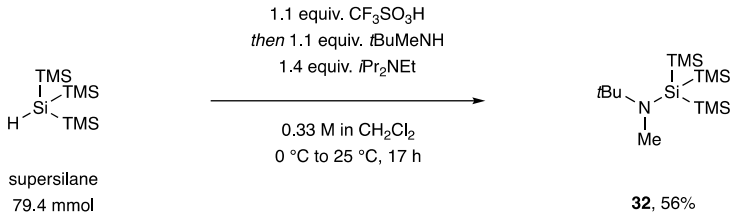

The reaction was conducted according to a modified literature procedure[50].

Caution: trifluoromethanesulfonic acid is incompatible with plastic syringes. Hence, dropping funnels or glass syringes should be used.

Trifluoromethanesulfonic acid (7.33 mL, 12.5 g, 83.0 mmol, 1.05 equiv.) was added to a flame-dried 250 mL Schlenk flask containing anhydrous CH_2Cl_2 (240 mL, 0.33 M) via a glass syringe. Dropwise addition of the silane (24.5 mL, 19.8 g, 79.4 mmol, 1.0 equiv.) at 0 °C was accompanied by evolution of H_2 gas. The mixture was allowed to warm up to room temperature over the course of 1 h. Then *N*,*N*-di*iso*propylethylamine (19.4 mL, 14.4 g, 111 mmol, 1.4 equiv.) and *tert*butyl-methyl amine (3.7 mL, 2.69 g, 30.9 mmol, 1.05 equiv.) were added slowly at 0 °C at the same time. The ice bath was removed, and the resulting solution was stirred for 16 h at room temperature. Then, the solvent was evaporated under an N_2 atmosphere by bubbling N_2 through the solution while stirring and opening the vial up to air. The residue was redissolved in dry pentane and filtered. The filtrate was concentrated again by bubbling N_2 through the solution to yield an oil. Dry acetonitrile (20 mL) was added, and precipitation was induced by sonification. The supernatant was taken out by syringe and filtered. This process was repeated (7x) and the remaining semi-solid was transferred with a large spatula and acetonitrile to a fritted funnel, crushed with a spatula, retransferred to a vial, and dried under high vacuum overnight yielding a sticky white solid. Yield: 16.5 g (90% purity), 46.5 mmol, 56%.

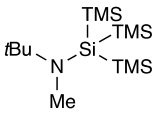

32, ^{1}H NMR (500 MHz, $CDCl_3$) δ 2.58 (s, 3H), 1.14 (s, 9H), 0.20 (s, 27H); ^{13}C NMR (126 MHz, $CDCl_3$) δ 52.85, 38.28, 30.37, 2.29. ESI-MS: calculated $[C_{14}H_{39}NSi_4+H]^+$: 334.2232, found: 334.2250. IR ν = 2949.1, 2893.4, 1358.6, 1242.8, 1215.0, 1081.1, 824.5, 679.8, 622.6, 474.0.

Comments:

1) The purity was measured by transfer of 34.0 mg of the product (0.1 mmol for 100% purity) into a vial followed by addition of mesitylene (14 μL, 0.1 mmol, 1.0 equiv.). The sample was dissolved in $CDCl_3$ (1 mL) and a ^{1}H NMR spectrum was obtained.

Synthesis of redox-active ester 30

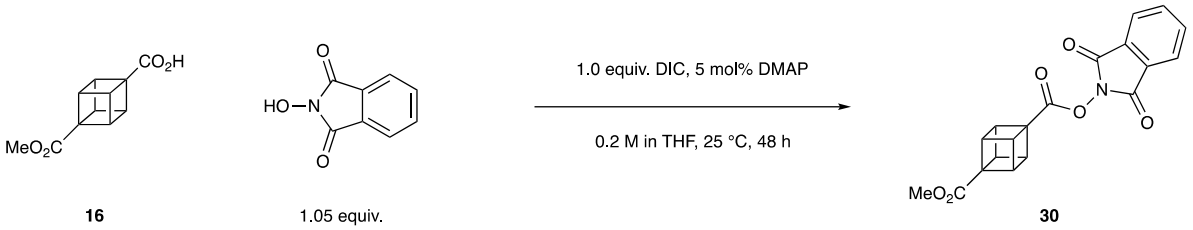

16 1.05 equiv. **30**

The reaction was conducted according to a modified literature procedure[11]. Purification was conducted by rapid column chromatography (gradient CH_2Cl_2 to 10% EtOAc in CH_2Cl_2).

The obtained analytical data were in good agreement with the literature[11].

Optimization

GP 2: The indicated silane (0.075 mmol, 1.5 equiv.), and subsequently the cubane redox-active ester **30** (17.6 mg, 0.05 mmol, 1.0 equiv.), the alkyl bromide (22.4 mg, 0.075 mmol, 1.5 equiv.), NaOAc (8.2 mg, 0.1 mmol, 2.0 equiv.), the copper catalyst (indicated amount), and the photocatalyst (1 mol%) were added to an oven-dried 4 mL vial equipped with a stir bar. The vial was degassed for 5 min by sparging with N_2 before degassed acetone (0.5 mL, 0.1 M) was added followed by the substrate (0.075 mmol, 1.5 equiv., if a liquid). The reaction vial was placed in an integrated photoreactor (450 nm, 100% light intensity, 5200 rpm fans, 500 rpm stirring, multi-vial holder). After the indicated reaction time, a 0.25 M stock solution of mesitylene was added (0.2 mL, 0.05 mmol, 1.0 equiv.) and the mixture was stirred vigorously for 2 min. A sample (ca. 0.4 mL was taken out and filtered over celite into an NMR tube (eluent: $CDCl_3$). The yields of the remaining redox-active ester **30**, the cubane carboxylic acid **16**, the hydrodecarboxylated redox-active ester (i.e., methylcubane carboxylate) and the amount of desired product (**S4**) were measured by ^1H NMR spectroscopy vs mesitylene.

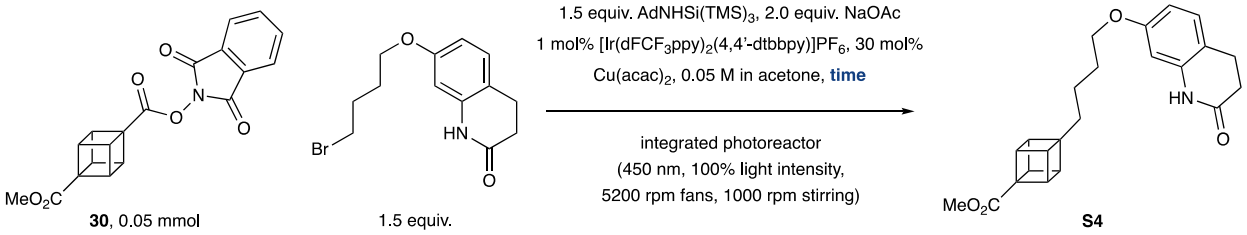

Entry	Reaction time	30	Cubane–CO_2H	Cubane–H	Yield of the desired product
1	1 min	22%	60%	0%	0%
2	2 min	0%	32%	5%	14%
3	3 min	0%	10%	8%	27%
4	4 min	0%	2%	9%	34%
5	5 min	0%	3%	10%	33%
6	15 min	0%	2%	8%	31%
7	30 min	0%	3%	10%	32%

Figure S11 | Screening of the reaction time.

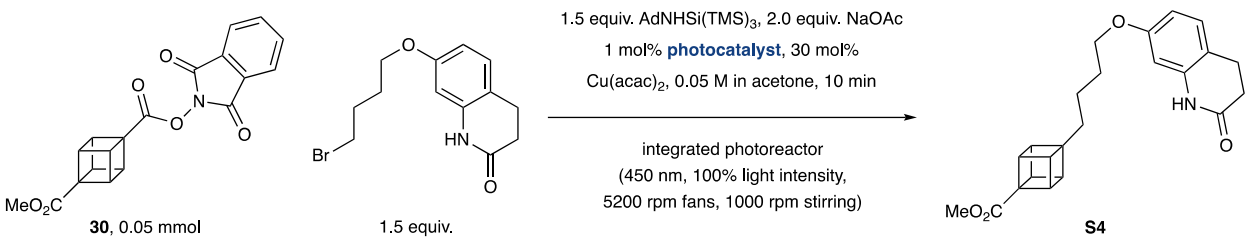

Entry	Photocatalyst	30	Cubane–CO_2H	Cubane–H	Yield of the desired product
1	$[Ir(dFCF_3ppy)_2(4,4'\text{-dtbbpy})]PF_6$	0%	2%	9%	32%
2	$[Ir(dFMeppy)_2(4,4'\text{-dtbbpy})]PF_6$	0%	5%	7%	24%
3	$[Ir(dFCF_3ppy)_2(4,4'\text{-d}(CF_3)bpy)]PF_6$	0%	38%	5%	4%
4	$[Ru(bpy)_3](PF_6)_2$	0%	71%	2%	0%
5	4-CzIPN	0%	3%	11%	34%

Figure S12 | First photocatalyst screening

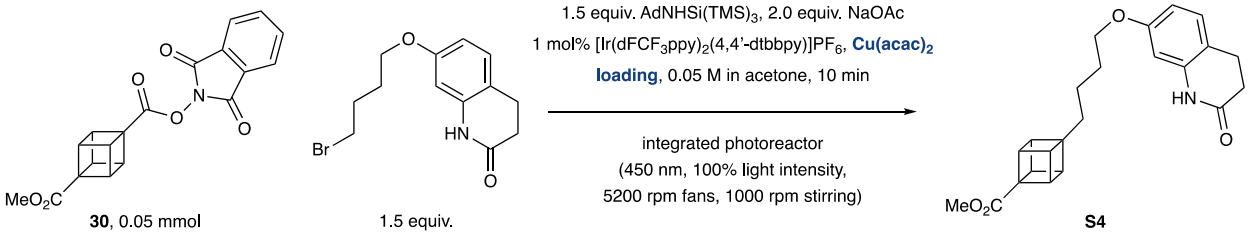

Entry	Copper loading	30	Cubane–CO_2H	Cubane–H	Yield of the desired product
1	5 mol%	0%	4%	25%	35%
2	10 mol%	0%	5%	10%	39%
3	20 mol%	0%	1%	8%	41%
4	30 mol%	0%	2%	9%	32%
5	50 mol%	0%	16%	5%	12%
6	75 mol%	6%	64%	0%	0%

Figure S13 | Screening of the copper catalyst loading.

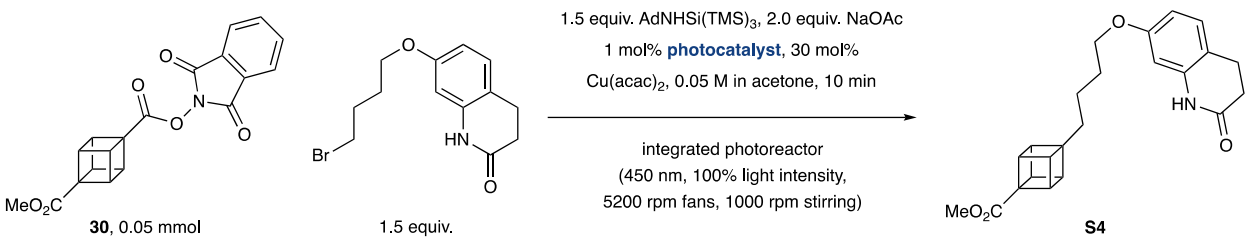

Entry	Photocatalyst	30	Cubane–CO_2H	Cubane–H	Yield of the desired product
1	$[Ir(dFCF_3ppy)_2(4,4'\text{-}dtbbpy)]PF_6$	0%	2%	9%	32%
2	$[Ir(dFMeppy)_2(4,4'\text{-}dtbbpy)]PF_6$	0%	5%	7%	24%
3	$[Ir(dFCF_3ppy)_2(4,4'\text{-}d(CF_3)bpy)]PF_6$	0%	38%	5%	4%
4	$[Ru(bpy)_3](PF_6)_2$	0%	71%	2%	0%
5	4-CzIPN	0%	3%	11%	34%

Figure S14 | Second photocatalyst screening.

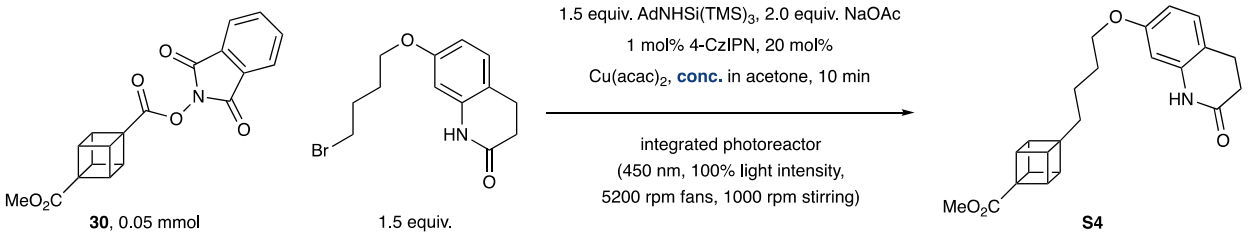

Entry	Concentration	30	Cubane–CO_2H	Cubane–H	Yield of the desired product
1	0.025 M	0%	4%	14%	40%
2	0.05 M	0%	5%	11%	48%
3	0.1 M	0%	5%	10%	51%
4	0.2 M	0%	4%	10%	50%

Figure S15 | Screening of the concentration.

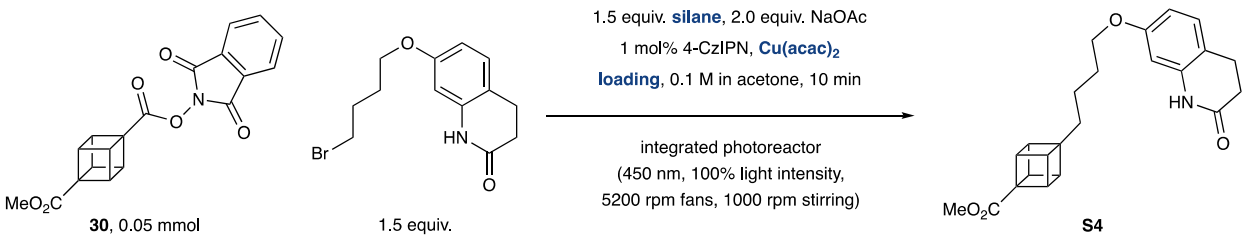

30, 0.05 mmol 1.5 equiv. **S4**

Entry	Silane	Copper loading	30	Cubane–CO_2H	Cubane–H	Yield of the desired product
1	AdNHSi(TMS)$_3$	10 mol%	0%	3%	15%	47%
2	AdNHSi(TMS)$_3$	20 mol%	0%	5%	10%	51%
3	MesNHSi(TMS)$_3$	10 mol%	12%	0%	20%	21%
4	MesNHSi(TMS)$_3$	20 mol%	26%	0%	22%	19%
5	MesNHSi(TMS)$_3$	10 mol%	0%	0%	29%	38%
6	MesNHSi(TMS)$_3$	20 mol%	0%	0%	20%	44%
7	*t*BuMeNSi(TMS)$_3$	5 mol%	0%	0%	15%	50%
8	*t*BuMeNSi(TMS)$_3$	10 mol%	0%	0%	14%	53%
9	*t*BuMeNSi(TMS)$_3$	20 mol%	0%	0%	11%	43%

Figure S16 | Screening of the silane.

Optimization of the Scale-Up

GP 3: The silane **32** (47% pure, 213 mg, 0.3 mmol, 1.5 equiv.), and subsequently the cubane redox-active ester **30** (70.3 mg, 0.2 mmol, 1.0 equiv.), the indicated alkyl bromide (0.3 mmol, 1.5 equiv.), NaOAc (32.8 mg, 0.4 mmol, 2.0 equiv.), the indicated copper catalyst (indicated amount), and 4-CzIPN (1.6 mg, 1 mol%) were added to an oven-dried 8 mL vial equipped with a stir bar. The vial was degassed for 5 min by sparging with N_2 before degassed acetone (indicated concentration) was added. The reaction vial was placed in an integrated photoreactor (450 nm, 100% light intensity, 5200 rpm fans, 500 rpm stirring, single vial holder). After the indicated reaction time, a 1 M stock solution of mesitylene was added (0.2 mL, 0.2 mmol, 1.0 equiv.) and the mixture was stirred vigorously for 2 min. A sample (ca. 0.4 mL) was taken out and filtered over celite into an NMR tube (eluent: $CDCl_3$). The yield of the desired product was measured by ^1H NMR spectroscopy vs mesitylene.

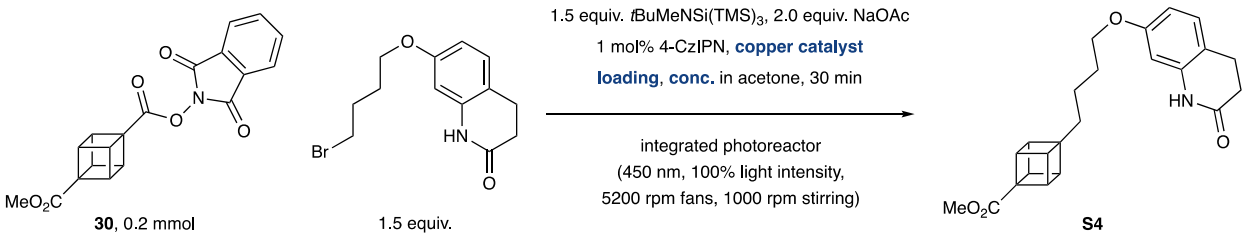

Entry	Copper catalyst	Copper catalyst loading	Concentration	Yield of the desired product
1	Cu(Me, tBu)2 (DMH)	20 mol%	0.05 M	34%
2	Cu(Me, Me)2 (acac)	20 mol%	0.05 M	41%
3	$Cu(acac)_2$	10 mol%	0.05 M	39%
4	$Cu(acac)_2$	10 mol%	0.1 M	48%
5	$Cu(acac)_2$	10 mol%	0.2 M	43%
6	$Cu(acac)_2$	5 mol%	0.2 M	42%

Figure S17 | Re-optimization for primary alkyl bromides.

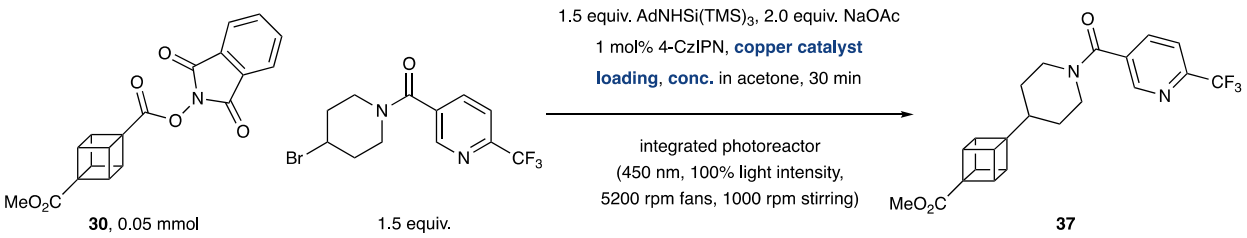

Entry	Copper catalyst	Copper catalyst loading	Concentration	Yield of the desired product
1	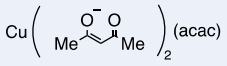	10 mol%	0.1 M	45%
2	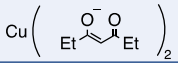	10 mol%	0.1 M	43%
3	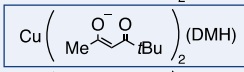	10 mol%	0.1 M	47%
4	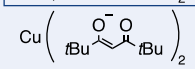	10 mol%	0.1 M	46%
5	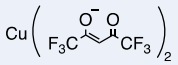	10 mol%	0.1 M	44%
6	$Cu(DMH)_2$	5 mol%	0.1 M	43%
7	$Cu(DMH)_2$	10 mol%	0.1 M	47%
8	$Cu(DMH)_2$	20 mol%	0.1 M	34%
9	$Cu(DMH)_2$	30 mol%	0.1 M	27%
10	$Cu(DMH)_2$	10 mol%	0.025 M	35%
11	$Cu(DMH)_2$	10 mol%	0.05 M	49%
12	$Cu(DMH)_2$	10 mol%	0.1 M	45%
13	$Cu(DMH)_2$	10 mol%	0.2 M	34%
14	$Cu(DMH)_2$	10 mol%	0.05 M	49%
15	$Cu(DMH)_2$	15 mol%	0.05 M	48%
16	$Cu(DMH)_2$	20 mol%	0.05 M	53%

Figure S18 | Re-optimization for secondary alkyl bromides.

Comments

1) Over the course of this optimization (Fig S11–15), we noticed that the reaction outcome was sensitive to the speed of the setup. A longer time for the setup would reduce the yield of the desired product with a concomitant increase in the formation of the hydrolyzed, 4-(methoxycarbonyl)cubane-1-carboxylic acid. A control reaction revealed that roughly 20% of the substrate was hydrolyzed to 4-(methoxycarbonyl)cubane-1-carboxylic acid in presence of just the adamantlyaminosilane over the course of 30 min. We rationalized that this decomposition proceeds via a silylamine-derived amide intermediate, which is subsequently hydrolyzed to the free carboxylic acid during filtration over celite (Fig. S19). We envision that a tertiary amine would no longer undergo this detrimental side reaction. Indeed, when utilizing *tert*-butyl-methyl aminosilane **32**, the reaction outcome was independent of the speed of the setup, 4-(methoxycarbonyl)cubane-1-carboxylic acid

was no longer detected, and the yield was slightly improved when using 10 mol% of the copper co-catalyst (Fig. S16, entry 8). Importantly, the exchange of the silane enabled us to utilize the tetrachlorophthalimide-derived redox-active ester, which is significantly more prone to hydrolysis, for the arylation reaction (vide infra). In fact, we were never able to obtain a reproducible yield with the tetrachlorophthalimide-derived redox-active ester when using adamantly aminosilane for neither the alkylation not the arylation reaction.

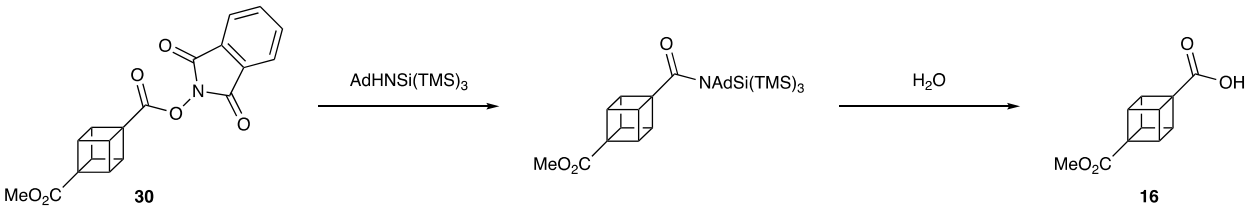

Figure S19 | Proposed pathway for the decomposition of the cubane redox-active ester by the adamantly aminosilane.

2) The purity of the aminosilane reagent **32** has no measurable influence on the yield of the reaction. However, its purity needs to be considered when calculating the amount needed (vide infra).
3) Additionally, we have evaluated the identity of the solvent (only acetone works, traces of product in acetonitrile and DMF), base (acetate bases are best and highest yields are observed with sodium as counterion), light intensity (wide plateau between 100% and 50% light intensity).
4) The photocatalyst loading with respect to the copper catalyst loading was investigated and showed little influence. Both 0.5 mol% and 2 mol% photocatalyst loading, for different copper catalyst loadings, gave similar yields.
5) The slight reduction in yield upon scaling up the reaction indicates that the reaction outcome is influenced by the light intensity (Fig. S17). We believe that this reduction is a result of an imperfect matching of the rates of the copper and photoredox catalytic cycles. We were easily able to solve that challenge by reducing the amount of copper, which slows down the copper catalytic cycle, while also increasing the concentration, which ensures rapid trapping of the generated radicals by copper (Fig. S17, 18). We strongly recommend using a light setup which guarantees a high light intensity such as the PennPhD photoreactor as the reaction has been optimized with this setup.
6) Under the optimized conditions we can identify the protodecarboxylated cubane (14% yield) as the major side product in addition to the desired product (53% yield). The crude NMR spectrum does not contain other major side products except for the excess alkylbromide coupling partner (Fig. S20). We believe that the majority of the remaining balance of cubane-derived products (33%) is taken up by the formation of copper-cubane dimers and resulting decomposition products. Such complexes would not undergo cross-coupling and lead to a dead-end in the catalytic cycle.

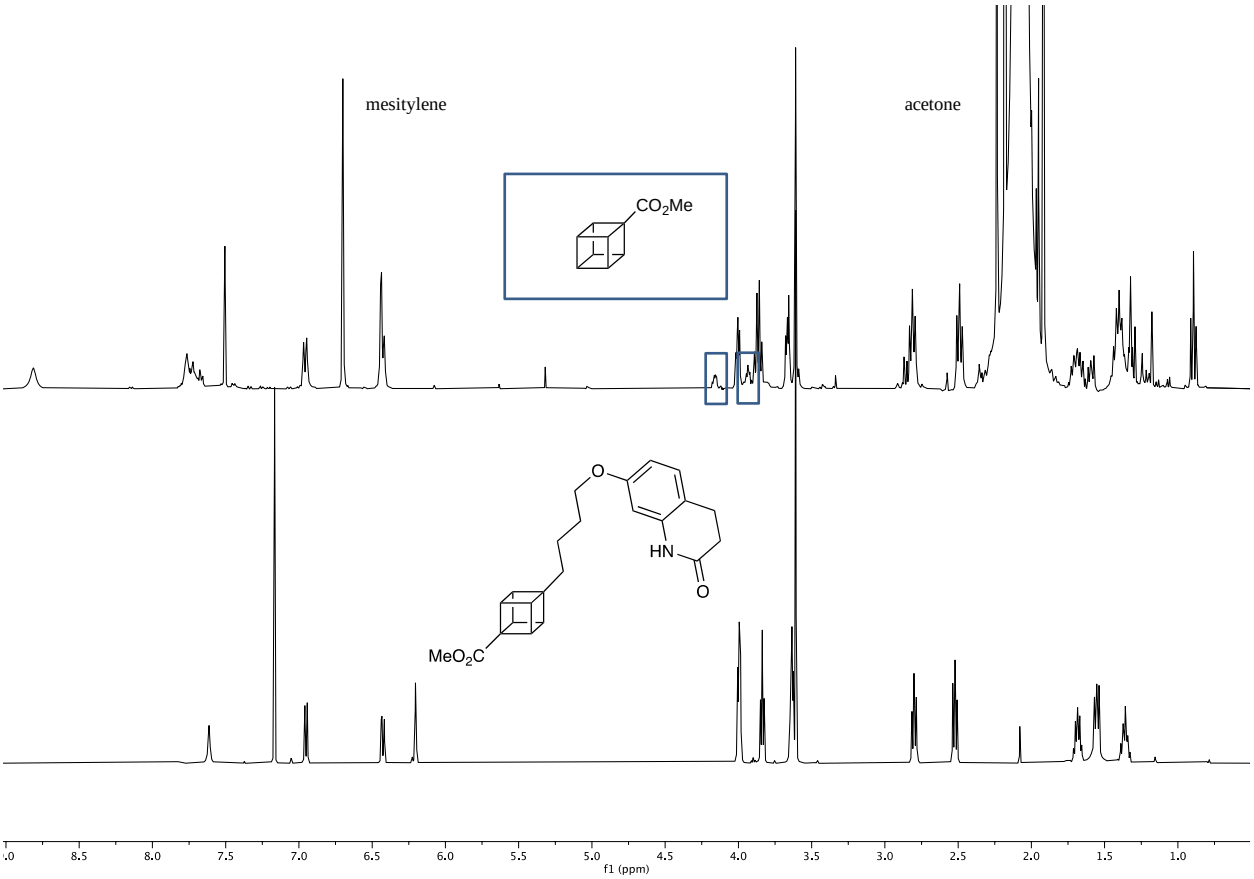

Figure S20 | Crude ^{1}H NMR spectrum of the alkylation reaction mixture.

Scope of primary alkyl bromides

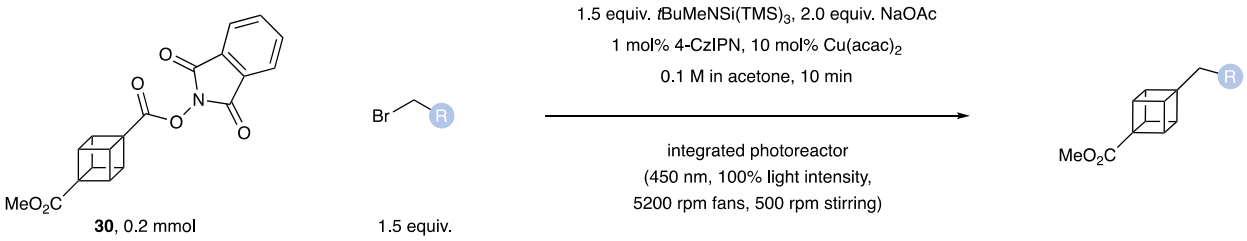

GP 4: The silane **32** (47% pure, 213 mg, 0.3 mmol, 1.5 equiv.), the cubane redox-active ester **30** (70.3 mg, 0.2 mmol, 1.0 equiv.), the indicated primary alkyl bromide (0.3 mmol, 1.5 equiv., if solid), NaOAc (32.8 mg, 0.4 mmol, 2.0 equiv.), $Cu(acac)_2$ (5.2 mg, 10 mol%), and 4-CzIPN (1.6 mg, 1 mol%) were added to an oven-dried 8 mL vial equipped with a stir bar. The vial was degassed for 5 min by sparging with N_2 before degassed acetone (2 mL, 0.1 M) and the indicated primary alkyl bromide (0.3 mmol, 1.5 equiv., if liquid) were added. The reaction vial was placed in an integrated photoreactor (450 nm, 100% light intensity, 5200 rpm fans, 500 rpm stirring, single-vial holder, 30 min). Subsequently the suspension was filtered over celite (eluent: EtOAc), concentrated, and purified by automatic column chromatography using a 40 g Isco RediSep Rf gold column (eluent: gradient from 0 to 100% EtOAc in hexane).

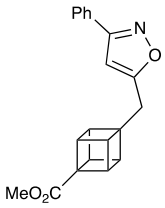

33, 50% yield, white solid. ^{1}H NMR (400 MHz, $CDCl_3$) δ 7.84–7.75 (m, 2H), 7.45 (tdd, *J* = 4.8, 3.5, 1.6 Hz, 3H), 6.27 (d, *J* = 0.9 Hz, 1H), 4.21–4.11 (m, 3H), 3.90 (t, *J* = 5.0 Hz, 3H), 3.71 (s, 3H), 3.14 (s, 2H); ^{13}C NMR (126 MHz, $CDCl_3$) δ 172.72, 170.69, 162.53, 130.06, 129.33, 129.04, 126.90, 99.24, 56.45, 56.37, 51.68, 46.41, 46.26, 30.68. ESI-MS: calculated $[C_{20}H_{17}NO_3+H]^+$: 320.1281, found: 320.1284. IR ν = 3124.2, 2985.4, 2951.0, 2917.4, 2848.9, 1720.4, 1601.0, 1579.1, 1435.2, 1309.0, 1210.8, 1084.6, 913.9, 768.8, 692.0.

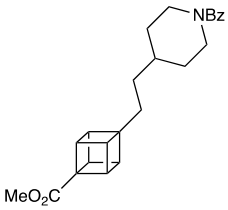

34, 51% yield, yellowish oil. ^{1}H NMR (300 MHz, $CDCl_3$) δ 7.39 (s, 5H), 4.69 (brs, 1H), 4.09 (t, *J* = 4.9 Hz, 3H), 3.74–3.67 (m, 6H), 2.86 (bd, *J* = 44.2 Hz, 2H), 1.90–1.43 (m, 8H), 1.30–1.22 (m, 2H); ^{13}C NMR (126 MHz, $CDCl_3$) δ 173.11, 170.39, 136.57, 129.52, 128.52, 126.93, 59.60, 56.44, 51.59, 46.17, 45.90, 45.41 (d, *J* = 700 Hz), 36.39, 32.61 (d, *J* = 119 Hz), 30.43, 29.80. ESI-MS: calculated $[C_{24}H_{27}NO_3+H]^+$: 378.2064, found: 378.2067. IR ν = 2982.8, 2914.5, 2848.1, 1719.7, 1625.6, 1432.8, 1314.0, 1204.6, 1085.4, 728.1, 707.6.

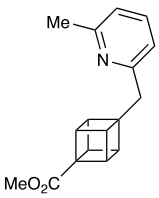

35, 51% yield, off-white solid. ^{1}H NMR (500 MHz, $CDCl_3$) δ 7.50 (t, *J* = 7.6 Hz, 1H), 6.99 (d, *J* = 7.7 Hz, 1H), 6.86 (d, *J* = 7.6 Hz, 1H), 4.12–4.01 (m, 3H), 3.83 (t, *J* = 4.7 Hz, 3H), 3.68 (s, 3H), 3.09 (s, 2H), 2.52 (s, 3H); ^{13}C NMR (126 MHz, $CDCl_3$) δ 173.05, 157.93, 157.86, 136.82, 120.90, 119.74, 58.33, 56.27, 51.57, 46.35, 46.26, 41.30, 24.55. ESI-MS: calculated $[C_{17}H_{17}NO_2+H]^+$: 268.1332, found: 268.1338. IR ν = 2981.9, 2951.5, 2920.8, 1717.3, 1591.0, 1451.4, 1315.5, 1208.6, 838.5, 748.9.

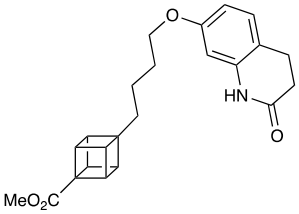

S4, 47% yield, off-white solid. ^{1}H NMR (500 MHz, $CDCl_3$) δ 7.71 (s, 1H), 7.05 (d, *J* = 8.3 Hz, 1H), 6.52 (dd, *J* = 8.3, 2.4 Hz, 1H), 6.30 (d, *J* = 2.5 Hz, 1H), 4.09 (t, *J* = 4.9 Hz, 3H), 3.93 (t, *J* = 6.4 Hz, 2H), 3.72 (t, *J* = 4.9 Hz, 3H), 3.74 (s, 3H), 2.89 (dd, *J* = 8.4, 6.5 Hz, 2H), 2.62 (dd, *J* = 8.5, 6.6 Hz, 2H), 1.78 (p, *J* = 6.7 Hz, 2H), 1.67–1.62 (m, 2H), 1.51–1.39 (m, 2H); ^{13}C NMR (126 MHz, $CDCl_3$) δ 173.20, 171.62, 158.80, 138.16, 128.86, 115.86, 108.74, 102.22, 68.18, 59.73, 56.42, 51.63, 46.23, 46.08, 32.50, 31.24, 29.50, 24.73, 20.84. ESI-MS: calculated $[C_{23}H_{25}NO_4+Na]^+$: 402.1676, found: 402.1680. IR ν = 3202.3, 2926.3, 2857.0, 1719.1, 1669.1, 1590.9, 1382.3, 1303.6, 1191.9, 1082.4, 831.2.

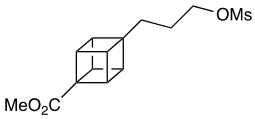

S5, 54% yield, off-white solid. ^{1}H NMR (500 MHz, $CDCl_3$) δ 4.24 (t, *J* = 6.1 Hz, 2H), 4.10 (t, *J* = 4.9 Hz, 3H), 3.74 (t, *J* = 4.9 Hz, 3H), 3.70 (s, 3H), 3.01 (s, 3H), 2.03–1.60 (m, 4H); ^{13}C NMR (126 MHz, $CDCl_3$) δ 172.97, 70.09, 58.86, 56.44, 51.64, 46.14, 45.87, 37.57, 28.70, 24.29. EI-MS: calculated $[C_{14}H_{18}O_5S]^+$: 298.0869, found: 298.0867. IR ν = 2984, 2357, 1719, 1336, 1174, 937.

Scope of secondary alkyl bromides

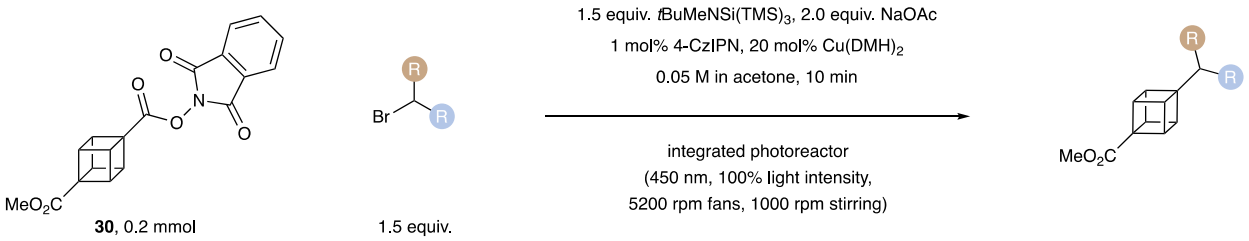

GP 5: The silane **32** (47% pure, 213 mg, 0.3 mmol, 1.5 equiv.), and subsequently the cubane redox-active ester **30** (70.3 mg, 0.2 mmol, 1.0 equiv.), the indicated secondary alkyl bromide (0.3 mmol, 1.5 equiv., if solid), NaOAc (32.8 mg, 0.4 mmol, 2.0 equiv.), $Cu(DMH)_2$ (10.6 mg, 20 mol%), and 4-CzIPN (1.6 mg, 1 mol%) were added to an oven-dried 8 mL vial equipped with a stir bar. The vial was degassed for 5 min by sparging with N_2 before degassed acetone (4 mL, 0.05 M) and the indicated primary alkyl bromide (0.3 mmol, 1.5 equiv., if liquid) were added. The reaction vial was placed in an integrated photoreactor (450 nm, 100% light intensity, 5200 rpm fans, 500 rpm stirring, single-vial holder, 30 min). Subsequently the suspension was filtered over celite (eluent: EtOAc), concentrated, and purified by automatic column chromatography using a 40 g Isco RediSep Rf gold column (eluent: gradient from 0 to 100% EtOAc in hexane).

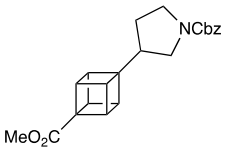

36, 48% yield, yellowish oil. ^{1}H NMR (300 MHz, $CDCl_3$) δ 7.43–7.29 (m, 5H), 5.13 (s, 2H), 4.10 (t, *J* = 5.0 Hz, 3H), 3.77 (t, *J* = 5.0 Hz, 3H), 3.70 (s, 3H), 3.62–3.42 (m, 2H), 3.43–3.29 (m, 1H), 3.05 (dt, *J* = 20.5, 9.5 Hz, 1H), 2.55–2.40 (m, 1H), 1.97–1.82 (m, 1H), 1.74–1.48 (m, 1H); ^{13}C NMR (126 MHz, $CDCl_3$) δ 172.76, 155.06 (d, *J* = 2.9 Hz), 137.08, 128.60 (d, *J* = 4.1 Hz), 128.15 (d, *J* = 6.0 Hz), 128.01 (d, *J* = 7.9 Hz), 66.89 (d, *J* = 9.5 Hz), 59.77 (d, *J* = 13.2 Hz), 56.66 (d, *J* = 3.6 Hz), 51.65, 46.77 (d, *J* = 64.6 Hz), 46.21 (d, *J* = 47.7 Hz), 46.13, 44.95, 40.42 (d, *J* = 122.3 Hz), 25.98 (d, *J* = 100.6 Hz). ESI-MS: calculated $[C_{22}H_{23}NO_4+H]^+$: 366.1700, found: 366.1703. IR ν = 2973.6, 2877.7, 1699.1, 1416.3, 1316.4, 1206.7, 1085.3, 840.6, 732.1, 697.0.

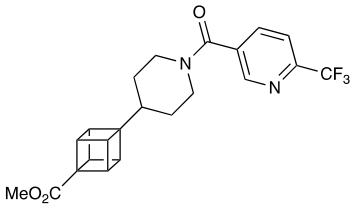

37, 51% yield, off-white solid. ^{1}H NMR (500 MHz, $CDCl_3$) δ 8.75 (d, *J* = 2.1 Hz, 1H), 7.93 (dd, *J* = 8.0, 2.1 Hz, 1H), 7.75 (d, *J* = 8.0 Hz, 1H), 4.91–4.72 (m, 1H), 4.09 (t, *J* = 4.9 Hz, 3H), 3.81 (t, *J* = 4.9 Hz, 3H), 3.74–3.64 (m, 4H), 3.16–3.02 (m, 1H), 2.77 (t, *J* = 12.2 Hz, 1H), 1.87–1.71 (m, 2H), 1.70–1.57 (m, 1H); ^{13}C NMR (126 MHz, $CDCl_3$) δ 172.82, 166.37, 148.95 (q, *J* = 34.8 Hz), 148.11, 136.46, 134.99, 121.22 (q, *J* = 274.0 Hz), 120.55 (q, *J* = 2.8 Hz), 61.94, 56.46, 51.68, 46.15, 45.24 (brd *J* = 685.8 Hz), 44.14, 37.69, 25.74 (brd *J* = 145.28 Hz); ^{19}F NMR (376 MHz, $CDCl_3$) δ −68.14. ESI-MS: calculated $[C_{22}H_{21}N_2O_3+H]^+$: 419.1577, found: 419.1588. IR ν = 2978.4, 2942.2, 2864.6, 1717.2, 1624.1, 1452.6, 1173.7, 1134.6, 1081.6, 997.8, 839.7, 611.3.

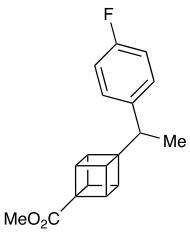

38, 52% yield, white solid. ^{1}H NMR (500 MHz, $CDCl_3$) δ 7.09 (dd, *J* = 8.4, 5.4 Hz, 2H), 6.98 (t, *J* = 8.6 Hz, 2H), 4.01 (t, *J* = 4.9 Hz, 3H), 3.78 (t, *J* = 5.0 Hz, 3H), 3.69 (s, 3H), 2.95 (q, *J* = 7.0 Hz, 1H), 1.20 (d, *J* = 7.1 Hz, 3H); ^{13}C NMR (126 MHz, $CDCl_3$) δ 172.96, 161.52 (d, *J* = 243.5 Hz), 138.94 (d, *J* = 3.4 Hz), 128.59 (d, *J* = 7.6 Hz), 115.19 (d, *J* = 21.0 Hz), 63.08, 56.42, 51.62, 45.80, 44.93, 40.50, 14.86; ^{19}F NMR (376 MHz, $CDCl_3$) δ −117.32. ESI-MS: calculated $[C_{18}H_{17}O_2F+H]^+$: 285.1285, found: 285.1285. IR ν = 2978.6, 2960.3, 2852.7, 1723.9, 1601.90, 1505.7, 1437.6, 1325.7, 1209.5, 1156.6, 1086.3, 1039.6, 823.3, 730.3, 515.5.

6. Arylation of cubanes

Synthesis of the tetrachlororedox-active ester S6

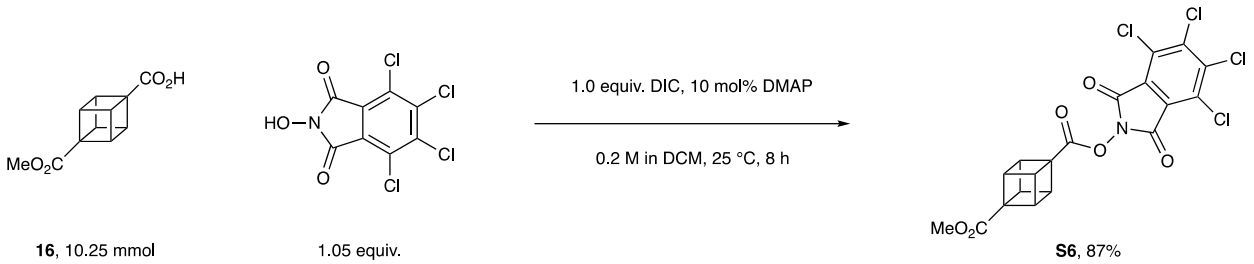

DIC (1.6 mL, 1.0 equiv.) was added dropwise to a rapidly stirred suspension of the cubane carboxylic acid **16** (2.11 g, 10.3 mmol, 1.0 equiv.), tetrachloro-*N*-hydroxyphthalimid (3.23 g, 10.9 mmol, 1.05 equiv.), and DMAP (125 mg, 1.03 mmol, 10 mol%) in dry CH_2Cl_2 (20 mL, 0.2 M) in a 100 mL oven-dried Schlenk flask under an N_2 atmosphere at room temperature. The reaction was stirred for 8 h, before being filtered over a celite pad (3 cm diameter and 3 cm height) with CH_2Cl_2 as eluent (ca. 200 mL). The filtrate was concentrated using a rotary evaporator with the water bath set to 30 °C to yield the crude product as a yellow to orange solid. The crude product was dissolved in minimal CH_2Cl_2 and filtered rapidly over silica gel using a fritted funnel (ca. 8 cm diameter, bottom layer: 1 cm (height) sand, then ca. 10 cm of silica gel, then another 2 cm sand; the solids were suspended with CH_2Cl_2 before the solution of crude product was added). Small amounts of an orange solid were not completely dissolved in the CH_2Cl_2 and remained in the flask or on top of the sand layer. The product was eluted with 4 L CH_2Cl_2 into 3 separate flasks (fraction 1: 300 mL CH_2Cl_2, fraction 2: 2.5 L, fraction 3: 1.2 L). A rapid filtration is crucial to prevent decomposition of the activated ester while a large amount of silica gel is required to prevent coelution with a yellow impurity. All flasks were concentrated using a rotary evaporator with the water bath set to 30 °C. Fraction 2 (occasionally also fraction 3) provided a white to slightly yellowish solid upon concentration. This solid was redissolved in minimal CH_2Cl_2 (ca. 80 mL) and added underneath a layer of pentane (400 mL) using a syringe with an attached needle. The biphasic mixture was stored at −20 °C for 16 h. After that time, the flask was allowed to warm up to room temperature, and a white solid was obtained by filtration. The filtrate was concentrated, and recrystallization was repeated to yield a second pure fraction. The third fraction was generally impure. Yield: 4.34 g, 8.87 mmol, 87%.

The obtained analytical data were in good agreement with the literature[11].

Optimization

GP 6: The silane (indicated amount), and subsequently the indicated cubane redox-active ester (0.05 mmol, 1.0 equiv.), NaOAc (8.2 mg, 0.1 mmol, 2.0 equiv.), the $Cu(acac)_2$ (indicated amount), and the photocatalyst (indicated amount) were added to an oven-dried 4 mL vial equipped with a stir bar. The vial was degassed for 5 min before degassed acetone (0.5 mL, 0.1 M) was added followed by the substrate (indicated amount). The reaction vial was placed in an integrated photoreactor (450 nm, 100% light intensity 5200 rpm fans, 1000 rpm stirring, multi-vial holder). After the indicated reaction time, a 0.25 M stock solution of the internal standards 1-bromo-3,5-bis(trifluoromethyl)benzene and mesitylene was added (0.2 mL, 0.05 mmol, 1.0 equiv. each) and the mixture was stirred vigorously for 2 min. A sample (ca. 0.4 mL was taken out and filtered over celite into an NMR tube (eluent: $CDCl_3$). The yields of the remaining redox-active ester (**30** or **S6**), the (net-) hydrolyzed cubane carboxylic acid **16**, and the hydrodecarboxylated redox-active ester (i.e., methyl cubane carboxylate) were measured by ^1H NMR spectroscopy vs mesitylene. The yields of the remaining aryl bromide, of the hydrodehalogenated arene, the aryl dimer, and of the desired product **40** were measured by ^{19}F NMR spectroscopy vs 1-bromo-3,5-bis(trifluoromethyl)benzene.

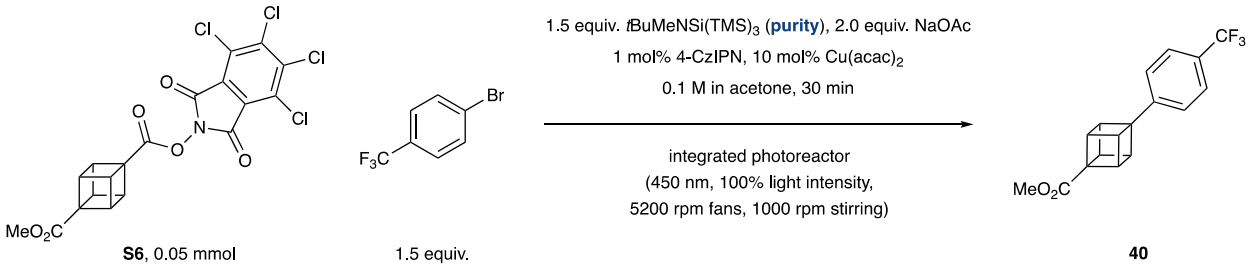

Entry	Purity of the silane	S6	Cubane–CO_2H	Cubane–H	4-(CF_3)Ph–Br	4-(CF_3)Ph–H	(4-(CF_3)Ph)$_2$	Yield of the desired product
1	47%	0%	2%	3%	6%	34%	12%	20%
2	80%	0%	2%	3%	1%	28%	13%	20%
3	90%	0%	2%	4%	1%	21%	20%	19%

Figure S21 | Influence of the purity of the silane.

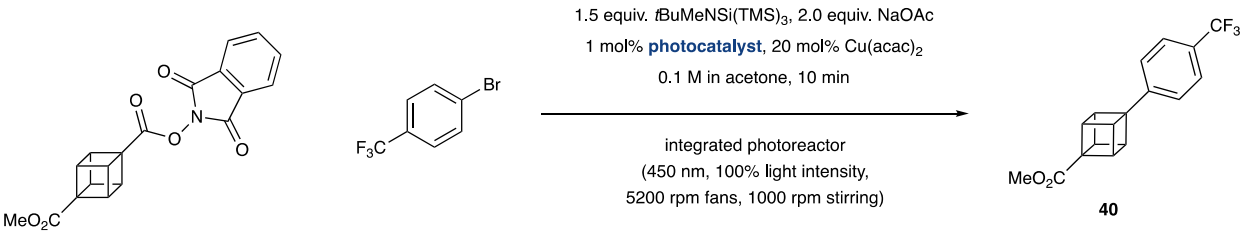

30, 0.05 mmol 1.5 equiv.

Entry	Photocatalyst	**30**	Cubane–CO_2H	Cubane–H	4-(CF_3)Ph–Br	4-(CF_3)Ph–H	(4-(CF_3)Ph)$_2$	Yield of the desired product
1	4-CzIPN	0%	0%	5%	7%	35%	13%	20%
2	Eosin Y	90%	0%	0%	147%	4%	0%	0%
3	$[Ir(dFCF_3)ppy)_2(4,4'\text{-dtbbpy})]PF_6$	3%	0%	4%	7%	37%	10%	22%
4	$[Ir(dFMeppy)_2(4,4'\text{-dtbbpy})]PF_6$	2%	0%	6%	18%	32%	14%	22%
5	$[Ir(dFCF_3ppy)_2(bpy)]PF_6$	13%	0%	8%	13%	22%	28%	16%
6	$[Ir(dFCF_3ppy)_2(4,4'\text{-dFbpy})]PF_6$	57%	0%	0%	71%	28%	8%	4%
7	$[Ir(dFCF_3ppy)_2(4,4'\text{-d}(CF_3)bpy)]PF_6$	86%	0%	0%	94%	37%	3%	0%
8	$[Ru(bpy)_3](PF_6)_2$	3%	0%	1%	40%	17%	19%	26%
9	$[Ru(4,4'\text{-dClbpy})_3](PF_6)_2$	50%	0%	0%	35%	24%	8%	3%

Figure S22 | Photocatalyst screening with the tetrahydroredox-active ester 30.

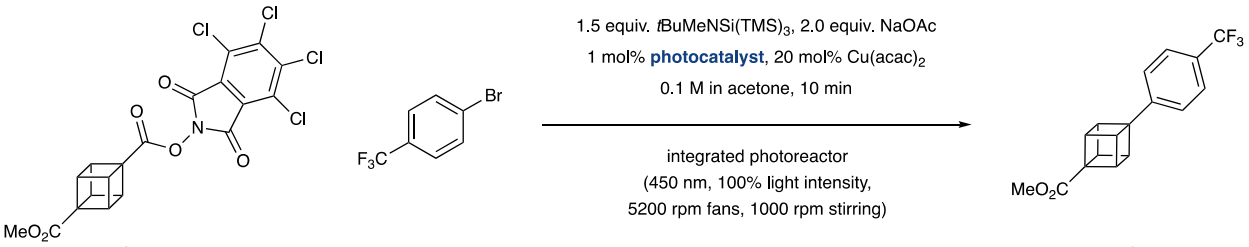

S6, 0.05 mmol 1.5 equiv. **40**

Entry	Photocatalyst	**S6**	Cubane–CO_2H	Cubane–H	4-(CF_3)Ph–Br	4-(CF_3)Ph–H	(4-(CF_3)Ph)$_2$	Yield of the desired product
1	4-CzIPN	2%	10%	5%	11%	48%	14%	19%
2	Eosin Y	24%	17%	0%	148%	3%	0%	1%
3	[Ir(dFCF_3ppy)$_2$(4,4'-dtbbpy)]PF_6	0%	8%	17%	88%	23%	17%	20%
4	[Ir(dFCF_3ppy)$_2$(bpy)]PF_6	4%	7%	19%	84%	23%	16%	22%
5	[Ir(dFCF_3ppy)$_2$(4,4'-dFbpy)]PF_6	4%	15%	7%	60%	20%	7%	12%
6	[Ir(dFCF_3ppy)$_2$(4,4'-d(CO_2Me)bpy)]PF_6	3%	9%	6%	59%	18%	6%	34%
7	[Ir(dFCF_3ppy)$_2$(5,5'-dFbpy)]PF_6	13%	10%	6%	110%	17%	9%	15%
8	[Ir(dFCF_3ppy)$_2$(4,4'-d(CF_3)bpy)]PF_6	2%	9%	0%	52%	26%	18%	39%
9	[Ir(dFCF_3ppy)$_2$(5,5'-d(CF_3)bpy)]PF_6	3%	7%	3%	111%	15%	5%	15%
10	[Ru(bpy)$_3$](PF_6)$_2$	24%	17%	0%	89%	20%	14%	29%
11	[Ru(4,4'-dClbpy)$_3$](PF_6)$_2$	0%	0%	7%	58%	26%	11%	41%
12	[Ru(bpm)$_3$](PF_6)$_2$	3%	2%	11%	143%	5%	1%	1%
13	[Ru(bpz)$_3$](PF_6)$_2$	19%	1%	13%	138%	11%	2%	1%

Figure S23 | Photocatalyst screening with the tetrachlororedox-active ester S6.

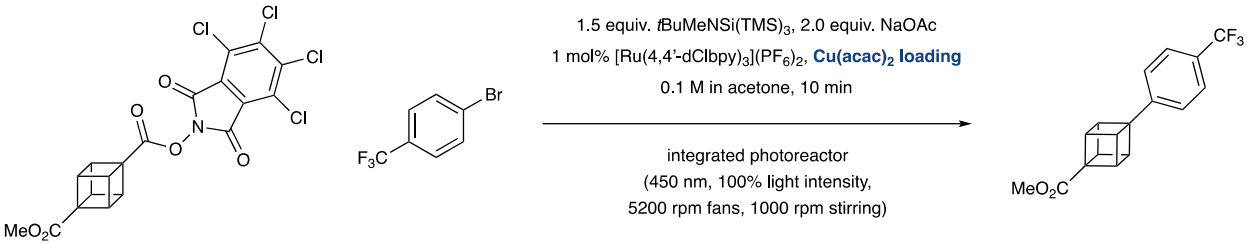

S6, 0.05 mmol 1.5 equiv. **40**

Entry	**Copper loading**	**S6**	Cubane–CO_2H	Cubane–H	4-(CF_3)Ph–Br	4-(CF_3)Ph–H	(4-(CF_3)Ph)$_2$	Yield of the desired product
1	5 mol%	2%	10%	5%	52%	62%	12%	26%
2	10 mol%	24%	17%	0%	69%	33%	12%	35%
3	15 mol%	0%	8%	17%	67%	27%	11%	38%
4	20 mol%	4%	7%	19%	58%	26%	11%	40%
5	30 mol%	4%	15%	7%	57%	26%	10%	39%
6	50 mol%	3%	9%	6%	56%	25%	11%	37%

Figure S24 | Screening of the copper catalyst loading.

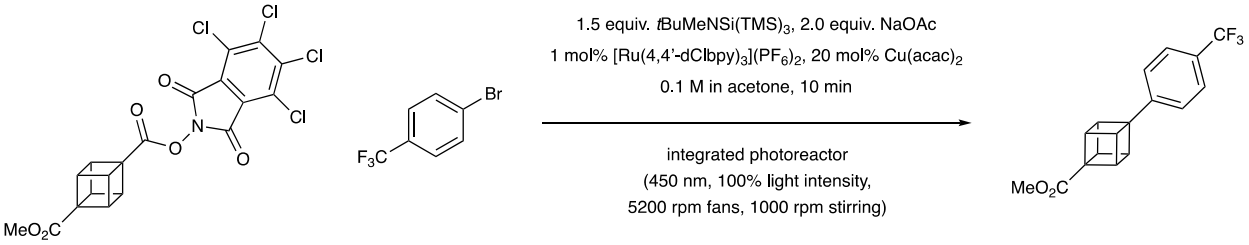

S6, 0.05 mmol **equiv.** **40**

Entry	**Amount of the aryl bromide**	**S6**	Cubane–CO_2H	Cubane–H	4-(CF_3)Ph–Br	4-(CF_3)Ph–H	(4-(CF_3)Ph)$_2$	Yield of the desired product
1	1	0%	7%	4%	16%	12%	6%	30%
2	1.5	0%	4%	2%	48%	16%	9%	39%
3	2	0%	5%	2%	90%	19%	11%	41%
4	2.5	0%	6%	2%	138%	20%	17%	42%
5	3	0%	5%	2%	181%	21%	12%	46%
6	5	0%	9%	2%	391%	26%	16%	48%

Figure S25 | Screening of the amount of the aryl bromide.

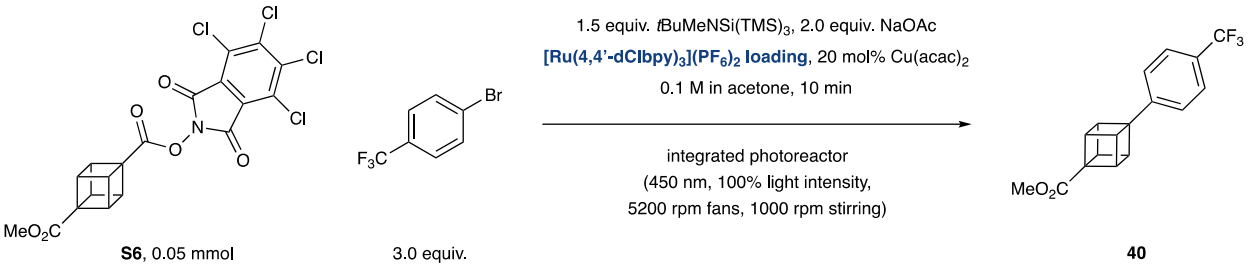

Entry	Photocatalyst loading	S6	Cubane–CO_2H	Cubane–H	4-(CF_3)Ph–Br	4-(CF_3)Ph–H	(4-CF_3)Ph)$_2$	Yield of the desired product
1	0.05 mol%	9%	9%	4%	196%	12%	15%	21%
2	0.1 mol%	0%	6%	4%	176%	16%	14%	41%
3	0.3 mol%	0%	6%	2%	164%	19%	11%	49%
4	0.6 mol%	0%	6%	2%	164%	19%	12%	45%
5	1 mol%	0%	8%	2%	166%	21%	12%	43%

Figure S26 | Screening of the photocatalyst loading.

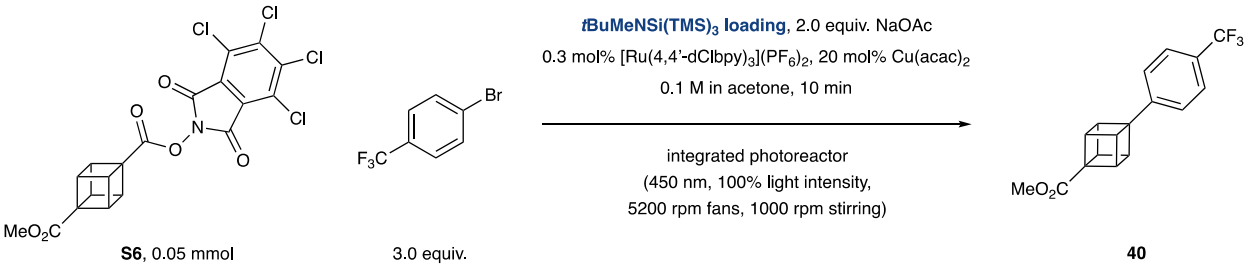

Entry	Silane loading	S6	Cubane–CO_2H	Cubane–H	4-(CF_3)Ph–Br	4-(CF_3)Ph–H	(4-CF_3)Ph)$_2$	Yield of the desired product
1	1.3 equiv.	0%	4%	2%	176%	29%	12%	43%
2	1.4 equiv.	0%	3%	2%	171%	31%	13%	46%
3	1.5 equiv.	0%	2%	2%	168%	35%	12%	48%
4	1.6 equiv.	0%	2%	2%	150%	38%	12%	48%
5	1.7 equiv.	0%	2%	2%	148%	40%	12%	49%
6	1.8 equiv.	0%	2%	2%	142%	44%	12%	50%
7	1.9 equiv.	0%	2%	2%	159%	41%	13%	50%
8	2.0 equiv.	0%	2%	2%	141%	42%	13%	50%

Figure S27 | Screening of the aminosilane loading.

Comments

1) The purity of the aminosilane reagent has no measurable influence on the yield of the reaction (Fig. S21). However, its purity needs to be considered when calculating the amount.

2) The respective redox-active esters (**30** and **S6**) perform similar when using the same photocatalyst (Figs. S22, 23, compare e.g., both entries 1 and 3). However, the tetrahydrophthalimid-derived redox-active ester (**30**) fails to provide any product (**40**) when using more oxidizing photocatalysts such as $[Ir(dFCF_3ppy)_2(4,4'\text{-}d(CF_3)bpy]PF_6$ or $[Ru(4,4'\text{-}dClbpy)_3](PF_6)_2$ (Fig. S22, entries 7, 9). At the same time, these two photocatalyst perform best for the tetrachlorophthalimid-derived redox-active ester (**S6**, Fig. S23, entries 8, 11). The former observation makes sense given that both photocatalysts should not be able to reduce the tetrahydroredox-active ester (**30**) to ultimately form the cubyl radical. The tetrachlorophthalimid-derived redox-active ester **S6** is more easily reducible and as such both catalysts are just about still competent in converting it to the cubyl radical. We further believe that a slow photoredox catalytic cycle is required. A rapid photoredox catalytic cycle might generate an excess of the cubyl radical which might saturate the copper catalyst thus preventing it from engaging in trapping of the more slowly generated aryl radical. This assumption is corroborated by the larger amounts of hydrodecarboxylated cubanes formed when using more reducing photocatalysts (Fig. S23, see e.g., entries 3, 4). Alternatively, it is possible that less reducing photocatalysts have a lower tendency to engage in an undesired redox process with the copper cocatalyst, which might ultimately lead to cubane decomposition. In either case, an even more oxidizing photocatalyst such as $[Ir(dFCF_3ppy)_2(4,4'\text{-}d(CF_3)bpy]PF_6$ (Fig. S23, entry 9) may render reduction of even the tetrachlorophthalimid-derived redox-active ester **S6** inefficient thus explaining its lower yield.
3) A copper catalyst loading of 20 mol% was found to be ideal (Fig. S24). We believe that a lower catalyst loading is detrimental to the reaction outcome since the radical trapping rate is too low whereas a higher catalyst loading will lead to cubane decomposition.
4) A higher loading of the aryl bromide was beneficial presumably as it benefits bromide abstraction over the undesired addition of the silyl radical into the redox-active ester (Fig. S25).
5) A lower catalyst loading of the photocatalyst leads to a higher yield presumably as it reduces the rate of the photoredox catalytic cycle (Fig. S26, vide supra). Similarly, an undesired interaction between photocatalyst and copper catalyst may offer an alternative explanation.
6) The loading of the aminosilane had a small effect on the yield but 1.8 equiv. was found to be more reproducible than 1.5 equiv (Fig. S27).
7) Under the optimized conditions we can identify the protodecarboxylated cubane (2% yield) and the free acid (2% yield) as cubane-derived side products in addition to the desired product (50% yield). Furthermore, we observe 142% of remaining aryl bromide, 44% of a protodehalogenated byproduct and 12% of a biaryl resulting from homocoupling of the aryl bromide. The crude NMR spectrum contains several weakly intensive peaks in the alkene region, which we assume to be indicative for minimal cubane decomposition under the reaction conditions (<1%). The crude NMR spectrum does not contain other major cubane-derived side products (Fig. S28). Hence, we believe that the majority of the remaining balance of cubane-derived products (45%) is taken up by the formation of copper-cubane dimers and resulting decomposition products. Such complexes would not undergo cross-coupling and lead to a dead-end in the catalytic cycle.

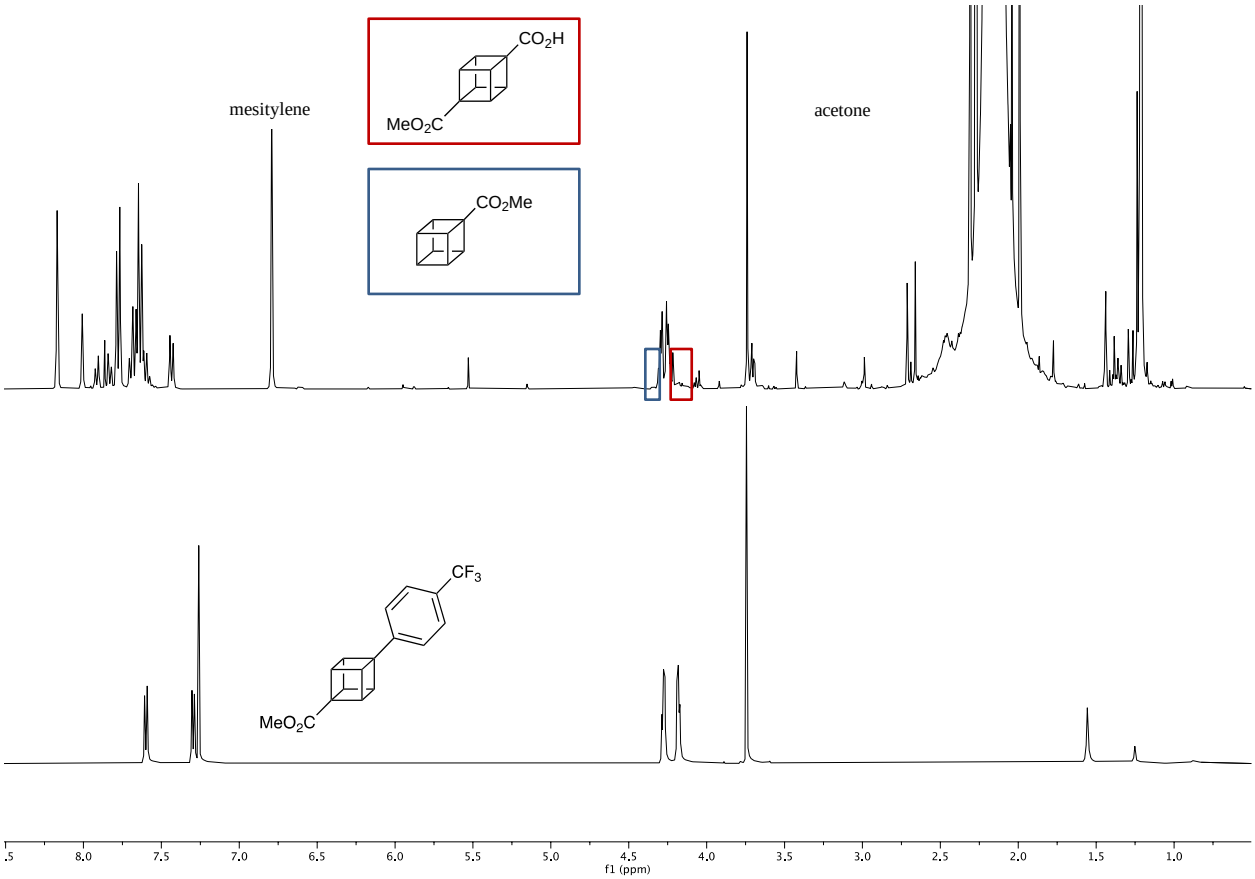

Figure S28 | Crude ^{1}H NMR spectrum of the arylation reaction mixture.

8) Additionally, we have evaluated the identity of the solvent (only acetone works, traces of product in acetonitrile), base (acetate bases are best but the counterions have a small effect), concentration (0.1 M and 0.2 M gave similar yields; both lower and higher concentrations gave a lower yield), and copper catalyst (several copper catalyst including $Cu(MeCN)_4PF_6$ all gave similar yields) but were unable to further optimize the yield.
9) We have evaluated the light intensity under the standard conditions and observed little influence between 30% and 100% light intensity on a 0.05 mmol scale but observed a sharp drop-off below that value. Upon scale-up, all reactions were run in an 8 mL vial using a multivial holder. Lower yields were observed when using in single vial holders for both 8 mL and 40 mL vials. This effect is likely a result of an increased light intensity. We strongly recommend using a light setup which guarantees a high light intensity such as the PennPhD photoreactor as the reaction has been optimized with this setup. We further recommend screening the light intensity when using a different light setup.

Synthesis of the heteroaryl bromide S7

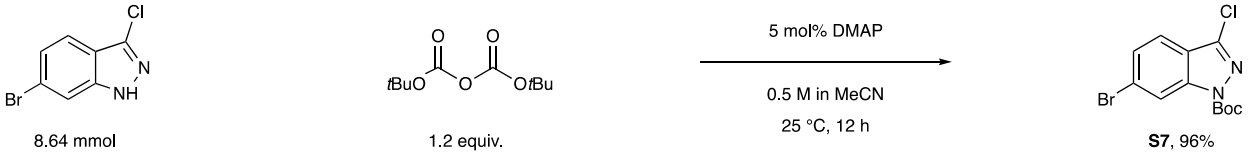

The reaction was conducted according to a modified literature procedure[57].

Boc_2O (2.38 mL, 2.26 g, 10.4 mmol, 1.2 equiv.) was added portion wise to a stirred solution of 1*H*-indazole (2 g, 8.64 mmol, 1.0 equiv.) and DMAP (52.8 mg, 0.432 mmol, 5 mol%) in MeCN (17.3 mL, 0.5 M) at room temperature leading to gas formation. After stirring for 16 h at room temperature, the solvent was evaporated under reduced pressure and the residue was partitioned between Et_2O (100 mL) and H_2O (100 mL). The aqueous phase was extracted with Et_2O (3 x 100 mL). The organic layer was washed with a saturated aqueous $NaHCO_3$ solution (100 mL) and brine (100 mL) before being dried over anhydrous Na_2SO_4. After filtration, the solvent was evaporated, and the crude product was purified by column chromatography (hexane/ EtOAc) to give the desired product as white solid. Yield: 2.75 g, 8.31 mmol, 96%.

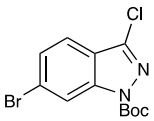

S7, ^1H NMR (500 MHz, $CDCl_3$) δ 8.40 (s, 1H), 7.55 (d, *J* = 8.5 Hz, 1H), 7.49 (dd, *J* = 8.5, 1.6 Hz, 1H), 1.71 (s, 9H); ^{13}C NMR (126 MHz, $CDCl_3$) δ 148.32, 141.38, 140.95, 128.08, 125.15, 122.48, 121.08, 118.25, 86.26, 28.20. ESI-MS: calculated $[C_{12}H_{12}{}^{79}BrClN_2O_2+Na]^+$: 354.9643, found: 354.9646. IR ν = 2983.9, 1770.4, 1744.8, 1606.8, 1571.8, 1476.2, 1397.5, 1368.6, 1330.6, 1304.4, 1222.8, 1152.5, 1070.6, 984.9, 846.5, 807.9, 780.0, 752.8, 623.1, 583.7, 459.7.

Arene scope

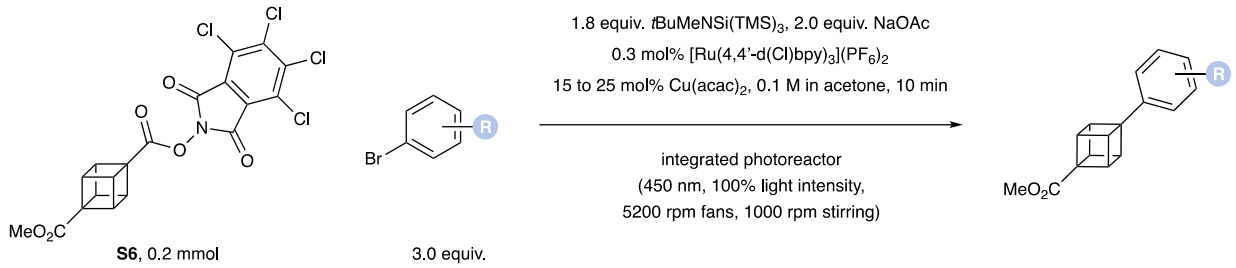

GP 7: The silane **32** (133.5 mg, 90% pure, 0.38 mmol, 1.8 equiv.), and subsequently the cubane redox-active ester **S6** (97.8 mg, 0.2 mmol, 1.0 equiv.), NaOAc (32.8 mg, 0.4 mmol, 2.0 equiv.), the copper catalyst (indicated amount), and the substrate (3.0 equiv., if solid) were added to an oven-dried 8 mL vial equipped with a stir bar. The vial was degassed for 5 min before a 0.3 mM stock solution of $[Ru(4,4'\text{-}dClbpy)_3](PF_6)_2$ in degassed acetone (2.0 mL, 0.6 µmol, 0.3 mol%, 0.1 M, for aromatic bromides,) or degassed acetone (2.0 mL, 0.1 M for heteroaromatic bromides) was added followed by the substrate (3.0 equiv., if liquid). Unless otherwise noted, two identical reactions were run in parallel, and placed inside the integrated photoreactor (450 nm, 100% light intensity, 5200 rpm fans, 1000 rpm stirring, multi-vial holder, 10 min). Both vials were combined and 40% KF on alumina (581 mg, 4 mmol) and tetra *n*-propylammonium bromide (266 mg, 1.00 mmol) were added and the suspension was stirred for 4–16 h. The suspension was filtered over celite (eluent: EtOAc), concentrated, and purified by automatic column chromatography using a 40 g Isco RediSep Rf gold column (eluent: gradient from 0 to 100% EtOAc in hexane).

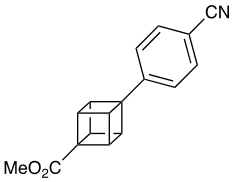

39, 47% yield, white solid. 15 mol% $Cu(acac)_2$ was used. No workup was conducted. Ca. 1% of a ring-opened isomeric product were inseparable from the reaction product. ^{1}H NMR (500 MHz, $CDCl_3$) δ 7.63 (d, *J* = 8.0 Hz, 2H), 7.28 (d, *J* = 8.0 Hz, 2H), 4.28 (dd, *J* = 5.7, 4.0 Hz, 3H), 4.18 (t, *J* = 4.9 Hz, 3H), 3.74 (s, 3H); ^{13}C NMR (126 MHz, $CDCl_3$) δ 172.44, 147.49, 132.49, 125.74, 119.23, 109.85, 60.03, 56.58, 51.80, 48.93, 46.30. ESI-MS: calculated $[C_{17}H_{13}NO_2+Na]^+$: 286.0838, found: 286.0839. IR ν = 2989.1, 2948.2, 2223.4, 1719.2, 1602.0, 1426.1, 1316.3, 1211.1, 1162.6, 1082.0, 857.9, 842.8, 552.9.

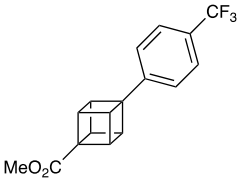

40, 46% yield, white solid. 20 mol% $Cu(acac)_2$ was used. The reaction was run on a 0.4 mmol scale. Two subsequent chromatographic separations were required to yield a pure product. ^{1}H NMR (500 MHz, $CDCl_3$) δ 7.60 (d, *J* = 8.0 Hz, 2H), 7.30 (d, *J* = 8.0 Hz, 2H), 4.28 (dd, *J* = 5.7, 4.1 Hz, 3H), 4.18 (dd, *J* = 5.7, 4.2 Hz, 3H), 3.74 (s, 3H); ^{13}C NMR (126 MHz, $CDCl_3$) δ 172.63, 146.10, 128.42 (q, *J* = 32.3 Hz), 124.49 (q, *J* = 272.2 Hz), 125.57 (q, *J* = 3.8 Hz), 125.28, 59.93, 56.59, 51.79, 48.88, 46.28; ^{19}F NMR (376 MHz, $CDCl_3$) δ −62.30. ESI-MS: calculated $[C_{17}H_{13}F_3O_2+H]^+$: 307.0940, found: 307.0947. IR ν = 2986.6, 2923.9, 1727.0, 1611.2, 1438.1, 1318.1, 1212.8, 1153.4, 1115.1, 1092.0, 1066.9, 1012.6, 823.4, 673.5, 595.7.

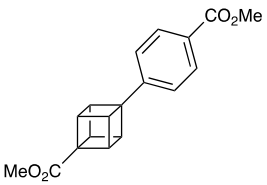

41, 48% yield, white solid. 15 mol% $Cu(acac)_2$ was used. ^1H NMR (500 MHz, $CDCl_3$) δ 8.02 (dt, *J* = 8.2, 2.0 Hz, 2H), 7.26–7.22 (m, 2H), 4.36–4.23 (m, 3H), 4.23–4.09 (m, 3H), 3.91 (s, 3H), 3.74 (s, 3H); ^{13}C NMR (126 MHz, $CDCl_3$) δ 172.68, 167.16, 147.40, 129.99, 128.00, 124.92, 60.20, 56.55, 52.20, 51.77, 48.96, 46.30. ESI-MS: calculated $[C_{18}H_{16}O_4+H]^+$: 297.1121, found: 297.1124. IR ν = 2951.8, 1708.8, 1603.3, 1431.7, 1317.6, 1277.0, 1217.3, 1086.7, 821.8, 763.1, 704.0.

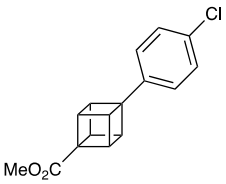

42, 46% yield, white solid. 20 mol% $Cu(acac)_2$ was used. The reaction was run on a 0.4 mmol scale. 0.5 mol% of $[Ru(4,4'\text{-}dClbpy)_3](PF_6)_2$ was used. The product was washed with small amounts of pentane after column chromatography to completely remove residual silane. ^1H NMR (400 MHz, $CDCl_3$) δ 7.37–7.27 (m, 2H), 7.17–7.08 (m, 2H), 4.25 (dd, *J* = 5.7, 4.1 Hz, 3H), 4.18–3.94 (m, 3H), 3.74 (s, 3H); ^{13}C NMR (101 MHz, $CDCl_3$) δ 172.58, 140.57, 131.80, 128.60, 126.25, 59.71, 56.48, 51.59, 48.74, 46.03. ESI-MS: calculated $[C_{16}H_{13}ClO_2+H]^+$: 273.0677, found: 273.0681. IR ν = 2998.8, 2984.2, 2967.2, 1729.9, 1492.3, 1439.1, 1321.3, 1215.0, 1089.3, 1009.8, 840.3, 814.4, 709.7.

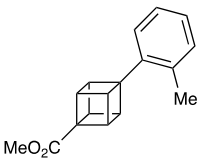

43, 41% yield, white solid. 25 mol% $Cu(acac)_2$ was used. The reaction was run 8 times on a 0.05 mmol scale at a 0.4 M concentration. The product was isolated alongside 0.11 equiv. of a ring-opened bisalkene-containing isomer of the desired product. The isomeric mixture was dissolved in CD_2Cl_2 (1 mL), *m*CPBA (9.8 mg, 56.7 μmol, 3.0 equiv. of the bisalkene isomer, 1.5 equiv. per alkene) was added, and the mixture was stirred for 3 h at room temperature before being repurified by column chromatography. ^1H NMR (500 MHz, $CDCl_3$) δ 7.21–7.11 (m, 3H), 7.09–7.04 (m, 1H), 4.26 (s, 6H), 3.74 (s, 3H), 2.28 (s, 3H); ^{13}C NMR (126 MHz, $CDCl_3$) δ 173.00, 138.90, 136.62, 130.55, 126.74, 125.68, 125.36, 61.68, 55.36, 51.74, 47.90, 45.86, 29.85. EI-MS: calculated $[C_{17}H_{16}O_2]^+$ 252.1145, found: 252.1156. IR ν = 2986, 1725, 1487, 1434, 1315, 1259, 1214, 1162, 1088, 906, 845, 752, 723, 453.

Heteroarene scope

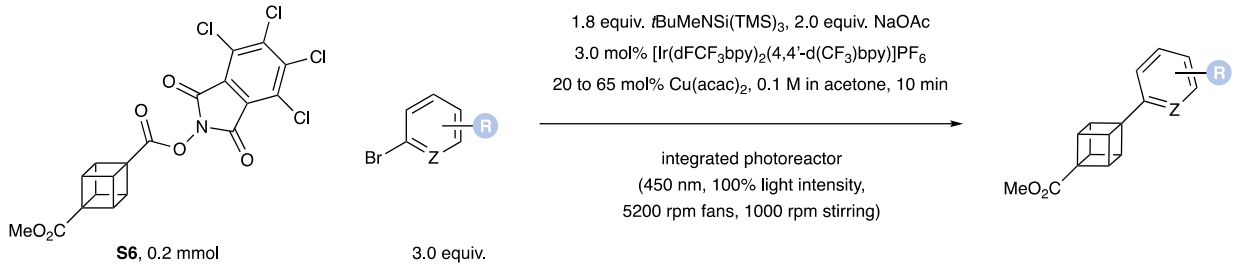

GP 8: The silane **32** (133.5 mg, 90% pure, 0.38 mmol, 1.8 equiv.), and subsequently the cubane redox-active ester **S6** (97.8 mg, 0.2 mmol, 1.0 equiv.), NaOAc (32.8 mg, 0.4 mmol, 2.0 equiv.), the copper catalyst (indicated amount), the substrate (3.0 equiv., if solid), and $[Ir(dFCF_3ppy)_2(4,4'\text{-}d(CF_3)bpy]PF_6$ (6.8 mg, 3 mol%) were added to an oven-dried 8 mL vial equipped with a stir bar. The vial was degassed for 5 min before degassed acetone (2 mL, 0.1 M) was added followed by the substrate (3.0 equiv., if liquid). Unless otherwise noted, two identical reactions were run in parallel, and placed inside the integrated photoreactor (450 nm, 100% light intensity, 5200 rpm fans, 1000 rpm stirring, multi-vial holder). Both vials were combined and purified by automatic column chromatography using a 40 g Isco RediSep Rf gold column as indicated.

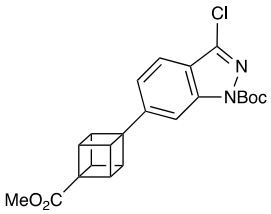

44, 46% yield, white solid. 30 mol% $Cu(acac)_2$ was used. The reaction was run 8 times on a 0.05 mmol scale. All reactions were combined, methanol (1.6 mL) was added, and the mixture was stirred for 2 h before it was purified by column chromatography (toluene/ acetone). ^{1}H NMR (500 MHz, $CDCl_3$) δ 7.95 (s, 1H), 7.66 (d, *J* = 8.3 Hz, 1H), 7.24 (dd, *J* = 8.2, 1.3 Hz, 1H), 4.35–4.26 (m, 3H), 4.23 (dd, *J* = 5.7, 4.0 Hz, 3H), 3.75 (s, 3H), 1.72 (s, 9H); ^{13}C NMR (126 MHz, $CDCl_3$) δ 172.65, 148.84, 145.25, 141.32, 141.10, 121.97, 121.89, 120.25, 111.00, 85.61, 60.71, 56.58, 51.80, 49.12, 46.27, 28.26. ESI-MS: calculated $[C_{22}H_{21}ClN_2O_4+Na]^+$: 435.1082, found: 435.1087. IR ν = 2974.3, 1720.8, 1614.1, 1473.7, 1387.1, 1315.7, 1321.28, 1207.5, 1148.6, 1055.8, 841.4, 753.0.

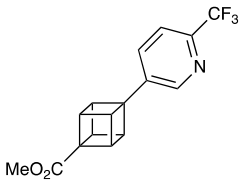

45, 48% yield, off-white solid. 20 mol% $Cu(acac)_2$ was used. 2.5 mol% of $[Ir(dFCF_3ppy)_2(4,4'\text{-}d(CF_3)bpy]PF_6$ were used. The crude product was dry-loaded onto silica gel prior to chromatographic separation to avoid coelution with an unidentified impurity. ^{1}H NMR (400 MHz, $CDCl_3$) δ 8.56 (d, *J* = 1.6 Hz, 1H), 7.65 (d, *J* = 1.4 Hz, 2H), 4.32 (dq, *J* = 4.2, 3.2 Hz, 3H), 4.25 (dq, *J* = 4.2, 3.2 Hz, 3H), 3.75 (s, 3H); ^{13}C NMR (101 MHz, $CDCl_3$) δ 172.26, 147.26, 146.10 (q, *J* = 34.7 Hz), 140.62, 133.73, 121.81 (q, *J* = 273.8 Hz), 120.31 (q, *J* = 2.8 Hz), 57.81, 56.62, 51.82, 48.78, 46.54. ESI-MS: calculated $[C_{16}H_{12}F_3NO_2+H]^+$: 308.0893, found: 308.0901. IR ν = 2954.2, 1711.5, 1313.8, 1132.0, 1083.7, 840.6, 690.4.

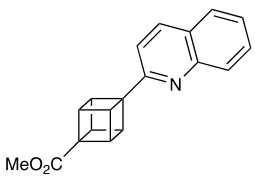

46, 47% yield, off-white solid. 65 mol% $Cu(acac)_2$ was used. The crude product was dry-loaded onto silica gel and purified by column chromatography with toluene/ acetone. ^{1}H NMR (500 MHz, d_6-acetone) δ 8.30 (d, *J* = 8.4 Hz, 1H), 8.00 (d, *J* = 8.5 Hz, 1H), 7.91 (dd, *J* = 8.3, 1.5 Hz, 1H), 7.73 (ddd, *J* = 8.4, 6.9, 1.5 Hz, 1H), 7.54 (ddd, *J* = 8.1, 6.8, 1.2 Hz, 1H),

7.48 (d, *J* = 8.5 Hz, 1H), 4.38 (dd, *J* = 5.6, 4.1 Hz, 3H), 4.35–4.19 (m, 3H), 3.70 (s, 3H); ^{13}C NMR (126 MHz, d_6-acetone) δ 172.37, 161.92, 149.02, 137.33, 130.26, 129.84, 128.73, 127.73, 126.72, 119.20, 62.38, 57.36, 51.63, 48.99, 47.18. ESI-MS: calculated $[C_{19}H_{15}NO_2+H]^+$: 290.1176, found: 290.1180. IR ν = 2993.5, 2943.7, 1720.8, 1596.1, 1435.5, 1354.5, 1215.2, 1168.0, 1085.0, 943.6, 820.6, 753.4, 619.3, 461.9.

Comments:

1) The reaction was run twice to ensure that sufficient material was present for a reproducible isolation (>40 mg).
2) We have chosen to run the reaction in multi-vial holders since this setup in principle allows for the highest throughput (4 x 0.2 mmol in one operation). However, it is worth noting that we evaluated the scale-up to a 0.4 mmol scale, which worked well with virtually identical yields using a single-vial holder after re-optimization of photocatalyst or copper loading (see products **40** and **42**). We anticipate that this re-optimization was required to ensure proper matching of the rates of the photoredox and copper catalytic cycles.
3) Products **43** and **44** were obtained in **38**% and **39**% analytical yield, respectively when run on a 0.2 mmol scale.

7. Trifluoromethylation of a cubane

Optimization

GP 9: 4-(methoxycarbonyl)cubane-1-carboxylate (**16**, 5.1 mg, 0.025 mmol, 1.0 equiv.), bis(2,5-dimethylphenyl)(trifluoromethyl)sulfonium trifluoromethanesulfonate (indicated amount), copper catalyst (indicated amount), photocatalyst (3 mol%), and Na_2CO_3 (7.8 mg, 0.075 mmol, 3.0 equiv.) were added to an oven-dried 8 mL vial equipped with a stir bar and placed under an N_2 atmosphere. Degassed DMSO (0.25 mL, 0.1 M) was added, and the vial was placed inside the integrated photoreactor (450 nm, indicated light intensity, 5200 rpm fans, 500 rpm stirring, multi-vial holder, 8 h). 1,4-difluorobenzene (1.0 equiv.) was added and the yield was measured by ^{19}F NMR spectroscopy vs 1,4-difluorobenzene.

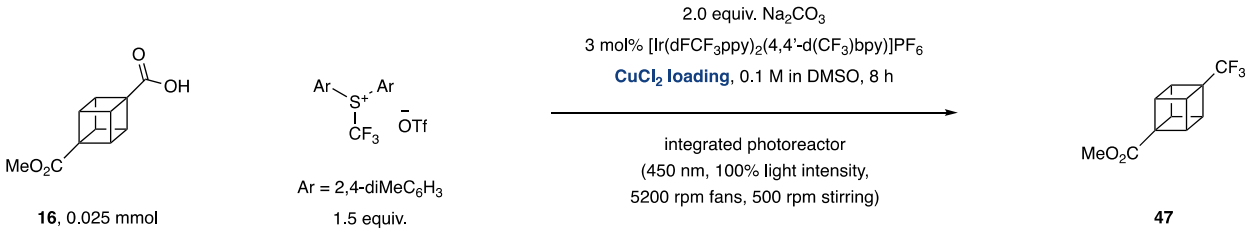

Entry	$CuCl_2$ loading	Yield of the desired product
1	5 mol%	21%
2	7.5 mol%	33%
3	10 mol%	40%
4	12.5 mol%	41%
5	15 mol%	25%
6	20 mol%	25%
7	25 mol%	23%

Figure S29 | Screening of the copper loading.

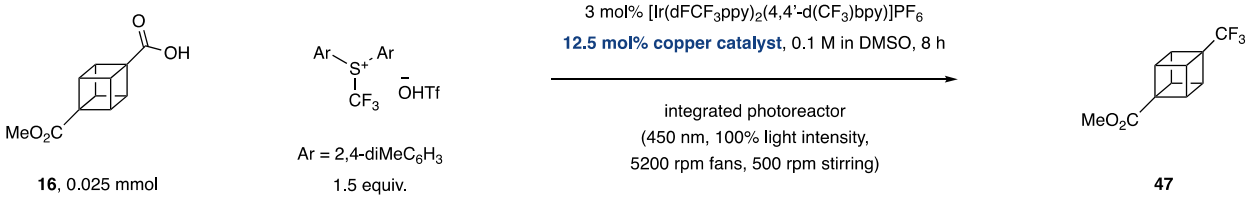

Entry	Copper catalyst	Yield of the desired product
1	$CuCl_2$	41%
2	$Cu(OAc)_2$	26%
3	CuCl	39%
4	CuBr	33%
5	CuI	26%
6	CuCN	31%
7	CuTc	43%
8	CuCN	23%
9	CuTc	9%

Figure S30 | Screening of the copper catalyst.

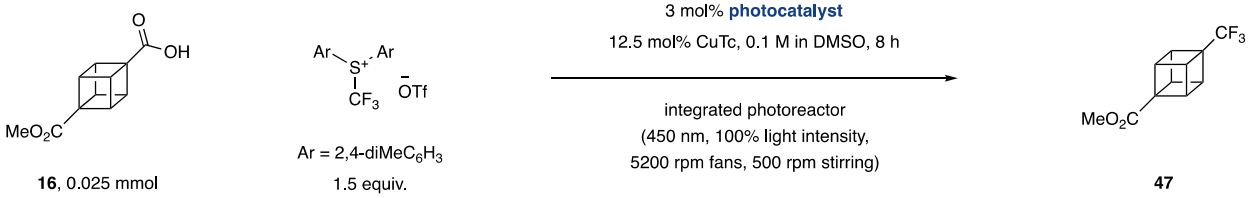

Entry	Photocatalyst	Yield of the desired product
1	4-CzIPN	3%
2	9-Mesityl-10-methylacridinium BF_4	5%
3	$[Ru(bpy)_3](PF_6)_2$	trace%
4	$[Ru(bpz)_3](PF_6)_2$	5%
5	$[Ir(dFCF_3ppy)_2(phen)]PF_6$	30%
6	$[Ir(dFCF_3ppy)_2(5,5'\text{-}d(CF_3)bpy)]PF_6$	45%
7	$[Ir(dFOMeppy)_2(5,5'\text{-}d(CF_3)bpy)]PF_6$	33%
8	$[Ir(dFCF_3ppy)_2(4,4'\text{-}d(CF_3)bpy)]PF_6$	41%
9	$[Ir(dFMeppy)_2(4,4'\text{-}d(CF_3)bpy)]PF_6$	34%
10	$[Ir(dFCF_3ppy)_2(dtbbpy)]PF_6$	33%
11	$[Ir(dFFppy)_2(dtbbpy)]PF_6$	23%

Figure S31 | Screening of the photocatalyst.

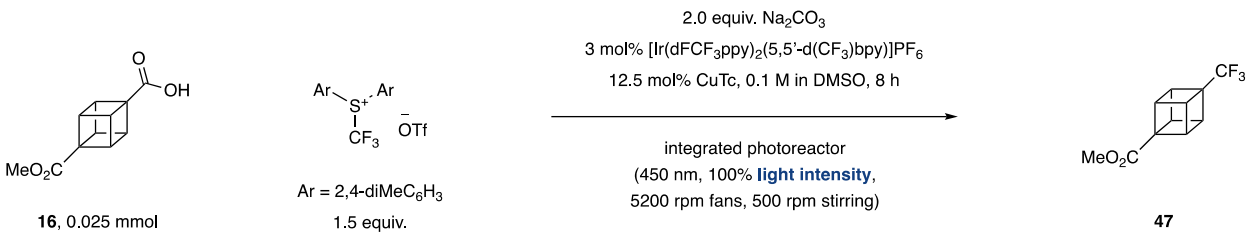

Entry	Light intensity	Yield of the desired product
1	100%	41%
2	75%	45%
3	50%	49%
4	40%	49%
5	30%	46%

Figure S32 | Screening of the light intensity.

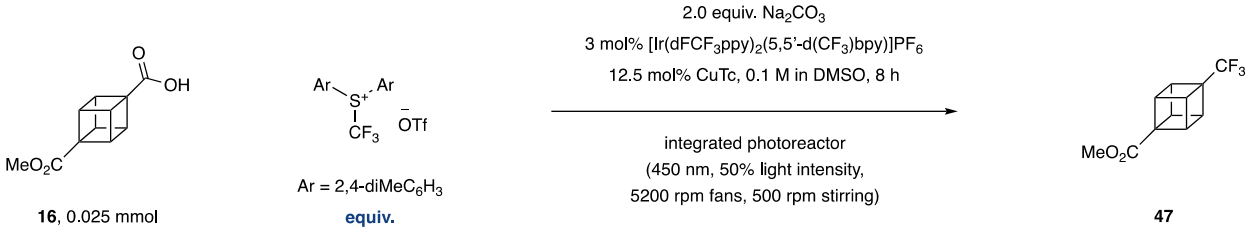

Entry	Amount of the sulfonium salt	Yield of the desired product
1	1 equiv.	42%
2	1.5 equiv.	49%
3	1 + 1 + 1 equiv.	52%
4	3 equiv.	17%
5	5 equiv.	19%
6	10 equiv.	10%

Figure S33 | Screening of the amount of the sulfonium salt.

Comments:

1) The influence of the light intensity on the reaction has been evaluated and a wide plateau between 30% and 100% was discovered when using the PennPhD photoreactor (Fig. S32). It is likely that other light sources with lower light intensity will lead to lower yields.
2) Under the optimized conditions we can identify the protodecarboxylated cubane (2% yield) as the major side product in addition to the desired product (49% yield). The crude NMR spectrum does not contain other major side products except for the expected degradation product the trifluoromethylation reagent (Fig. S34). As with the preceding reactions we

believe that the majority of the remaining balance of cubane-derived products (49%) is taken up by the formation of copper-cubane dimers and resulting decomposition products. Such complexes would not undergo cross-coupling and lead to a dead-end in the catalytic cycle.

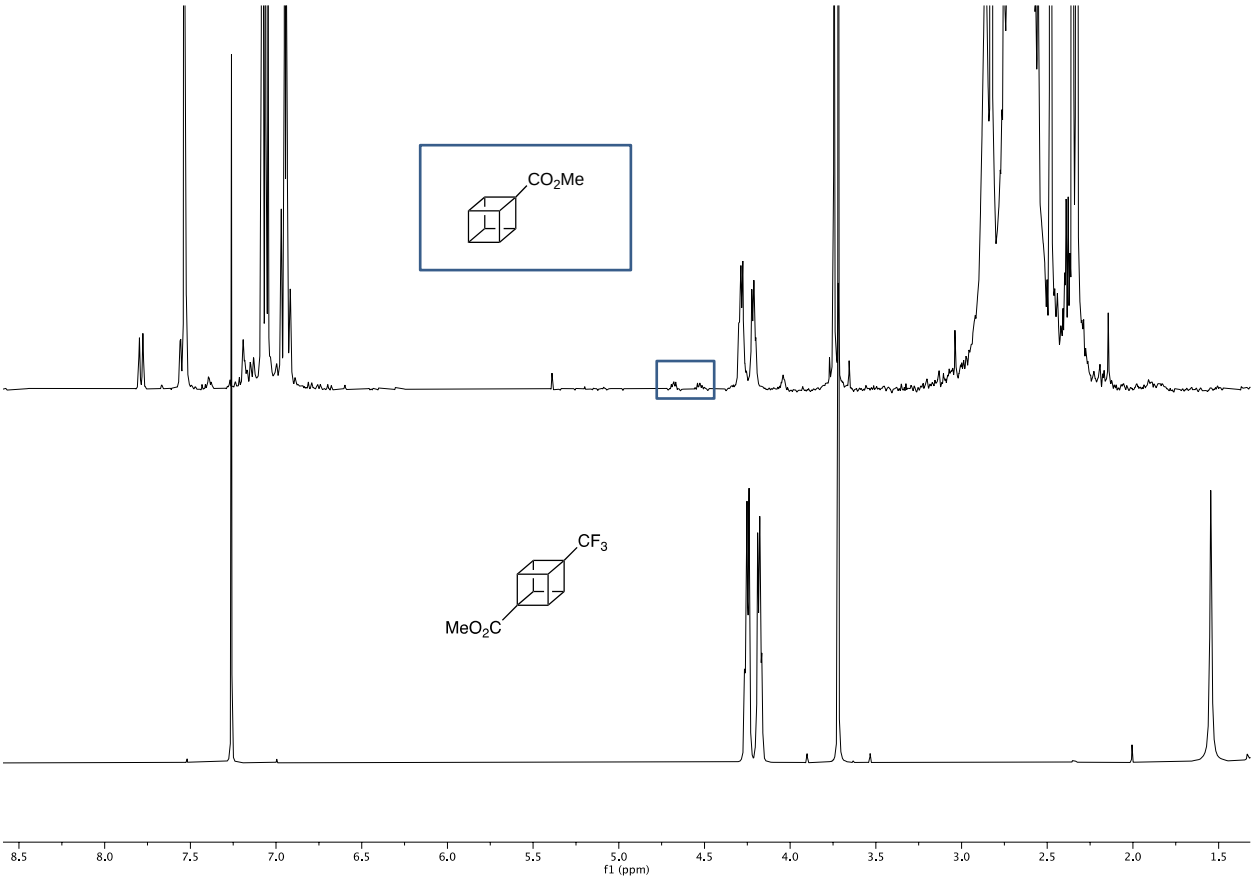

Figure S34 | Crude ^{1}H NMR spectrum of the trifluoromethylation reaction mixture.

Optimized procedure

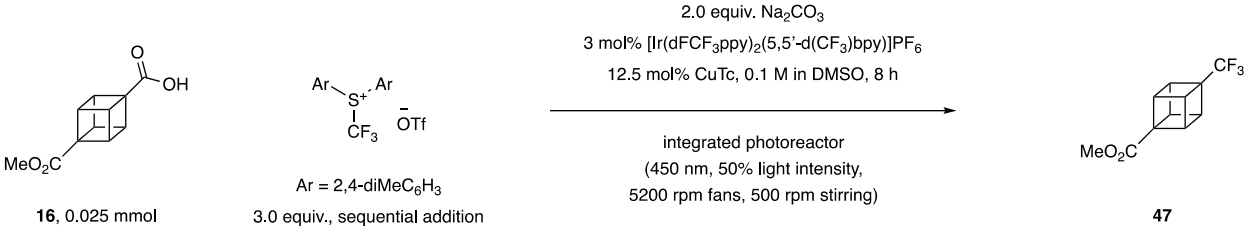

4-(methoxycarbonyl)cubane-1-carboxylate (**16**, 10.3 mg, 0.05 mmol, 1.0 equiv.), bis(2,5-dimethylphenyl)(trifluoromethyl)sulfonium trifluoromethanesulfonate (23.0 mg, 0.05 mmol, 1.0 equiv.), Copper(I) thiophene-2-carboxylate (1.2 mg, 12.5 mol%), $[Ir(dFCF_3ppy)_2(5,5'\text{-}d(CF_3)bpy)]PF_6$ (1.7 mg, 3 mol%) and Na_2CO_3 (15.6 mg, 0.15 mmol, 3.0 equiv.) were added to an oven-dried 8 mL vial equipped with a stir bar and placed under an N_2 atmosphere. Degassed DMSO (0.5 mL, 0.1 M) was added, and the vial was placed inside the integrated photoreactor (450 nm, 50% light intensity, 5200 rpm fans, 500 rpm stirring, multi-vial holder, 4 h). After 1 h and again after 2 h, additional bis(2,5-dimethylphenyl)(trifluoromethyl)sulfonium trifluoromethanesulfonate (23.0 mg, 0.05 mmol, 1.0 equiv.) in degassed DMSO (0.5 mL) were added and the irradiation was continued. The reaction was run 4 times on a 0.05 mmol scale and an average ^{19}F NMR yield was measured vs 1,4-difluorobenzene. In order to provide characterization data and verify product formation, the combined reaction mixtures were purified by automatic column chromatography using a 24 g Isco RediSep Rf gold column (eluent: gradient from 0 to 50% Et_2O in hexane) to afford a yellow, volatile solid.

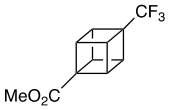

47, 49% yield, yellow solid. ^1H NMR (500 MHz, $CDCl_3$) δ 4.35–4.21 (m, 3H), 4.18 (t, J = 5.1 Hz, 3H), 3.72 (s, 3H); ^{13}C NMR (126 MHz, $CDCl_3$) δ 171.70, 125.03 (q, J = 272.5 Hz), 56.39, 54.52 (q, J = 36.2 Hz), 51.87, 46.74, 43.89 (q, J = 4.4 Hz); ^{19}F NMR (376 MHz, CDCl3) δ −77.57. EI-MS: calculated $[C_{11}H_9F_3O_2]^+$: 230.0549, found: 230.0543. IR ν = 2999, 2355, 1728, 1379, 1225, 1176, 1058.

8. Cross-coupling of new cubane isomers

Synthesis of 3-methoxycarbonylcubanecarboxylic acid (54)

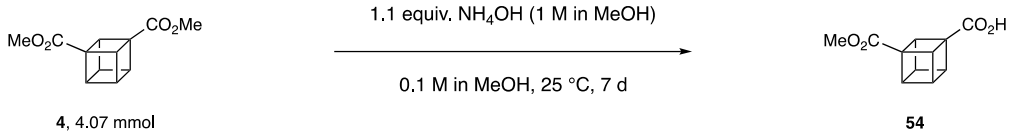

4, 4.07 mmol

54

A 1 M solution of ammonium hydroxide in methanol (4.48 mL, 4.48 mmol, 1.1 equiv.) was added dropwise over 5 min to a solution of the diester **4** (896 mg, 4.07 mmol, 1.0 equiv.) in dry MeOH (40 mL) at 0 °C under an N_2 atmosphere. The mixture was stirred at 0 °C for 3 h before being allowed to warm up to room temperature. Following stirring at that temperature for 7 d, the solution was diluted with H_2O (ca. 100 mL). NaCl (3 g) was added, and the solution was neutralized with 1 M $KHSO_4$ (5 mL) and immediately extracted with EtOAc (8 x 70 mL). The combined organic extracts were concentrated using a rotary evaporator before being purified by column chromatography (CH_2Cl_2 to 0.25% $MeCO_2H$ in 90:10 CH_2Cl_2/MeOH). Yield: 588.1 mg, 2.85 mmol, 70%.

54, ^{1}H NMR (500 MHz, d_6-acetone) δ 4.39 (dt, *J* = 4.8, 2.4 Hz, 2H), 4.27–4.16 (m, 2H), 3.99 (q, *J* = 5.0 Hz, 2H), 3.66 (s, 3H); ^{13}C NMR (126 MHz, d_6-acetone) δ 171.17, 170.72, 53.33, 53.20, 50.88, 50.79, 49.75, 49.72, 42.45. ESI-MS: calculated $[C_{11}H_{10}O_4+Na]^+$: 229.0471, found: 229.0466. IR ν = 3003.1, 2988.8, 1721.3, 1670.2, 1418.8, 1301.0, 1214.8, 1129.8, 998.9, 697.5, 474.0, 440.5.

Comments:

1) A rapid workup is important since the halfester slowly hydrolyses during the workup.
2) 15% of the diacid and 11% of the diester substrate were isolated by column chromatography as well.

Synthesis of 2-methoxycarbonylcubanecarboxylic acid (S8)

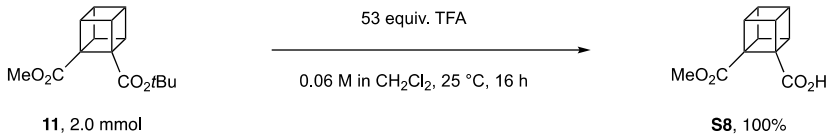

TFA (8 mL, 53 equiv.) was added dropwise to a stirring solution of 1-(*tert*-butyl) 2-methyl-cubane-1,2-dicarboxylate (**11**, 525 mg, 2.0 mmol, 1.0 equiv.) in dry CH_2Cl_2 (34 mL, 0.06 M) under an N_2 atmosphere. The resulting solution was stirred at room temperature for 16 h and then concentrated. The oil was dissolved in Et_2O (2 mL), hexane was added (7 mL), the solution was sonicated (1 min), and concentrated slowly to remove the Et_2O prior to the hexane. This procedure was repeated until a solid formed.

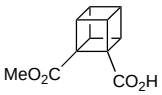

S8, 100% yield, slightly pink solid. ^{1}H NMR (500 MHz, $CDCl_3$) δ 4.29 (td, *J* = 6.1, 3.4 Hz, 4H), 4.00 (ddp, *J* = 7.2, 5.0, 2.5 Hz, 2H), 3.76 (d, *J* = 2.1 Hz, 3H); ^{13}C NMR (126 MHz, $CDCl_3$) δ 173.92, 172.22, 57.69, 57.30, 52.40, 48.11, 47.88, 45.79, 45.62. ESI-MS: calculated $[C_{11}H_{10}O_4+H]^+$: 207.0652 found: 207.0662. IR ν = 2996, 1726, 1700, 1438, 1322, 1223, 1205, 1169, 1093, 1028, 949, 677, 428.

Amination of non-linear cubane isomers

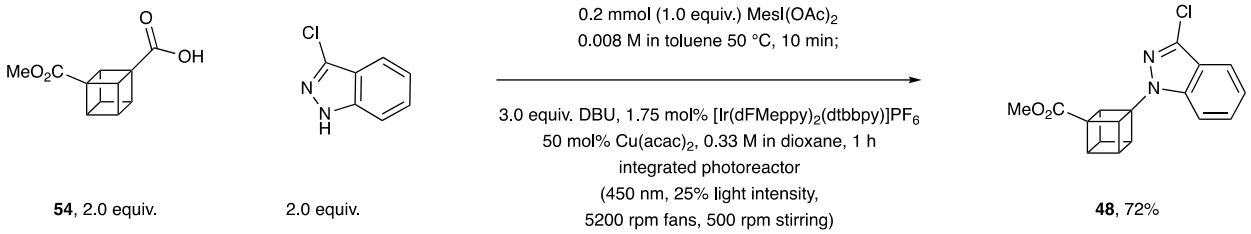

A 250 mL round-bottom flask was charged with iodomesitylene diacetate (0.146 mg, 0.4 mmol), 3-(methoxycarbonyl)cubane-1-carboxylic acid (**54**, 0.164 mg, 0.8 mmol, 2.0 equiv.), and 50 mL toluene (0.008 M). The flask was attached to a rotary evaporator with the water bath heated to 50 ºC and the solvent (and the generated acetic acid) was removed over ca. 10 min. A second 50 mL aliquot of toluene was added to the flask and the evaporation was repeated. The evaporation was repeated two more times. After further removal of residual toluene under high vacuum, hexane was added to the viscous oil and the suspension was sonicated followed by removal of the hexane to provide iodomesitylene bis(4-(methoxycarbonyl)cubane-1-carboxylate) as a solid, which can be directly used in the following amination reactions.

Iodomesitylene bis(3-(methoxycarbonyl)cubane-1-carboxylate) (131.3 mg, 0.2 mmol, 1.0 equiv.), 3-chloroindazole (0.4 mmol, 2.0 equiv.), $Cu(acac)_2$ (26.2 mg, 0.1 mmol, 50 mol%), and $[Ir(dFMeppy)_2(dtbbpy)]PF_6$ (3.6 mg, 1.75 mol%), were added to an oven-dried 40 mL vial equipped with a stir bar and placed under an N_2 atmosphere. Degassed 1,4-dioxane (6 mL, 0.033 M) was added followed by DBU (0.09 mL, 3.0 equiv.) and the vial was placed inside the integrated photoreactor (450 nm, 25% light intensity, 1500 rpm fans, 500 rpm stirring, single-vial holder, 60 min). The reactions were concentrated and purified by automatic column chromatography using a 24 g Isco RediSep Rf gold column (eluent: gradient from 0 to 100% EtOAc in hexane).

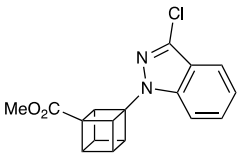

48, 72% yield, white solid. ^{1}H NMR (500 MHz, $CDCl_3$) 7.68 (dt, *J* = 8.2, 1.1 Hz, 1H), 7.50 (dd, *J* = 8.5, 1.1 Hz, 1H), 7.43 (ddd, *J* = 8.3, 6.9, 1.1 Hz, 1H), 7.26–7.21 (m, 1H), 4.84 (dt, *J* = 4.9, 2.4 Hz, 2H), 4.70 (tq, *J* = 5.3, 2.6 Hz, 1H), 4.33 (tq, *J* = 4.5, 2.1 Hz, 1H), 4.10 (q, *J* = 5.0 Hz, 2H), 3.78 (s, 3H); ^{13}C NMR (126 MHz, $CDCl_3$) δ 171.82, 139.81, 133.90, 127.75, 122.18, 121.89, 120.09, 110.63, 69.14, 55.51, 52.39, 51.96, 51.54, 50.12, 40.87. ESI-MS: calculated $[C_{17}H_{13}ClN_2O_2+H]^+$: 313.0738, found: 313.0751. IR ν = 2999, 2354, 1722, 1467, 1375, 1244, 766.

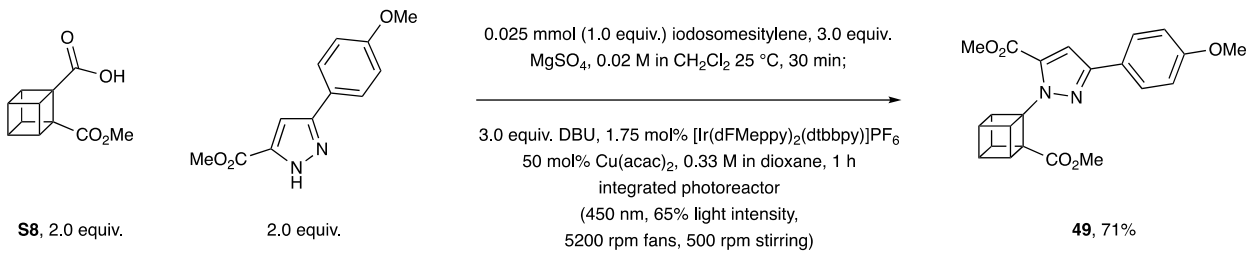

S8, 2.0 equiv. 2.0 equiv. **49**, 71%

To a 50 mL round-bottom flask was added iodosomesitylene (0.105 g, 0.4 mmol, 1.0 equiv.), 2-(methoxycarbonyl)cubane-1-carboxylic acid (**S8**, 0.164 mg, 0.8 mmol, 2.0 equiv.), and CH_2Cl_2 (4 mL, 0.1 M). The mixture was sonicated until it became homogenous, typically resulting in a slightly cloudy solution due to the liberation of water. Magnesium sulfate (0.144 g, 1.2 mmol, 3.0 equiv.) was added, and the reaction was stirred at room temperature for 30 min. The suspension was filtered, and the filtrate was concentrated in vacuo to provide iodomesitylene bis(4-(methoxycarbonyl)cubane-1-carboxylate), which can be directly used in the following amination reaction.

Iodomesitylene bis(2-(methoxycarbonyl)cubane-1-carboxylate) (16.4 mg, 0.025 mmol, 1.0 equiv.), ethyl 3-(4-methoxyphenyl)-pyrazole-5-carboxylate (12.3 mg, 0.05 mmol, 2.0 equiv.), $Cu(acac)_2$ (4.9 mg, 0.019 mmol, 75 mol%), $[Ir(dFMeppy)_2(dtbbpy)]PF_6$ (0.5 mg, 1.75 mol%), were added to an oven-dried 8 mL vial equipped with a stir bar and placed under an N_2 atmosphere. Degassed 1,4-dioxane (0.5 mL, 0.05 M) was added followed by DBU (11.2 μL, 3.0 equiv.) and the vial was placed inside the integrated photoreactor (450 nm, 65% light intensity, 1500 rpm fans, 500 rpm stirring, multi-vial holder, 60 min). The reaction was run 4 times, the reaction mixtures were combined, concentrated, and purified by reversed phase (C18) chromatography (eluent: gradient from 0 to 100% H_2O in MeCN with 0.1% NH_4OH). The compound is particularly acid-sensitive, undergoing opening of the cubane core upon exposure to acid. Thus purification under basic conditions is necessary.

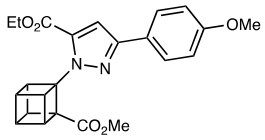

49, 71% yield, white solid. ^{1}H NMR (500 MHz, $CDCl_3$) δ 7.77 (d, *J* = 8.8 Hz, 2H), 7.14 (s, 1H), 6.94 (d, *J* = 8.8 Hz, 2H), 4.66–4.64 (m, 2H), 4.38–4.21 (m, 4H), 3.98 (dtq, *J* = 12.6, 4.9, 2.4 Hz, 2H), 3.84 (s, 3H), 3.52 (s, 3H), 1.36 (t, *J* = 7.1 Hz, 3H); ^{13}C NMR (126 MHz, $CDCl_3$) δ 170.50, 159.80, 159.68, 150.05, 134.05, 127.02, 125.52, 114.15, 108.39, 73.83, 62.30, 61.28, 55.45, 51.45, 51.40, 45.87, 45.22, 43.16, 14.45. ESI-MS: calculated $[C_{23}H_{22}N_2O_5+Na]^+$: 429.1421, found: 429.1451. IR ν = 2998, 2355, 1720, 1558, 1446, 1286, 1246, 1106, 767.

Alkylation of non-linear cubane isomers

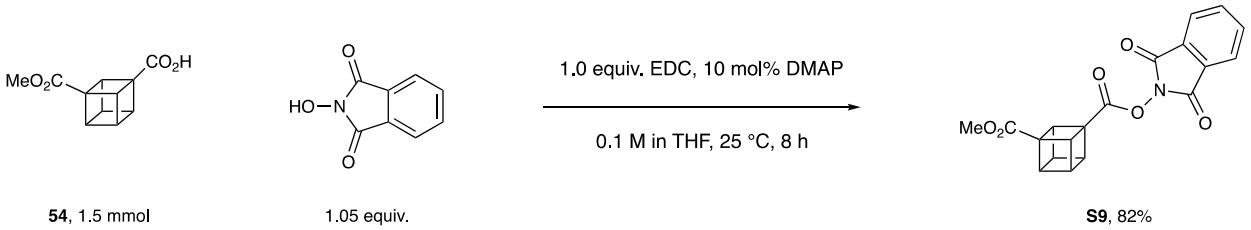

54, 1.5 mmol 1.05 equiv. **S9**, 82%

EDC (0.288 g, 1 equiv.), cubane carboxylic acid **54** (0.309 g, 1.50 mmol, 1.0 equiv.), *N*-hydroxyphthalimide (0.256 g, 1.05 equiv.), and DMAP (18.4 mg, 10 mol%) were taken up in dry THF (15 mL, 0.1 M) in a 40 mL oven-dried vial under an N_2 atmosphere at room temperature. The reaction was stirred for 8 h, before being concentrated, and purified by automatic column chromatography using a 24 g Isco RediSep Rf gold column (eluent: gradient from 0 to 10% EtOAc in CH_2Cl_2).

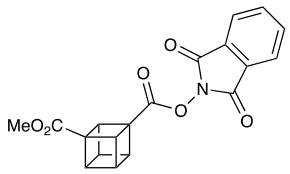

S9, 82% yield, white solid. ^{1}H NMR (500 MHz, $CDCl_3$) δ 7.90 (dd, *J* = 5.4, 3.1 Hz, 2H), 7.80 (dd, *J* = 5.5, 3.1 Hz, 2H), 4.71 (dt, *J* = 4.7, 2.4 Hz, 2H), 4.47 (dq, *J* = 5.1, 2.5 Hz, 1H), 4.26 (dq, *J* = 5.0, 2.5 Hz, 1H), 4.13 (q, *J* = 5.0 Hz, 2H), 3.74 (s, 3H); ^{13}C NMR (126 MHz, $CDCl_3$) δ 171.13, 166.74, 162.12, 134.91, 129.09, 124.12, 53.97, 51.97, 51.58, 50.72, 50.52, 49.98, 43.66. ESI-MS: calculated $[C_{19}H_{13}NO_6+Na]^+$: 374.0635, found: 374.0640. IR ν = 3003, 1777, 1742, 1468, 1436, 1361, 1330, 1292, 1218, 1186, 1157, 1067, 981, 697.

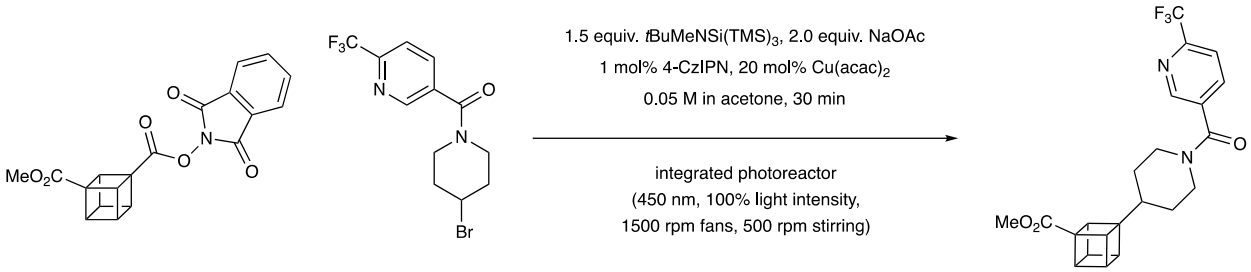

S9, 0.2 mmol 1.5 equiv. **50**, 49%

The silane **32** (110.2 mg, 90% pure, 0.3 mmol, 1.8 equiv.), the cubane redox-active ester **S9** (70.3 mg, 0.2 mmol, 1.0 equiv.), NaOAc (54.4 mg, 0.4 mmol, 2.0 equiv.), $Cu(acac)_2$ (10.5 mg, 40 µmol, 20 mol%), (4-bromopiperidin-1-yl)(6-(trifluoromethyl)pyridin-3-yl)methanone (101.1 mg, 0.3 mmol, 1.5 equiv.), and 4-CzIPN (1.6 mg, 1 mol%), were added to an oven-dried 40 mL vial equipped with a stir bar and placed under an N_2 atmosphere. Degassed acetone (4.0 mL, 0.05 M) was added, and the vial was placed inside the integrated photoreactor (450 nm, 100% light intensity, 1500 rpm fans, 500 rpm stirring, single vial holder, 30 min). The reaction was concentrated and purified by automatic column chromatography using a 24 g Isco RediSep Rf gold column (eluent: gradient from 0 to 100% EtOAc in hexane).

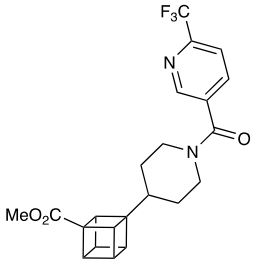

50, 49% yield, white solid.[1]H NMR (500 MHz, $CDCl_3$) δ 8.74 (s, 1H), 7.92 (dd, *J* = 7.9, 2.1 Hz, 1H), 7.74 (d, *J* = 8.0 Hz, 1H), 4.81 (d, *J* = 13.1 Hz, 1H), 4.25 (dq, *J* = 5.0, 2.5 Hz, 1H), 4.14–3.96 (m, 2H), 3.87–3.77 (m, 3H), 3.68 (s, 4H), 3.19–3.01 (m, 1H), 2.76 (t, *J* = 12.9 Hz, 1H), 1.87–1.73 (m, 2H), 1.61 (d, *J* = 13.2 Hz, 1H), 1.36–1.21 (m, 1H), 1.20–1.04 (m, 1H); ^{13}C NMR (126 MHz, $CDCl_3$) δ 172.69, 166.33, 148.88 (q, *J* = 35.1 Hz), 148.10, 136.46, 134.97, 121.28 (q, *J* = 274.4 Hz), 120.54 (d, *J* = 2.9 Hz), 59.13, 52.51, 51.67, 50.20, 48.58 (d, *J* = 5.5 Hz), 46.72, 45.19 (brd, *J* = 686.8 Hz), 41.69, 37.36, 25.61 (brd, *J* = 142.8 Hz); ^{19}F NMR (376 MHz, $CDCl_3$) δ −68.14. ESI-MS: calculated $[C_{22}H_{21}F_3N_2O_3+Na]^+$: 441.1396, found: 441.1411; IR ν = 2985, 2354, 1668, 1332, 1137, 731.

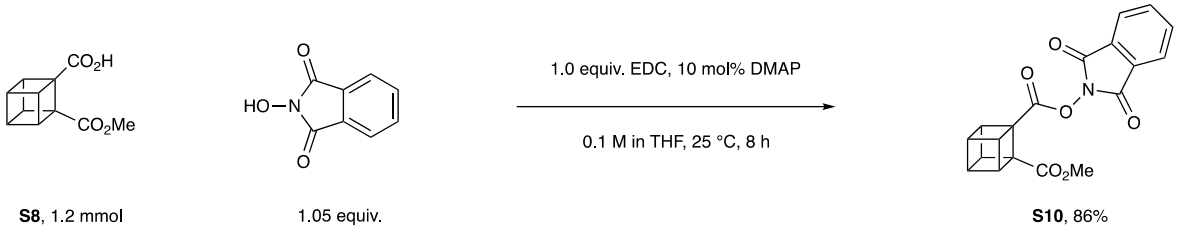

EDC (0.230 g, 1 equiv.), cubane carboxylic acid **S8** (0.247 g, 1.20 mmol, 1.0 equiv.), *N*-hydroxyphthalimide (0.205 g, 1.05 equiv.), and DMAP (14.7 mg, 10 mol%) were taken up in dry THF (12 mL, 0.1 M) in an oven-dried vial 40 mL under an N_2 atmosphere at room temperature. The reaction was stirred for 8 h, before being concentrated, and purified by automatic column chromatography using a 24 g Isco RediSep Rf gold column (eluent: gradient from 0 to 10% EtOAc in CH_2Cl_2).

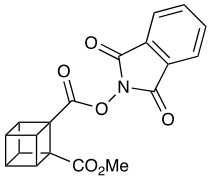

S10, 86% yield, white solid. ^{1}H NMR (500 MHz, $CDCl_3$) δ 7.88 (dd, *J* = 5.5, 3.1 Hz, 2H), 7.78 (dd, *J* = 5.5, 3.1 Hz, 2H), 4.49 (td, *J* = 5.0, 2.3 Hz, 2H), 4.38 (td, *J* = 4.9, 2.3 Hz, 2H), 4.11 (qt, *J* = 4.9, 2.3 Hz, 1H), 4.02 (qt, *J* = 4.8, 2.2 Hz, 1H), 3.82 (s, 3H); ^{13}C NMR (126 MHz, $CDCl_3$) δ 169.68, 165.66, 161.91, 134.84, 129.12, 124.07, 58.38, 55.05, 52.29, 47.97, 47.93, 46.40, 45.53. ESI-MS: calculated $[C_{19}H_{13}NO_6+Na]^+$: 374.0635 found: 374.0632; IR ν = 2998, 2357, 1742, 1725, 1220, 902, 695.

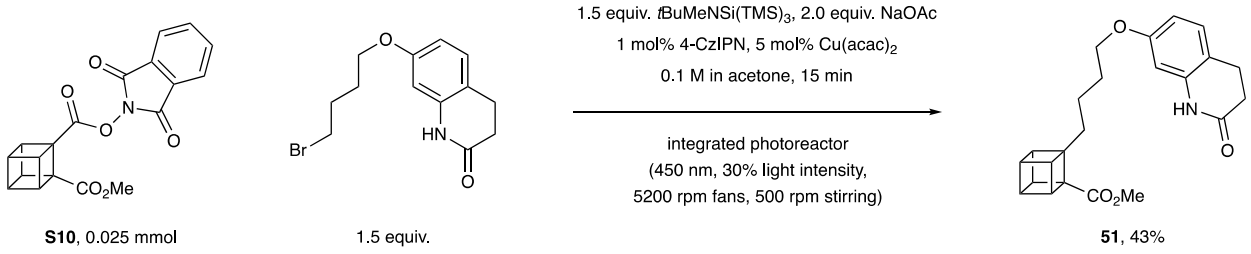

The silane **32** (13.8 mg, 90% pure, 0.0375 mmol, 1.5 equiv.), cubane redox-active ester **S10** (8.8 mg, 0.025 mmol, 1.0 equiv.), NaOAc (6.8 mg, 0.05 mmol, 2.0 equiv.), $Cu(acac)_2$ (0.3 mg, 5 mol%), 7-(4-bromobutoxy)-3,4-dihydroquinolin-2-one (11.2 mg, 0.0375 mmol, 1.5 equiv.), and 4-CzIPN (0.2 mg, 1 mol%), were added to an oven-dried 8 mL vial equipped with a stir bar and placed under an N_2 atmosphere. Degassed acetone (0.25 mL, 0.1 M) was added, and the vial was

placed inside the integrated photoreactor (450 nm, 30% light intensity, 1500 rpm fans, 500 rpm stirring, multi-vial holder, 15 min). The reaction was repeated 4 times and an average ^{1}H NMR yield was recorded with respect to 1,3,5-trimethoxybenzene. The product was purified using reversed phase (C18) chromatography (eluent: gradient from 0 to 100% H_2O in MeCN with 0.1% NH_4OH). The compound is particularly acid sensitive, undergoing opening of the cubane core upon exposure to acid. Thus purification under basic conditions is necessary.

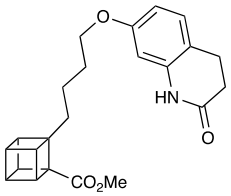

51, 43% yield, white solid. ^{1}H NMR (500 MHz, $CDCl_3$) δ 7.66 (s, 1H), 7.04 (d, *J* = 8.3 Hz, 1H), 6.51 (dd, *J* = 8.3, 2.4 Hz, 1H), 6.29 (d, *J* = 2.5 Hz, 1H), 4.11 (td, *J* = 4.9, 2.2 Hz, 2H), 3.99 (tp, *J* = 4.8, 2.4 Hz, 1H), 3.91 (t, *J* = 6.4 Hz, 2H), 3.81–3.75 (m, 3H), 3.68 (s, 3H), 2.89 (dd, *J* = 8.5, 6.5 Hz, 2H), 2.61 (dd, *J* = 8.5, 6.5 Hz, 2H), 1.80–1.70 (m, 4H), 1.46–1.38 (m, 2H); ^{13}C NMR (126 MHz, $CDCl_3$) δ 172.36, 171.57, 158.78, 138.14, 128.85, 115.83, 108.82, 102.23, 68.12, 61.76, 56.85, 51.39, 46.59, 46.42, 46.09, 44.48, 31.27, 30.40, 29.49, 24.73, 20.30. ESI-MS: calculated $[C_{23}H_{25}NO_4+H]^+$: 380.1856, found: 380.1856. IR ν = 2981, 2925, 1716, 1678, 1190, 1123, 730.

Arylation of non-linear cubane isomers

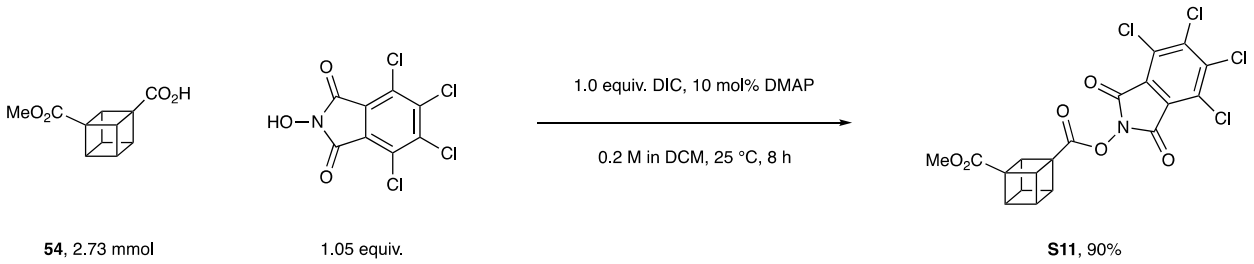

DIC (0.423 mL, 1.0 equiv.) was added dropwise to a rapidly stirred suspension of the cubane carboxylic acid **54** (0.563 g, 2.73 mmol, 1.0 equiv.), tetrachloro-*N*-hydroxyphthalimide (0.862 g, 1.05 equiv.), and DMAP (33.4 mg, 10 mol%) in dry CH_2Cl_2 (14 mL, 0.2 M) in an oven-dried 40 mL vial under an N_2 atmosphere at room temperature. The reaction was stirred for 8 h, before being concentrated using a rotary evaporator with the water bath set to 30 °C. The crude product was dissolved in minimal CH_2Cl_2 and passed rapidly through a short silica gel column (eluent: CH_2Cl_2).

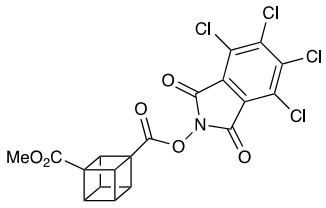

S11, 90% yield, white solid. ^{1}H NMR (500 MHz, $CDCl_3$) δ 4.70 (dt, *J* = 4.8, 2.4 Hz, 2H), 4.47 (tq, *J* = 4.9, 2.3 Hz, 1H), 4.27 (tq, *J* = 4.8, 2.3 Hz, 1H), 4.14 (q, *J* = 4.9 Hz, 2H), 3.74 (s, 3H); ^{13}C NMR (126 MHz, $CDCl_3$) δ 171.00, 166.25, 157.76, 141.20, 130.63, 124.89, 52.01, 51.60, 50.55, 50.02, 43.73. ESI-MS: calculated $[C_{19}H_9Cl_4NO_6+Na]^+$: 509.9076, found: 509.9105. IR ν = 3001, 2355, 1743, 1377, 1215, 1153, 753.

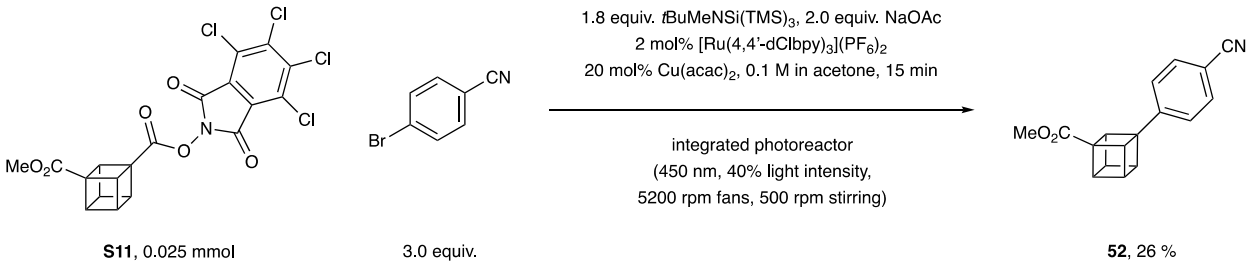

The silane **32** (16.5 mg, 90% pure, 0.045 mmol, 1.8 equiv.), cubane redox-active ester **S11** (12.2 mg, 0.025 mmol, 1.0 equiv.), NaOAc (6.8 mg, 0.05 mmol, 2.0 equiv.), $Cu(acac)_2$ (1.3 mg, 20 mol%), 4-bromobenzonitrile (13.7 mg, 0.075 mmol, 3.0 equiv.), and $[Ru(4,4'\text{-}dClbpy)_3](PF_6)_2$ (0.5 mg, 2 mol%), were added to an oven-dried 8 mL vial equipped with a stir bar and placed under an N_2 atmosphere. Degassed acetone (0.25 mL, 0.1 M) was added, and the vial was placed inside the integrated photoreactor (450 nm, 40% light intensity, 1500 rpm fans, 500 rpm stirring, multi-vial holder, 15 min). The reaction was run 4 times, on a 0.025 mmol scale and the reaction mixtures were combined, concentrated, and purified by automatic column chromatography using a 12 g Isco RediSep Rf gold column (eluent: gradient from 0 to 100% EtOAc in hexane).

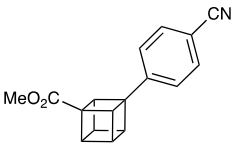

52, 26% yield, white solid. ^{1}H NMR (500 MHz, $CDCl_3$) δ 7.64 (d, *J* = 7.7 Hz, 2H), 7.30 (d, *J* = 7.7 Hz, 2H), 4.47–4.30 (m, 3H), 4.26–4.15 (m, 1H), 4.03 (q, *J* = 4.7 Hz, 2H), 3.73 (s, 3H); ^{13}C NMR (126 MHz, $CDCl_3$) δ 172.23, 147.11, 132.52, 125.85, 119.27, 109.95, 57.38, 53.33, 52.62, 51.85, 51.23, 50.50, 41.95. EI-MS: calculated $[C_{17}H_{13}NO_2]^+$: 263.0941, found: 263.0943. IR ν = 2989, 2225, 1722, 1606, 1506, 1435, 1317, 1213, 1163, 1081, 971, 883, 827, 554.

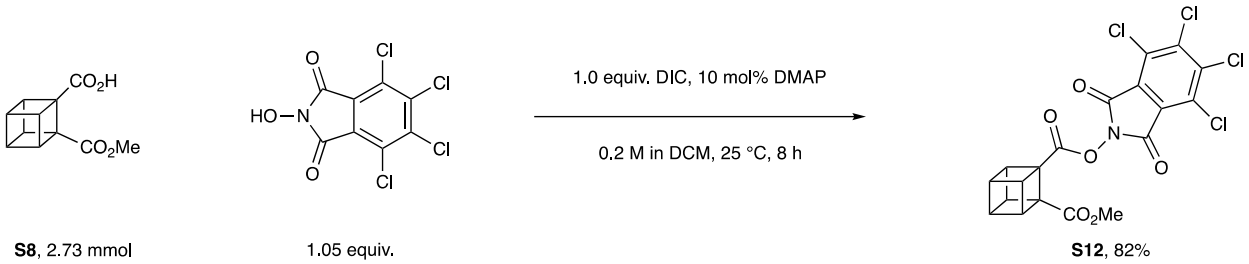

S8, 2.73 mmol 1.05 equiv. **S12**, 82%

DIC (0.081 mL, 1.0 equiv.) was added dropwise to a rapidly stirred suspension of cubane carboxylic acid **S8** (0.163 g, 0.79 mmol, 1.0 equiv.), tetrachloro-*N*-hydroxyphthalimide (0.2496 g, 1.05 equiv.), and DMAP (9.7 mg, 10 mol%) in dry CH_2Cl_2 (4 mL, 0.2 M) in an oven-dried 40 mL vial under an N_2 atmosphere at room temperature. The reaction was stirred for 8 h, before being concentrated using a rotary evaporator with the water bath set to 30 °C. The crude product was dissolved in minimal CH_2Cl_2 and passed rapidly through a short silica gel column (eluent: CH_2Cl_2).

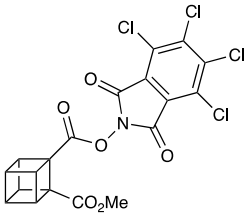

S12, 82% yield, white solid. ^{1}H NMR (500 MHz, $CDCl_3$) δ 4.48 (td, *J* = 4.9, 2.2 Hz, 2H), 4.38 (td, *J* = 4.9, 2.3 Hz, 2H), 4.12 (qt, *J* = 4.9, 2.3 Hz, 1H), 4.02 (qt, *J* = 4.9, 2.2 Hz, 1H), 3.82 (s, 3H); ^{13}C NMR (126 MHz, $CDCl_3$) δ 169.53, 165.23, 157.52, 141.11, 130.57, 124.88, 58.34, 54.77, 52.36, 48.03, 47.94, 46.48, 45.58. ESI-MS: calculated $[C_{19}H_9Cl_4NO_6+Na]^+$: 509.9076, found: 509.9084. IR ν = 3001, 2356, 1745, 1723, 1377, 1196, 724.

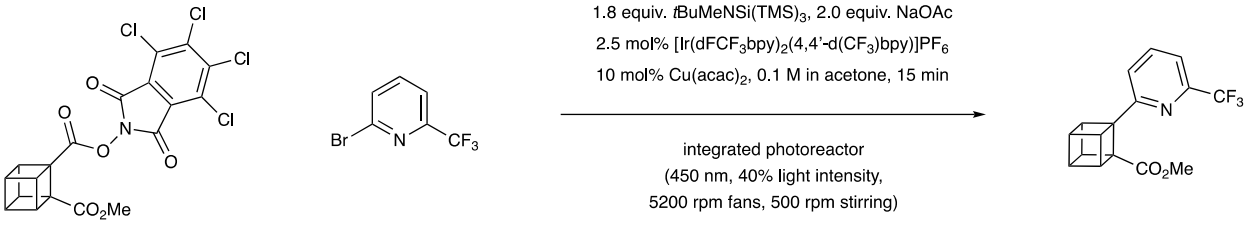

S12, 0.025 mmol 3.0 equiv. **53**, 18%

The silane **32** (16.5 mg, 90% pure, 0.045 mmol, 1.8 equiv.), the cubane redox-active ester **S12** (12.2 mg, 0.025 mmol, 1.0 equiv.), NaOAc (6.8 mg, 0.05 mmol, 2.0 equiv.), $Cu(acac)_2$ (0.7 mg, 10 mol%), 2-bromo-6-(trifluoromethyl)pyridine (16.9 mg, 0.075 mmol, 3.0 equiv.), and $[Ir(dFCF_3ppy)(4,4'\text{-}d(CF_3)bpy)]PF_6$ (0.72 mg, 2.5 mol%), were added to an oven-dried 8 mL vial equipped with a stir bar and placed under an N_2 atmosphere. Degassed acetone (0.25 mL, 0.1 M) was added, and the vial was placed inside the integrated photoreactor (450 nm, 40% light intensity, 5200 rpm fans, 500 rpm stirring, multi-vial holder, 15 min). The reaction was run 4 times on a

0.025 mmol scale and the reaction mixtures were combined, concentrated, and purified by automatic column chromatography using a 12 g Isco RediSep Rf gold column.

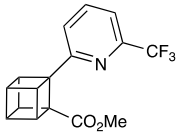

53, 18% yield, white solid. ^{1}H NMR (500 MHz, $CDCl_3$) δ 7.80 (t, *J* = 7.8 Hz, 1H), 7.47 (dd, *J* = 7.7, 1.0 Hz, 1H), 7.36 (d, *J* = 7.9 Hz, 1H), 4.34 (tt, *J* = 5.7, 2.8 Hz, 4H), 4.05 (dddd, *J* = 20.5, 7.4, 4.9, 2.5 Hz, 2H), 3.57 (s, 3H); ^{13}C NMR (126 MHz, $CDCl_3$) δ 171.15, 159.77, 147.92 (q, *J* = 34.3 Hz), 137.45, 122.77, 121.64 (q, *J* = 274.3 Hz), 117.88 (q, *J* = 2.9 Hz), 62.51, 59.29, 51.42, 48.78, 46.87, 45.98, 44.91; ^{19}F NMR (376 MHz, $CDCl_3$) δ −68.01. ESI-MS: calculated $[C_{16}H_{12}F_3NO_2+Na]^+$: 330.0712, found: 330.0717. IR ν = 2996, 2357, 1722, 1466, 1358, 1139, 1120.

9. Synthesis of pharmaceutical analogs

Synthesis of Cuba-Lumacaftor (56)

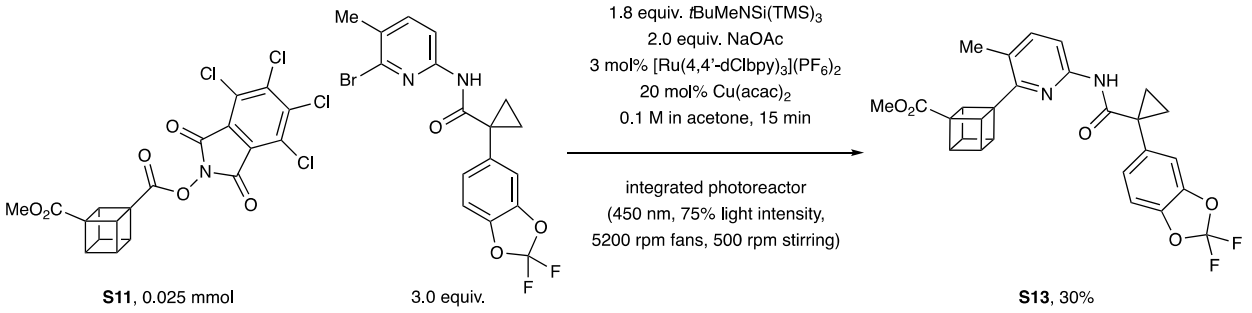

The silane **32** (16.5 mg, 90% pure, 0.045 mmol, 1.8 equiv.), the cubane redox-active ester **S11** (12.2 mg, 0.025 mmol, 1.0 equiv.), NaOAc (6.8 mg, 0.05 mmol, 2.0 equiv.), $Cu(acac)_2$ (1.3 mg, 20 mol%), the 2-bromopyridine (30.8 mg, 0.075 mmol, 3.0 equiv.), and $[Ru(4,4'\text{-}dClbpy)_3](PF_6)_2$ (0.8 mg, 0.75 μmol, 3 mol%), were added to an oven-dried 8 mL vial equipped with a stir bar and placed under an N_2 atmosphere. Degassed acetone (0.25 mL, 0.1 M) was added, and the vial was placed inside the integrated photoreactor (450 nm, 40% light intensity, 5200 rpm fans, 500 rpm stirring, multi-vial holder, 15 min). The reactions were concentrated and purified by automatic column chromatography using a 12 g Isco RediSep Rf gold column (eluent: gradient from 0 to 100% EtOAc in hexane). 30% yield, white solid. The above reaction was repeated, and the combined product was taken directly onto the hydrolysis.

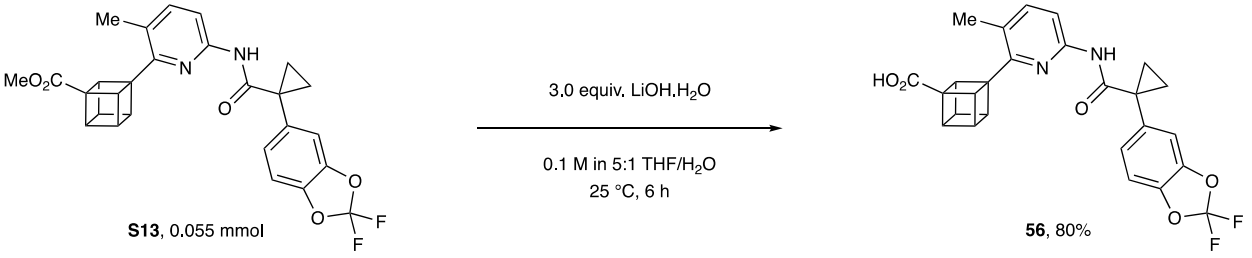

The cubane methyl ester **S13** (0.055 mmol, 1.0 equiv.) was dissolved in THF:H_2O (5:1, 0.6 mL, 0.1 M) in an 8 mL vial equipped with a stir bar. To this solution was added $LiOH.H_2O$ (6.9 mg, 0.165 mmol, 3.0 equiv.). The mixture was sonicated (5 min) and stirred at room temperature for 6 h. The solution was diluted with water (2 mL) and then acidified (pH 3) with 1 M HCl before being extracted using EtOAc to provide the product as a slightly impure pinkish solid in 80% yield. A sample for biological studies was purified by reversed phase chromatography (MeCN/H_2O = 15–70% with 0.1% TFA) and provided the TFA salt of **56**, which was spectroscopically characterized.

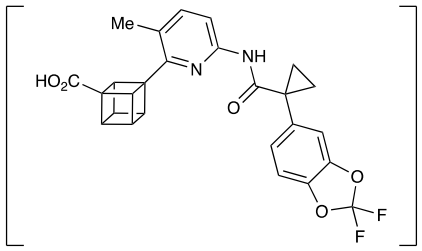

56.TFA, ^{1}H NMR (600 MHz, DMSO) δ 8.73 (s, 1H), 7.70 (d, *J* = 8.3 Hz, 1H), 7.56 (s, 1H), 7.55 (s, 1H), 7.43 (d, *J* = 8.3 Hz, 1H), 7.35 (d, *J* = 8.3 Hz, 1H), 7.10 (d, *J* = 52 Hz, 1H), 4.50–4.42 (m, 2H), 4.25 (dd, *J* = 4.7, 2.4 Hz, 1H), 4.18 (dd, *J* = 4.7, 2.4 Hz, 1H), 3.95 (q, *J* = 4.6 Hz, 2H), 2.17 (s, 3H), 1.50 (q, *J* = 4.1 Hz, 2H), 1.17 (q, *J* = 4.2 Hz, 2H); ^{13}C NMR (151 MHz, DMSO) δ 172.62, 171.14, 158.21 (q, *J* = 37.0 Hz), 154.70, 147.96, 142.86, 142.13, 140.13, 136. 25, 131.24 (t, *J* = 252.6 Hz), 127.51, 126.55, 115.45 (q, *J* = 290.8 Hz), 112.21, 111.83, 110.17, 57.71, 52.21, 50.78, 49.19, 48.43, 40.87, 31.28, 16.44, 15.74; ^{19}F NMR (564 MHz, DMSO) δ −48.93, −74.88. ESI-MS: calculated $[C_{26}H_{20}F_2N_2O_5+H]^+$: 479.1413, found: 479.1423.

Biological studies of Cuba-Lumacaftor (56)

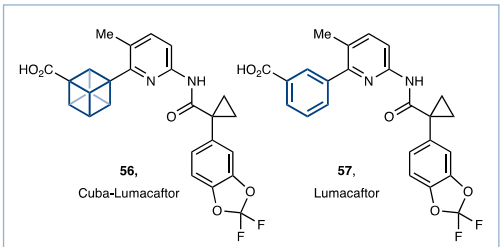

Property	Cuba-Lumacaftor	Lumacaftor
RC50 CFTR [μM]	2.1	0.15
logD	2.03	1.99
Solubility pH 7 [mg/mL]	171	139
Solubility pH 2 [mg/mL]	155	1
EPSA	101	113
Human CL_{int} [μL/min/10^6 cells]	6.98	11.96

Figure S35 | Biological studies of Cuba-Lumacaftor (56).

The biological properties of Cuba-Lumacaftor (**56**) were studied utilizing standard biological setups at Merck (Fig. S35). The results indicate that the compound is significantly more metabolically stable than the parent, optimized benzene-containing drug (CL_{int} < 6.98 μL/min/10^6 cells vs 11.96 μL/min/10^6 cells) while displaying a similar lipophilicity (logD) and cell permeability compared to the parent benzene-containing drug (**57**). The activity (RC50 CFTR) is only reduced by one order of magnitude despite the significant change to the structure of the heavily optimized marketed drug (**57**), which is conducted close to a binding carboxylic acid moiety. At the same time, the cubane-containing drug **56** has a significantly improved solubility at both pH 7 and pH 2. This can be rationalized either by a modulation of the pKa value of the carboxylic acid or by a disruption of π-stacking interactions by the sp^3-hybridized cubane and indicates a significantly improved absorption throughout the gastrointestinal tract.

Synthesis of Cuba-Acecainide (58)

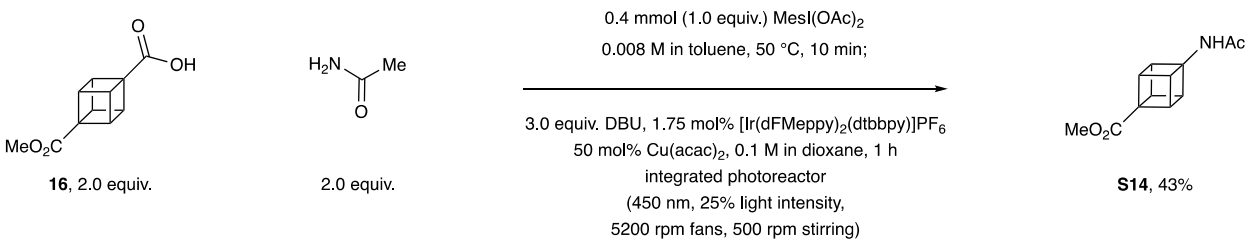

The reaction was conducted according to **GP 1**. A 250 mL round-bottom flask was charged with iodomesitylene diacetate (0.146 mg, 0.4 mmol), 4-(methoxycarbonyl)cubane-1-carboxylic acid (**16**, 0.164 mg, 0.8 mmol, 2.0 equiv.), and 50 mL toluene. The flask was attached to a rotary evaporator with the water bath heated to 50 ºC and the solvent (and the generated acetic acid) was removed over ca. 10 min. A second 50 mL aliquot of toluene was added to the flask and the evaporation was repeated. The evaporation was repeated two more times. After further removal of residual toluene under high vacuum, Iodomesitylene bis(4-(methoxycarbonyl)cubane-1-carboxylate) can be directly used in the following amination reaction.

Iodomesitylene bis(4-(methoxycarbonyl)cubane-1-carboxylate) (262.6 mg, 0.4 mmol, 1.0 equiv.), the nitrogen nucleophile (0.8 mmol, 2.0 equiv.), $[Ir(dFMeppy)_2(dtbbpy)]PF_6$ (7.1 mg, 1.75 mol%), and $Cu(acac)_2$ (52.4 mg, 50 mol%), were added to an oven-dried 40 mL vial equipped with a stir bar and placed under an N_2 atmosphere. Degassed 1,4-dioxane (12 mL, 0.33 M) was added followed by DBU (0.180 mL, 3.0 equiv.) and the vial was placed inside the integrated photoreactor (450 nm, 25% light intensity, 5200 rpm fans, 500 rpm stirring, single vial holder, 60 min). The reaction was concentrated and purified by automatic column chromatography using a 40 g Isco RediSep Rf gold column (eluent: gradient from 0 to 100% EtOAc in hexane).

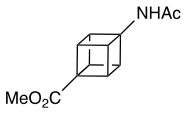

S14, 43% yield, white solid. ^{1}H NMR (500 MHz, $CDCl_3$) δ 6.03 (s, 1H), 4.20–4.08 (m, 6H), 3.70 (s, 3H), 1.99 (s, 3H); ^{13}C NMR (126 MHz, $CDCl_3$) δ 172.87, 169.62, 66.75, 55.86, 51.70, 50.32, 45.16, 23.26. ESI-MS: calculated $[C_{12}H_{13}NO_3+H]^+$: 220.0968, found: 220.0973. IR ν = 2357, 1723, 1697, 1316, 1092, 677.

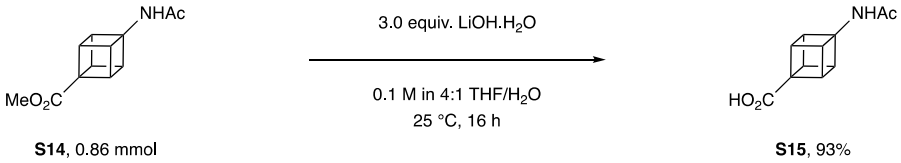

The cubane methyl ester (**S14**, 0.860 mmol, 1.0 equiv.) was dissolved in THF/H_2O (4:1, 8.6 mL, 0.1 M) in a 40 mL vial equipped with a stir bar. To this solution was added $LiOH.H_2O$ (108.3 mg, 2.58 mmol, 3.0 equiv.). The mixture was sonicated (10 min) and stirred at room temperature for 16 h. The solution was diluted with water (4 mL) and then acidified (pH 3) with 1 M HCl, and extracted using EtOAc (6 x 20 mL), and concentrated.

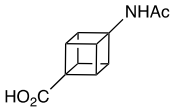

S15, 93% yield, yellow foam. ^{1}H NMR (500 MHz, D_2O) δ 4.23–4.09 (m, 6H), 2.03 (s, 3H); ^{13}C NMR (126 MHz, D_2O) δ 177.78, 173.67, 65.69, 55.89, 49.42, 44.81, 21.73. IR ν = 2995, 2355, 2340, 1702, 1654, 1535, 1295.

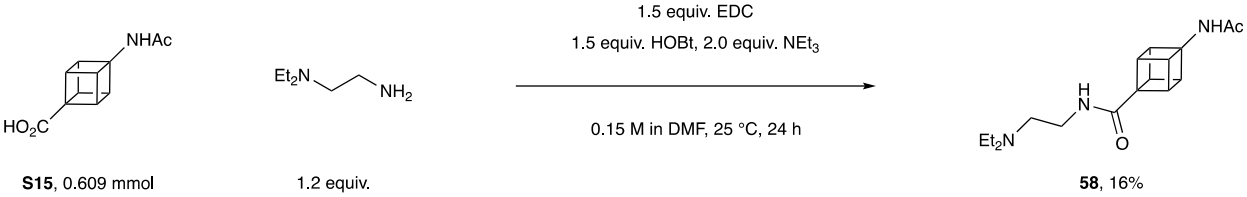

The cubane monoacid **S15** (125 mg, 0.609 mmol, 1.0 equiv.), EDC (175 mg, 0.914 mmol, 1.5 equiv.), and HOBt (140 mg, 0.914 mmol, 1.5 equiv.) were added to an 8 mL vial equipped with a stir bar. After addition of DMF (4 mL, 0.15 M), triethylamine (0.169 mL, 2.0 equiv.) and then diethylethane-1,2-diamine (0.104 mL, 1.2 equiv.) were added. The reaction mixture was stirred for 24 h at room temperature and then quenched by the addition of water, and extracted with EtOAc. Purification was conducted by reversed phase (C18) chromatography (eluent: gradient from 0 to 100% H_2O in MeCN with 0.1% formic acid).

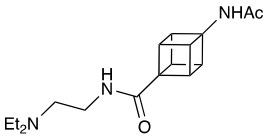

58, 16% yield, brown solid. ^{1}H NMR (500 MHz, $CDCl_3$) δ 6.13 (s, 1H), 4.10 (q, *J* = 5.4 Hz, 6H), 3.48 (q, *J* = 5.6 Hz, 2H), 2.88–2.76 (m, 6H), 1.98 (s, 3H), 1.16 (t, *J* = 7.2 Hz, 6H); ^{13}C NMR (126 MHz, $CDCl_3$) δ 172.83, 169.62, 66.75, 57.80, 51.50, 49.93, 47.13, 45.02, 35.58, 23.27, 10.12. ESI-MS: calculated $[C_{17}H_{25}N_3O_2+H]^+$: 304.2020, found: 304.2031. IR ν = 3243, 2980, 1624, 1598, 1324, 636.

Biological studies of Cuba-Acecainide (58)

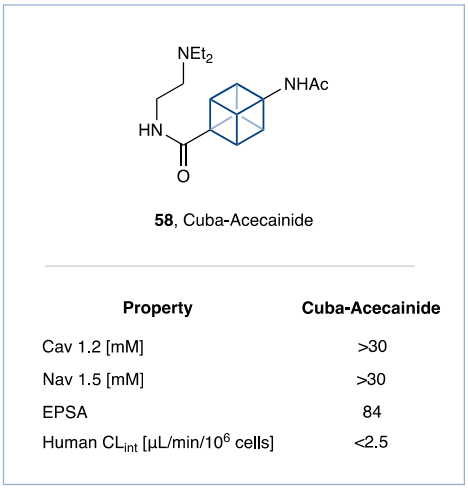

Figure S36 | Biological studies of Cuba-Acecainide (58).

Cuba-Acecainide was found to be metabolically stable (CL_{int} < 2.5 µL/min/10^6 cells) but was inactive in both calcium and sodium channel assays (Fig. S36).

10. Procedure for the Scifinder© search

Four structures were searched via Scifinder (Fig. S37). All substructures were selected, and the selection was filtered by the structures containing ^{1}H, ^{13}C, ^{19}F, and/or mass spectra. All references for the selected structures were obtained and the number of patents were obtained from the document type window. The search was conducted on the 12th of January 2023 at 1 pm Central European time (CET).

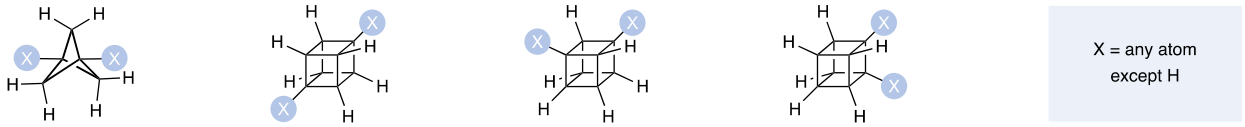

Figure S37 | Structures investigated in the patent search.

11. NMR Spectra

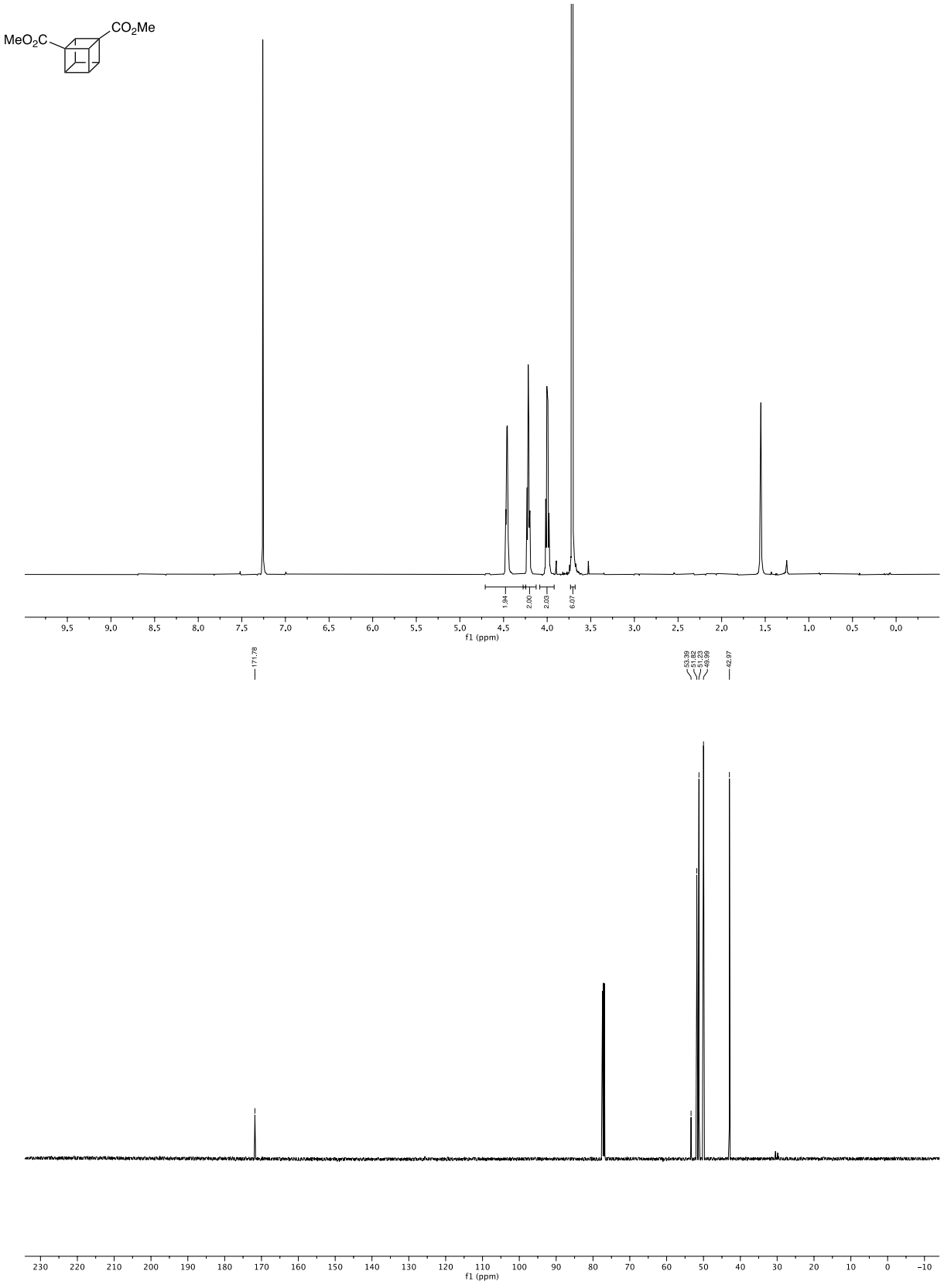

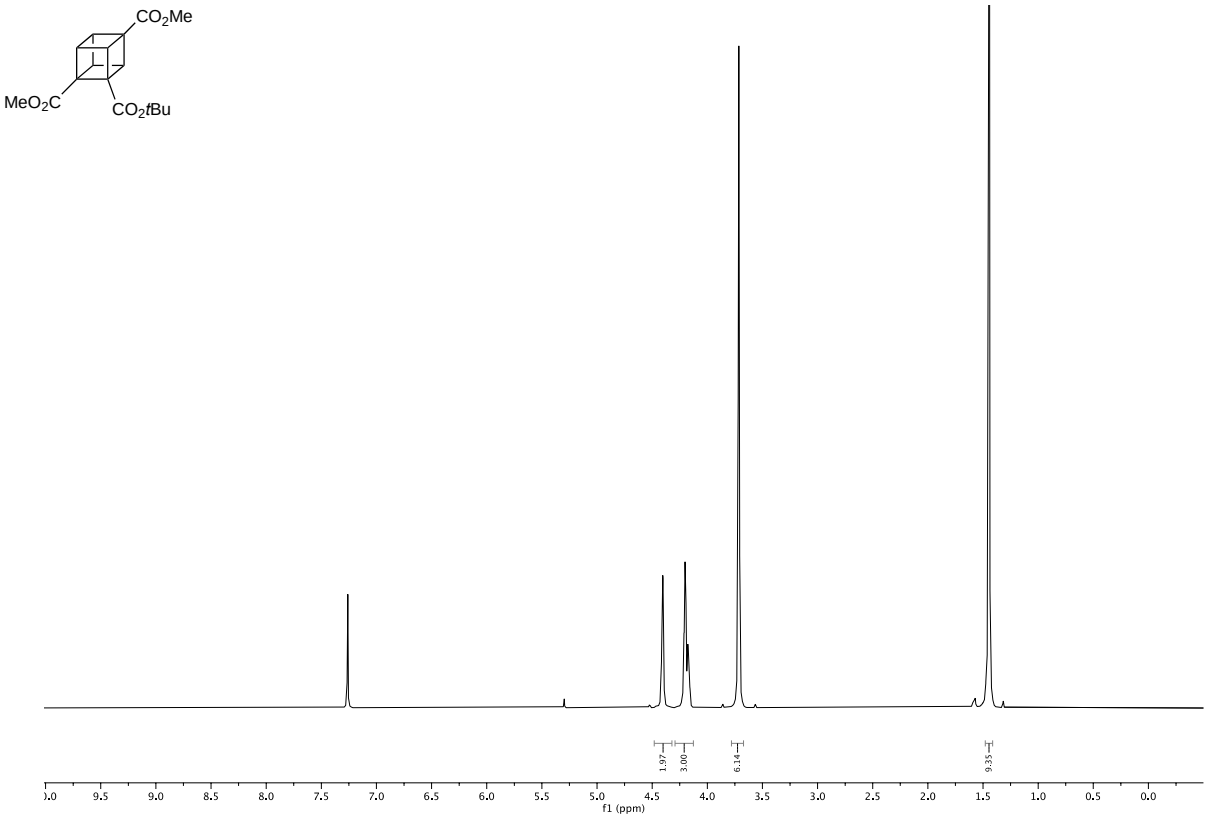
CO2Me
MeO2C
CO2tBu
1.97
3.00
6.14
9.35
f1 (ppm)

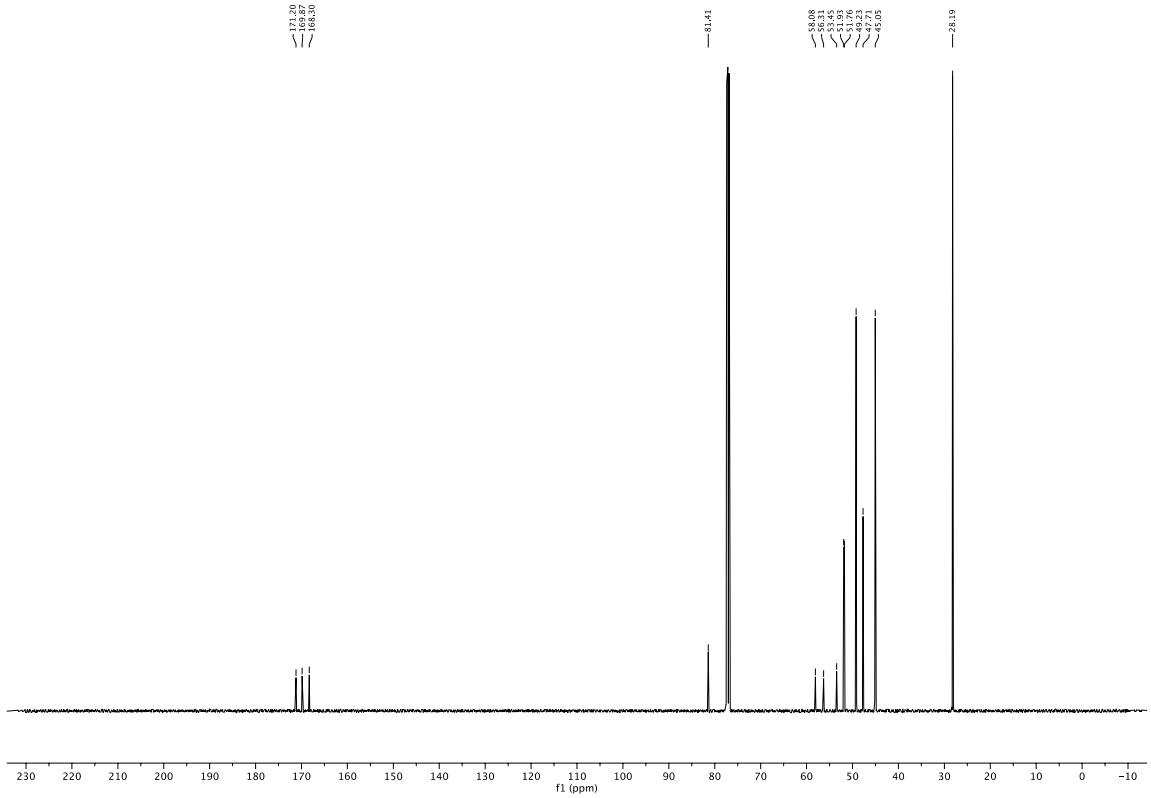
171.20
169.87
168.30
81.41
58.08
56.31
53.45
51.98
51.76
49.23
47.71
45.16
28.19
f1 (ppm)

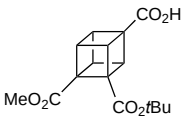
CO2H
MeO2C
CO2tBu

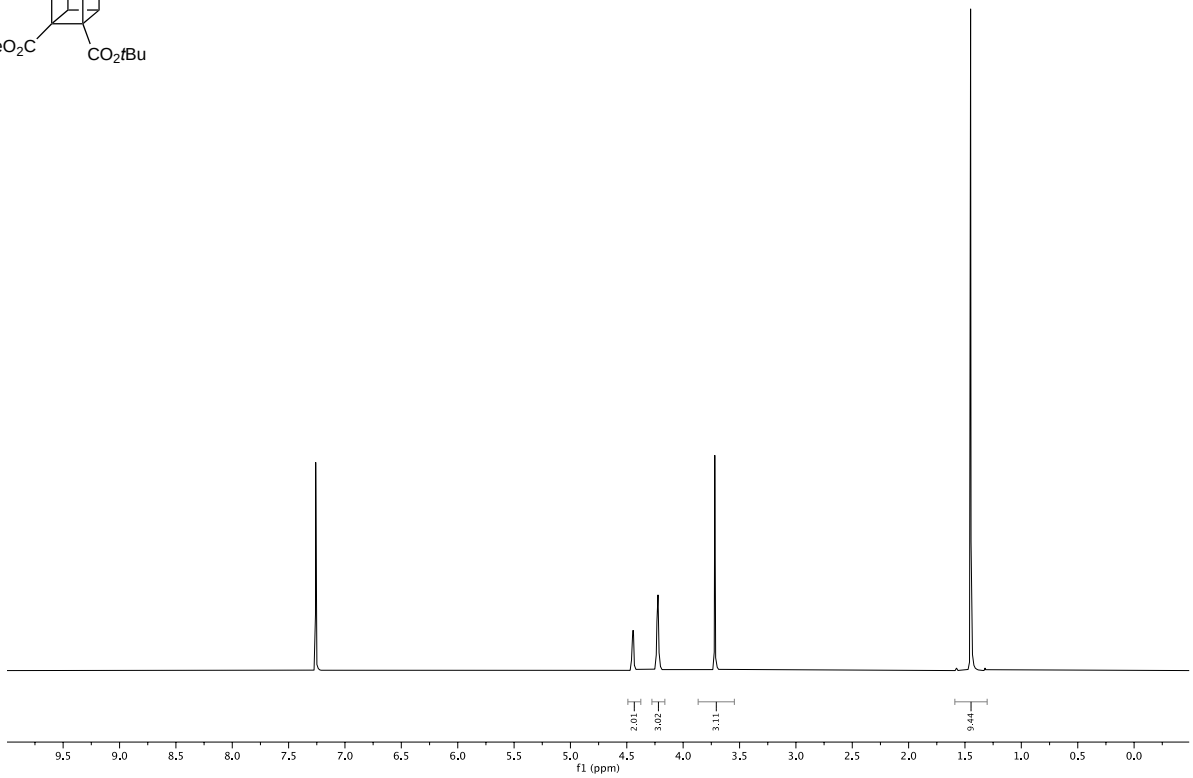
2.01
3.02
3.11
9.44
f1 (ppm)

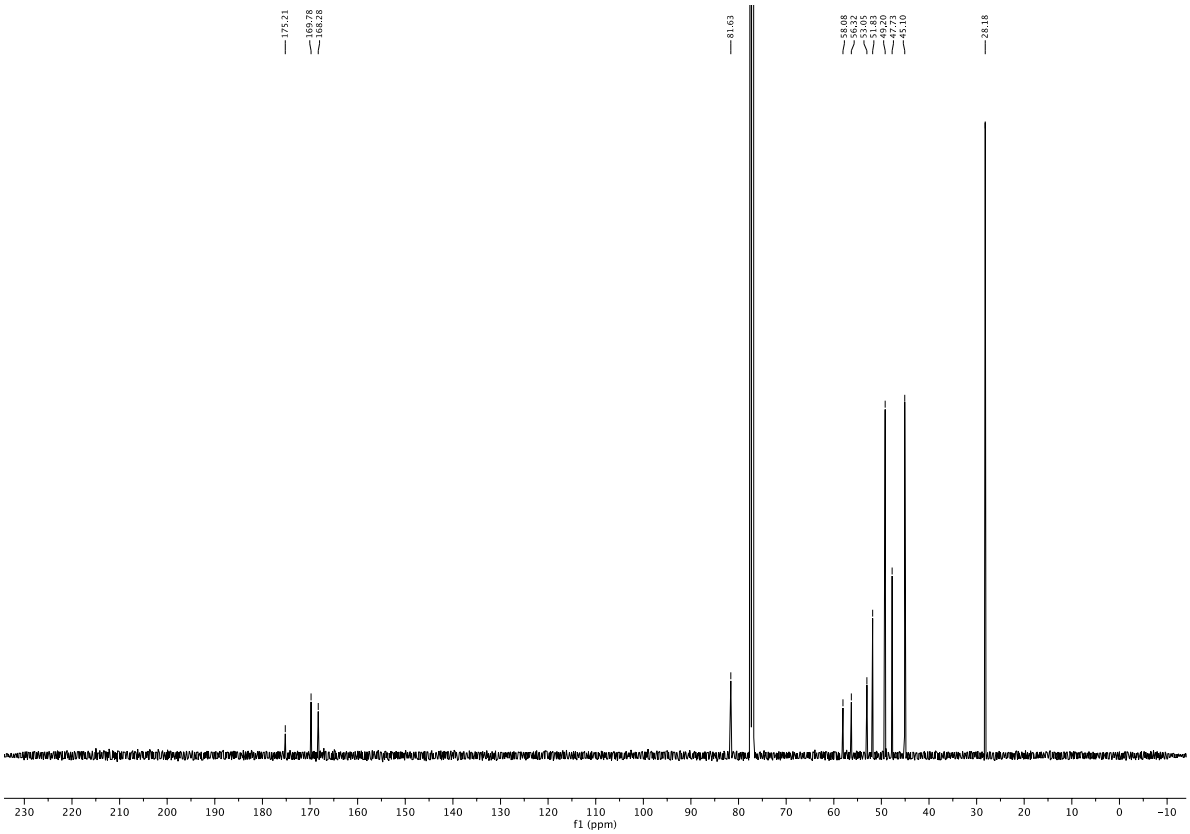
175.21
169.78
168.28
81.63
58.08
56.32
53.05
51.83
49.20
47.73
45.10
28.18
f1 (ppm)

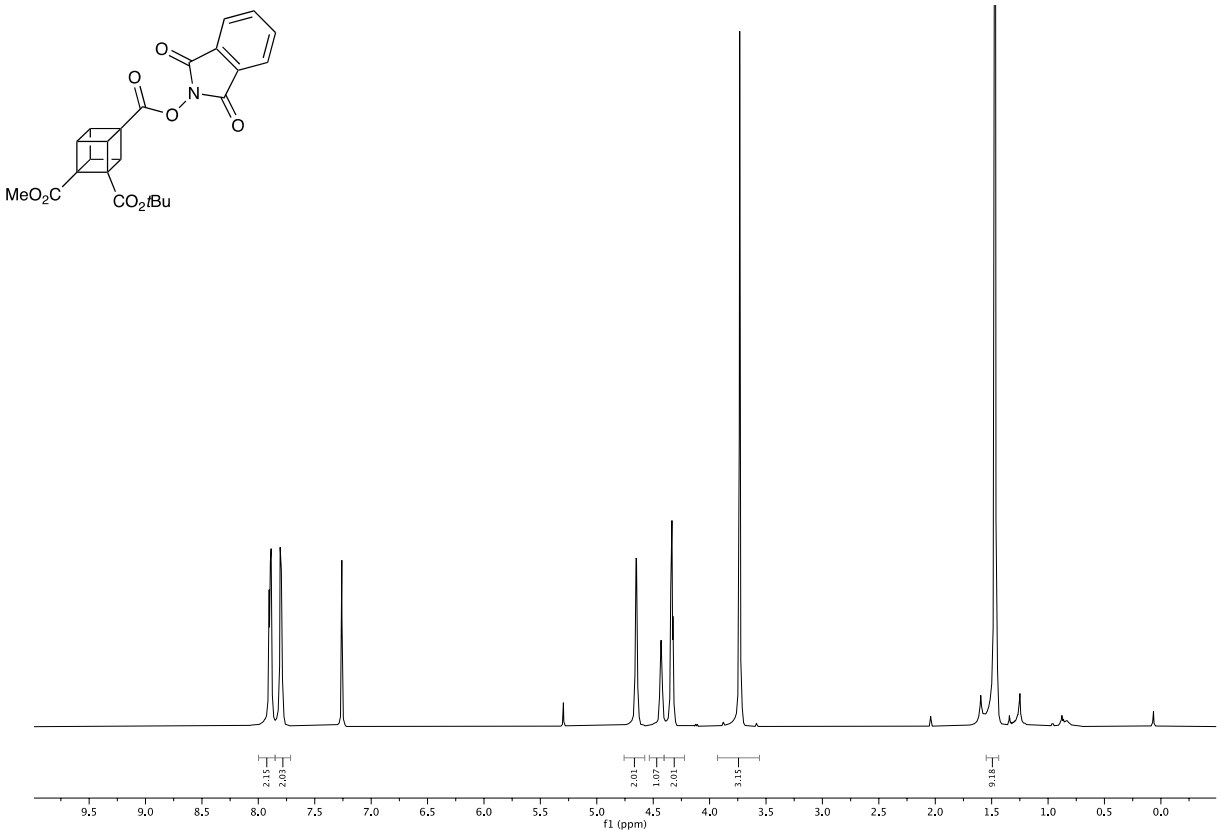
MeO2C
CO2tBu
2.15
2.03
2.01
1.07
2.01
3.15
9.18
f1 (ppm)

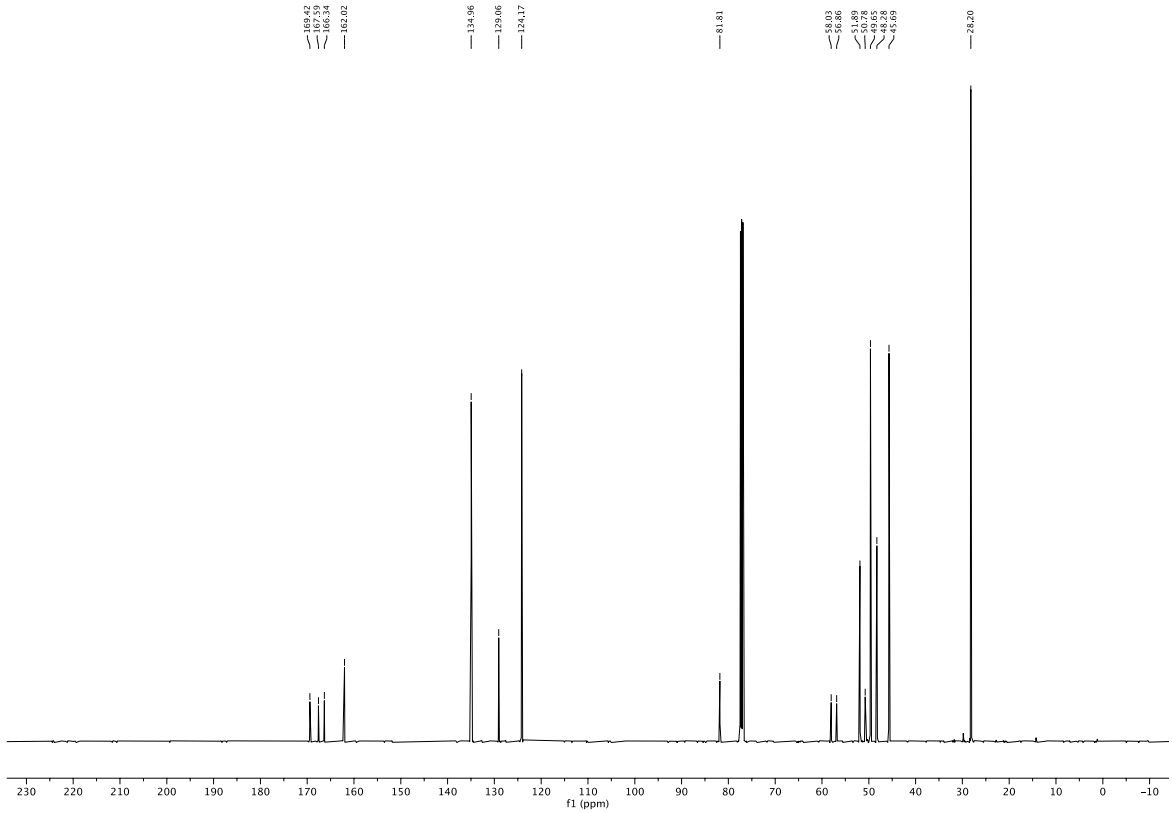
169.42
167.59
166.34
162.02
134.96
129.06
124.17
81.81
58.03
56.86
51.89
50.28
49.65
48.28
45.69
28.20
f1 (ppm)

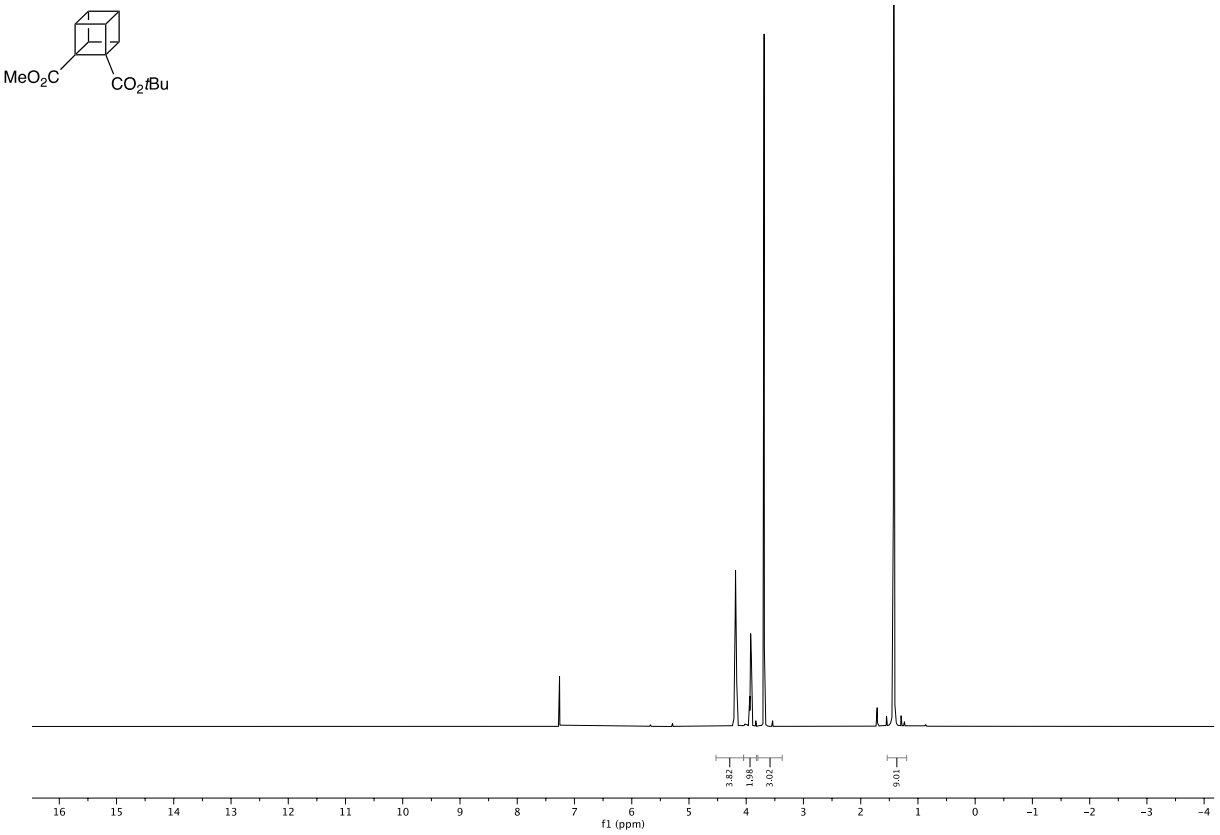
MeO2C
CO2tBu
3.82
1.98
3.02
9.01
f1 (ppm)

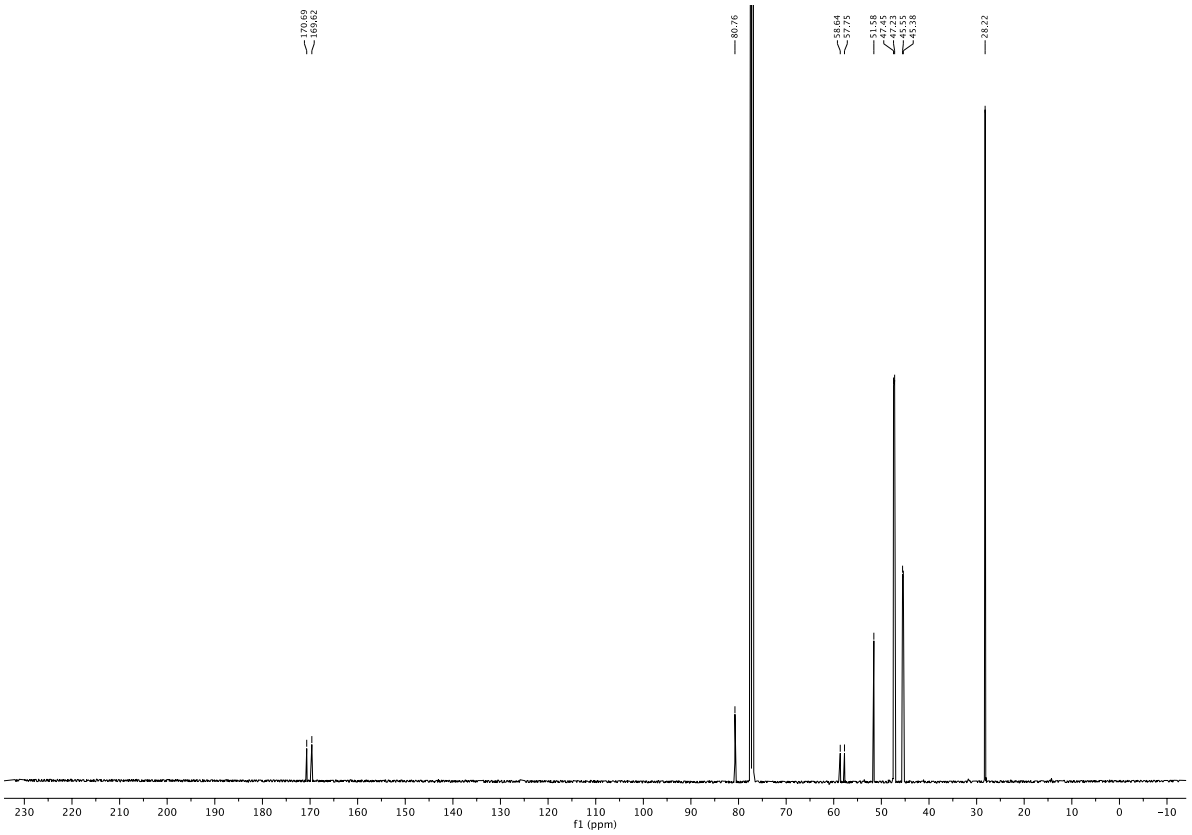
170.69
169.62
80.76
58.64
57.75
51.58
47.45
47.23
45.55
45.38
28.22
f1 (ppm)

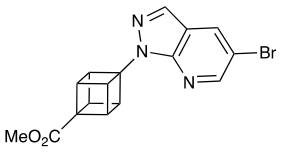
N
N
N
Br
MeO2C

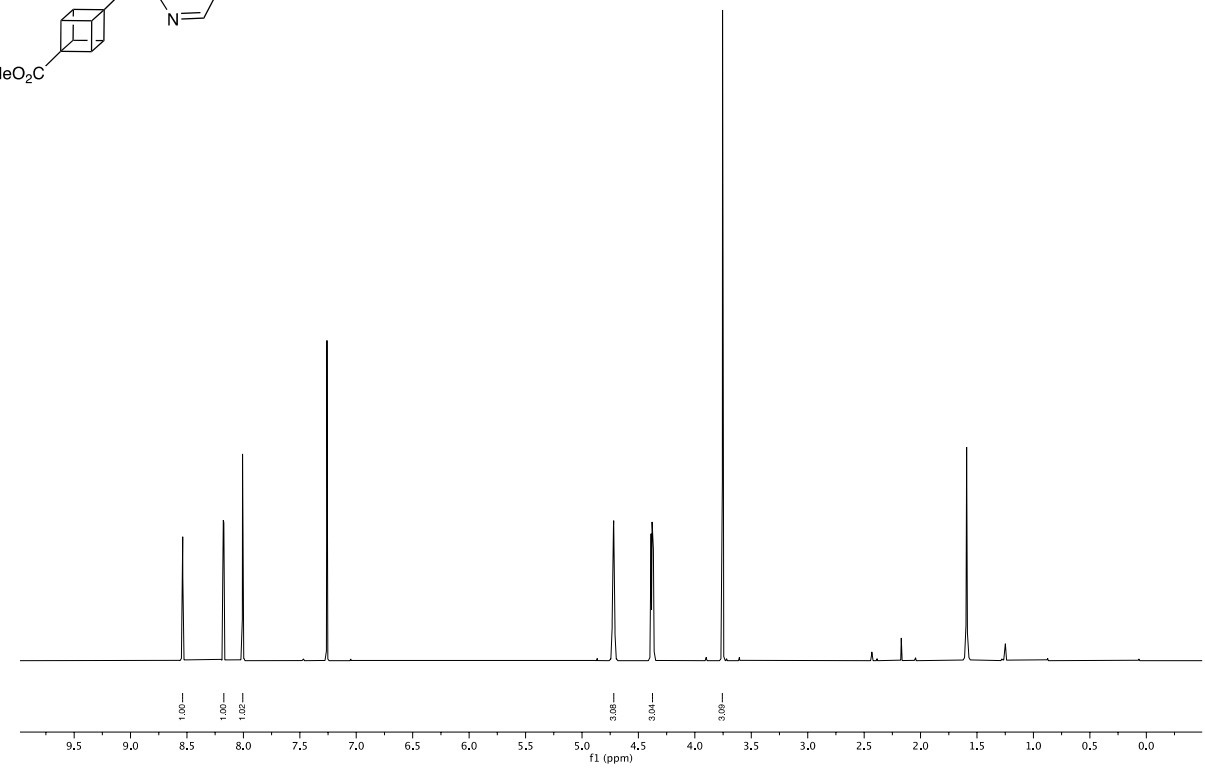
1.00
1.00
1.02
3.08
3.04
3.09
9.5 9.0 8.5 8.0 7.5 7.0 6.5 6.0 5.5 5.0 4.5 4.0 3.5 3.0 2.5 2.0 1.5 1.0 0.5 0.0
f1 (ppm)

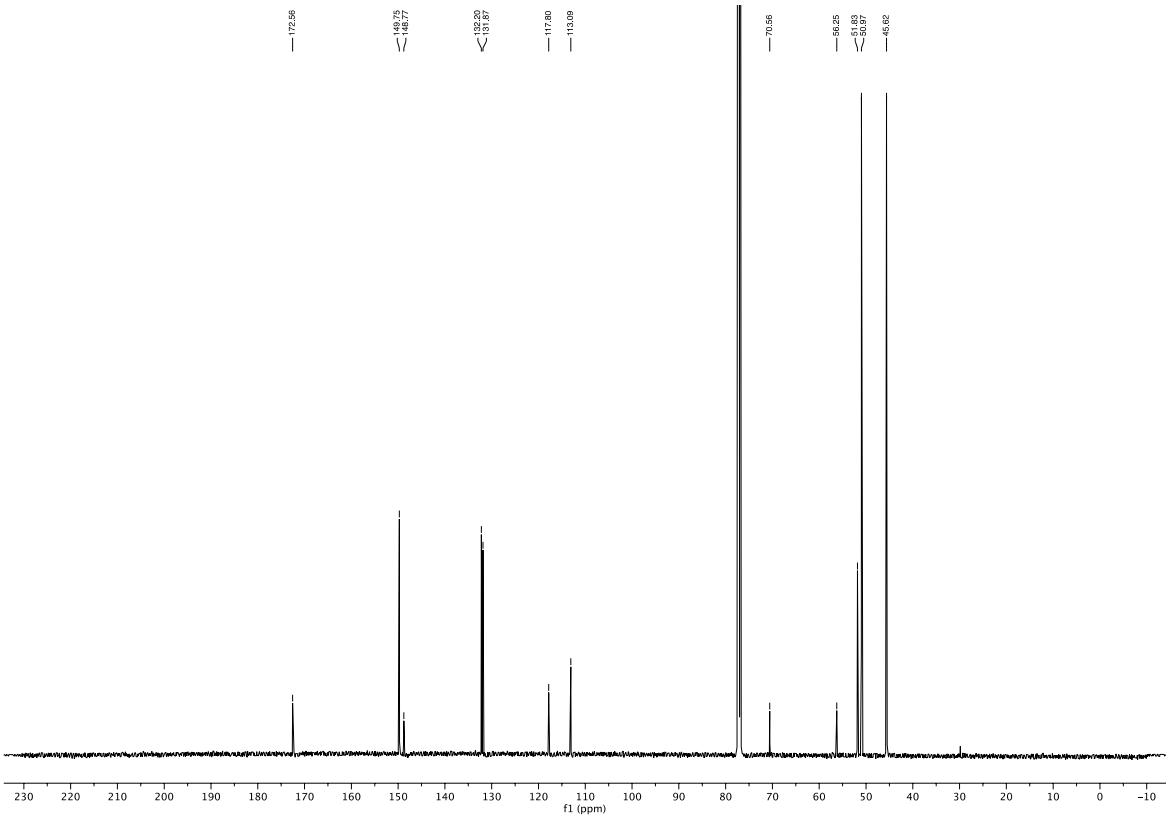
172.56
149.75
148.77
132.20
131.87
117.80
113.09
70.56
56.25
51.83
50.97
45.62
230 220 210 200 190 180 170 160 150 140 130 120 110 100 90 80 70 60 50 40 30 20 10 0 -10
f1 (ppm)

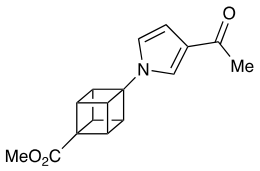
O
Me
N
MeO2C

1.00
1.99
2.92
2.91
3.27
3.29
f1 (ppm)

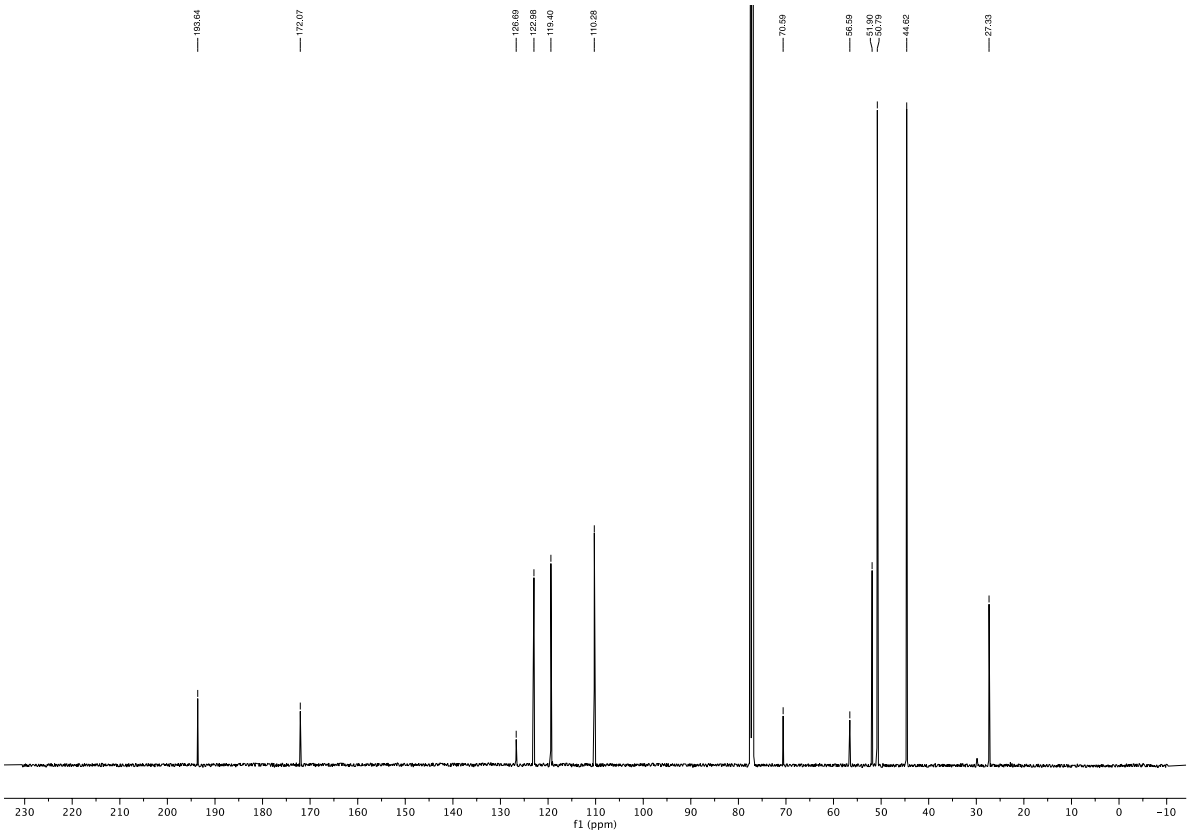
193.64
172.07
126.69
122.98
119.40
110.28
70.59
56.59
51.90
50.79
44.62
27.33
f1 (ppm)

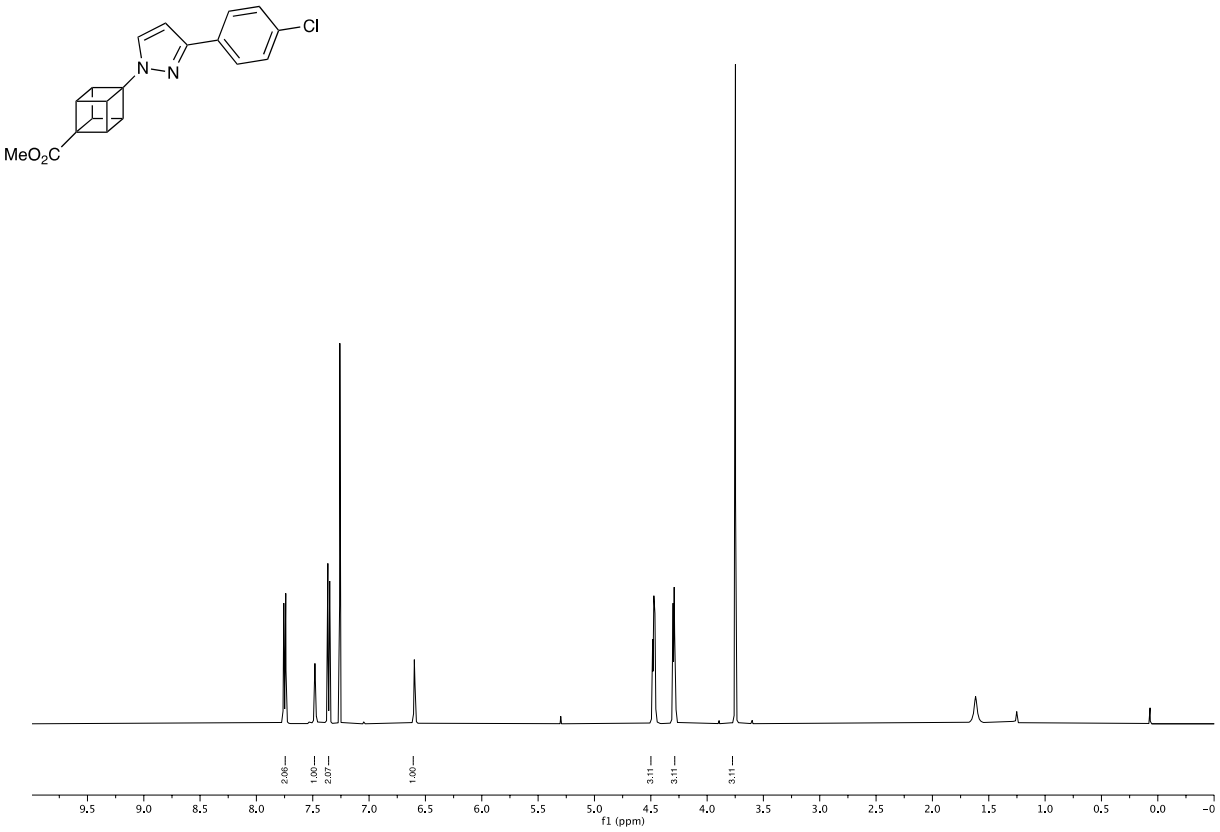
Cl
N
N
MeO2C
2.06
1.00
2.07
1.00
3.11
3.11
3.11
f1 (ppm)

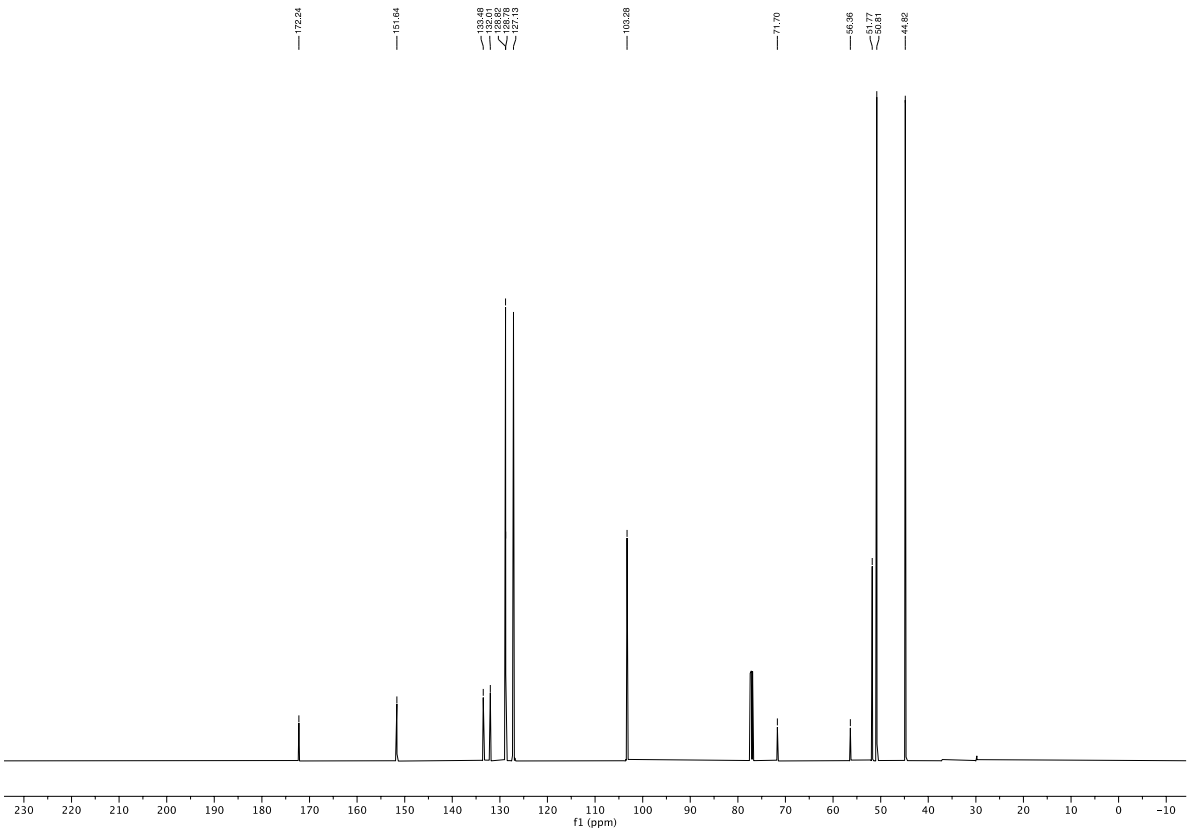
172.24
151.64
133.48
132.01
128.82
128.29
127.13
103.28
71.70
56.36
51.77
50.81
44.82
f1 (ppm)

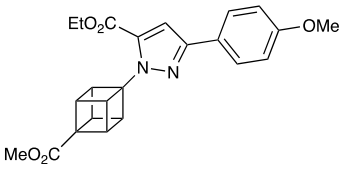
EtO2C
OMe
N
N
MeO2C

2.03
0.98
2.02
2.98
1.99
2.95
3.03
2.85
2.98
f1 (ppm)

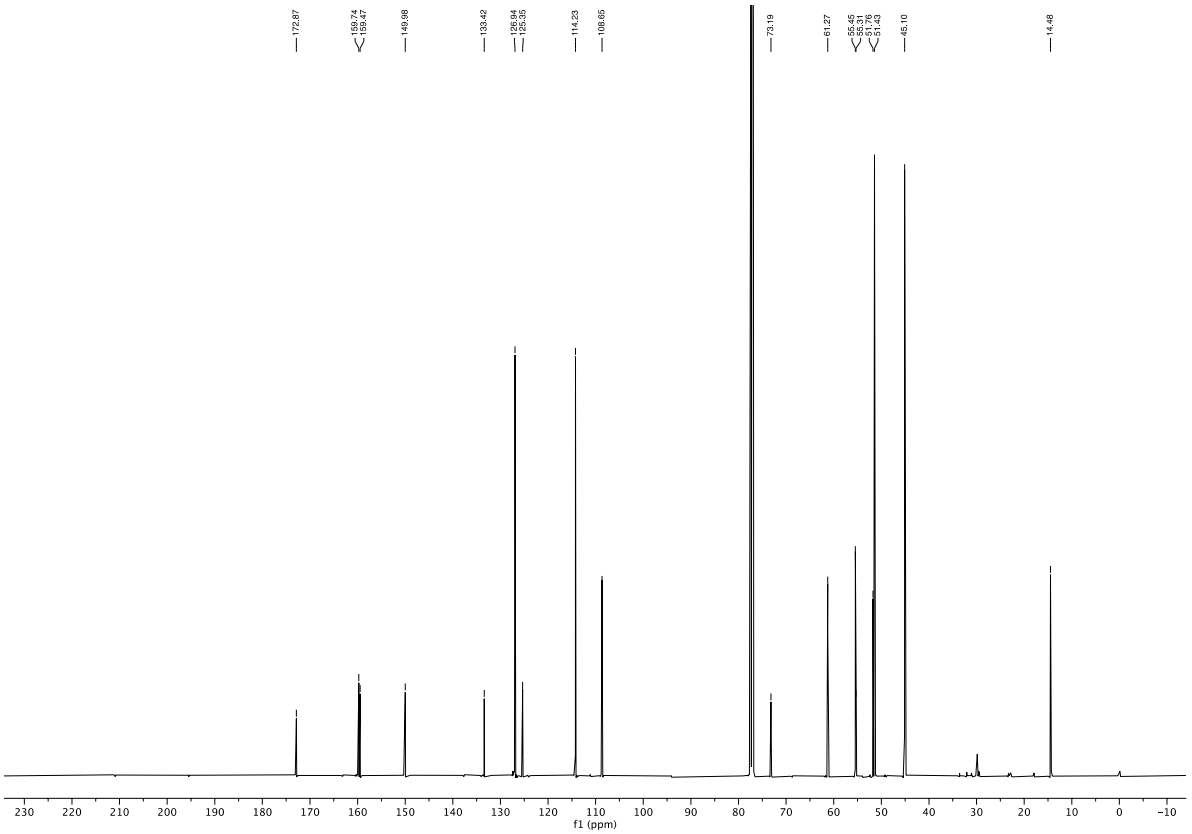
172.87
159.74
159.47
149.98
133.42
126.94
125.35
114.23
108.65
73.19
61.27
55.45
53.31
53.10
51.43
45.10
14.48
f1 (ppm)

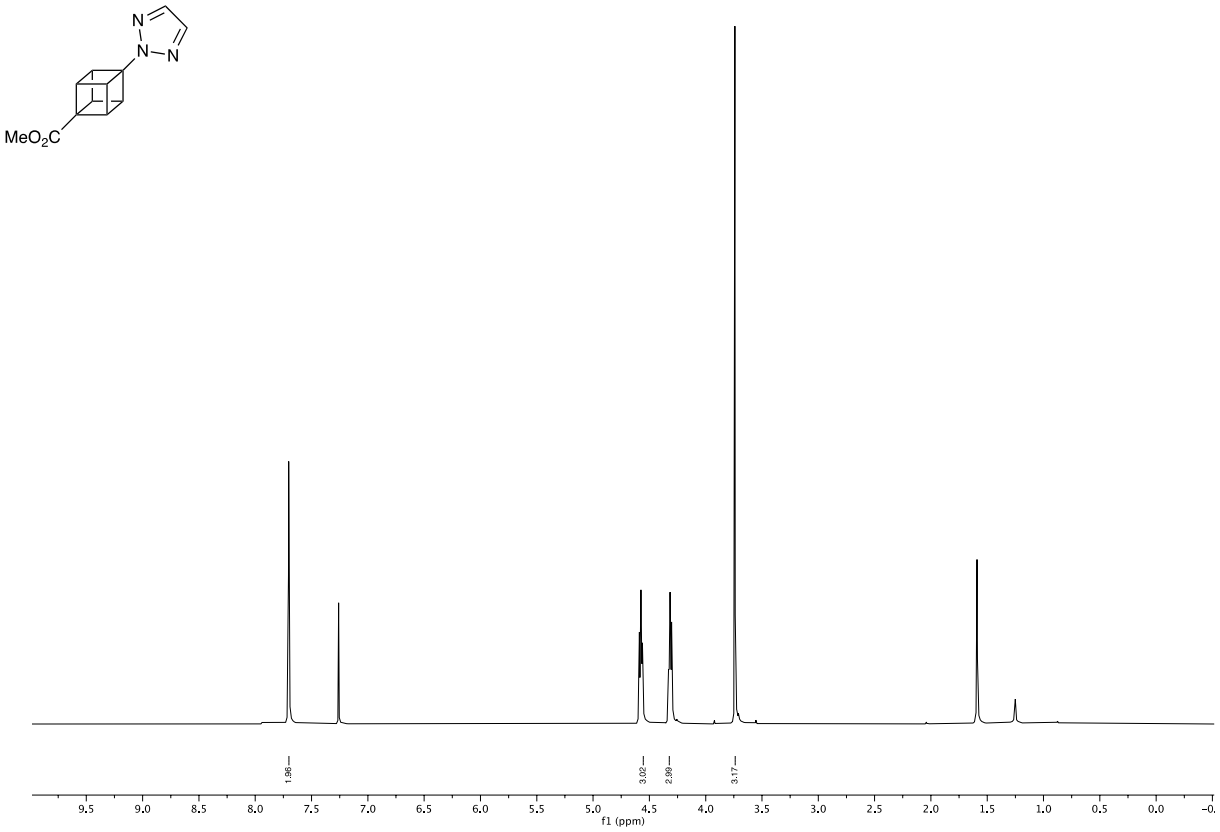
MeO2C
1.96
3.02
2.99
3.17
f1 (ppm)

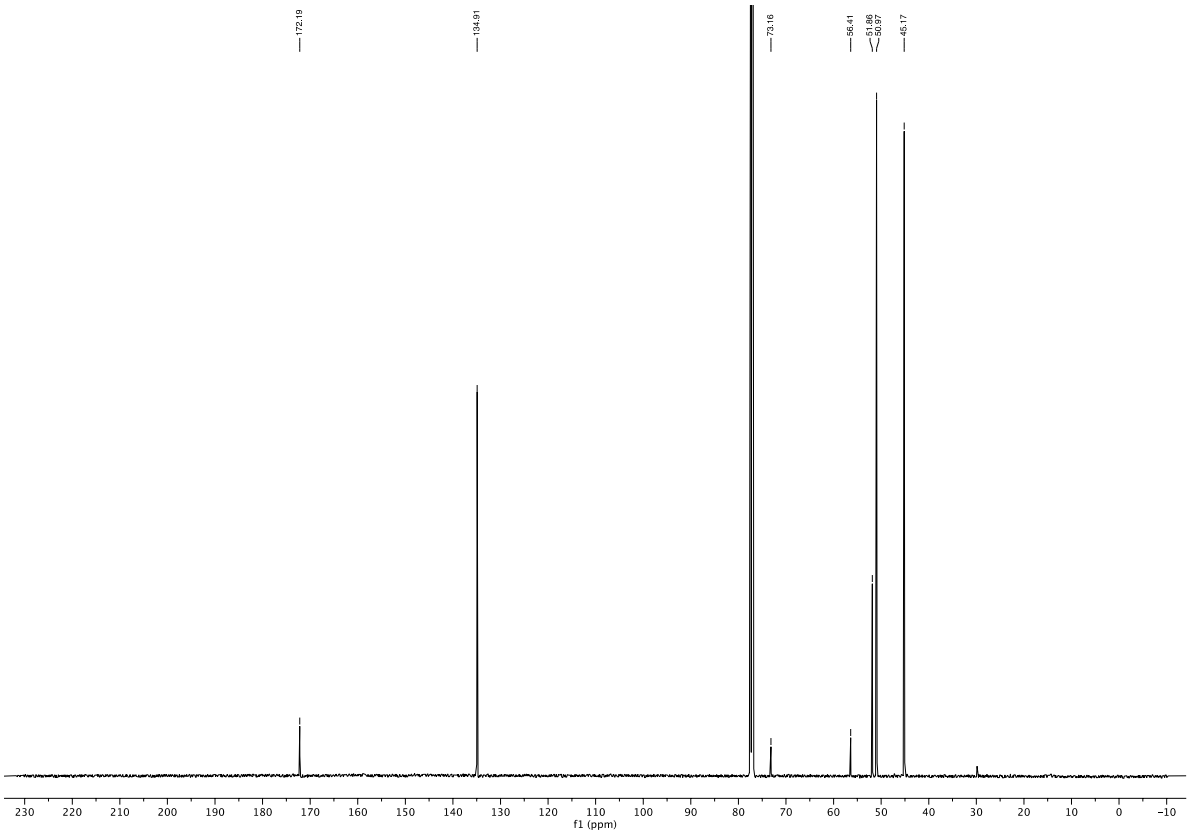
172.19
134.91
73.16
56.41
51.86
50.97
45.17
f1 (ppm)

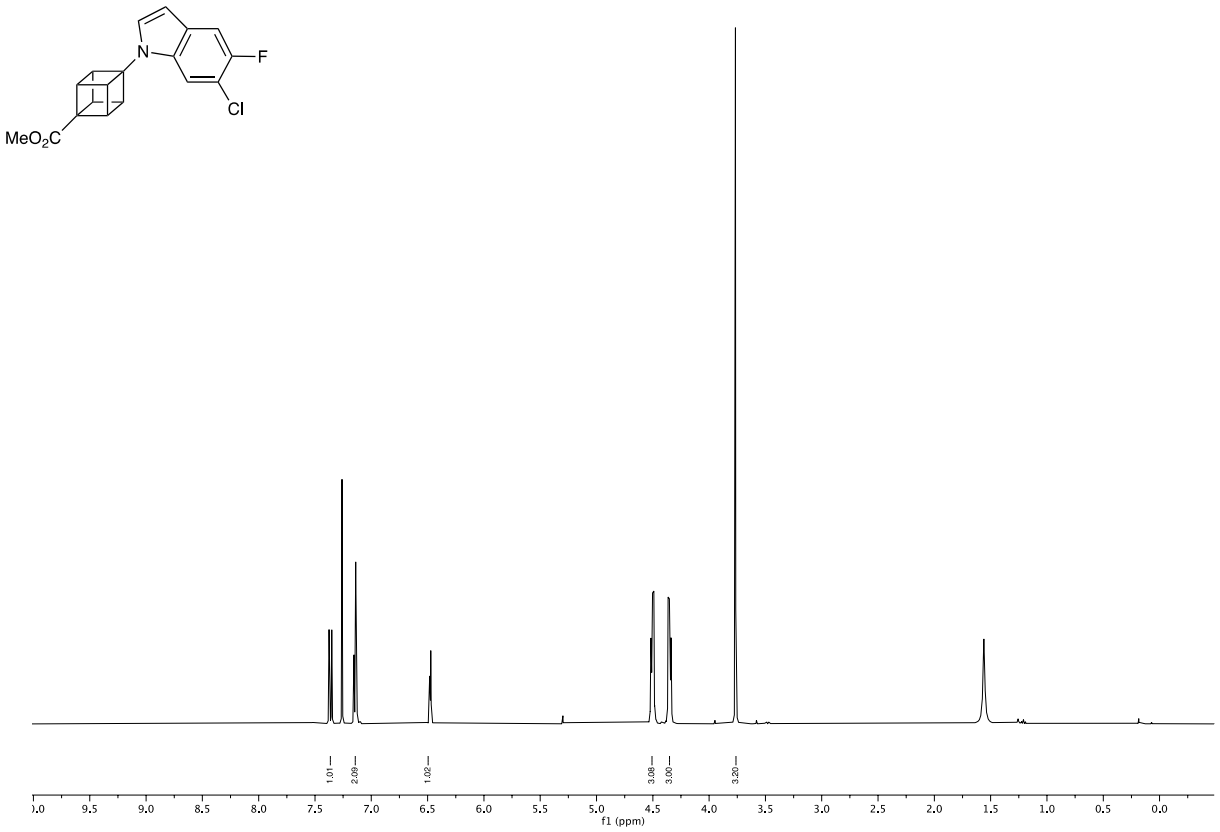
N
F
Cl
MeO2C
1.01
2.09
1.02
3.08
3.00
3.20
f1 (ppm)

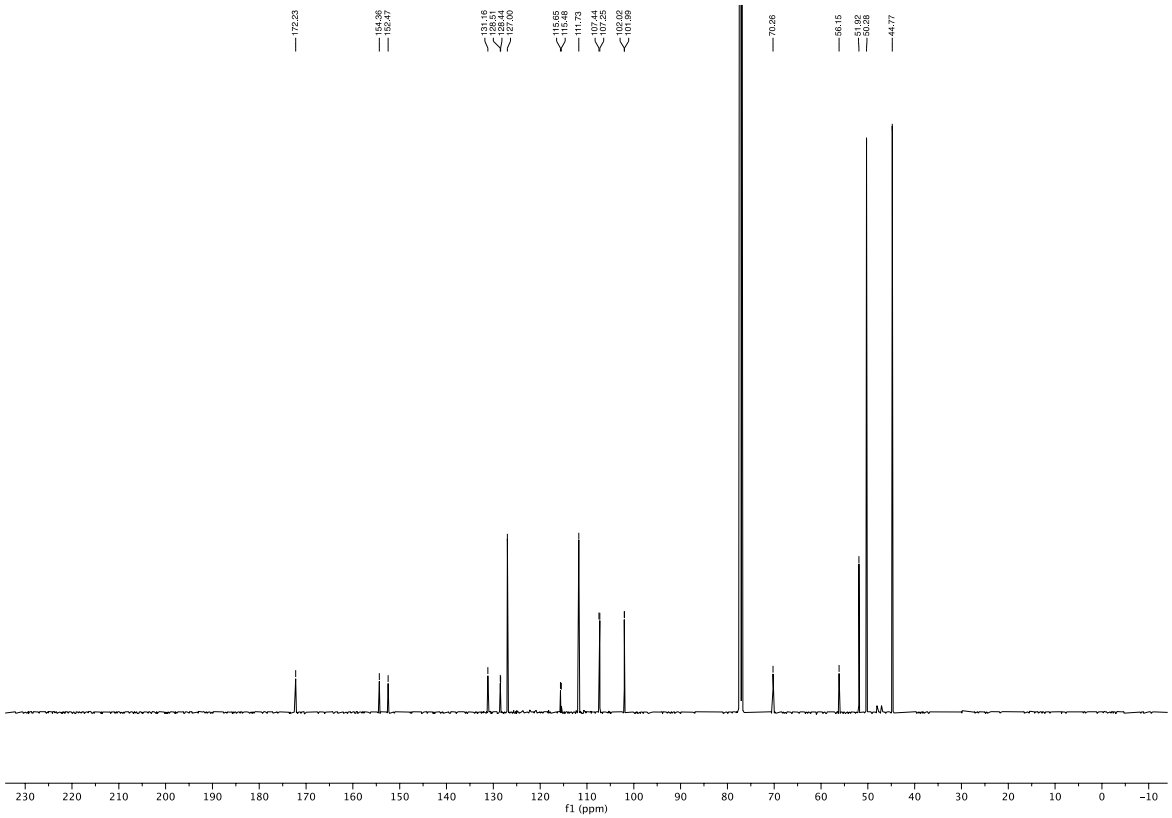
172.23
154.36
152.47
131.16
128.51
128.44
127.06
115.65
115.48
111.73
107.44
107.25
102.02
101.99
70.26
56.15
51.92
50.28
44.77
f1 (ppm)

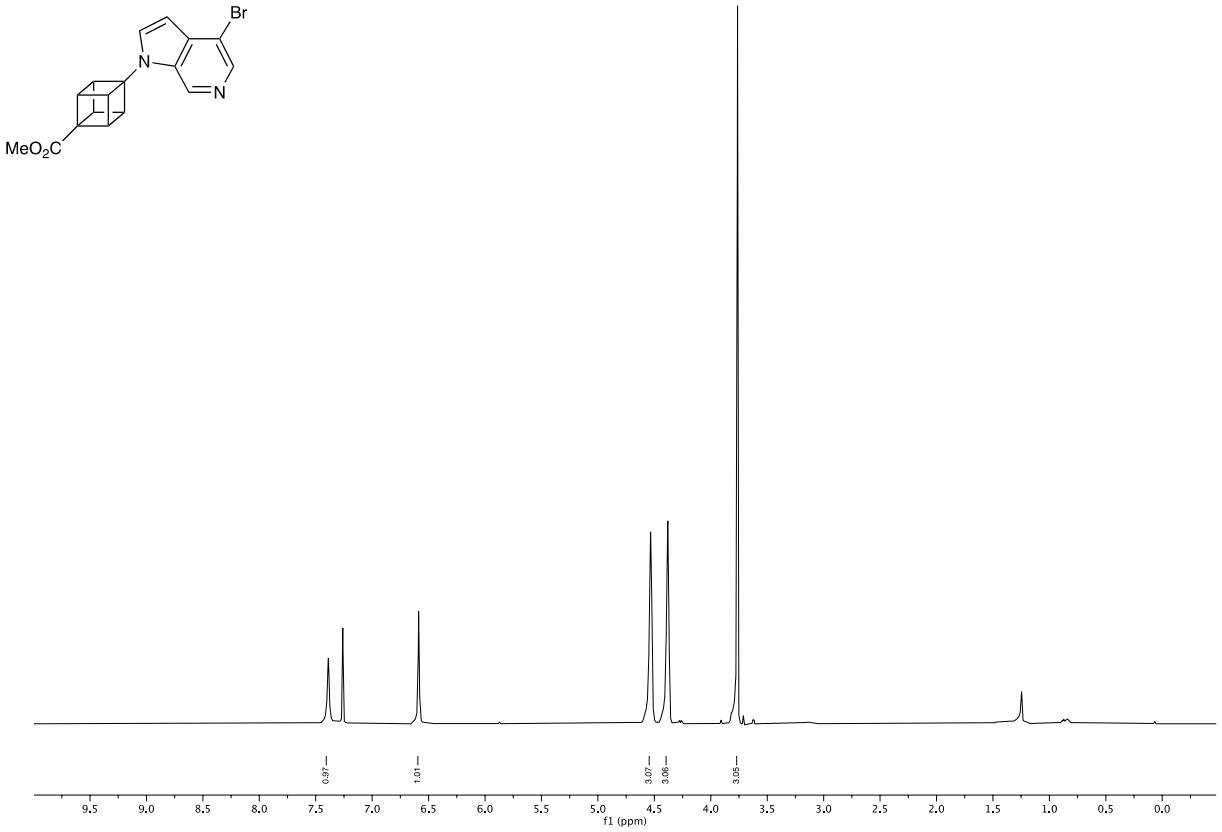
Br
N
N
MeO2C
0.97
1.01
3.07
3.06
3.05
f1 (ppm)

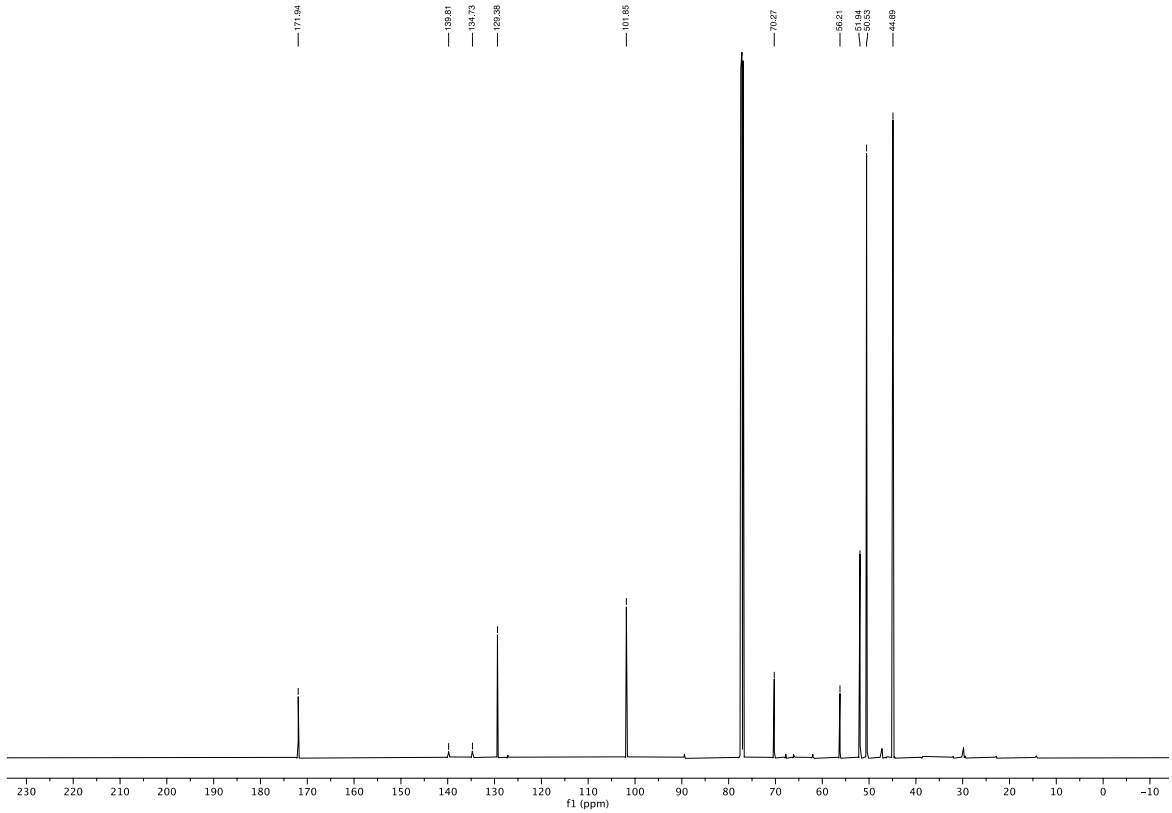
171.94
139.81
134.73
129.38
101.85
70.27
56.21
51.94
50.53
44.89
f1 (ppm)

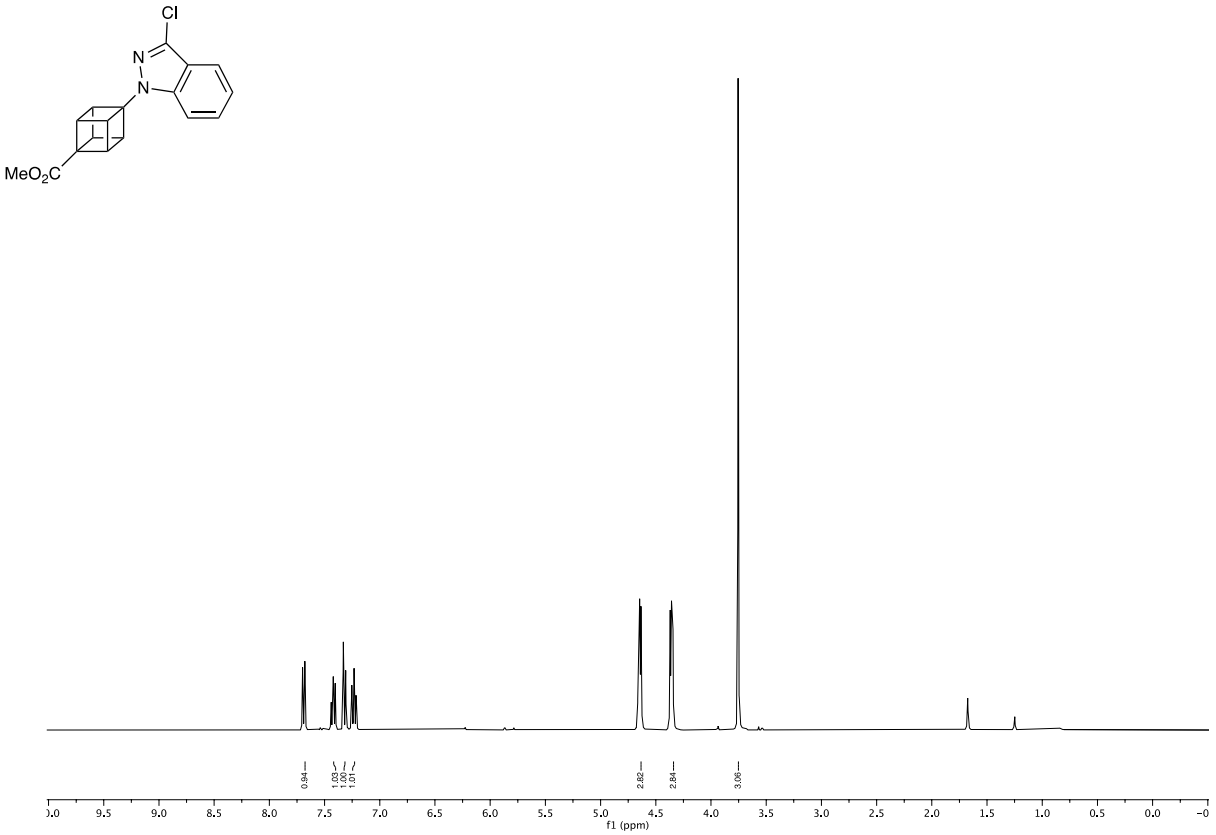
Cl
N
N
MeO2C
0.94
1.03
1.00
1.01
2.82
2.84
3.06
f1 (ppm)

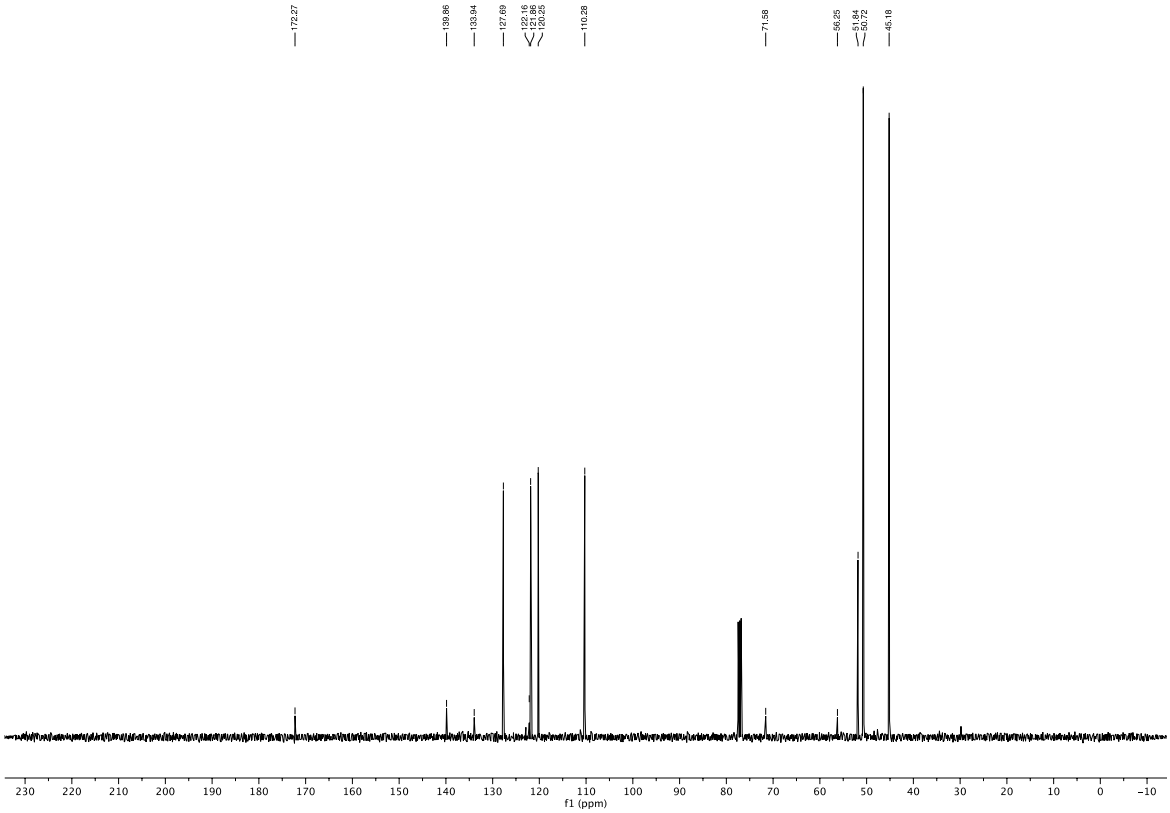
172.27
139.86
133.94
127.69
122.16
121.86
120.25
110.28
71.58
56.25
51.84
50.72
45.18
f1 (ppm)

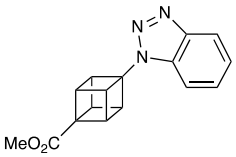
N
N
N
MeO2C

0.78
0.76
2.05
2.89
3.05
3.08
9.5 9.0 8.5 8.0 7.5 7.0 6.5 6.0 5.5 5.0 4.5 4.0 3.5 3.0 2.5 2.0 1.5 1.0 0.5 0.0
f1 (ppm)

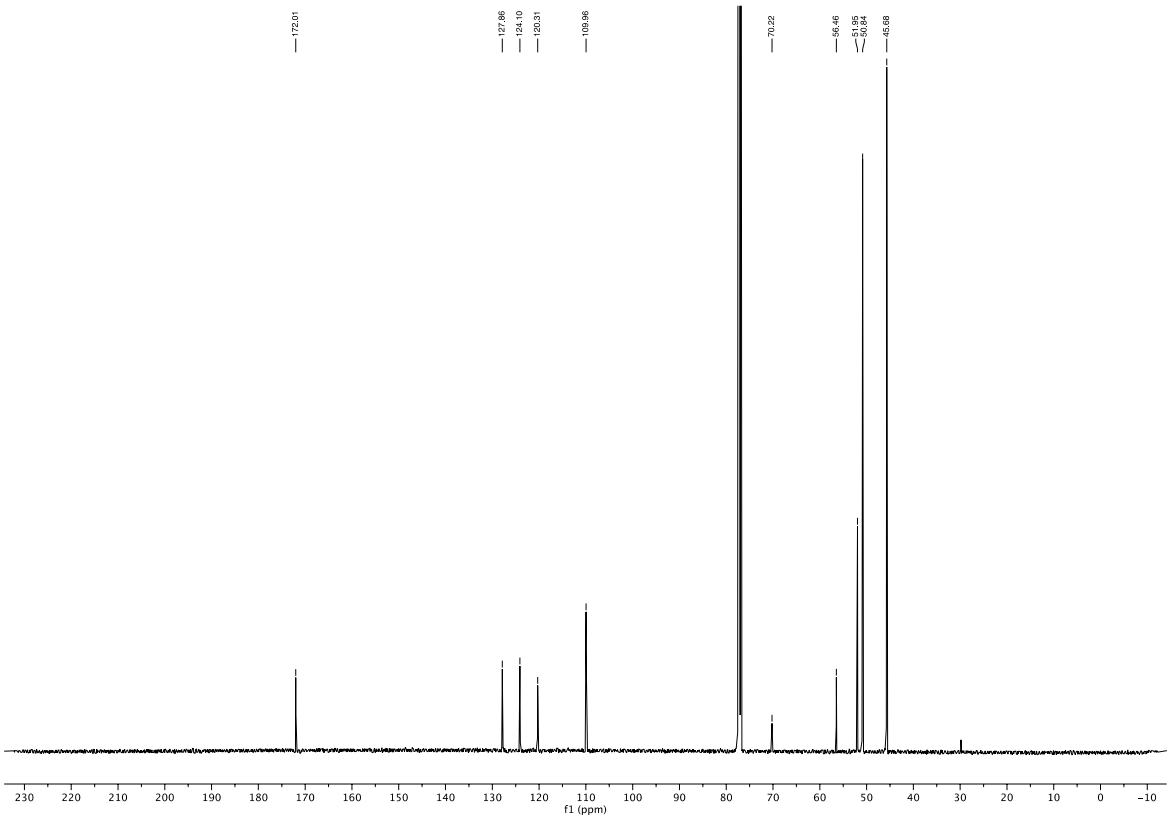
172.01
127.86
124.10
120.31
109.96
70.22
56.46
51.95
50.84
45.68
230 220 210 200 190 180 170 160 150 140 130 120 110 100 90 80 70 60 50 40 30 20 10 0 −10
f1 (ppm)

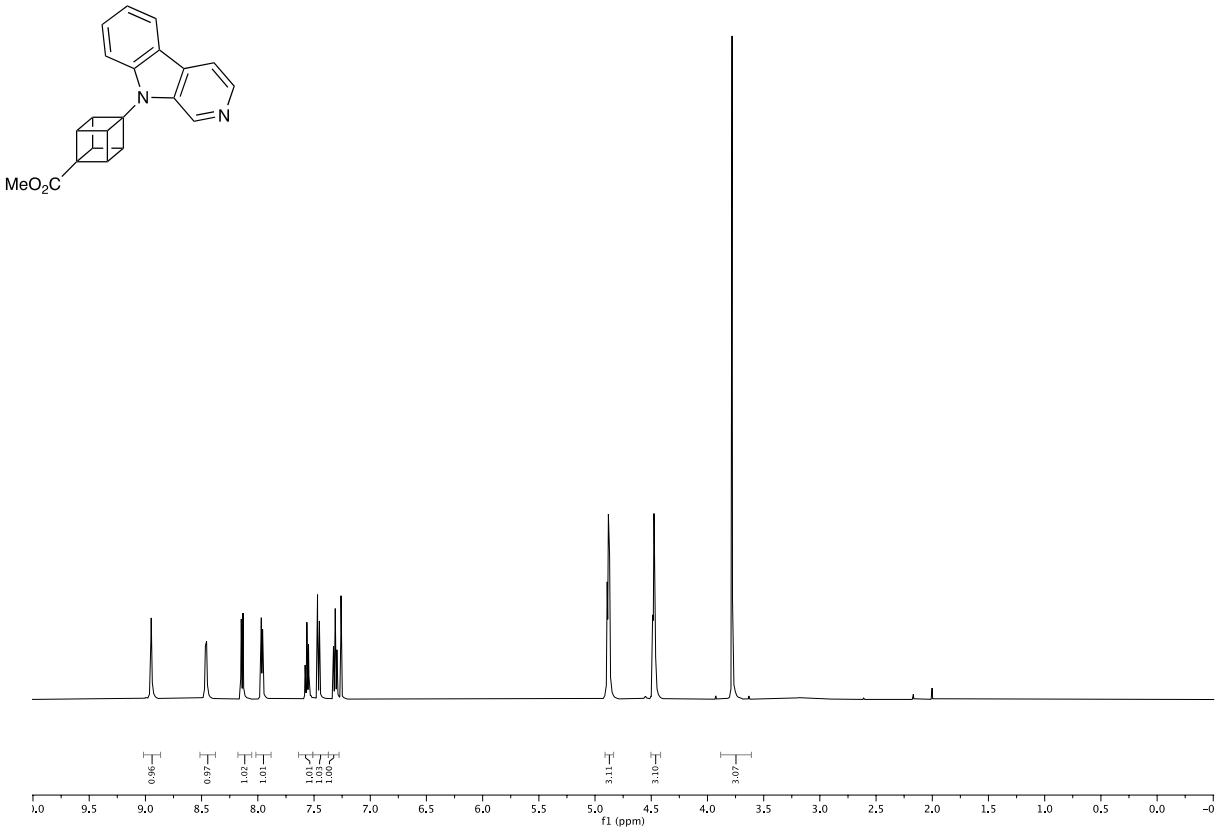
MeO2C
N
N
0.96
0.97
1.02
1.01
1.01
1.03
1.00
3.11
3.10
3.07
f1 (ppm)

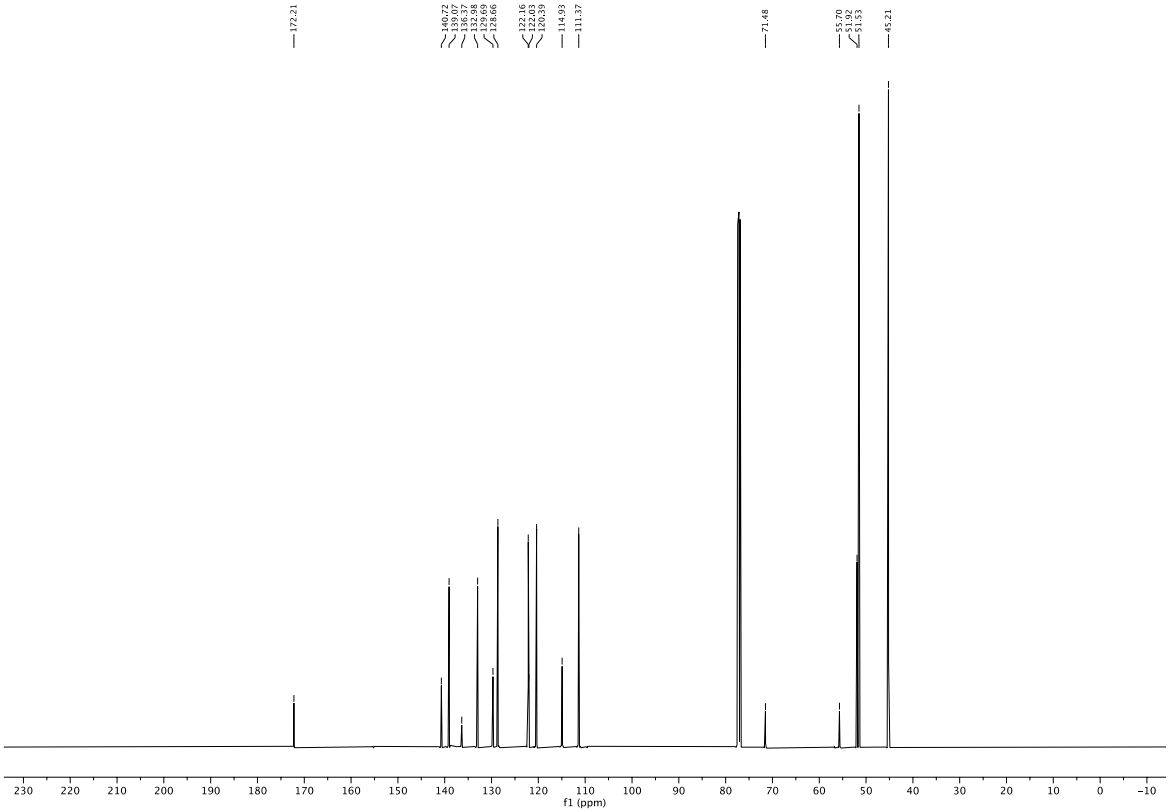
172.21
140.72
139.07
136.37
132.98
130.60
128.66
122.16
122.03
120.39
114.93
111.37
71.48
55.70
53.92
53.53
45.21
f1 (ppm)

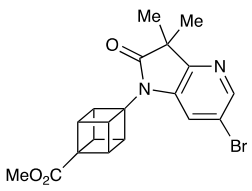
Me
Me
O
N
N
Br
MeO2C

1.06
0.98
3.00
2.99
3.09
6.14
10.5 10.0 9.5 9.0 8.5 8.0 7.5 7.0 6.5 6.0 5.5 5.0 4.5 4.0 3.5 3.0 2.5 2.0 1.5 1.0 0.5 0.0 -0.5 -1.0 -1.5
f1 (ppm)

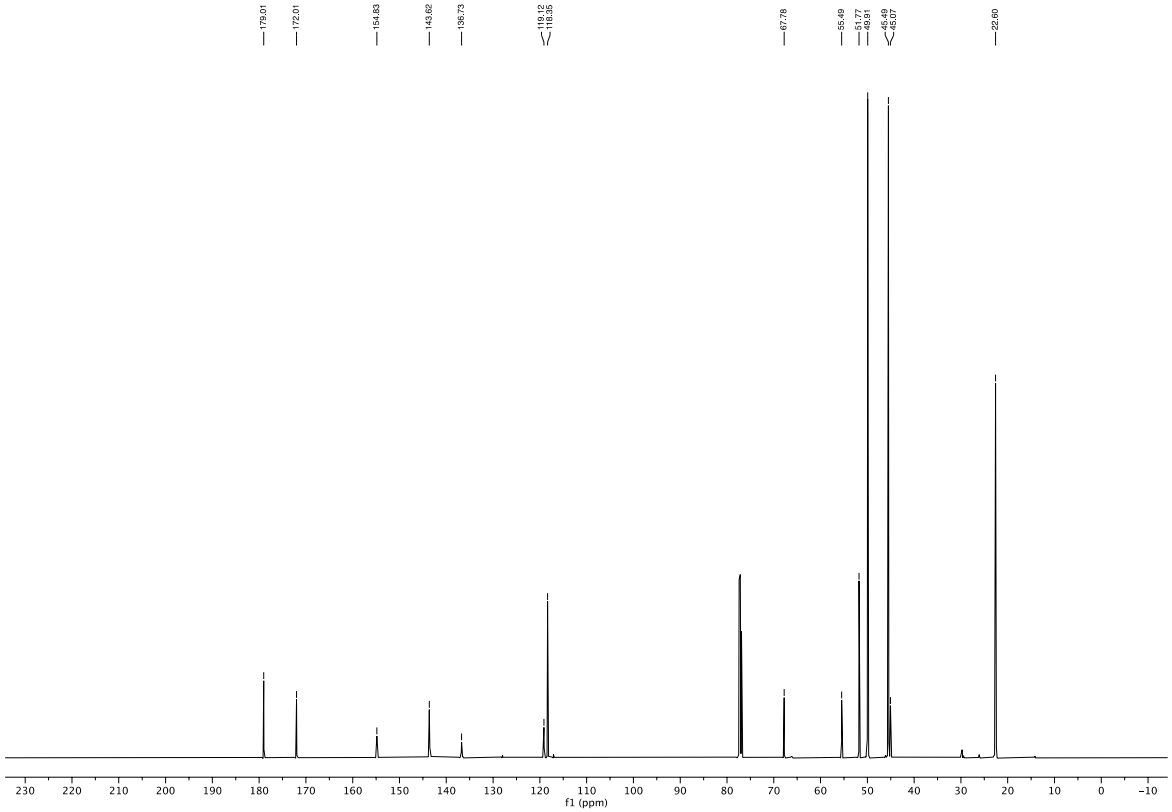
179.01
172.01
154.83
143.62
136.73
119.12
118.35
67.78
55.49
51.77
49.91
45.49
45.07
22.60
230 220 210 200 190 180 170 160 150 140 130 120 110 100 90 80 70 60 50 40 30 20 10 0 -10
f1 (ppm)

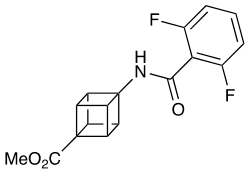
F
H
N
O
F
MeO2C

1.06
2.06
1.01
5.83
3.08
f1 (ppm)

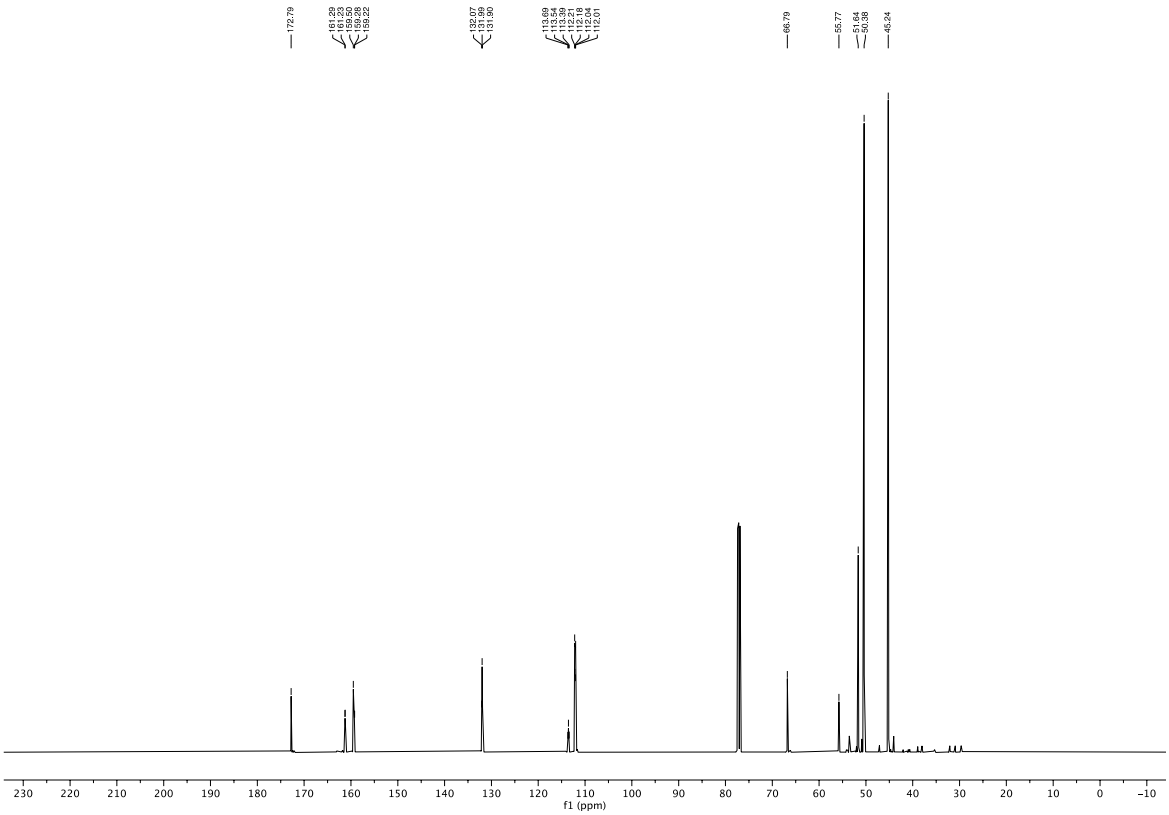
172.79
161.29
161.20
159.50
159.38
159.22
132.07
131.98
131.90
113.69
113.54
113.39
112.21
112.16
112.04
112.01
66.79
55.77
51.64
50.38
45.24
f1 (ppm)

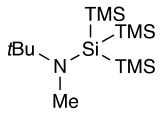
TMS
TMS
tBu
Si
N
TMS
Me

3.00
9.37
27.17
f1 (ppm)

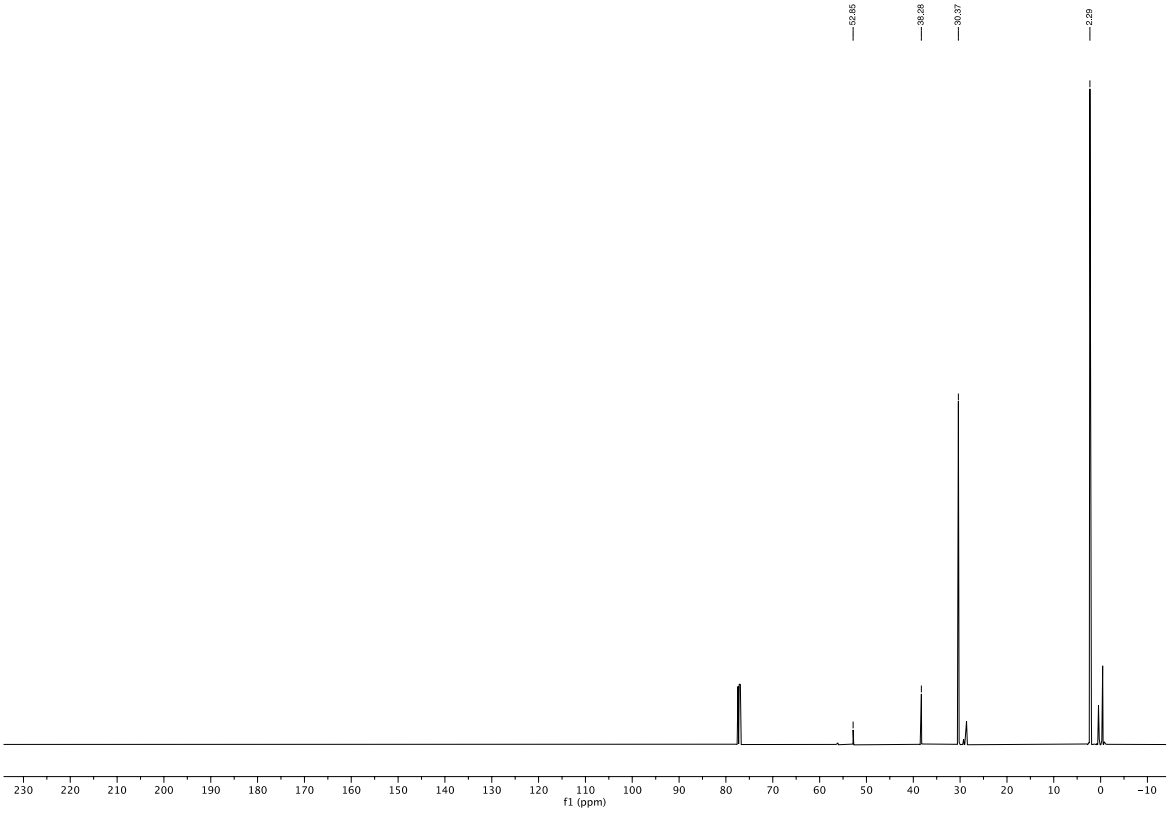
62.85
38.28
30.57
2.89
f1 (ppm)

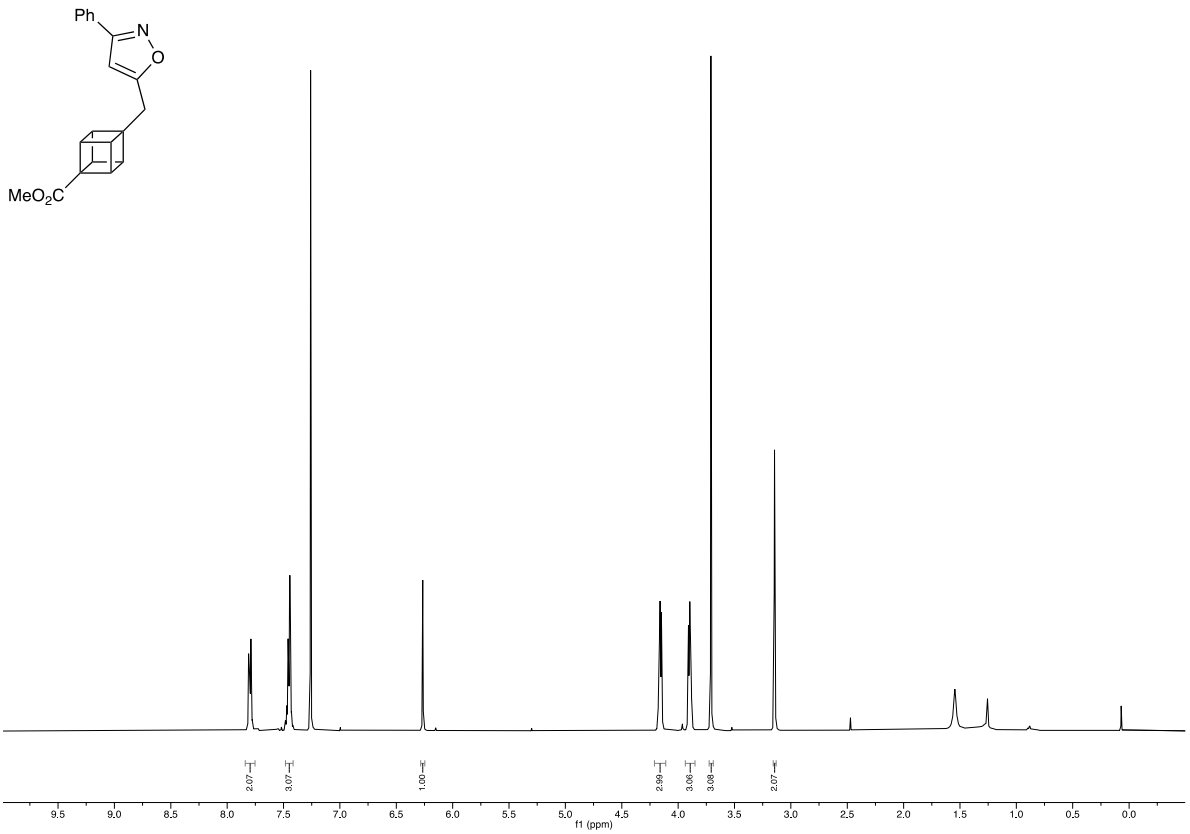
Ph
N
O
MeO2C
2.07
3.07
1.00
2.99
3.06
3.08
2.07
f1 (ppm)

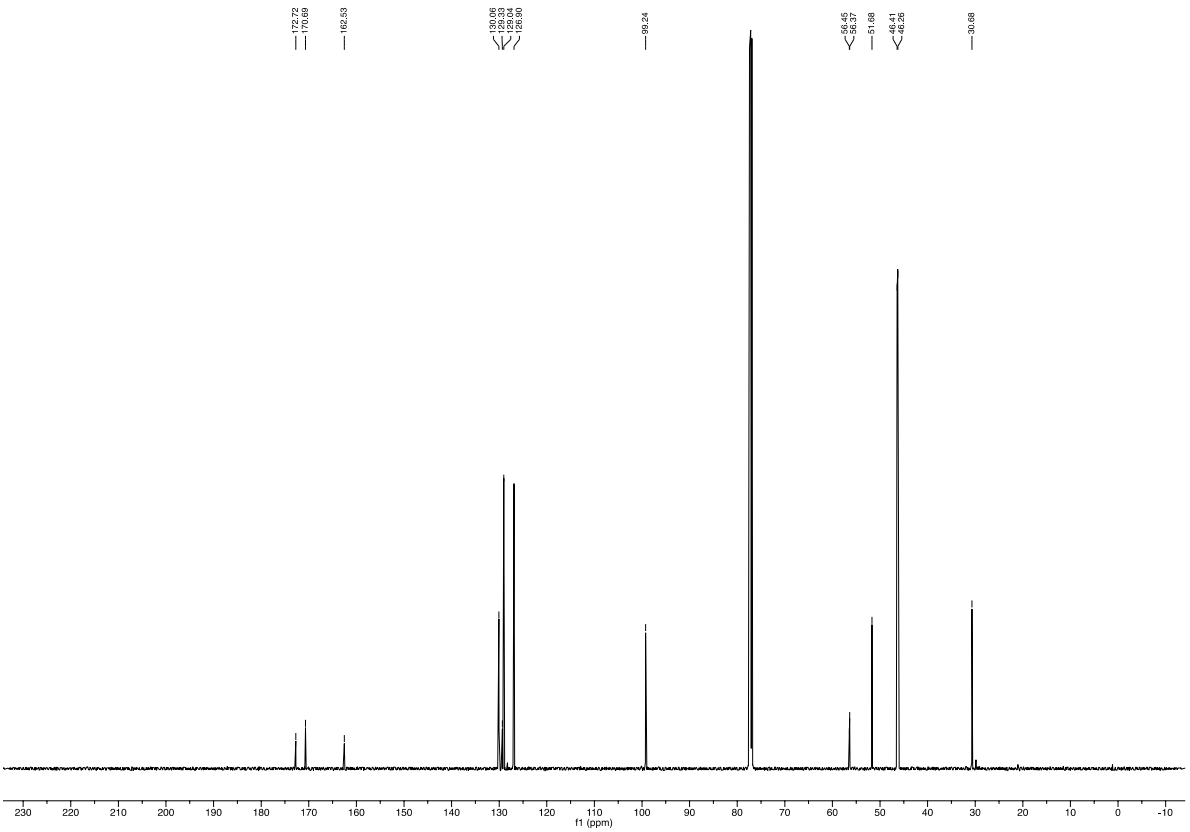
172.72
170.69
162.53
130.06
129.33
129.14
126.90
99.24
56.45
56.37
51.68
46.41
46.25
30.68
f1 (ppm)

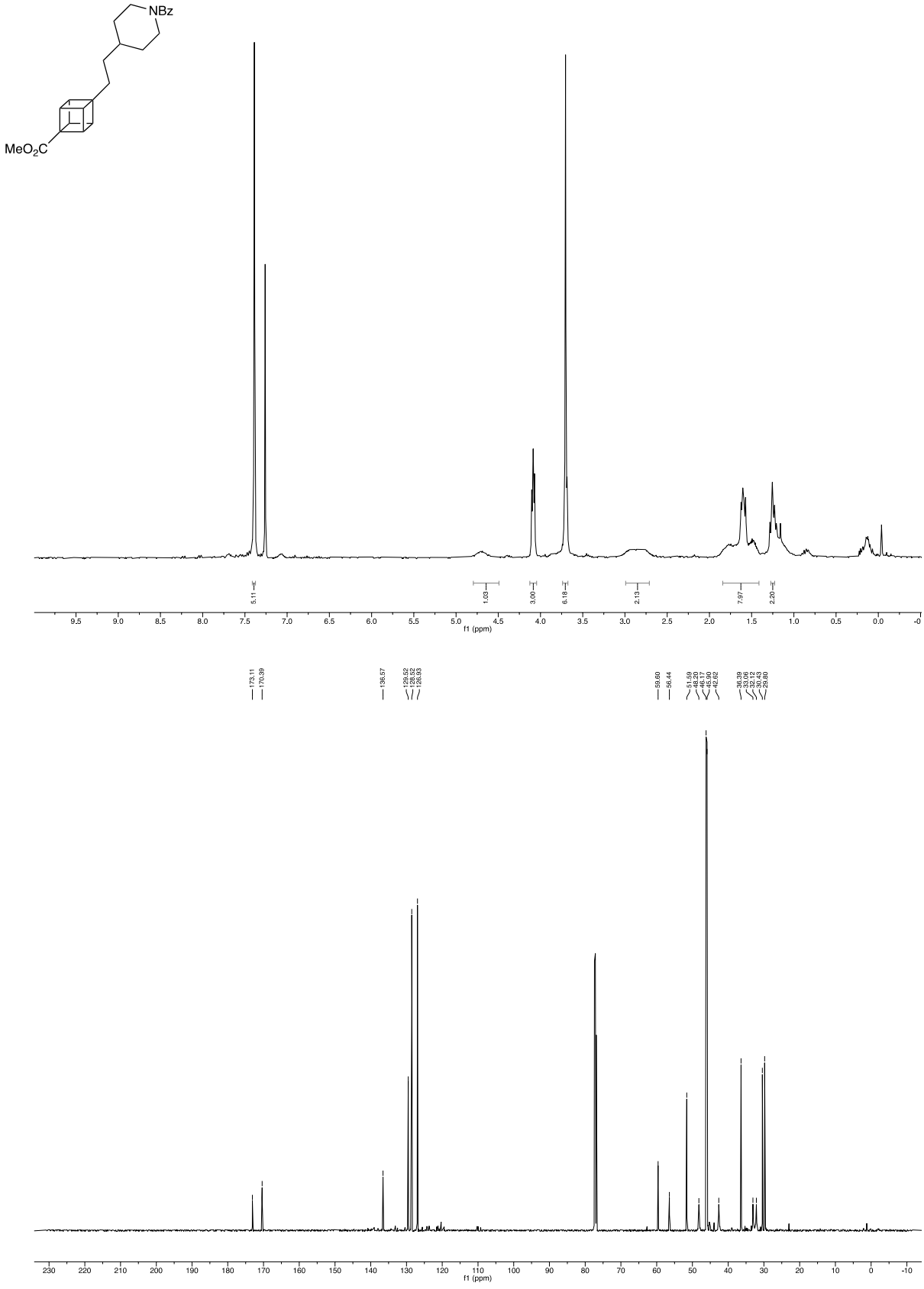
NBz
MeO2C
5.11
1.03
3.00
6.18
2.13
7.97
2.20
f1 (ppm)
173.11
170.39
136.57
129.52
128.33
126.93
59.60
56.44
51.19
48.20
46.17
45.00
42.62
36.39
33.06
32.73
30.43
29.80
f1 (ppm)

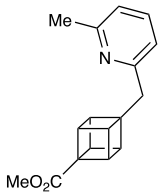
Me
N
MeO2C

1.07
1.00
0.98
2.96
3.02
3.06
2.01
3.10
f1 (ppm)

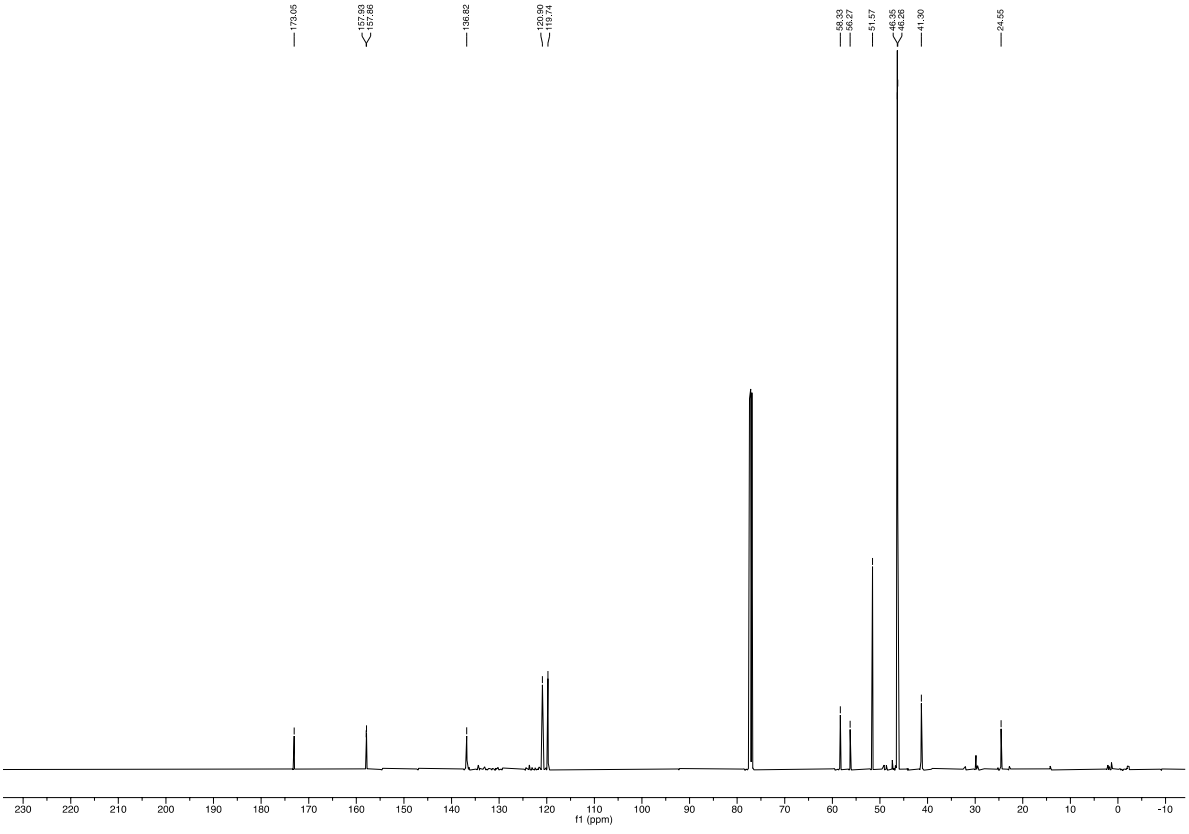
173.05
157.93
157.66
136.82
120.60
119.74
58.33
56.27
51.57
46.35
45.85
41.30
24.55
f1 (ppm)

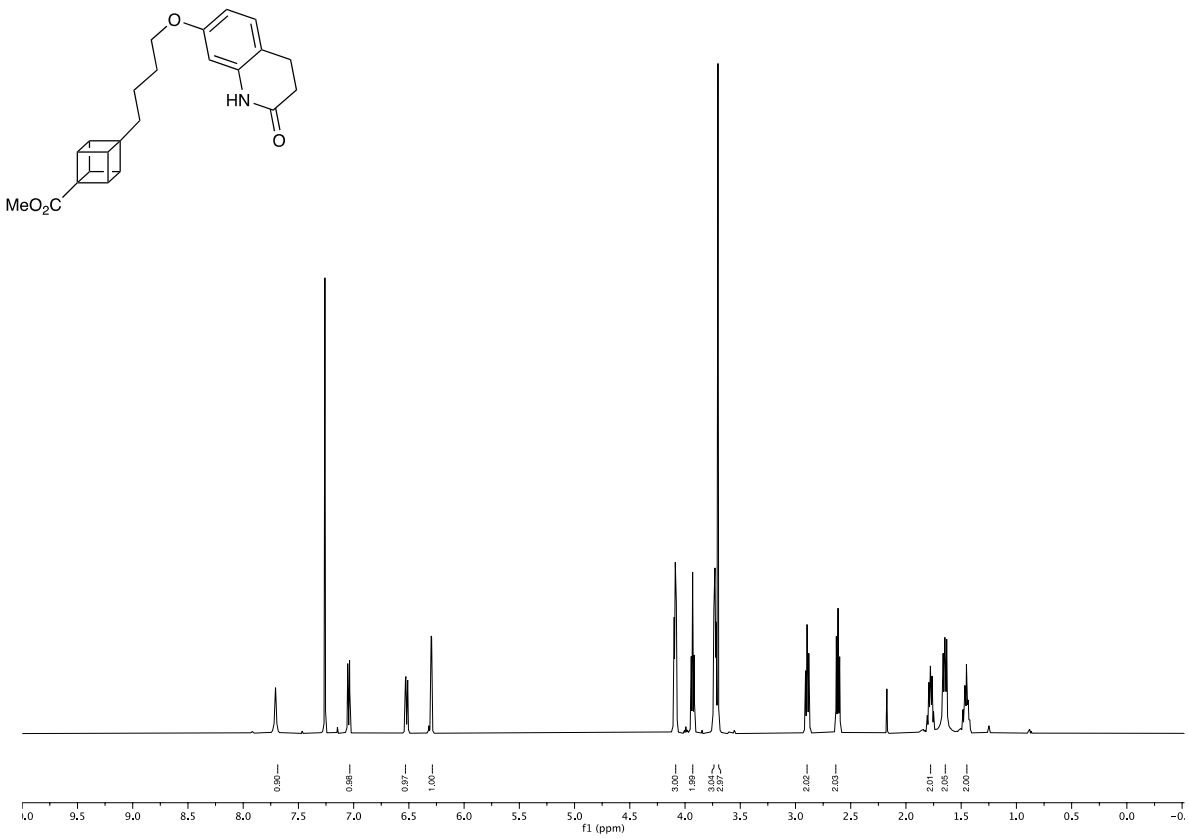
O
HN
O
MeO2C
0.90
0.98
0.97
1.00
3.00
1.89
3.04
2.97
2.02
2.03
2.01
2.08
2.00
f1 (ppm)

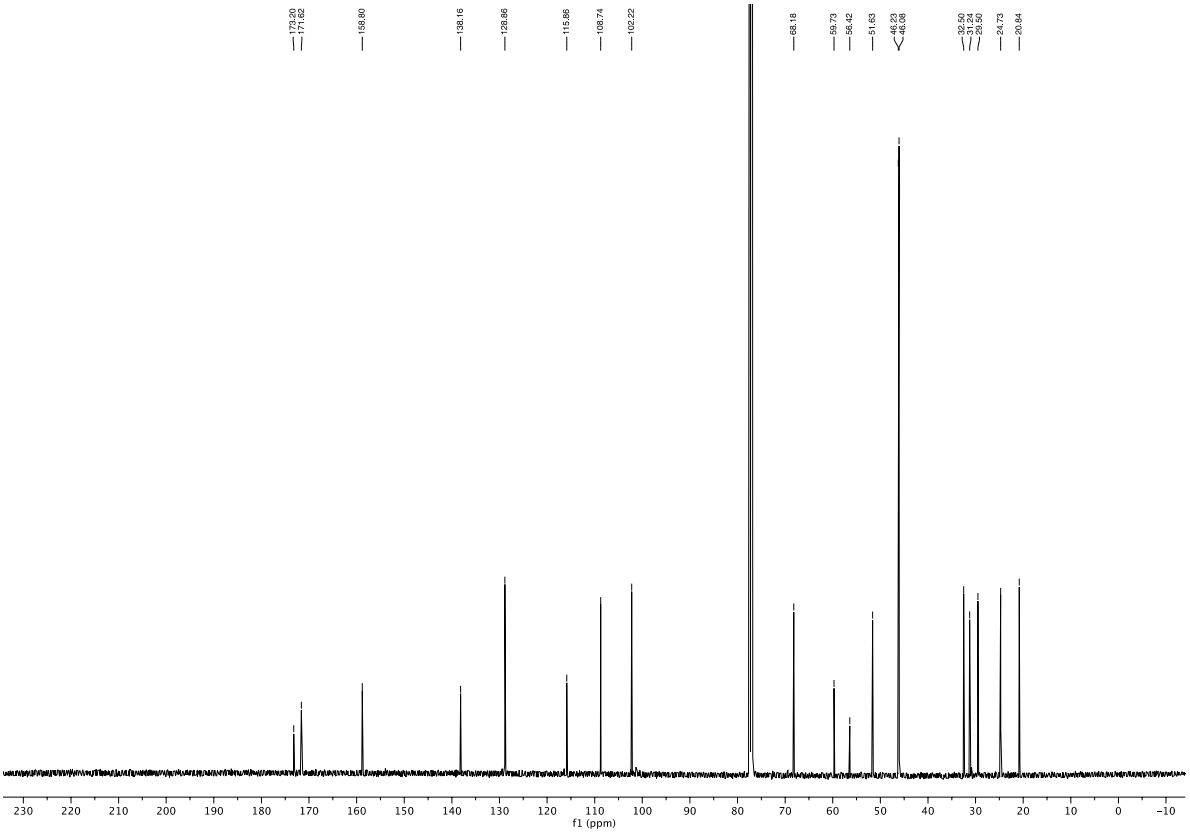
173.20
171.62
158.80
138.16
128.86
115.86
108.74
102.22
68.18
59.73
58.42
51.63
46.23
46.08
36.50
31.24
29.50
24.73
20.84
f1 (ppm)

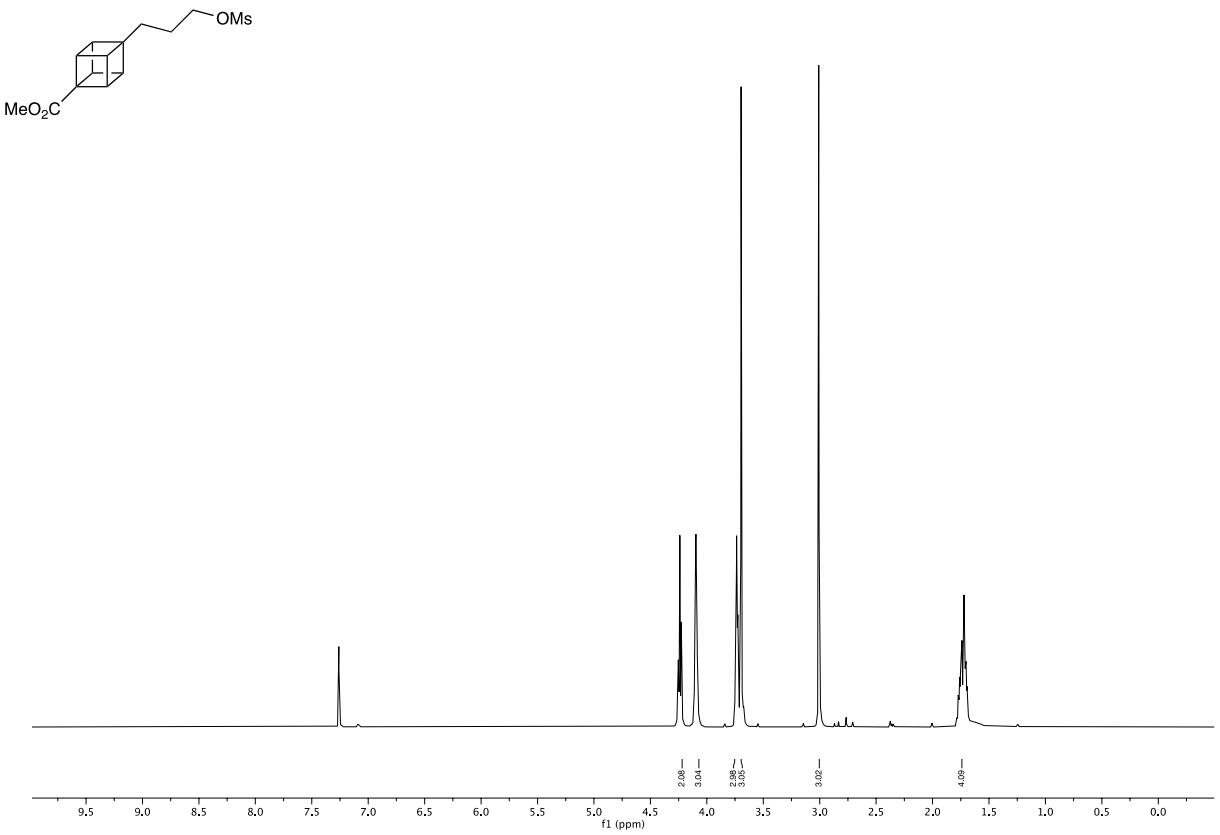
OMs
MeO2C
2.08
3.04
2.98
3.05
3.02
4.09
f1 (ppm)

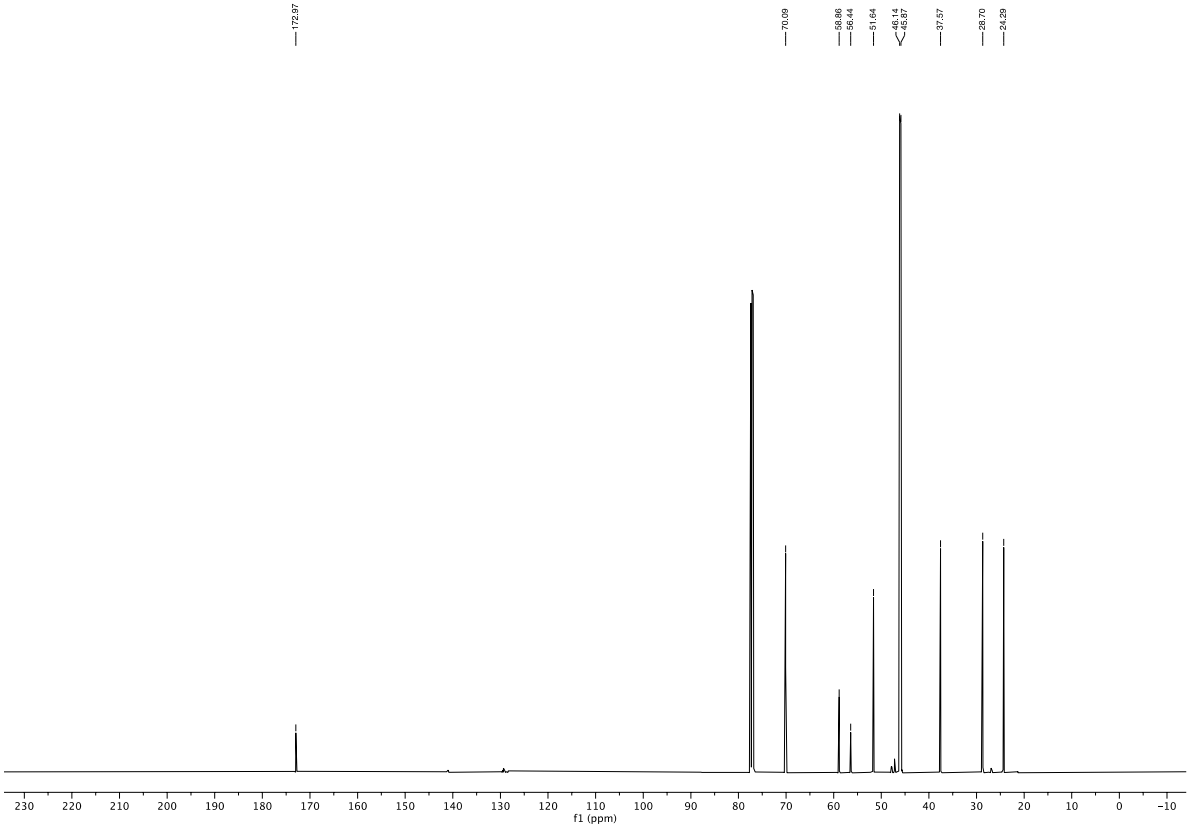
172.97
70.09
58.86
56.44
51.64
46.14
45.87
37.57
28.70
24.29
f1 (ppm)

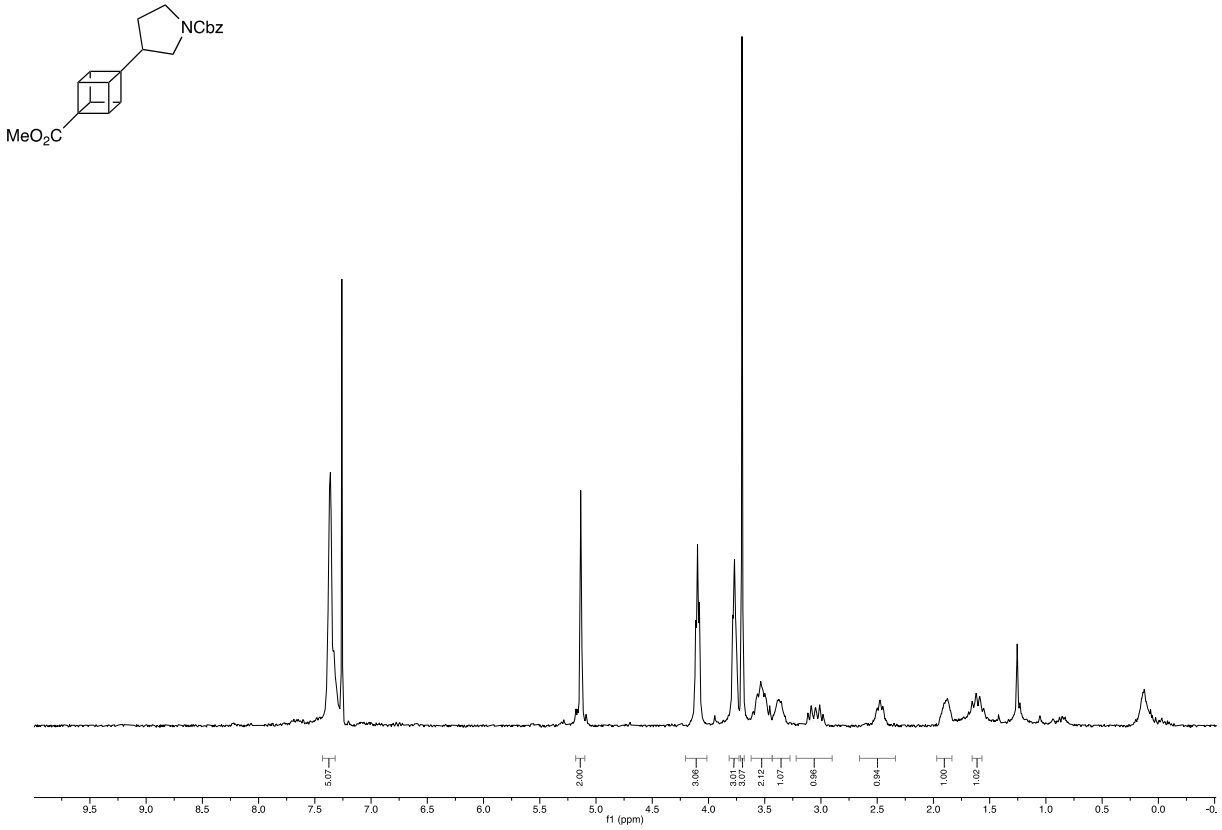
NCbz
MeO2C
5.07
2.00
3.06
3.01
3.07
2.12
1.07
0.96
0.94
1.00
1.02
f1 (ppm)

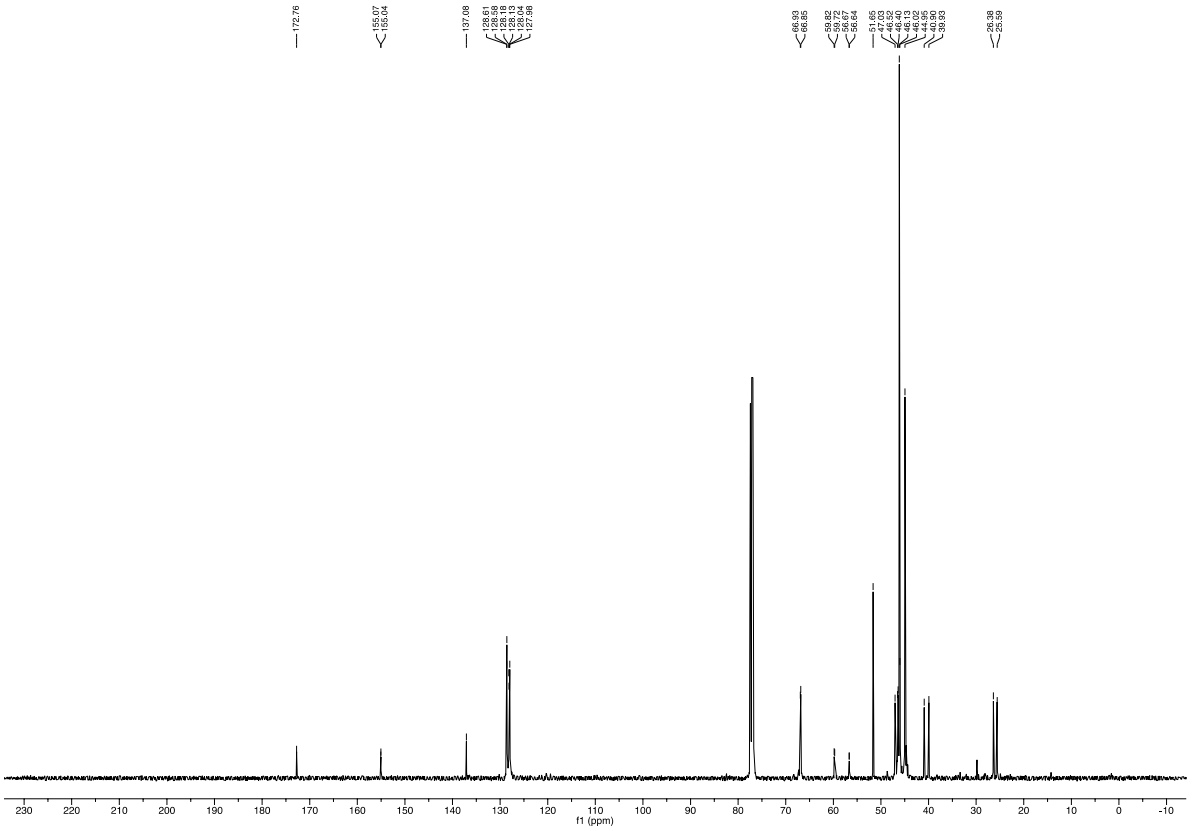
172.78
155.07
155.04
137.08
128.61
128.49
128.18
128.13
128.04
127.98
66.93
66.85
59.82
59.72
58.77
58.64
51.66
47.03
46.92
44.40
44.13
44.02
41.95
40.90
39.93
26.38
25.59
f1 (ppm)

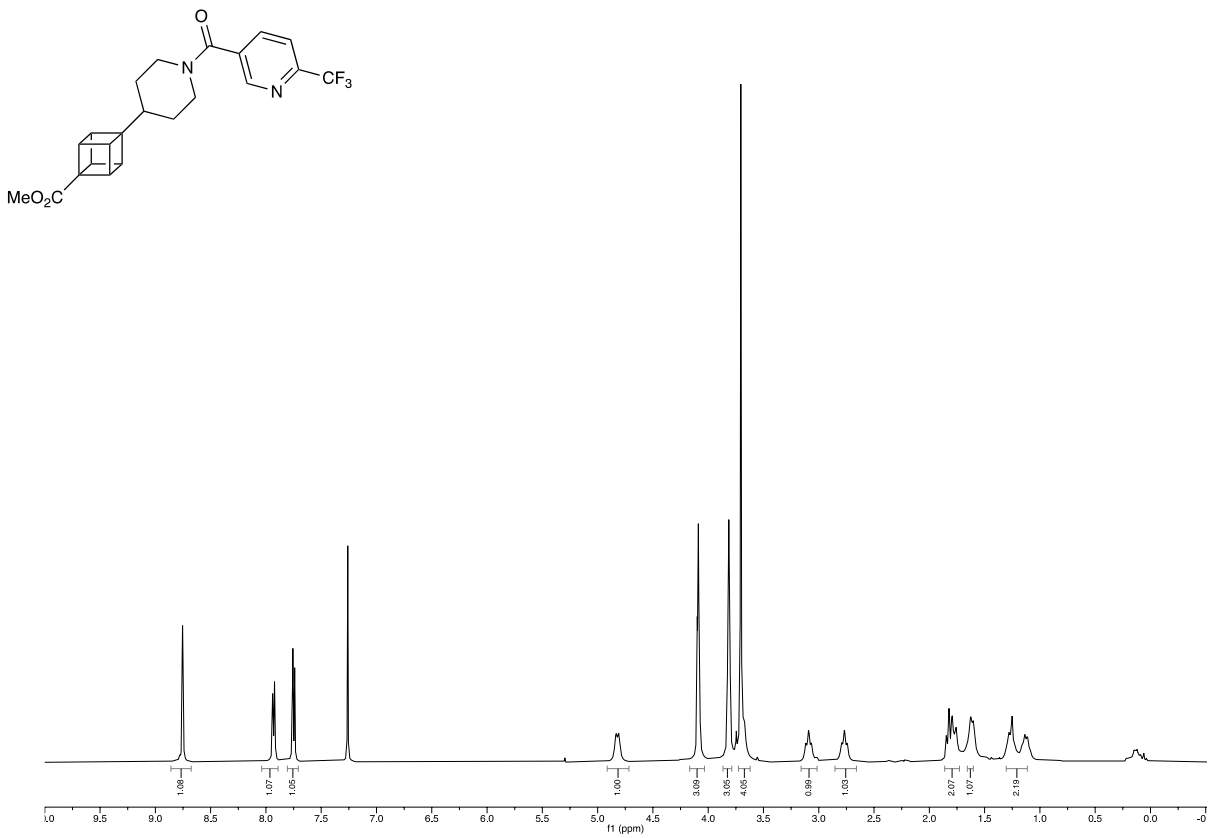
O
N
N
CF3
MeO2C
1.08
1.07
1.05
1.00
3.09
3.05
4.05
0.99
1.03
2.07
1.07
2.19
f1 (ppm)

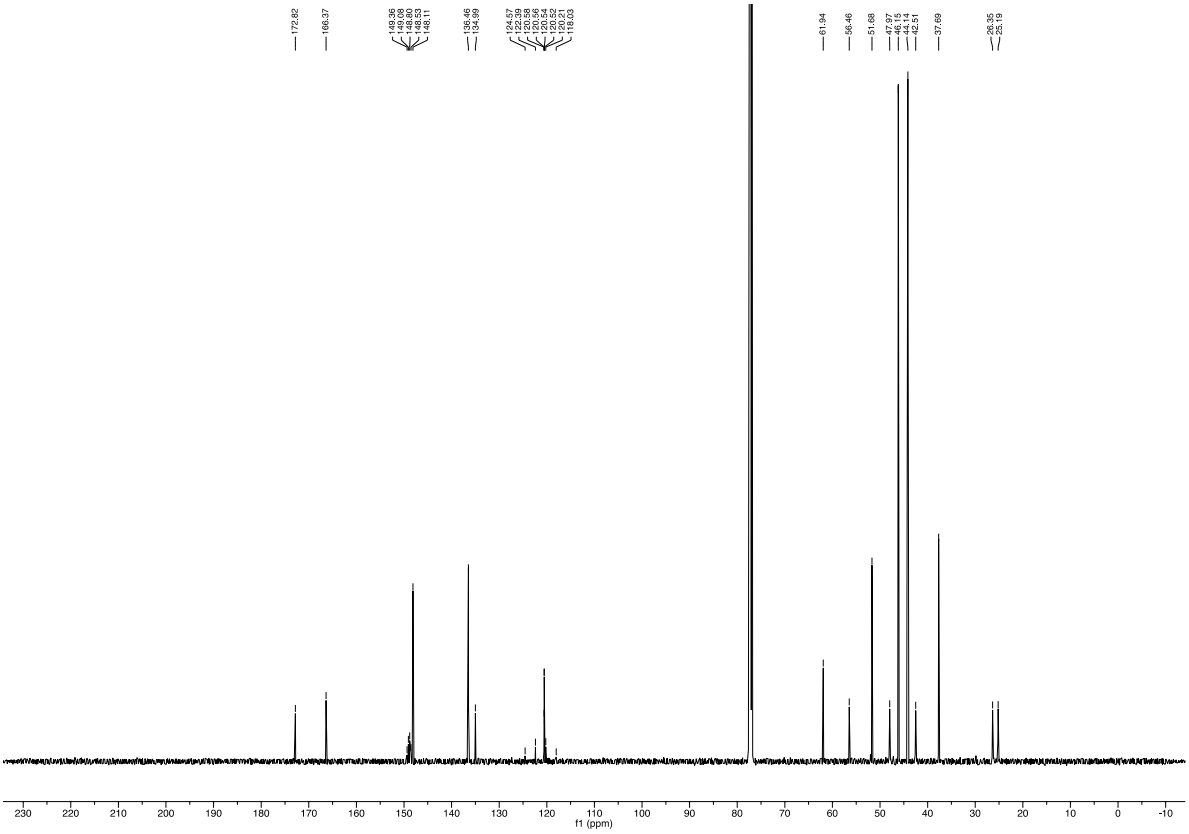
172.82
166.37
149.36
149.08
148.80
148.53
146.11
135.46
134.99
124.57
122.39
120.58
120.36
120.54
120.33
120.21
118.03
61.94
56.46
51.88
47.97
46.15
44.14
42.91
37.69
26.35
25.19
f1 (ppm)

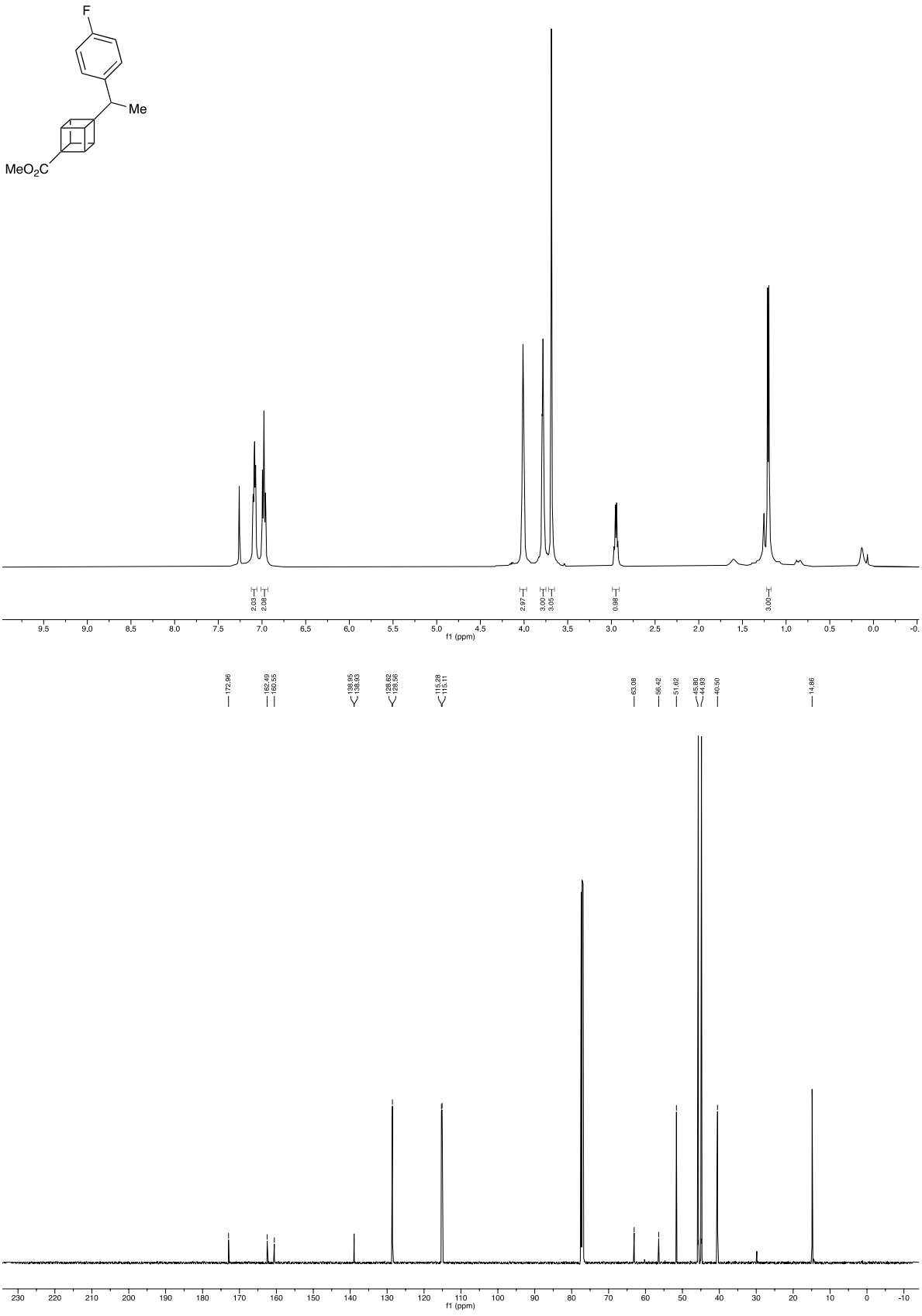
F
Me
MeO2C
2.03
2.08
2.97
3.00
3.05
0.98
3.00
f1 (ppm)
172.96
160.49
160.55
138.95
138.93
128.62
128.56
115.28
115.11
63.08
56.42
51.62
45.80
44.93
40.50
14.86
f1 (ppm)

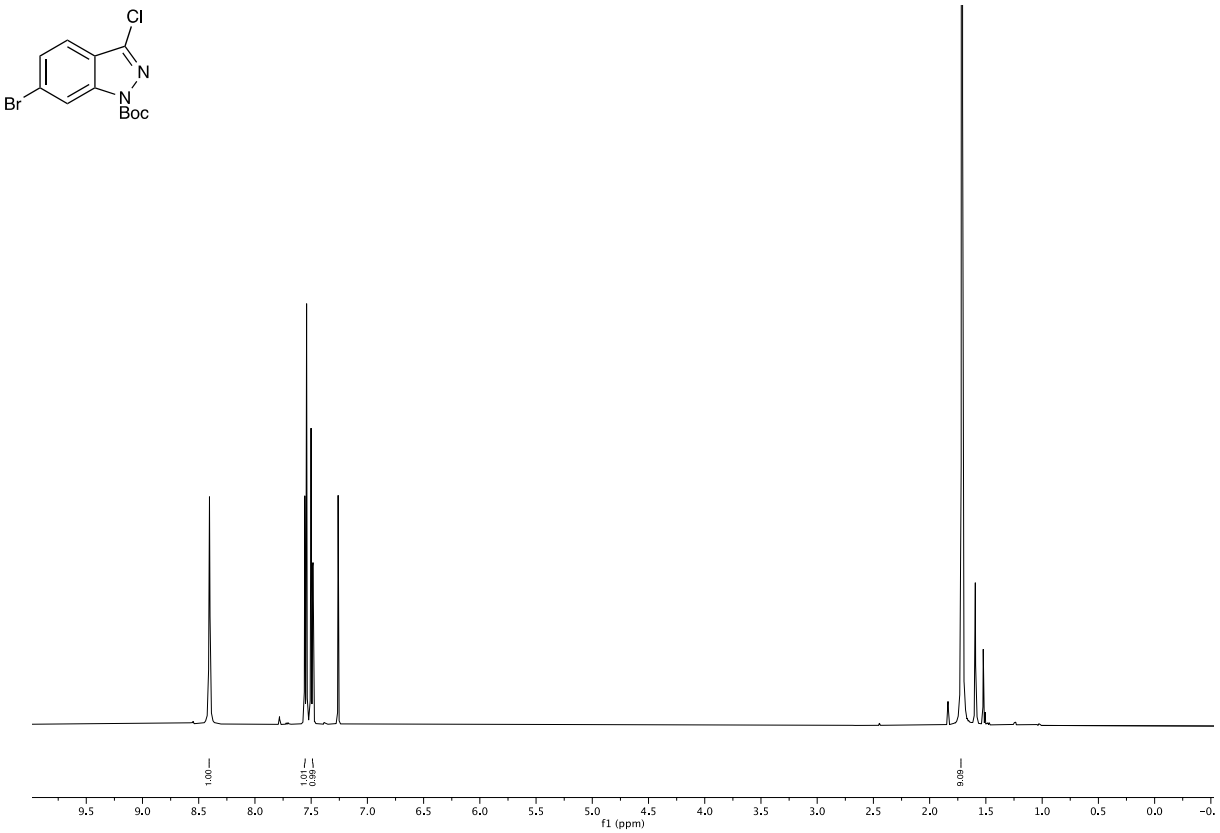
Cl
N
N
Boc
Br
1.00
1.01
0.99
9.09
f1 (ppm)

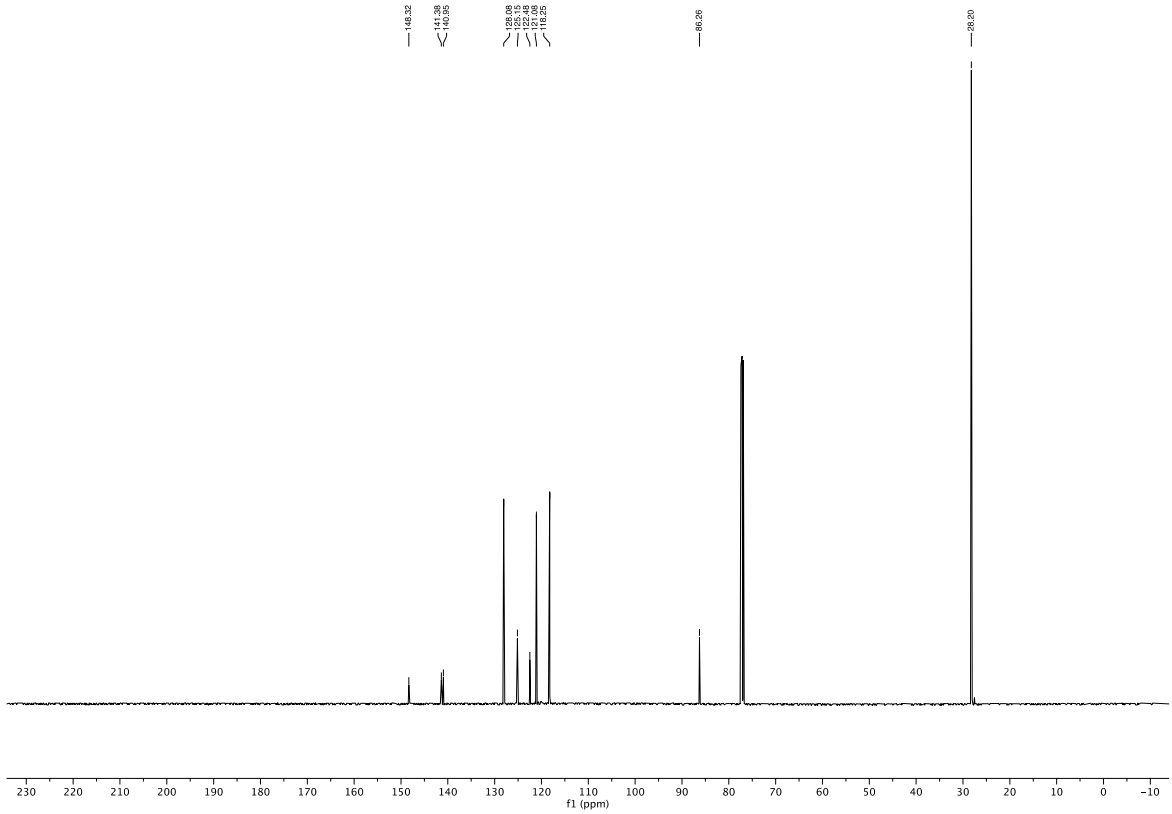
148.32
141.38
140.95
128.08
125.15
122.48
121.08
116.25
86.26
28.20
f1 (ppm)

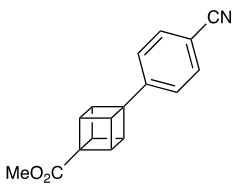
CN
MeO2C

1.99
2.01
3.00
2.98
3.14
f1 (ppm)

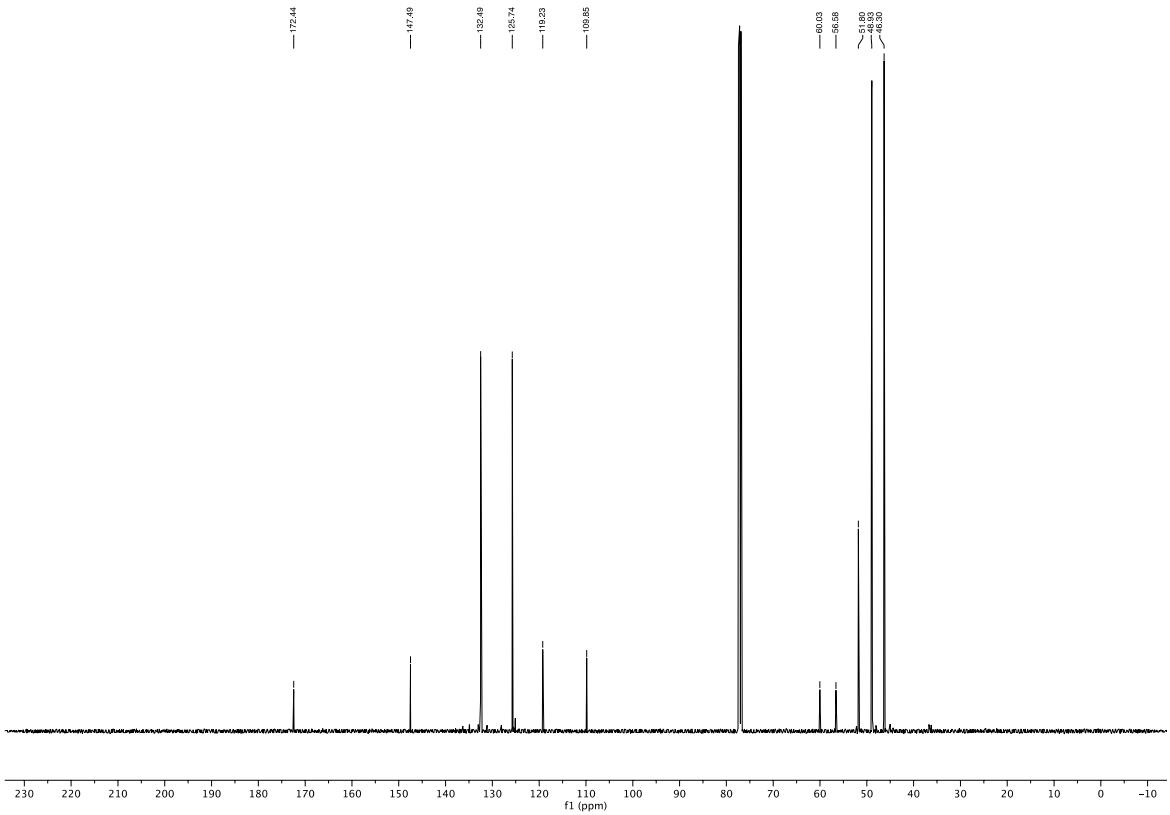
172.44
147.49
132.49
125.74
119.23
109.85
60.03
56.58
51.80
48.93
46.30
f1 (ppm)

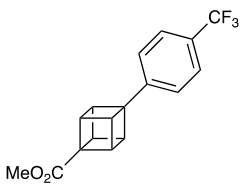
CF3
MeO2C

2.00
1.98
3.02
3.03
3.00
f1 (ppm)

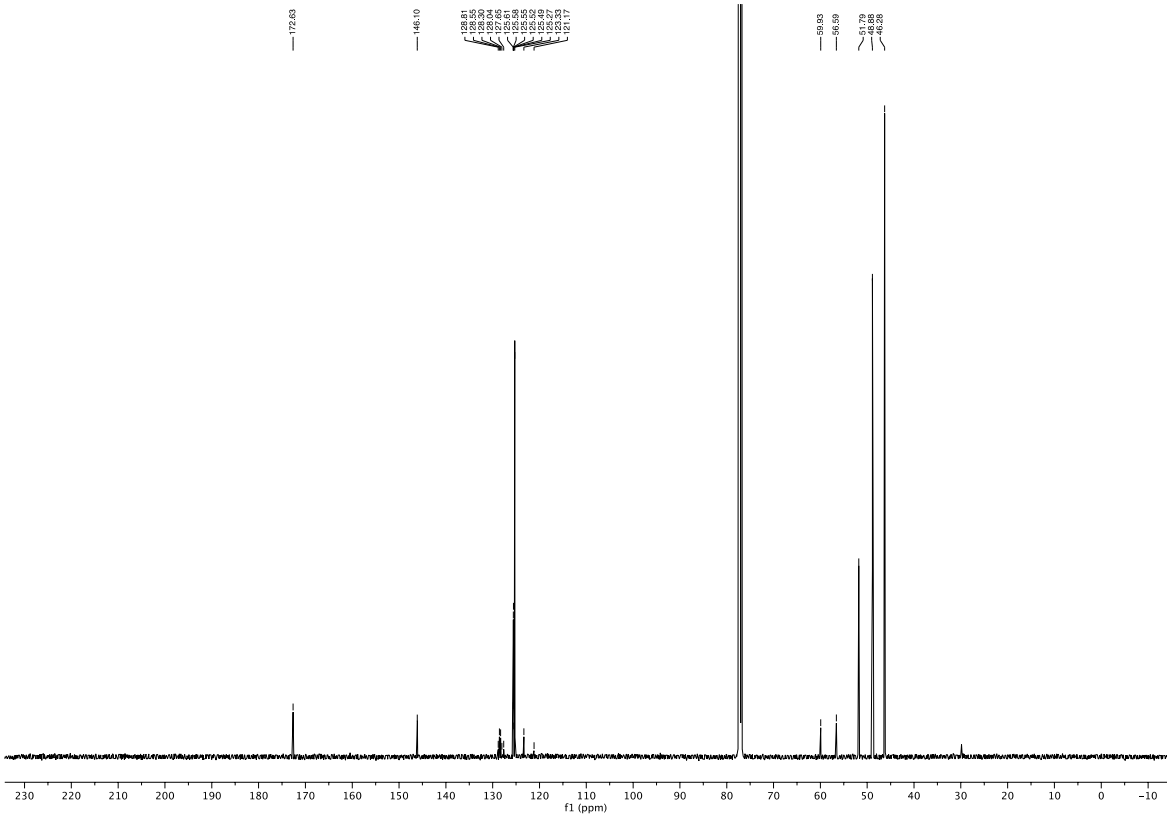
172.63
146.10
128.81
128.55
128.30
128.04
127.45
125.61
125.58
125.55
126.52
125.49
125.27
123.33
121.17
59.93
56.59
51.79
46.88
46.28
f1 (ppm)

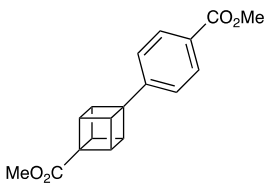
CO2Me
MeO2C

2.03
1.98
2.96
3.00
3.03
2.99
f1 (ppm)

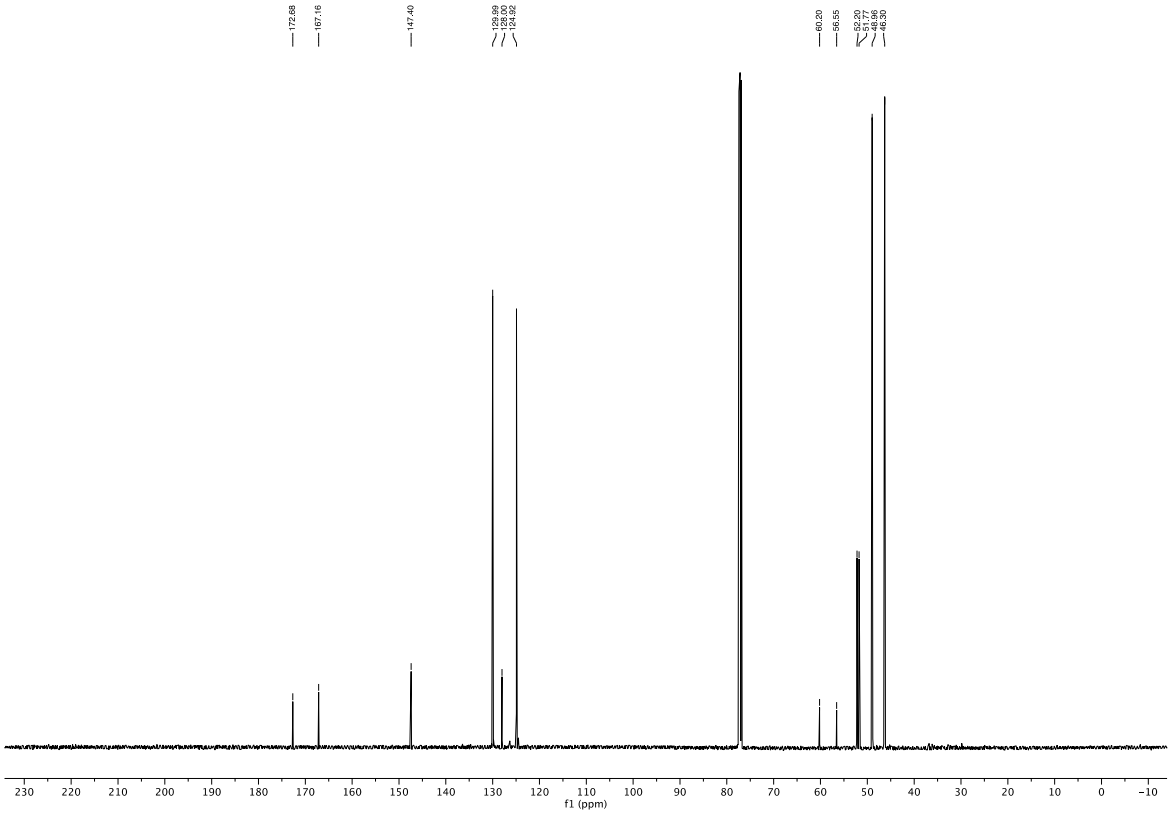
172.68
167.16
147.40
129.99
128.00
124.92
60.20
56.85
52.20
51.77
49.66
46.30
f1 (ppm)

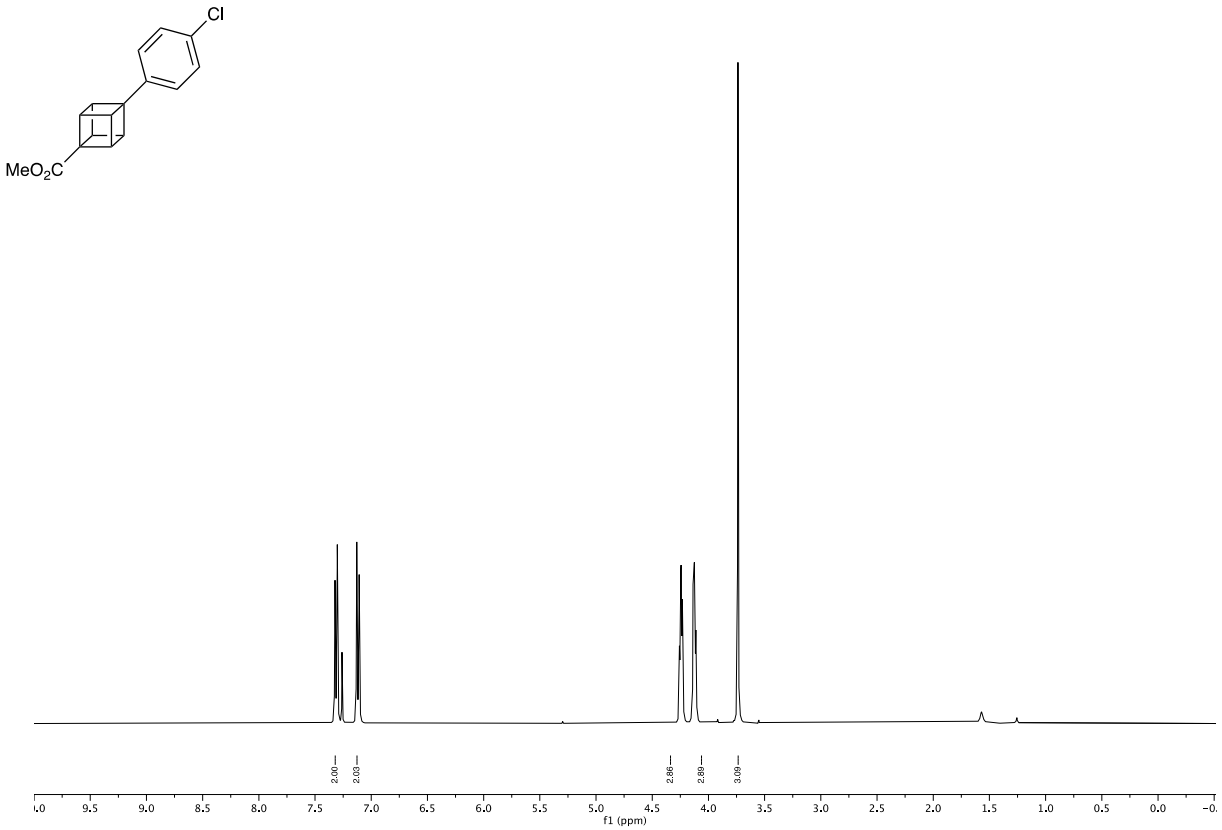
Cl
MeO2C
2.00
2.03
2.86
2.89
3.09
f1 (ppm)

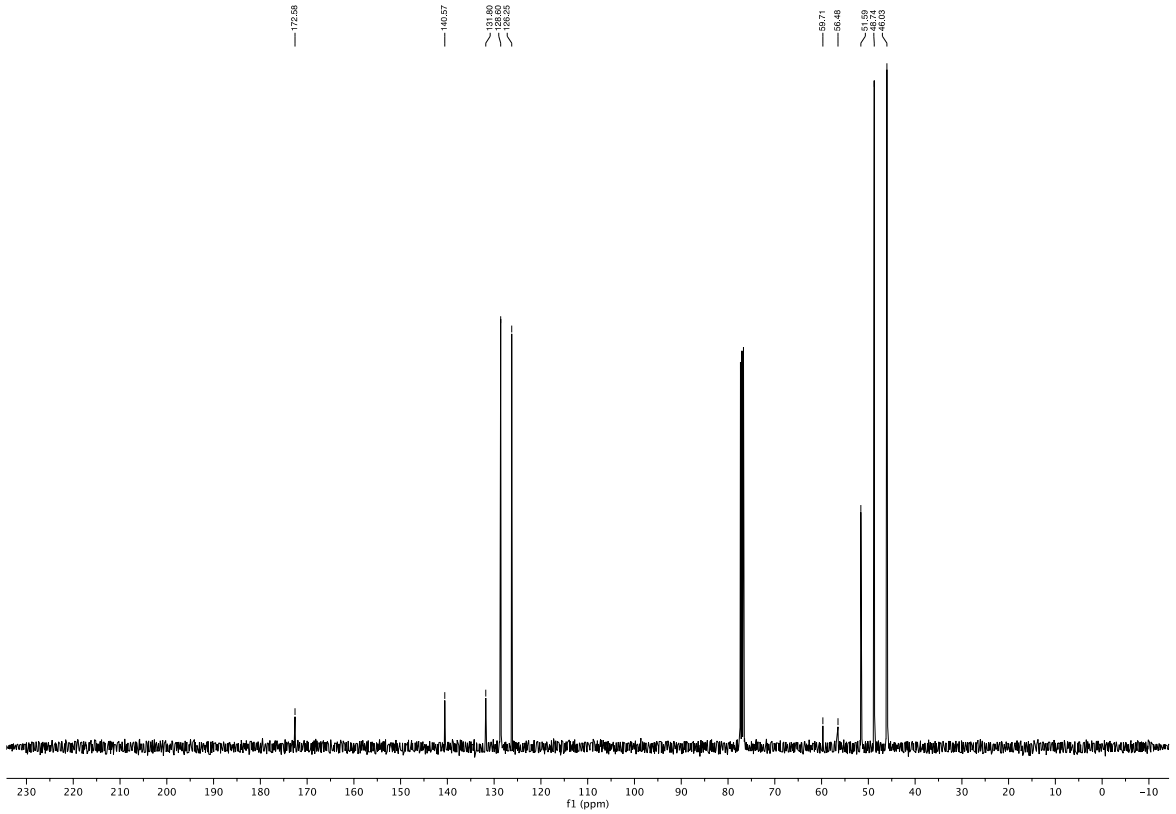
172.58
140.57
131.80
130.69
128.25
59.71
56.48
51.69
48.74
46.03
f1 (ppm)

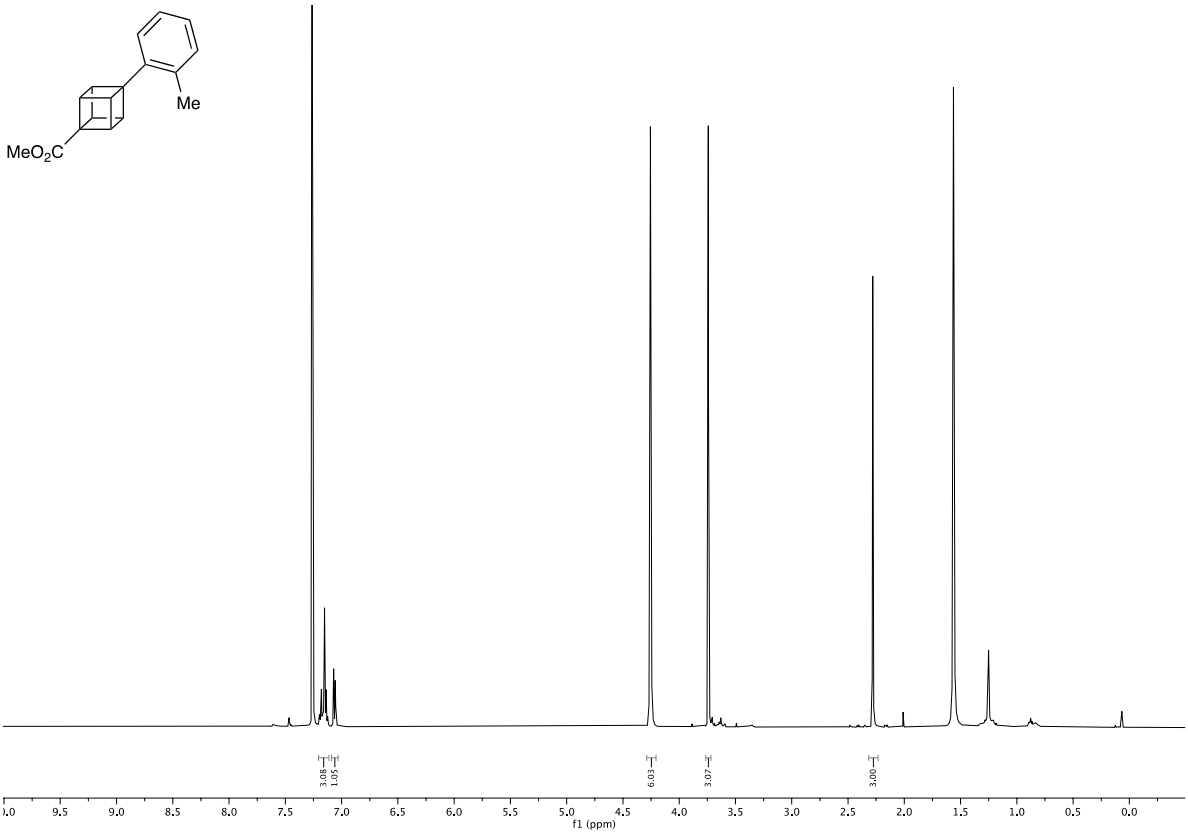
Me
MeO2C
3.08
1.05
6.03
3.07
3.00
f1 (ppm)

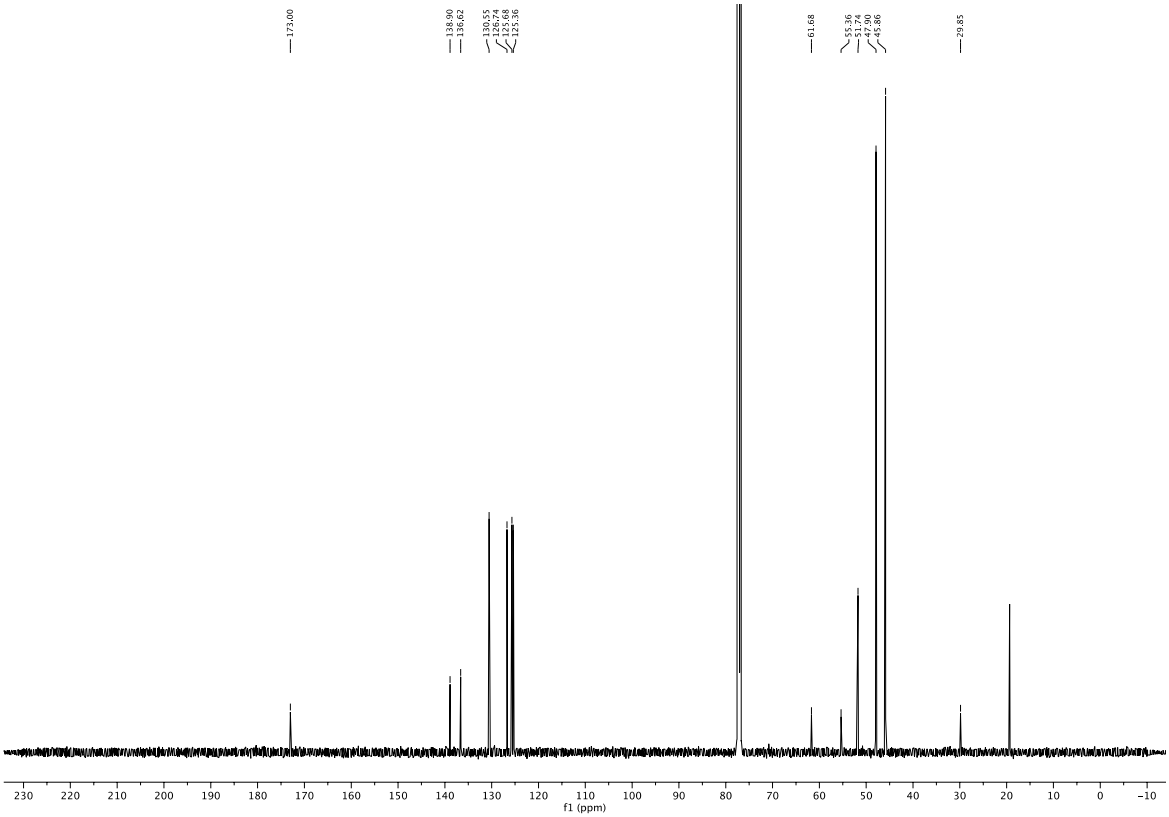
173.00
138.90
136.62
130.55
126.74
125.68
125.36
61.68
55.36
53.74
47.90
45.86
29.85
f1 (ppm)

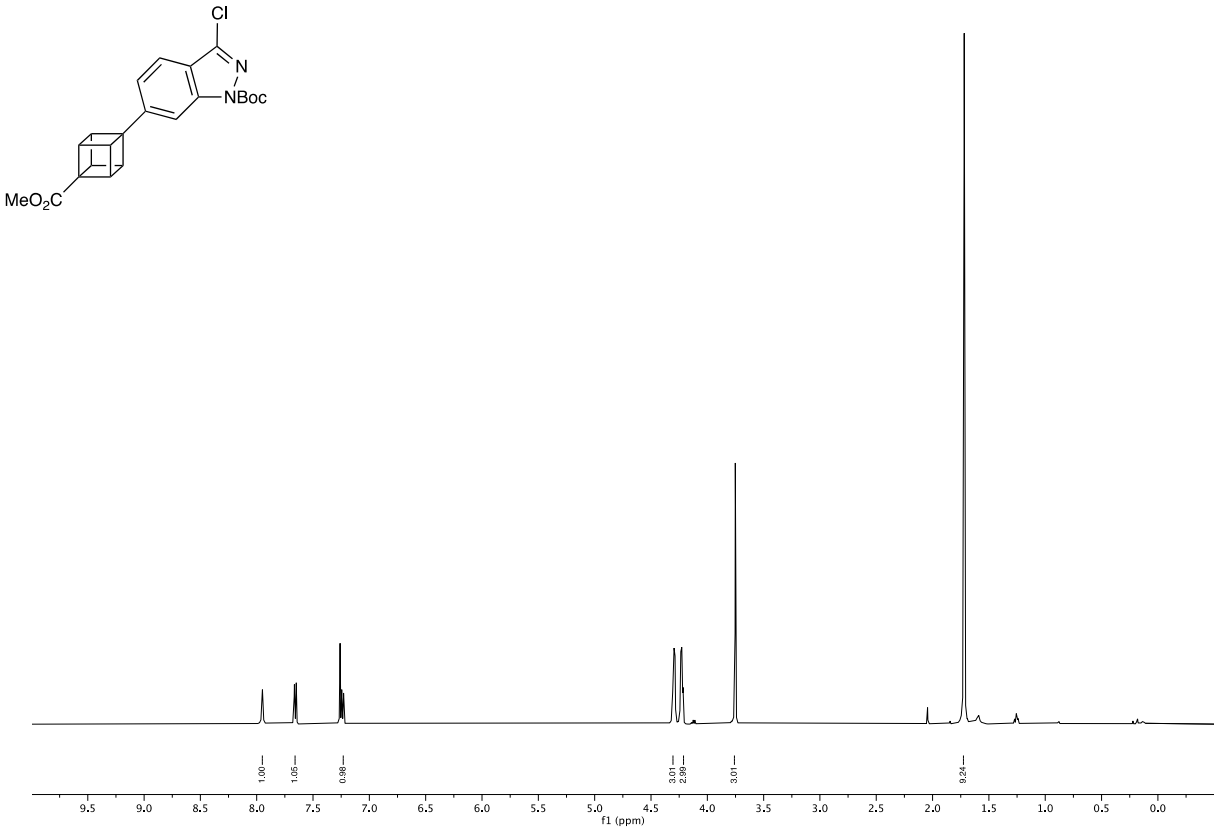
Cl
N
NBoc
MeO2C
1.00
1.05
0.98
3.01
2.99
3.01
9.24
f1 (ppm)

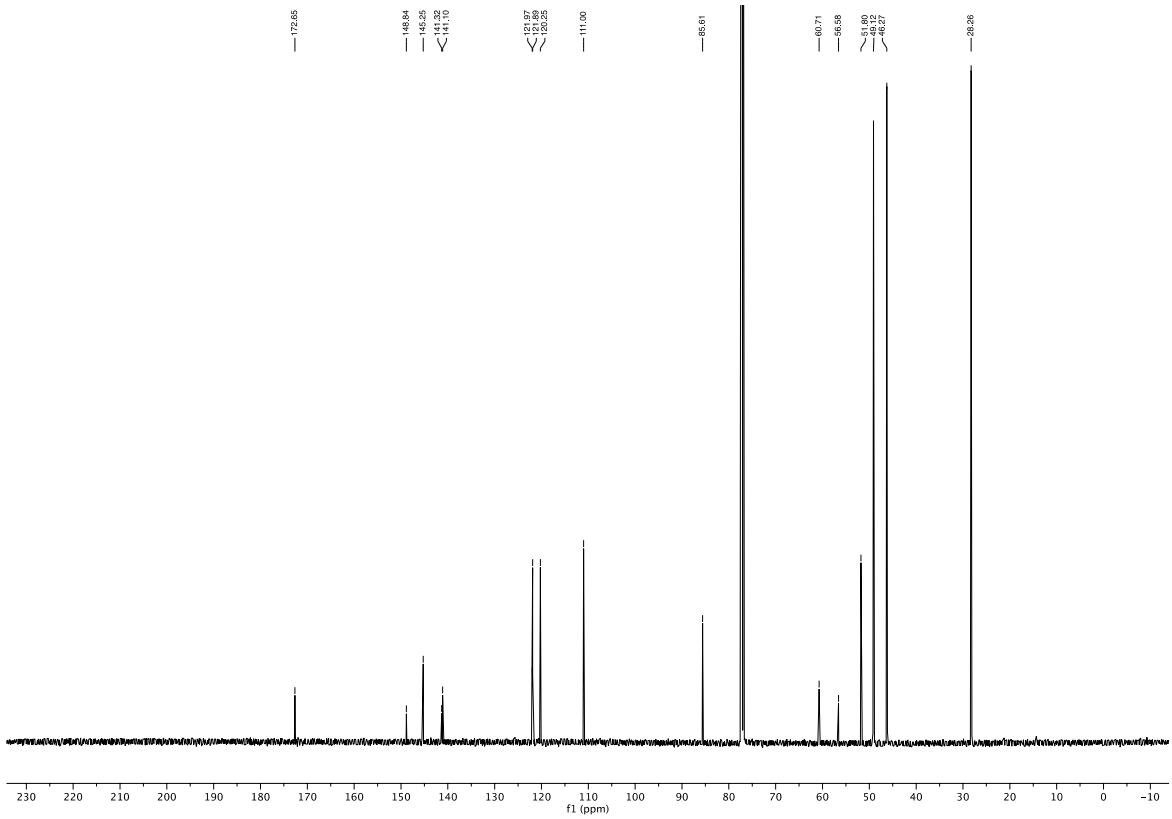
172.65
148.84
145.25
141.32
141.10
121.97
121.89
120.25
111.00
85.61
60.71
56.58
51.90
49.12
46.27
28.26
f1 (ppm)

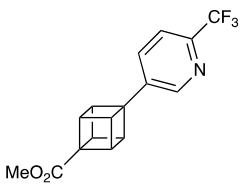
CF3
N
MeO2C

0.98
2.07
2.98
3.00
3.09
f1 (ppm)

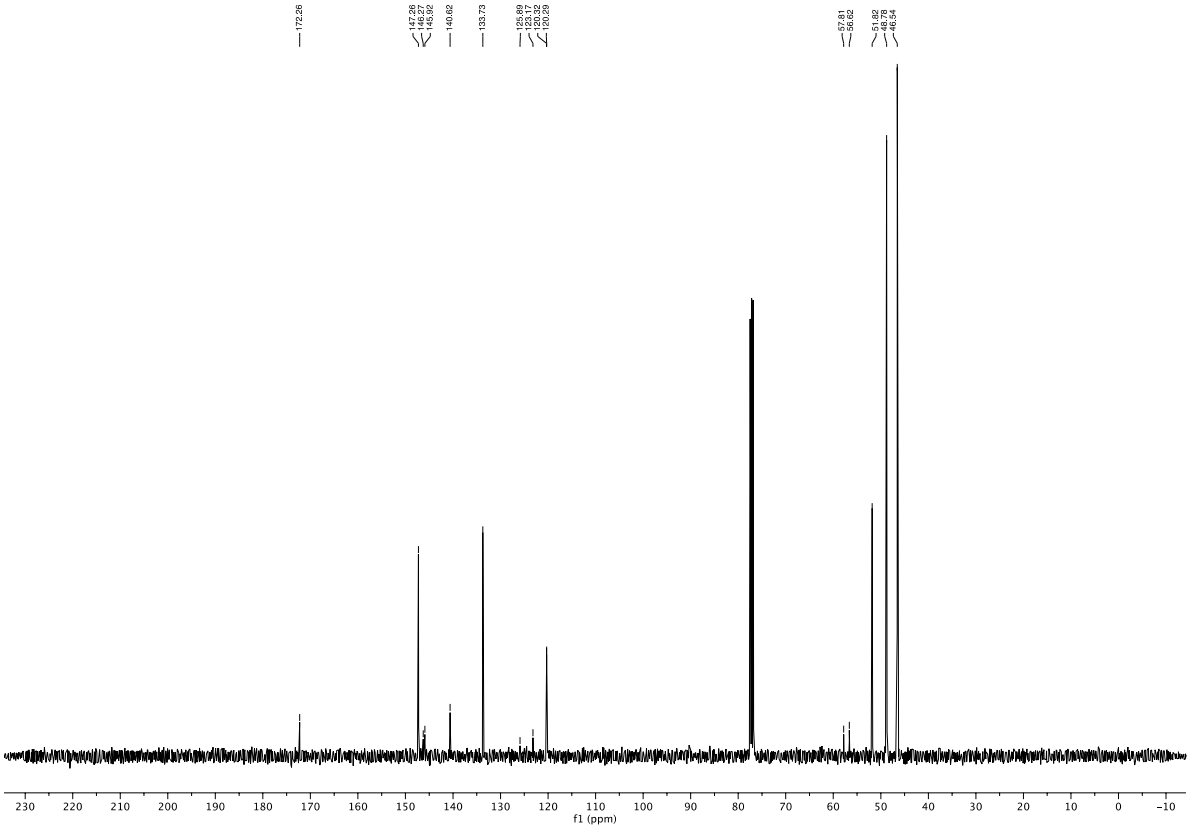
172.26
147.26
146.27
145.92
140.62
133.73
125.89
123.17
120.73
120.29
57.81
56.62
51.82
47.70
46.54
f1 (ppm)

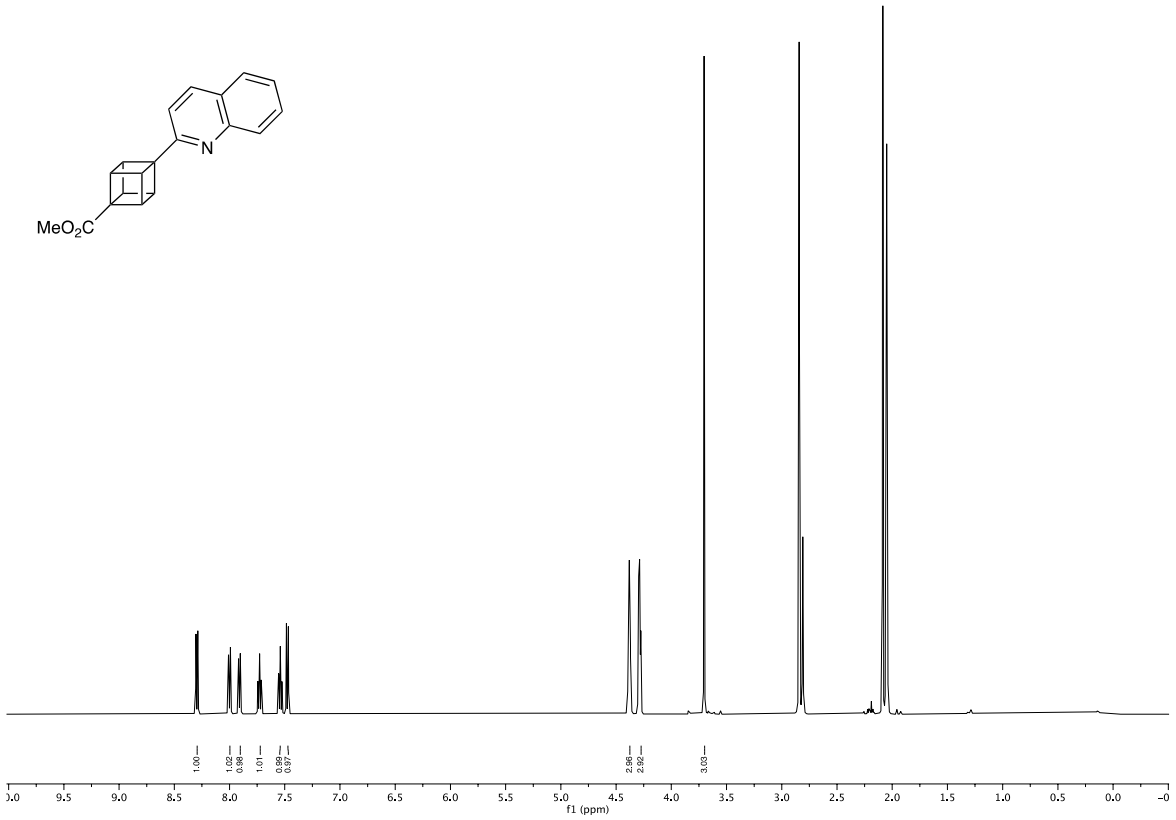
N
MeO2C
1.00
1.02
0.98
1.01
0.99
0.97
2.96
2.92
3.03
f1 (ppm)

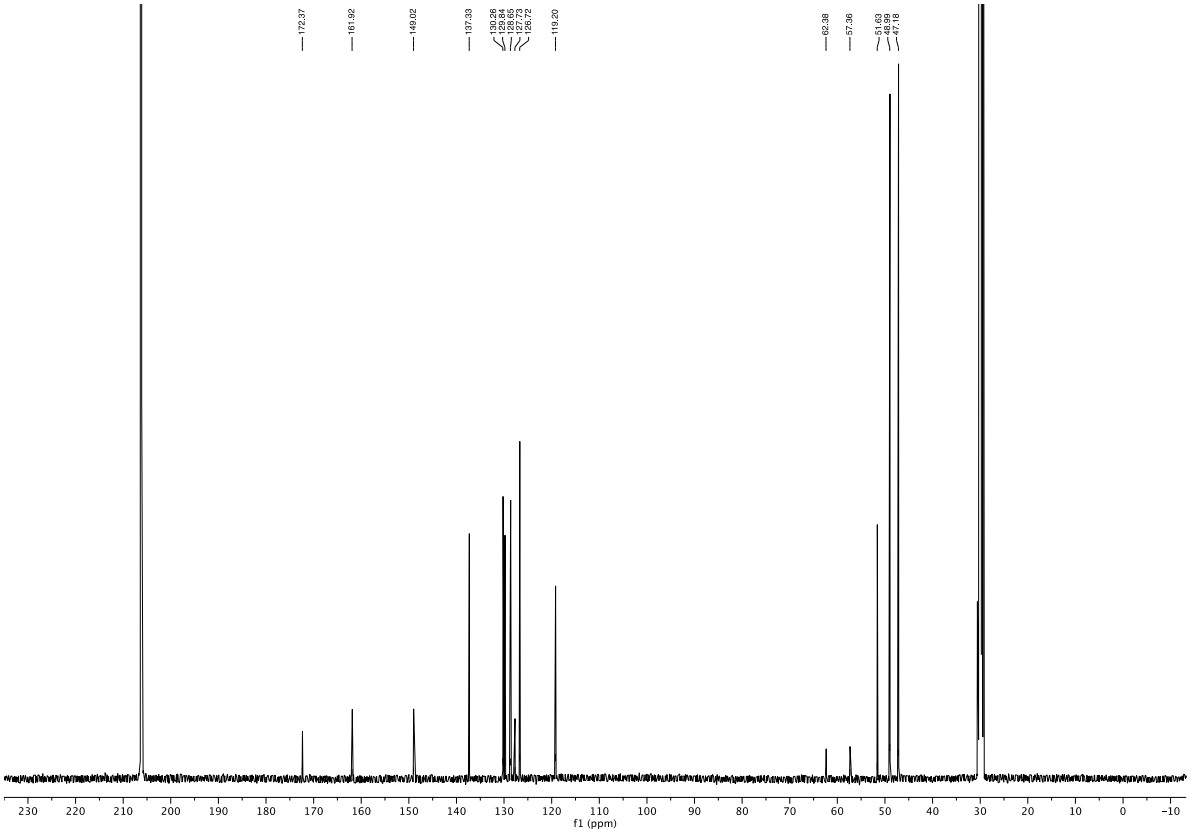
172.37
161.92
149.02
137.33
130.26
129.84
128.65
127.73
126.72
119.20
62.38
57.36
51.63
49.98
47.18
f1 (ppm)

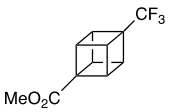
CF3
MeO2C

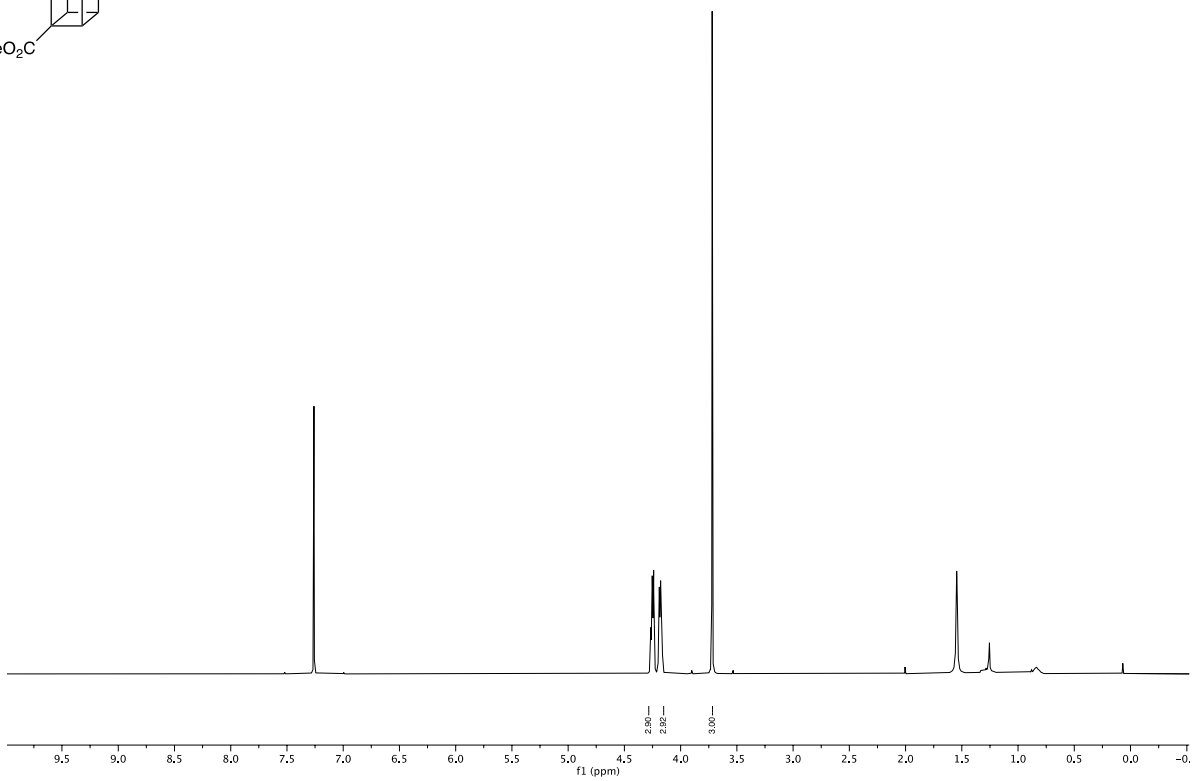
2.90
2.92
3.00
f1 (ppm)

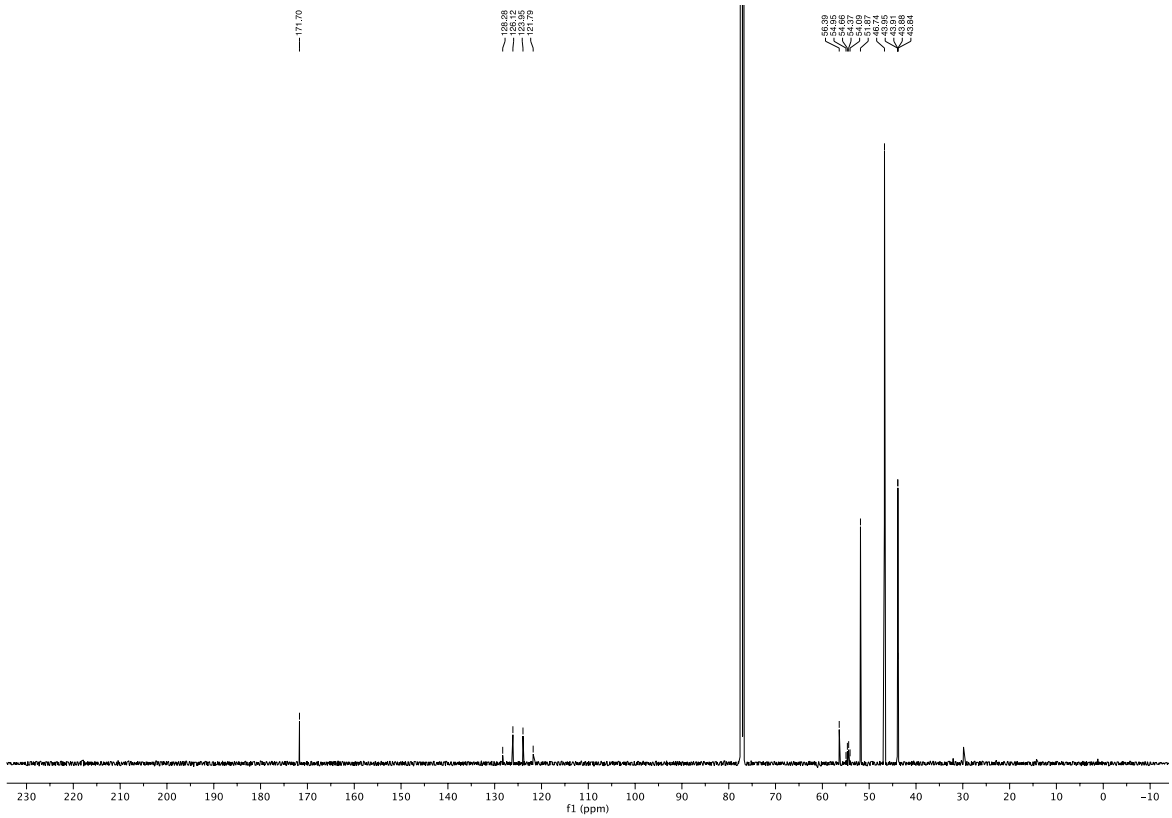
171.70
128.28
125.22
123.95
121.79
66.39
56.30
54.66
54.47
54.09
51.87
49.74
43.95
43.91
43.88
43.84
f1 (ppm)

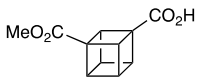
MeO2C
CO2H

1.98
2.02
2.00
3.02
f1 (ppm)

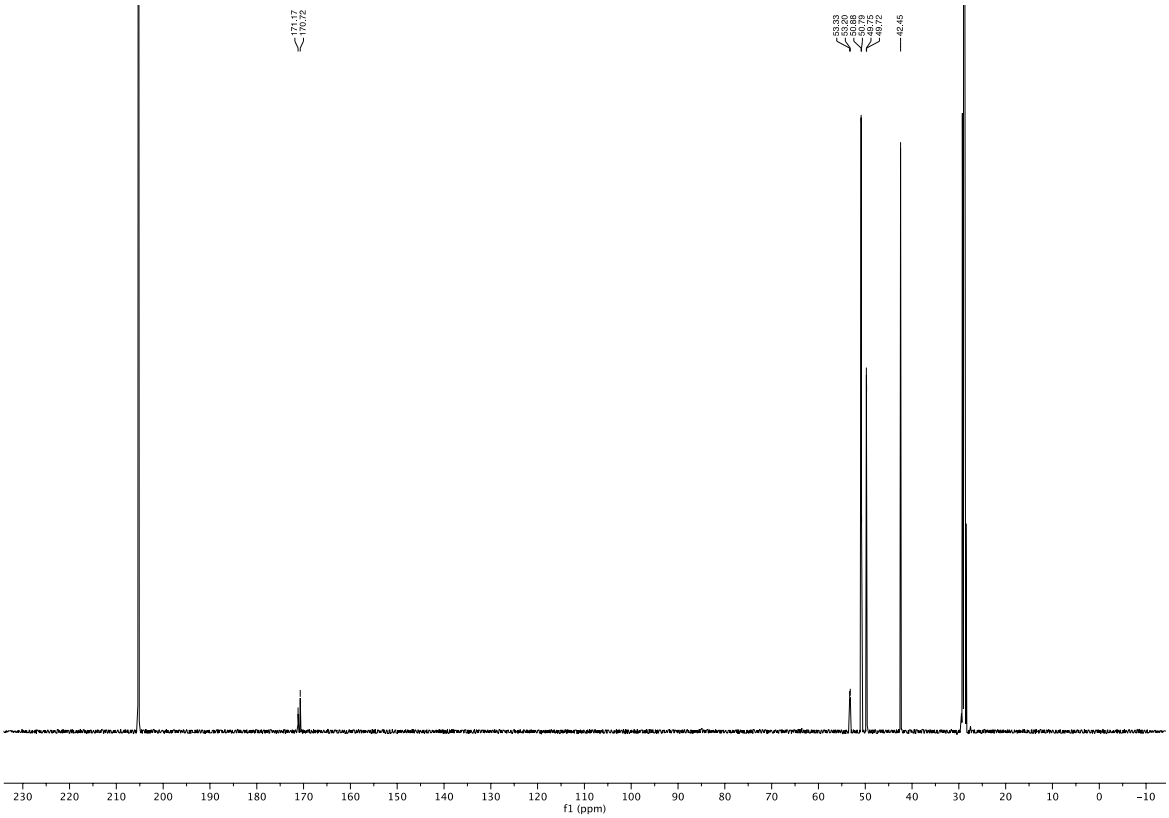
171.17
170.72
53.33
53.20
53.08
50.79
49.45
49.72
42.45
f1 (ppm)

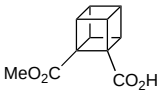
MeO2C
CO2H

3.95
1.99
3.00
f1 (ppm)

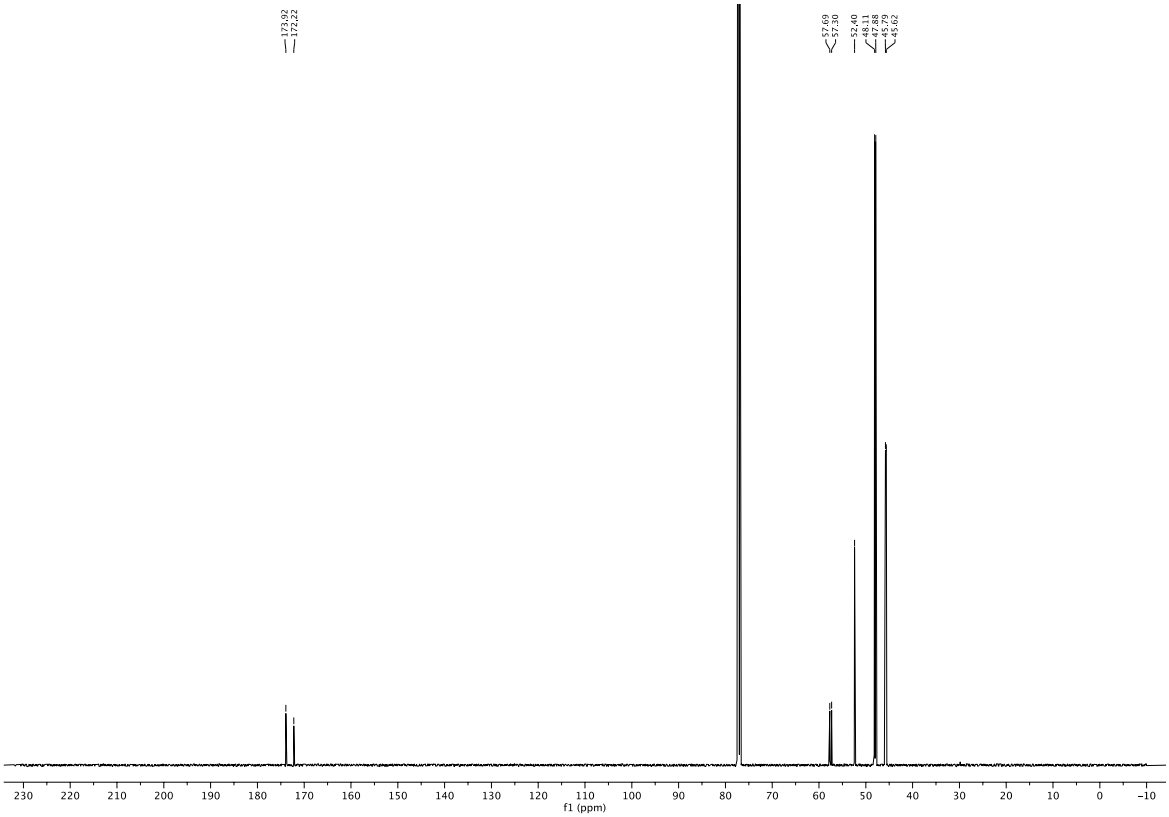
173.92
172.22
57.69
57.30
52.40
48.11
47.98
45.79
45.62
f1 (ppm)

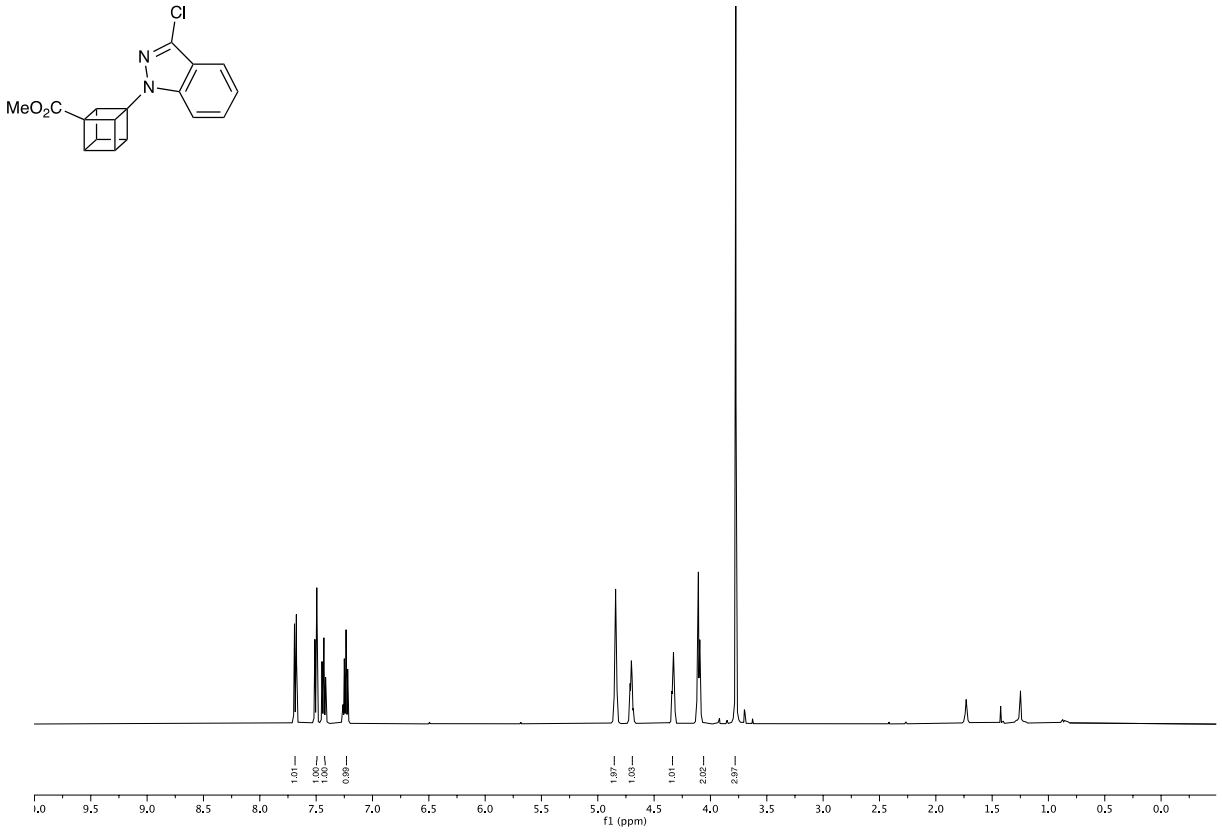
Cl
N
N
MeO2C
1.01
1.00
1.00
0.89
1.97
1.03
1.01
2.02
2.97
f1 (ppm)

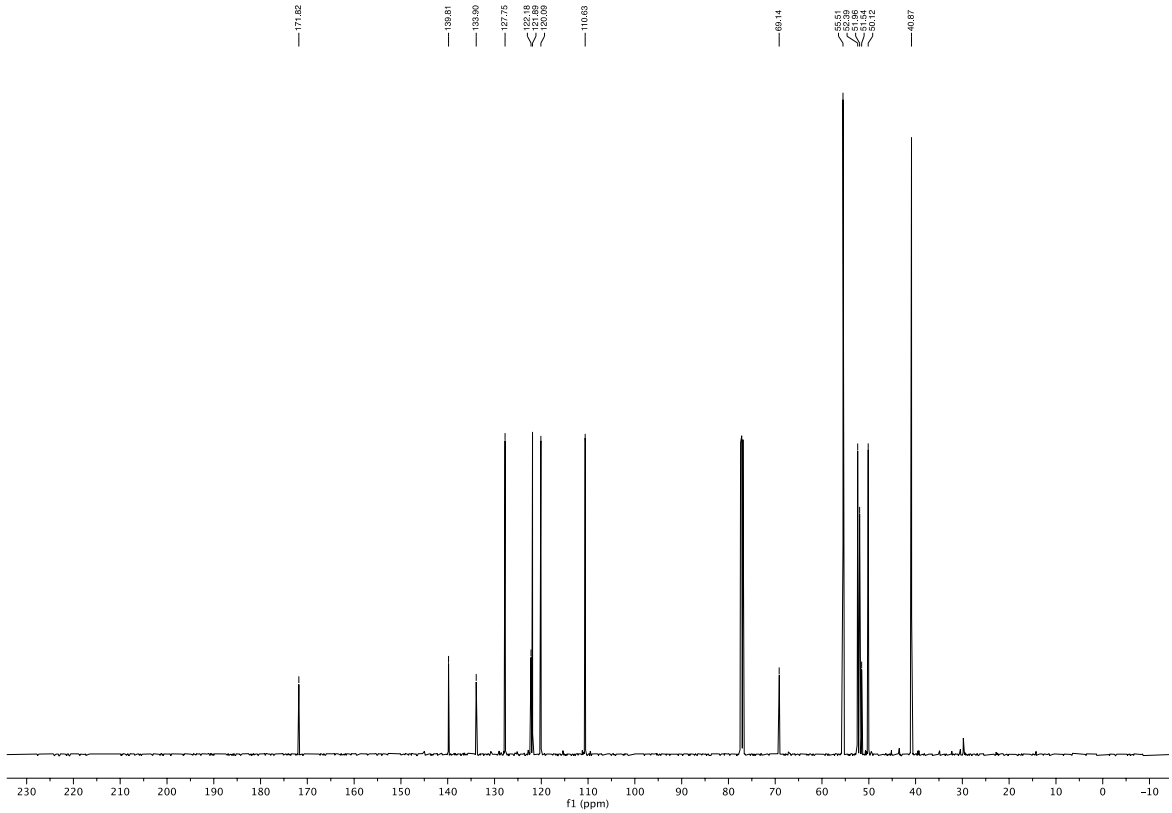
171.82
139.81
133.90
127.75
122.18
121.89
120.09
110.63
69.14
55.51
55.39
51.96
51.54
50.12
40.87
f1 (ppm)

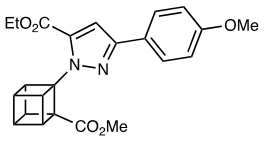
EtO2C
OMe
N
N
CO2Me

2.00
0.97
2.01
1.93
3.97
1.93
3.06
2.97
3.10
f1 (ppm)

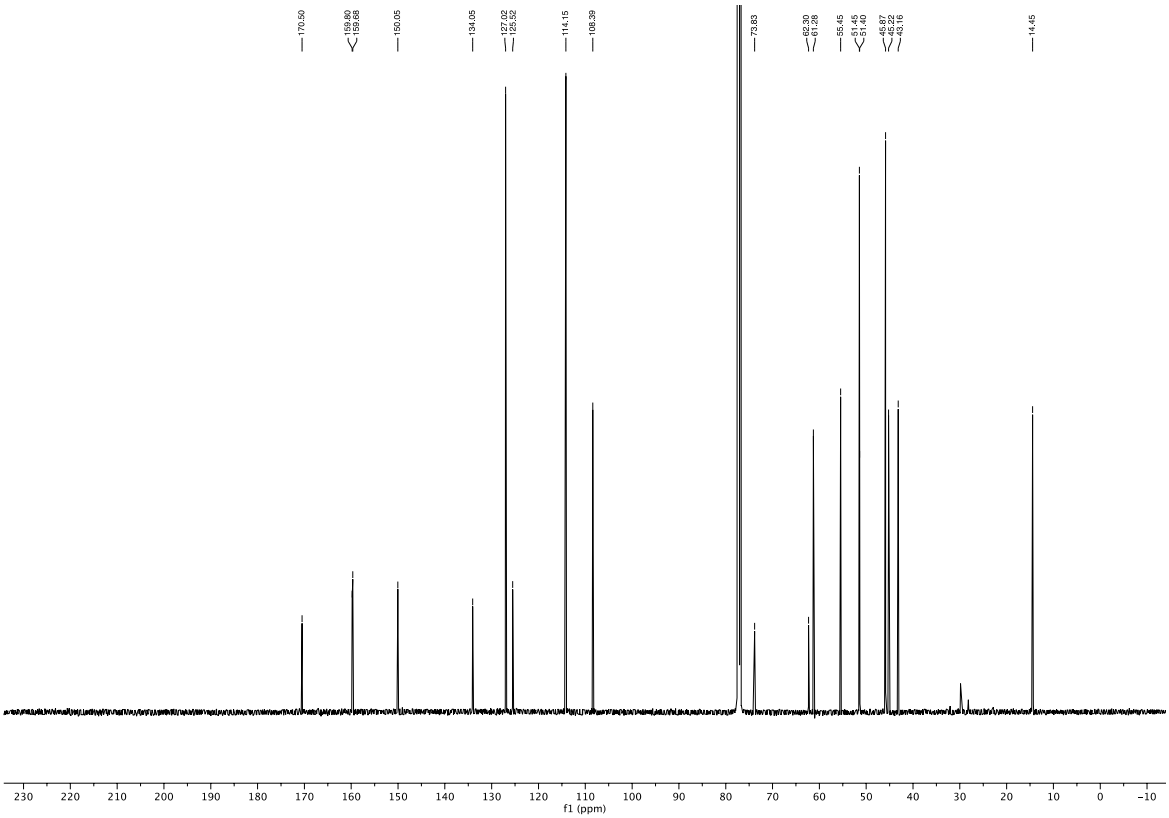
170.50
159.80
159.68
150.05
134.05
127.02
125.52
114.15
108.39
73.83
62.20
61.28
55.45
51.45
51.40
46.87
45.22
43.16
14.45
f1 (ppm)

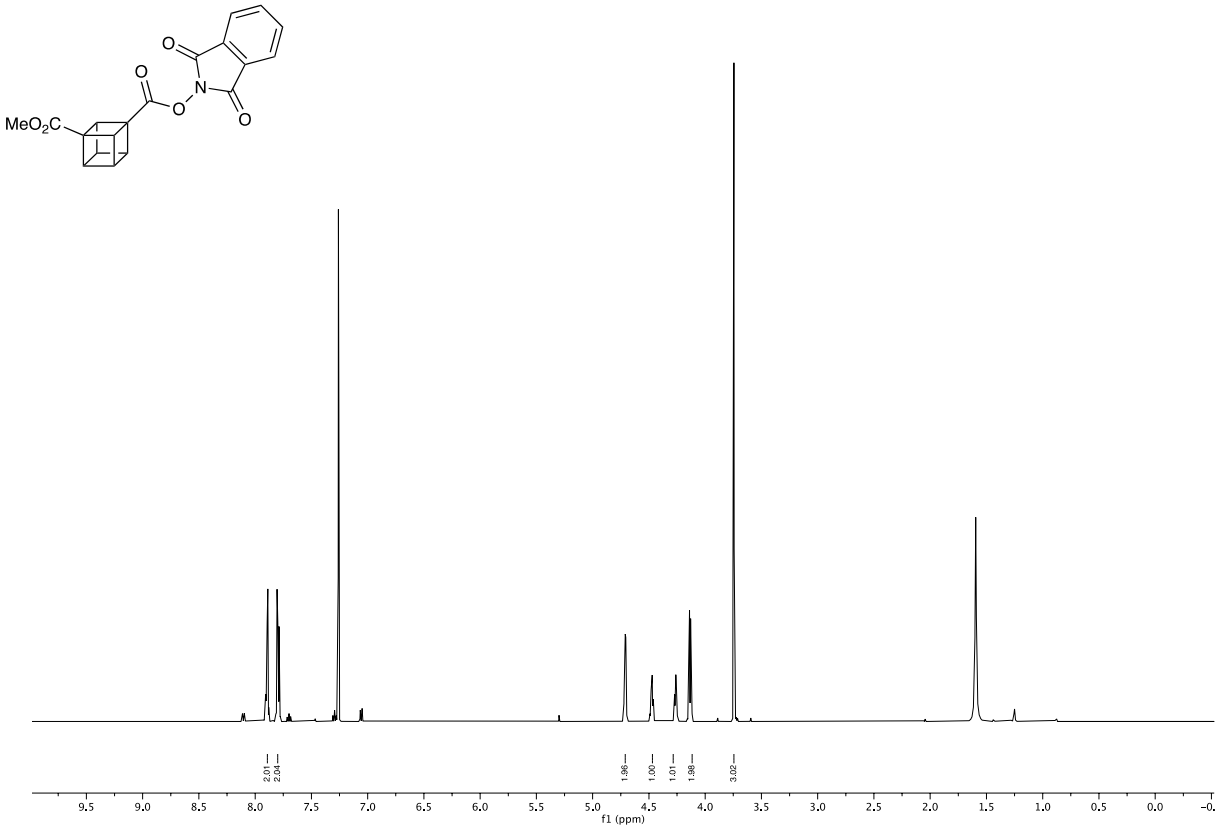
MeO2C
O
O
N
O
O
2.01
2.04
1.96
1.00
1.01
1.98
3.02
f1 (ppm)

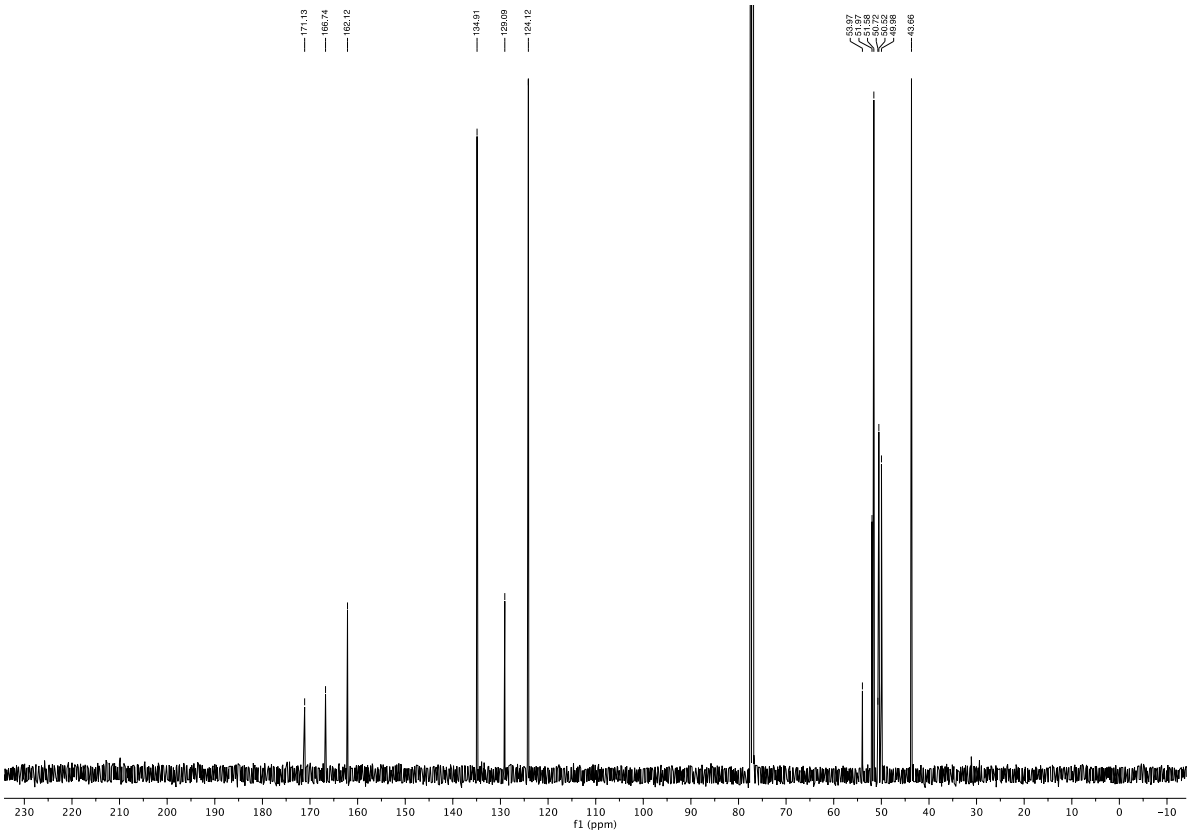
171.13
166.74
162.12
134.91
129.09
124.12
53.97
53.87
51.58
50.72
50.52
49.98
43.66
f1 (ppm)

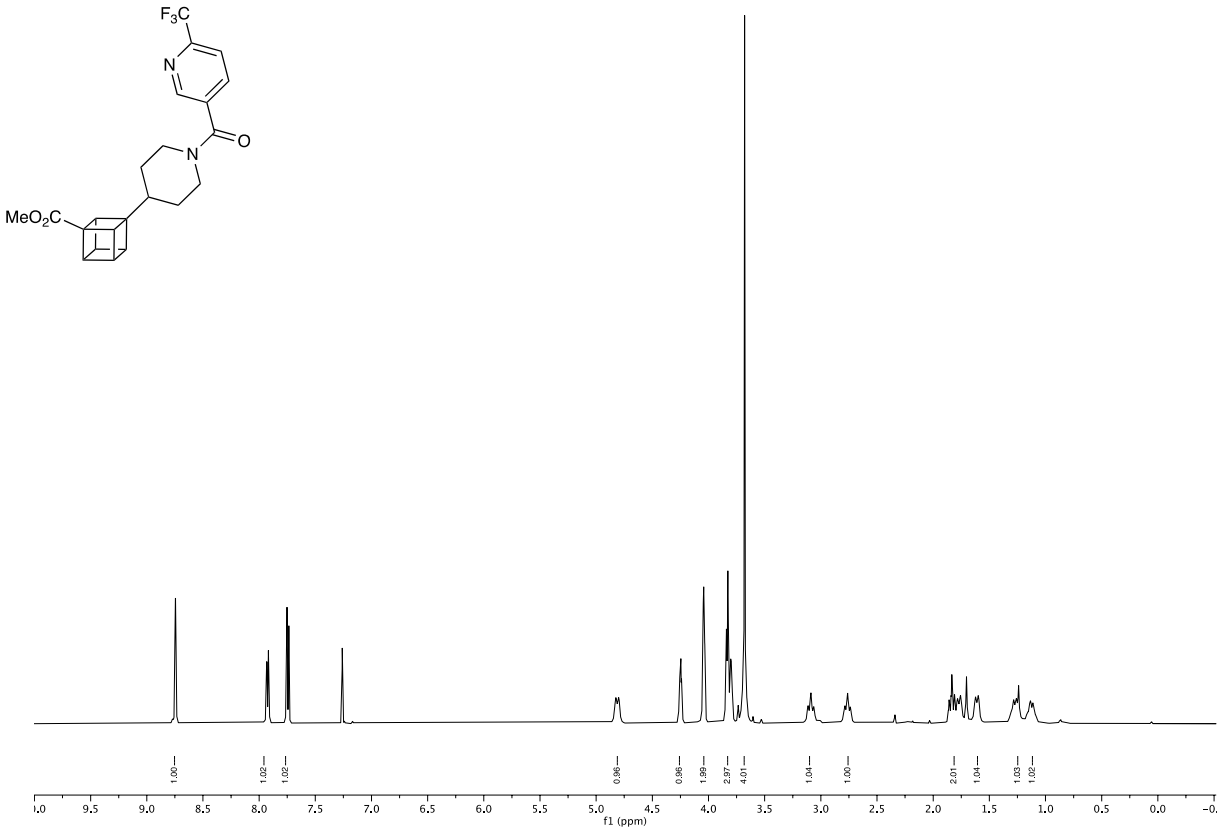
F3C
N
O
N
MeO2C
1.00
1.02
1.02
0.96
0.96
1.99
2.97
4.01
1.04
1.00
2.01
1.04
1.03
1.02
f1 (ppm)

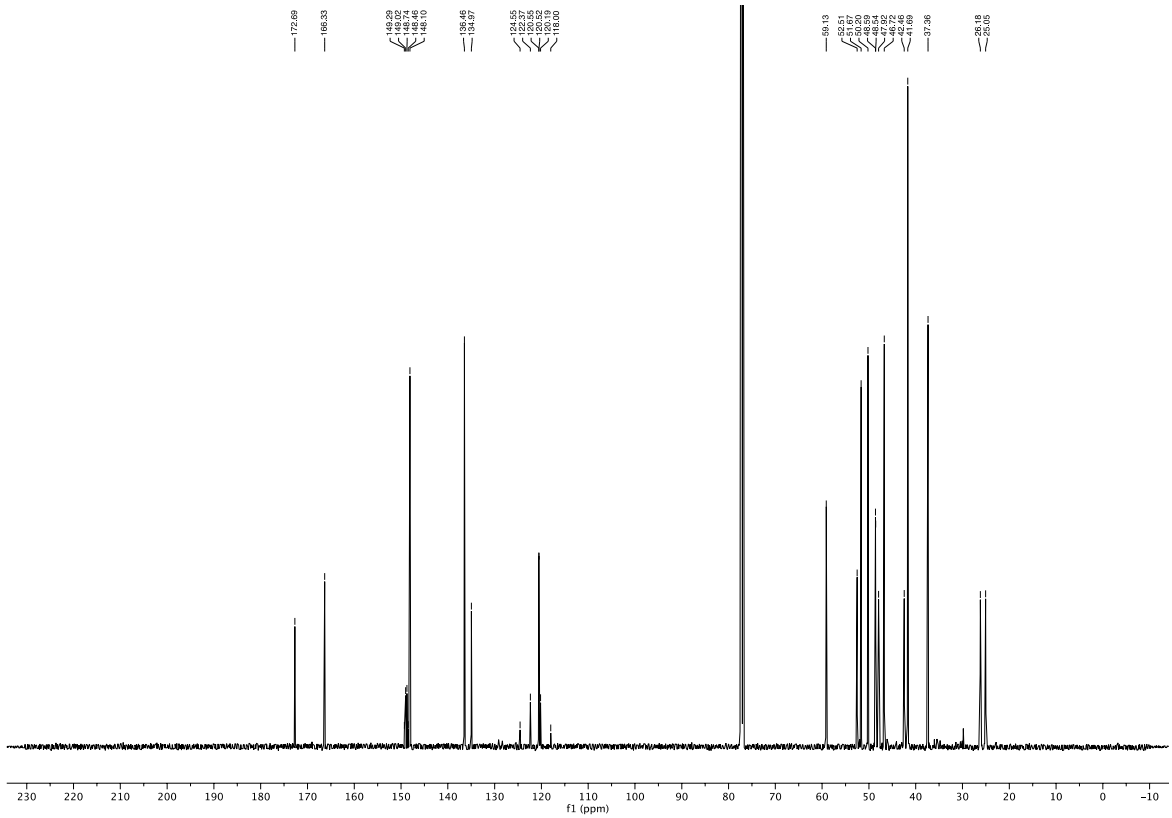
172.69
166.33
149.28
149.02
148.74
148.46
148.10
138.46
134.97
124.55
122.37
120.35
120.25
120.19
118.00
99.13
52.61
51.97
50.20
48.59
48.34
47.92
47.79
42.46
41.69
37.36
26.18
25.10
f1 (ppm)

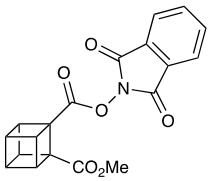
O
O
N
O
O
O
CO2Me

2.00
2.05
1.96
1.97
1.00
1.05
3.07
9.5 9.0 8.5 8.0 7.5 7.0 6.5 6.0 5.5 5.0 4.5 4.0 3.5 3.0 2.5 2.0 1.5 1.0 0.5 0.0
f1 (ppm)

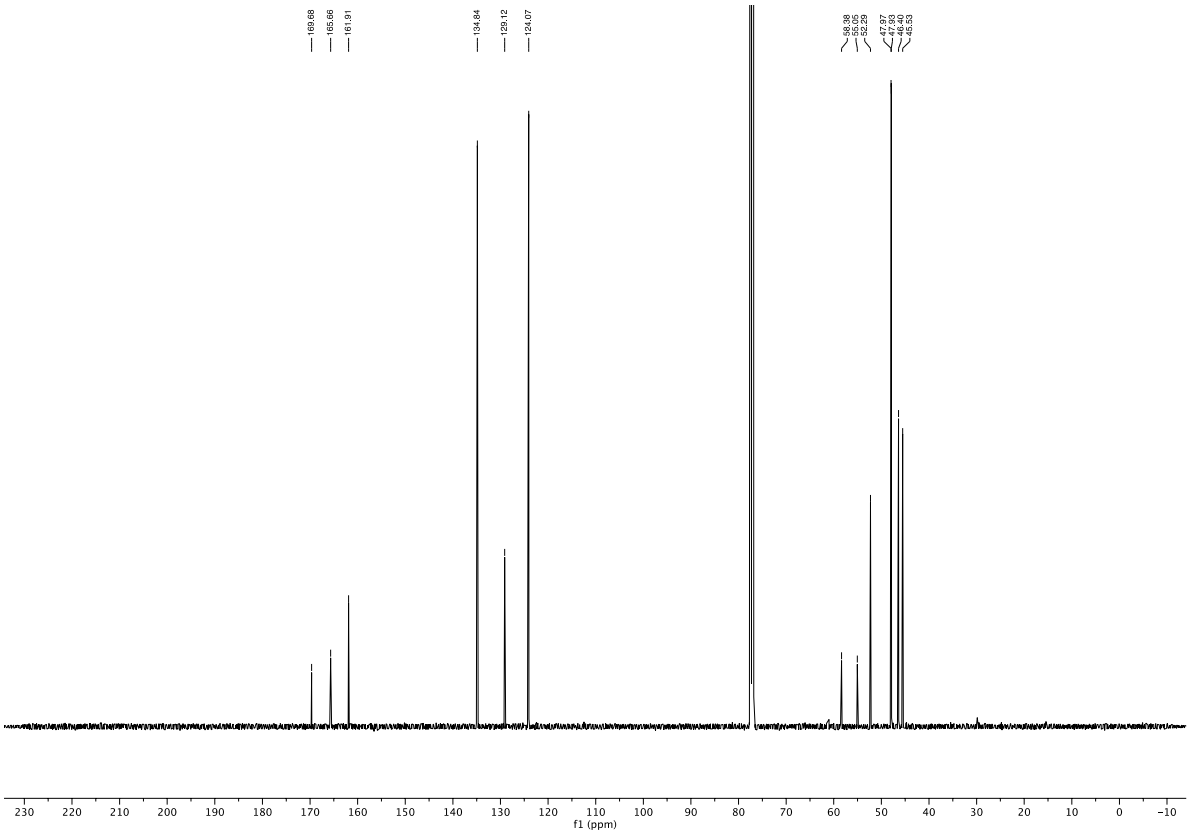
169.68
165.66
161.91
134.84
129.12
124.07
68.38
53.05
52.29
47.97
47.93
47.40
45.53
230 220 210 200 190 180 170 160 150 140 130 120 110 100 90 80 70 60 50 40 30 20 10 0 -10
f1 (ppm)

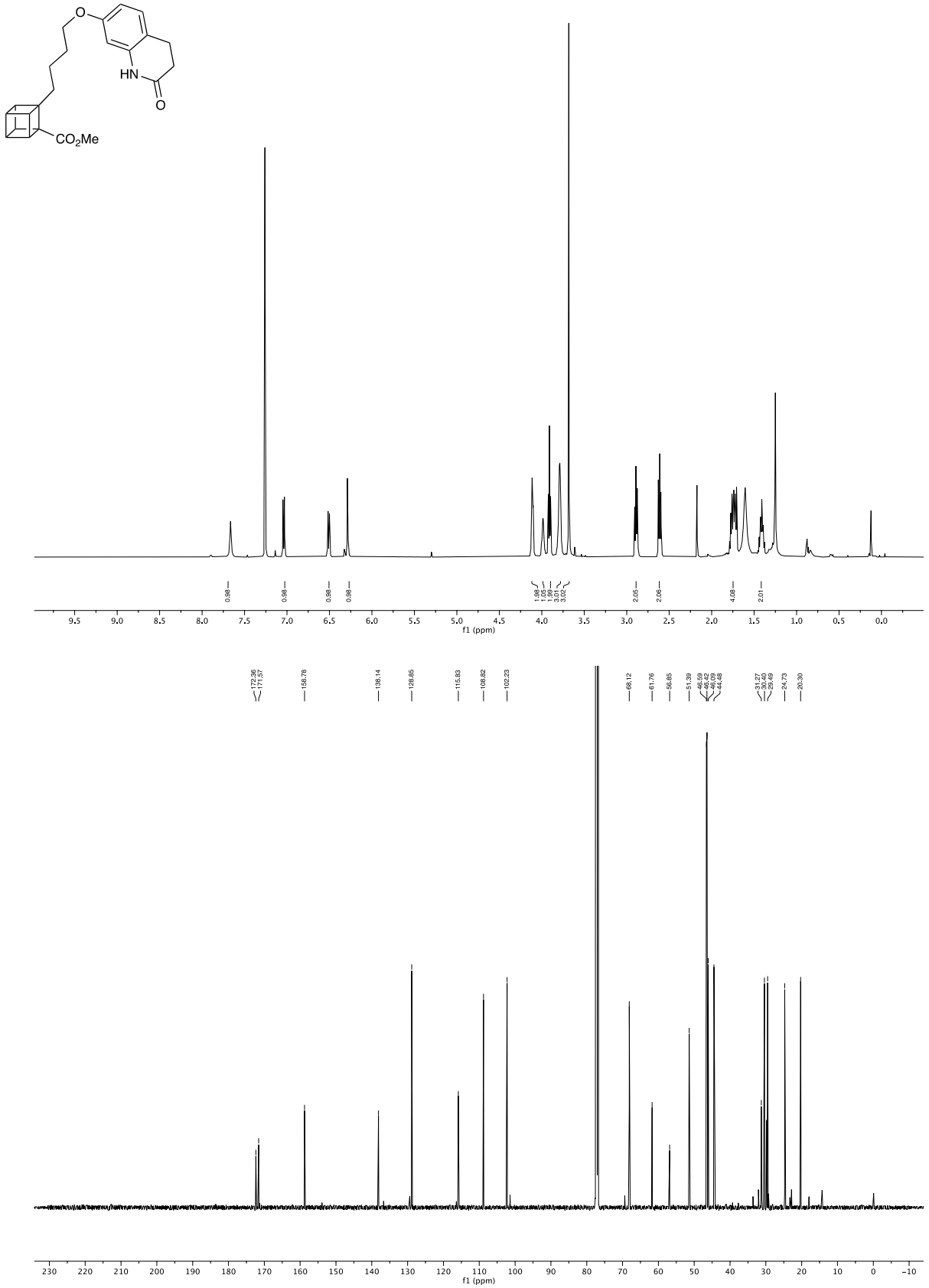
O
HN
O
CO2Me
0.98
0.98
0.98
0.98
1.98
1.05
1.00
3.01
3.02
2.05
2.06
4.08
2.01
f1 (ppm)
172.36
171.07
158.78
138.14
128.85
115.83
108.82
102.23
68.12
61.76
56.85
51.39
46.59
46.42
46.28
44.48
31.27
30.40
29.49
24.73
20.30
f1 (ppm)

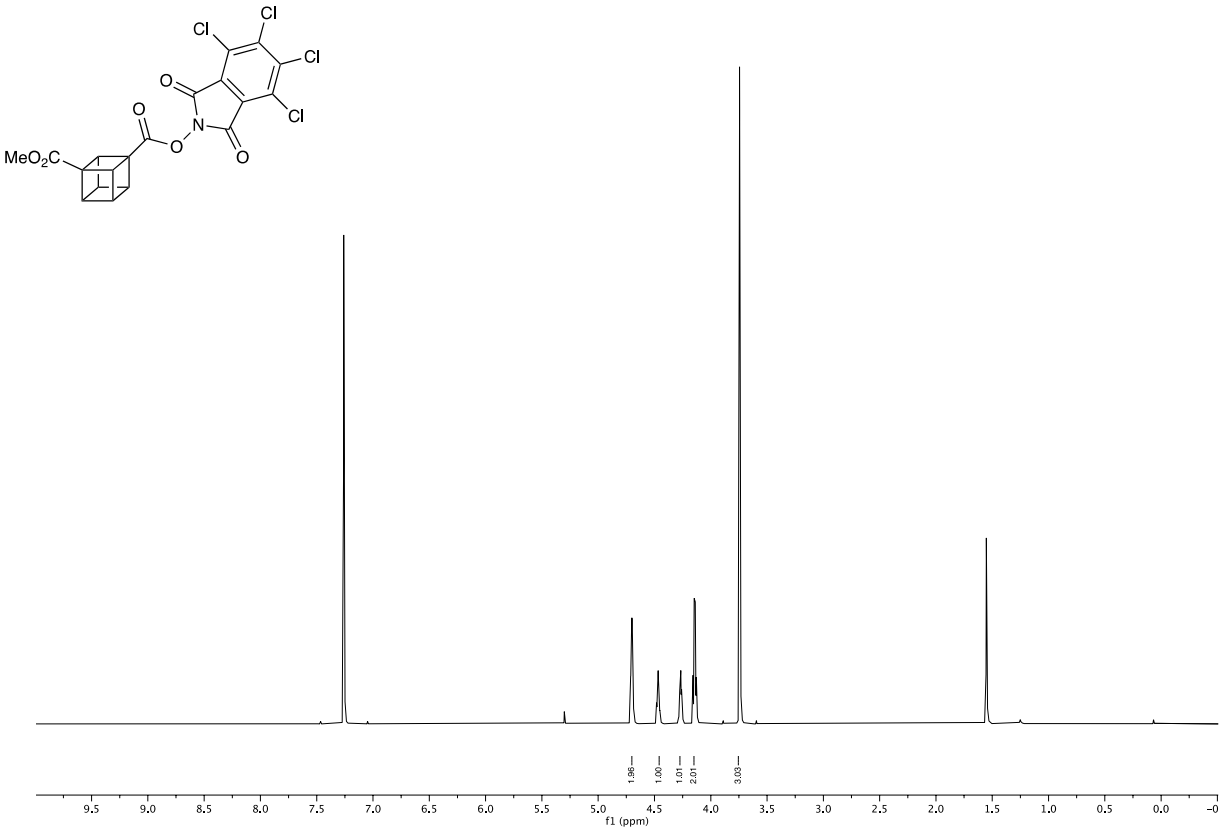
Cl
Cl
Cl
Cl
O
O
N
O
O
O
MeO2C
1.96
1.00
1.01
2.01
3.03
f1 (ppm)

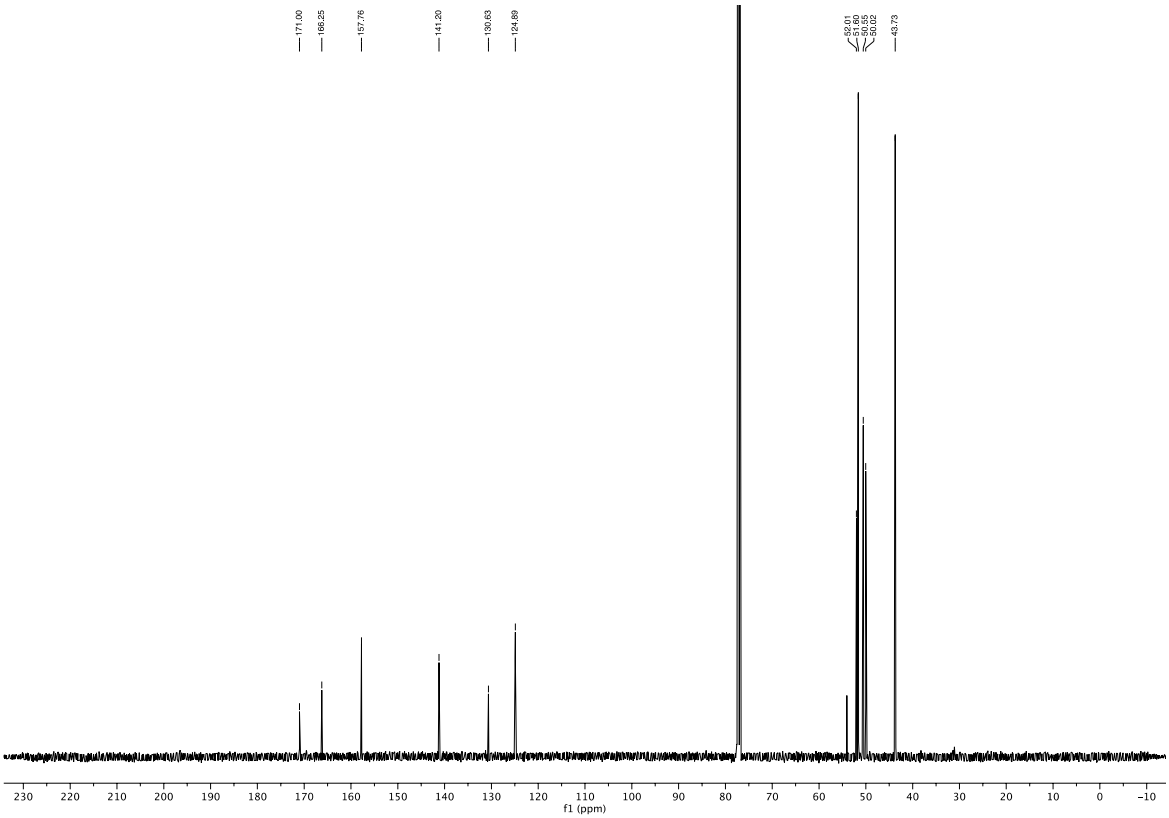
171.00
166.25
157.76
141.20
130.63
124.89
52.01
51.80
50.55
50.02
43.73
f1 (ppm)

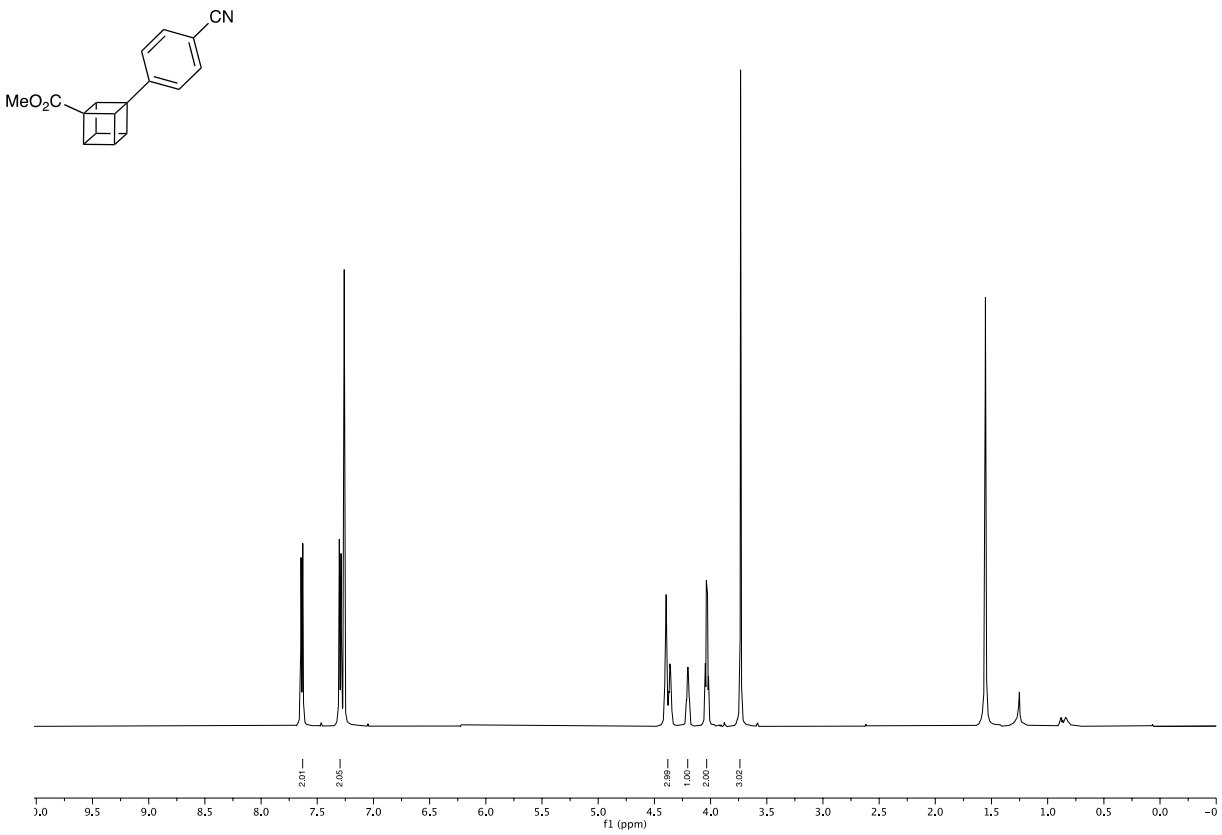
CN
MeO2C
2.01
2.05
2.99
1.00
2.00
3.02
f1 (ppm)

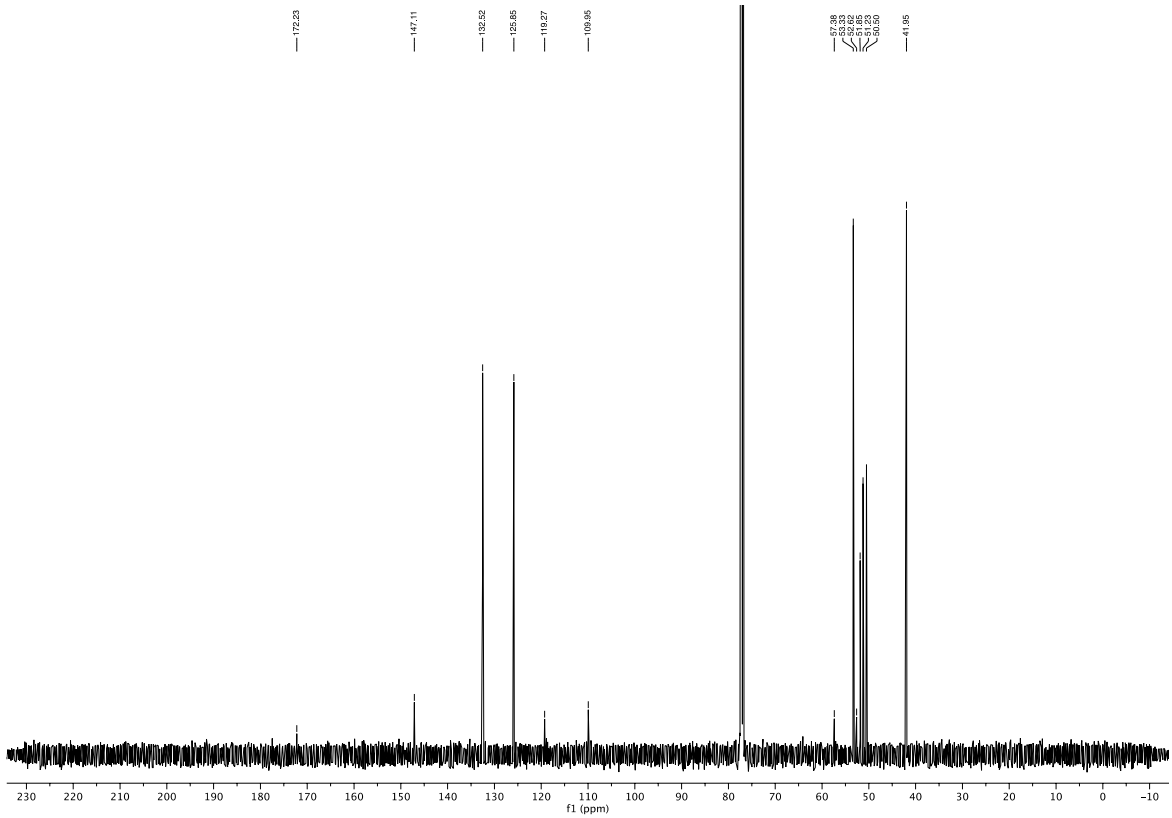
172.23
147.11
132.52
125.85
119.27
109.95
67.38
53.33
52.07
51.85
51.23
50.00
41.95
f1 (ppm)

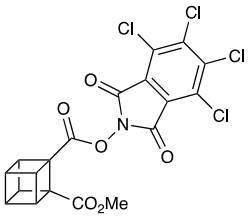
Cl
Cl
Cl
Cl
O
O
N
O
O
O
CO2Me

1.96
1.97
0.99
1.01
3.03
f1 (ppm)

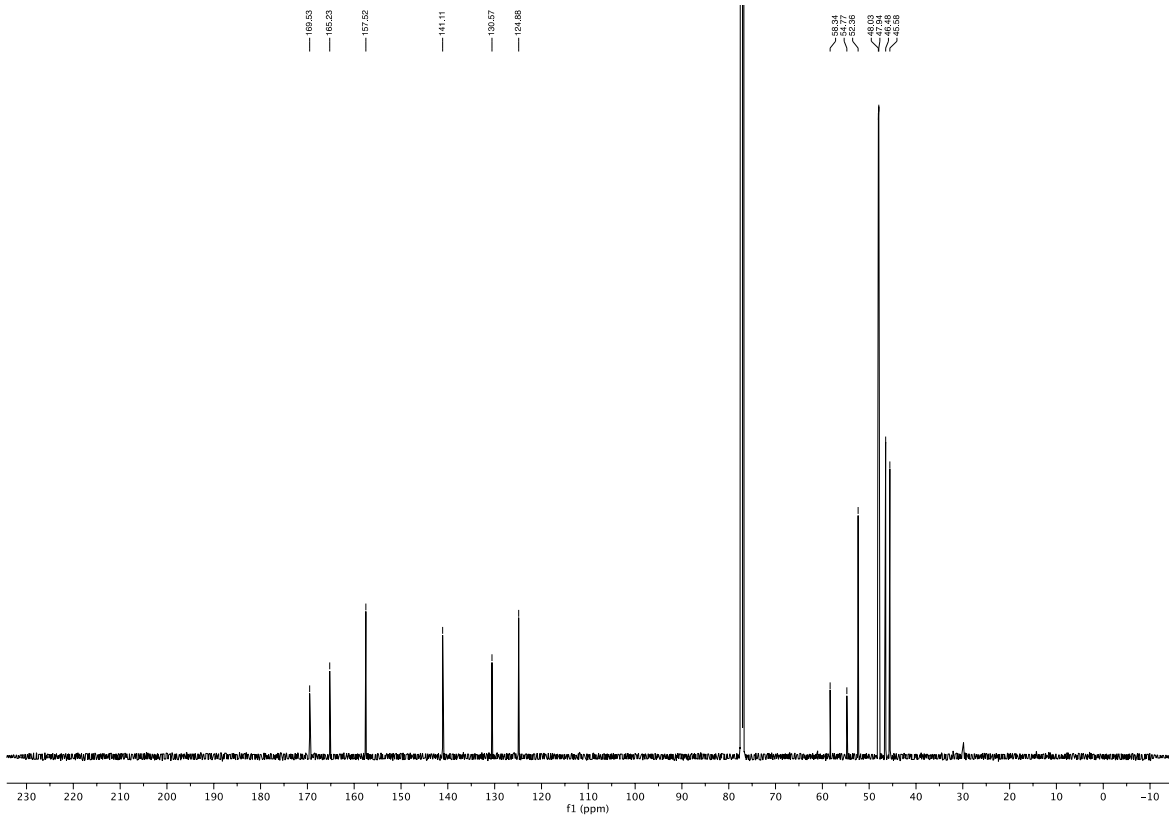
169.53
165.23
157.52
141.11
130.57
124.88
58.34
54.77
52.36
48.03
47.74
46.48
45.58
f1 (ppm)

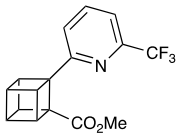
CF3
N
CO2Me

1.02
0.98
1.00
3.99
2.04
3.09
f1 (ppm)

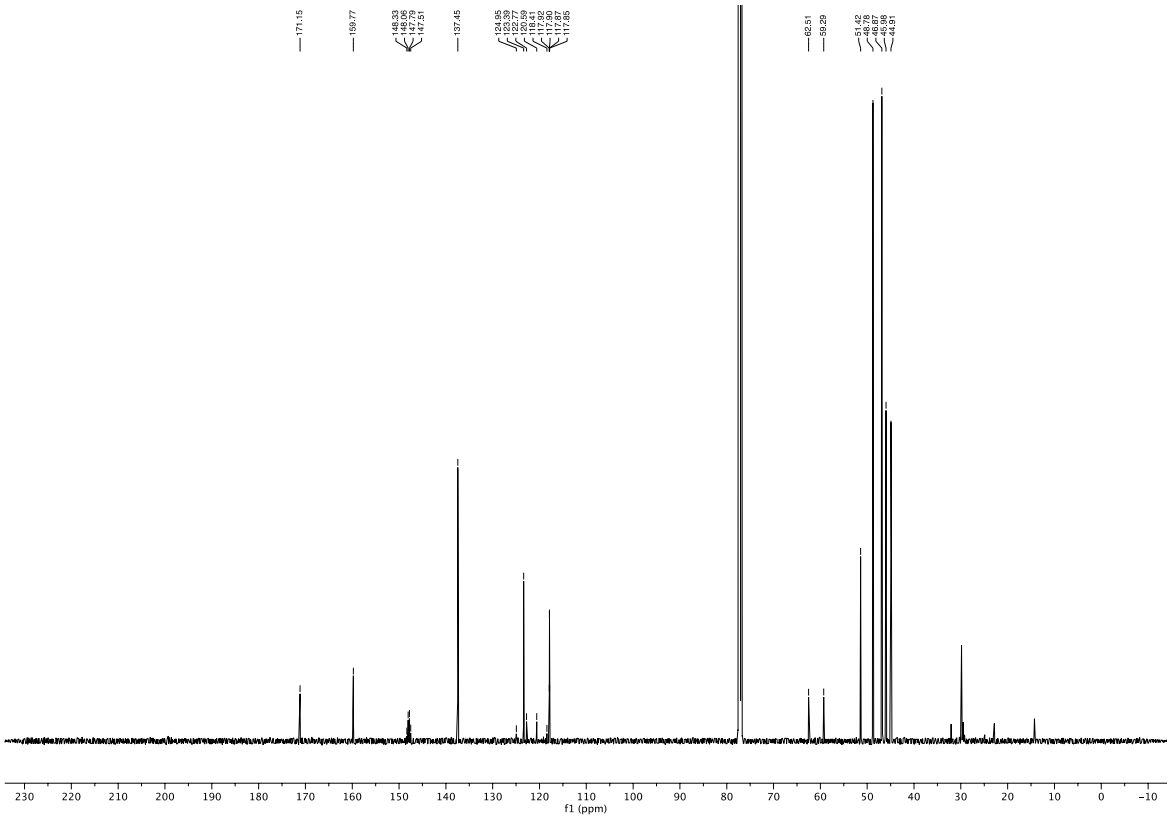
171.15
169.77
148.33
148.06
147.29
147.51
137.45
134.95
123.39
122.77
120.99
118.41
117.99
117.90
117.87
117.68
82.51
59.29
51.42
48.78
48.67
46.98
44.91
f1 (ppm)

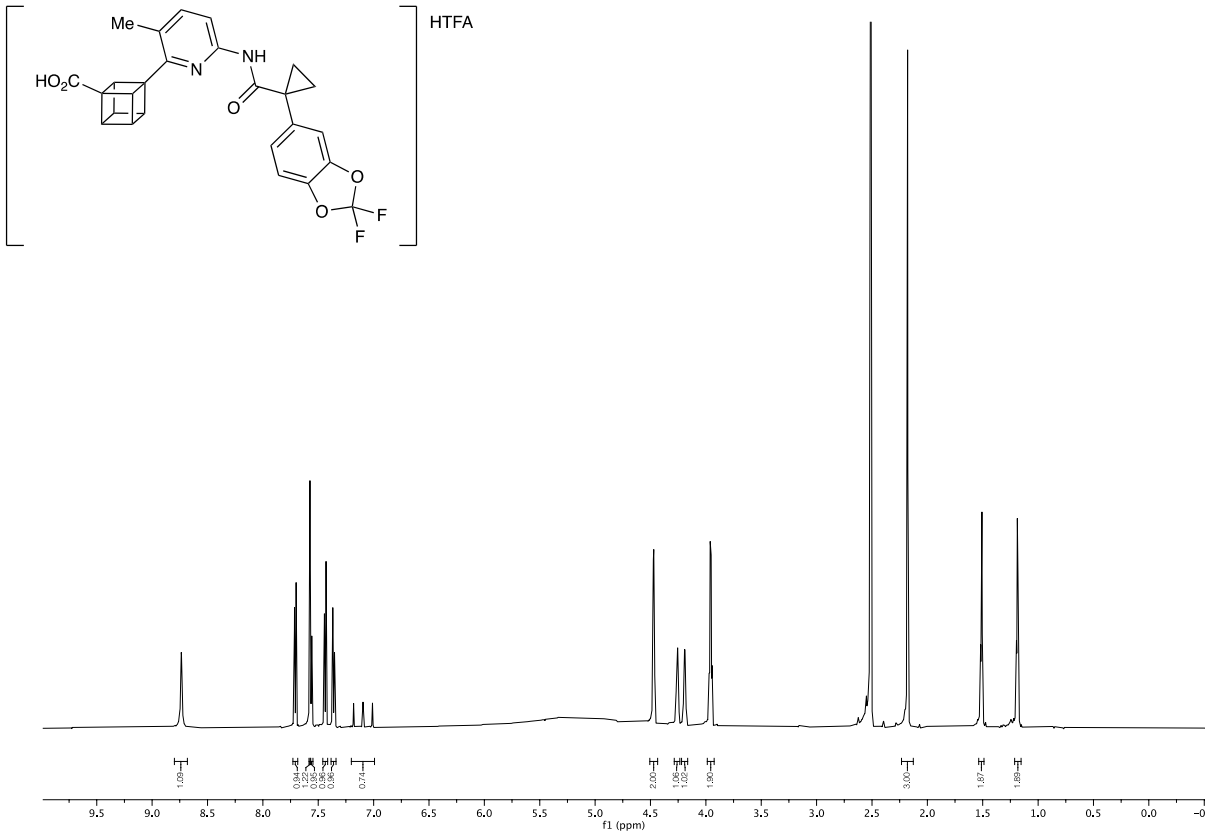
Me
NH
N
HO2C
O
O
O
F
F
HTFA
f1 (ppm)

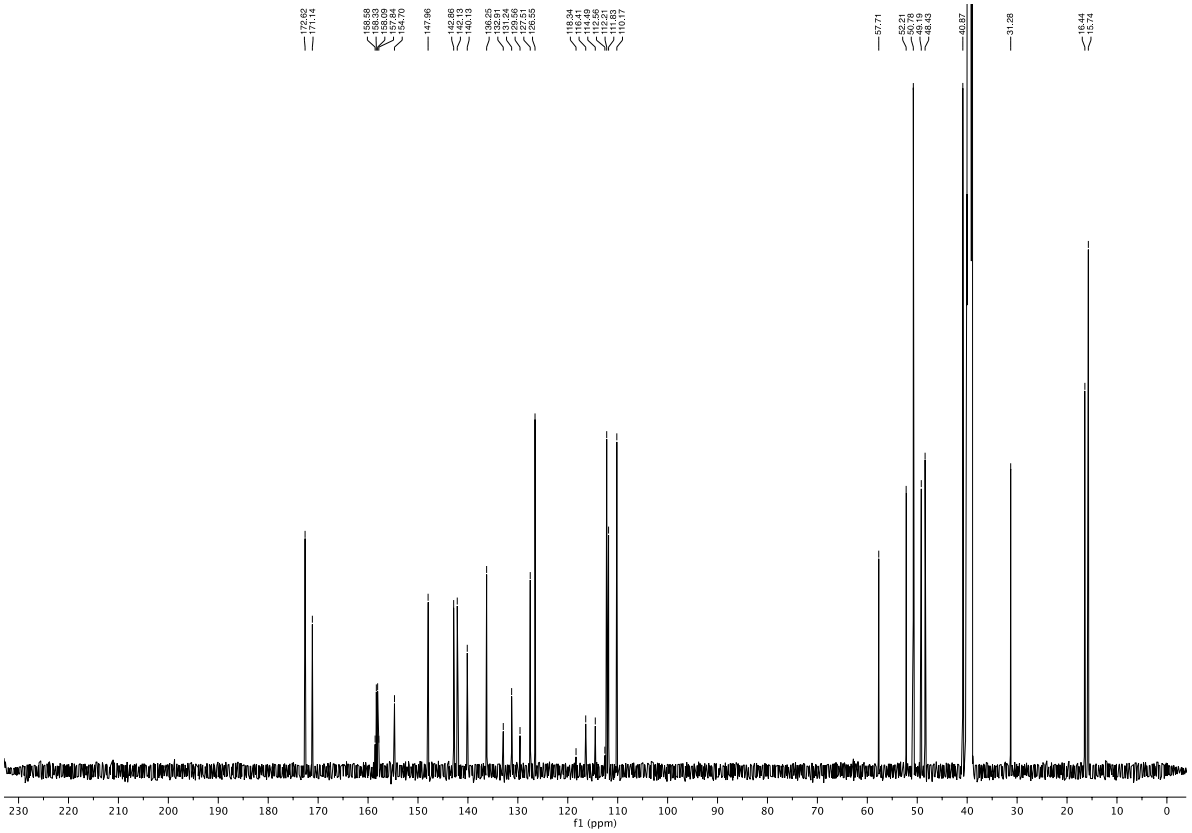
172.62
171.14
158.58
158.33
158.09
157.84
154.70
147.96
142.86
142.13
140.13
136.25
132.51
131.34
129.56
127.51
126.51
118.34
116.41
114.49
112.56
112.21
111.83
110.17
57.71
52.71
50.29
49.19
48.43
40.87
31.28
16.44
15.74
f1 (ppm)

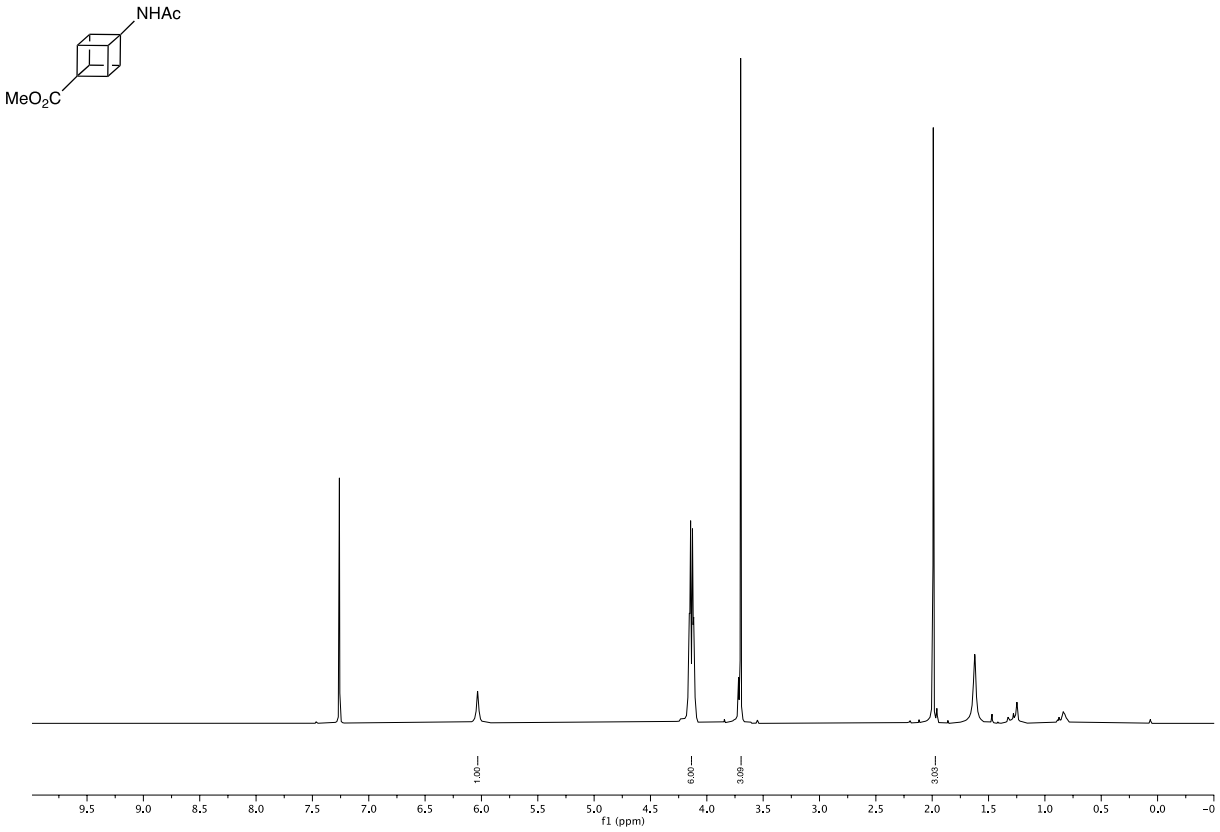
NHAc
MeO2C
1.00
6.00
3.09
3.03
f1 (ppm)

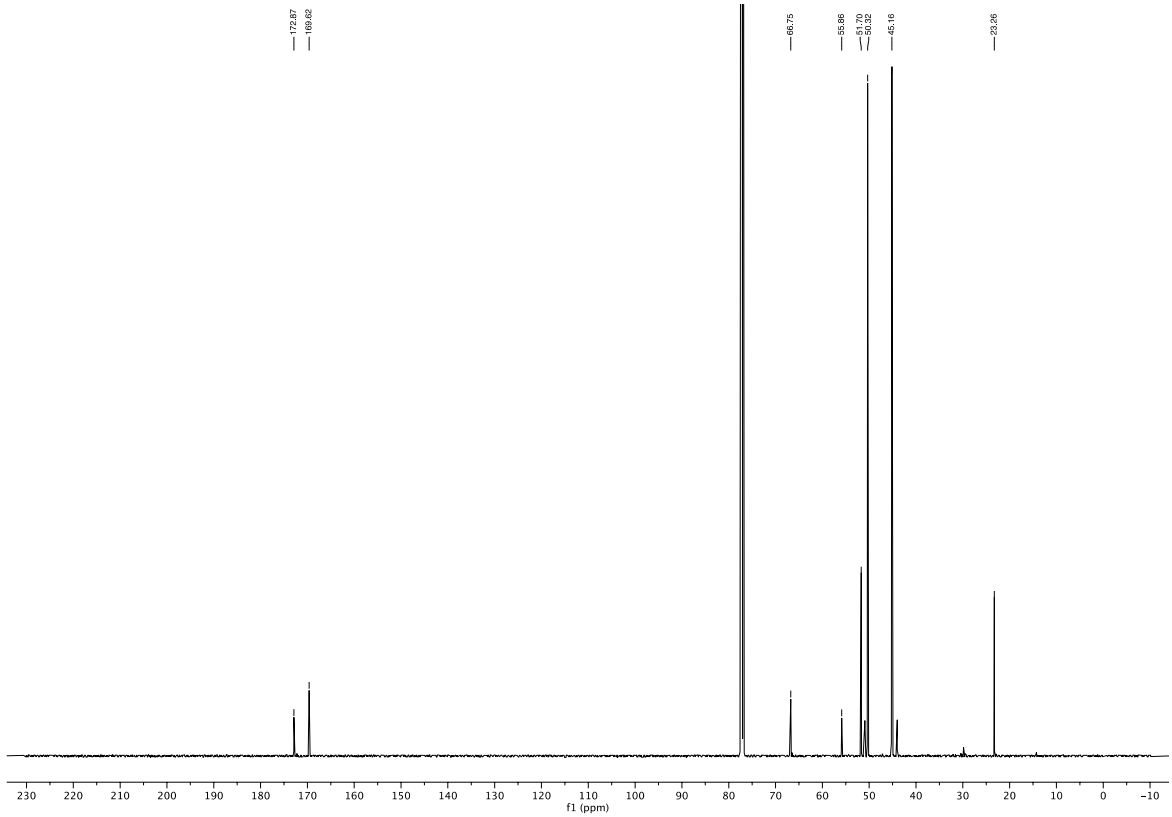
172.87
169.62
66.75
55.86
51.70
50.32
45.16
23.26
f1 (ppm)

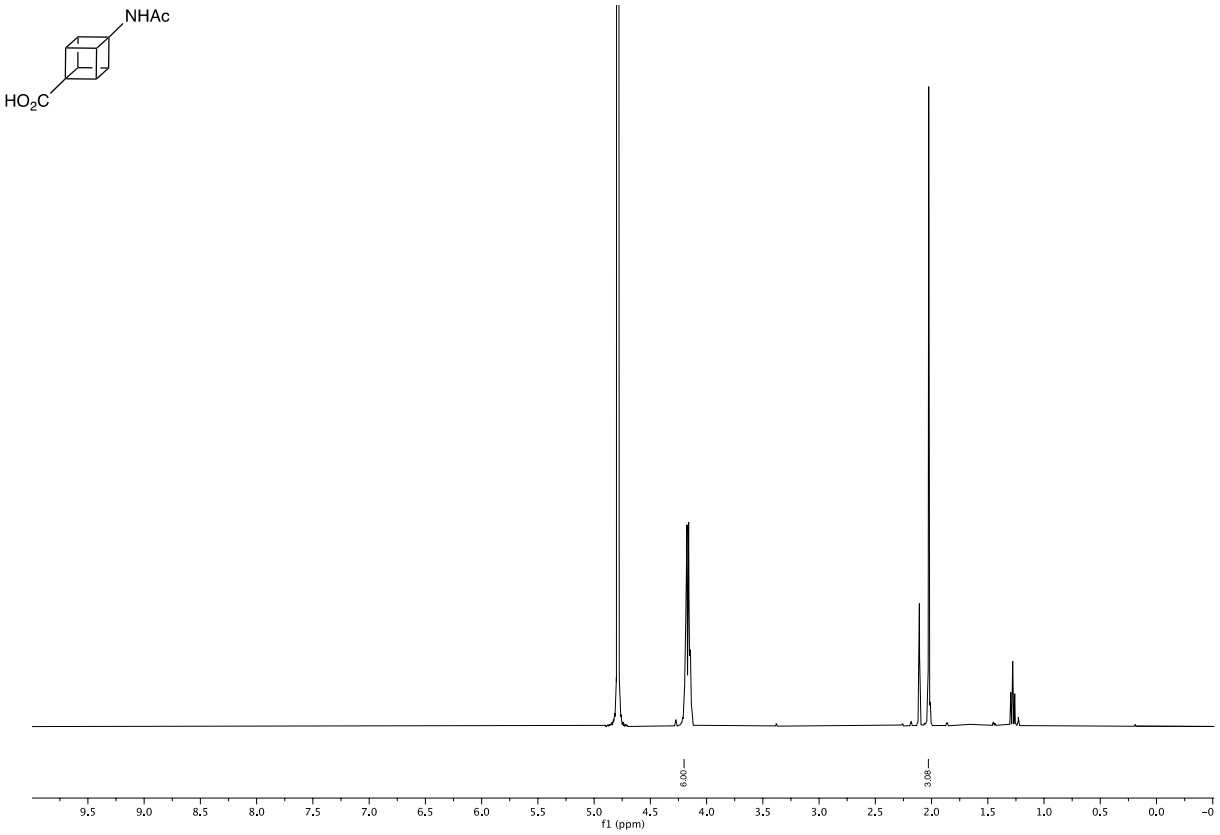
NHAc
HO2C
6.00
3.08
f1 (ppm)

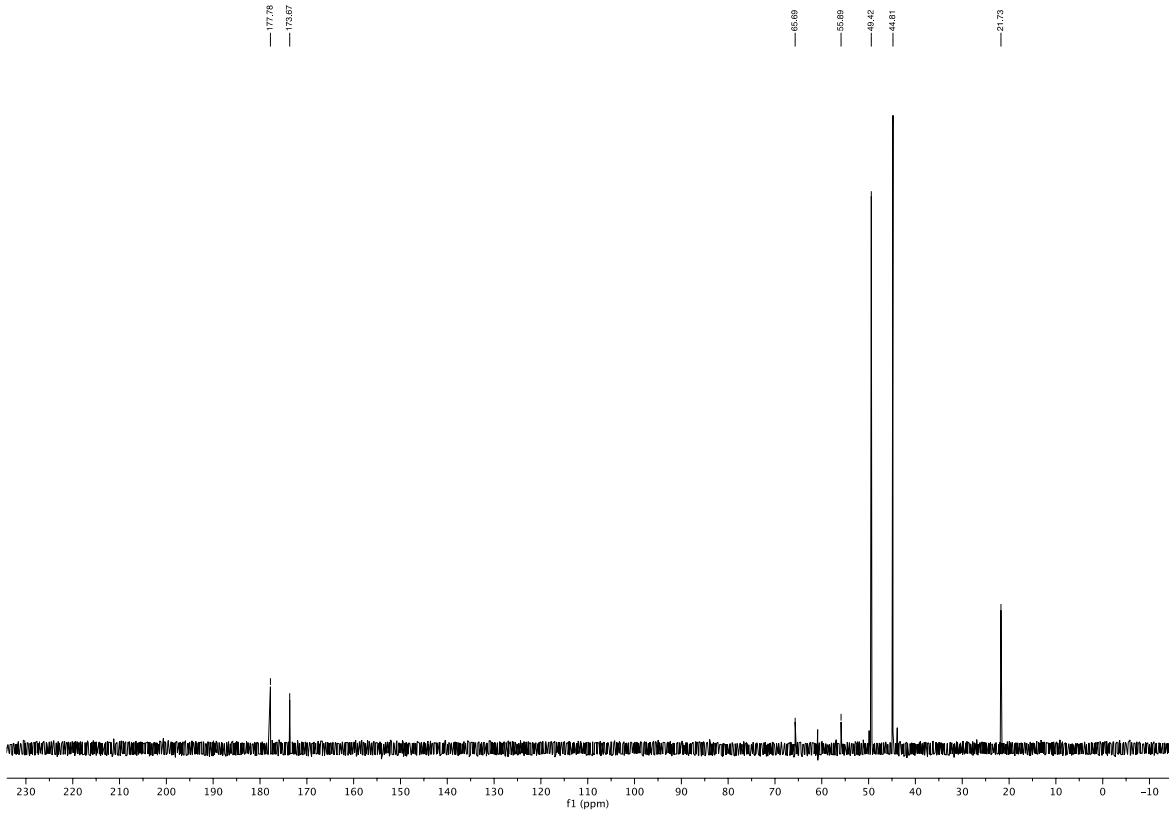
177.78
173.67
65.69
55.89
49.42
44.81
21.73
f1 (ppm)

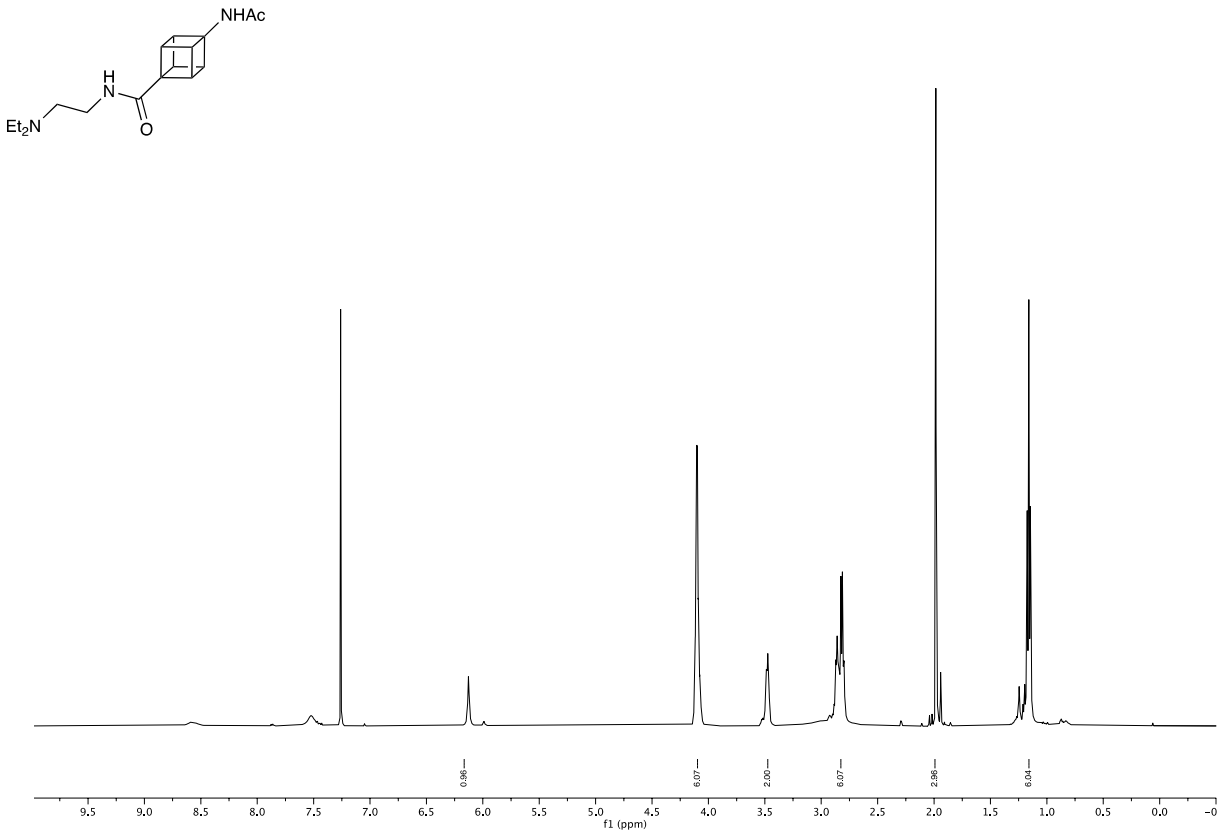
NHAc
H
N
O
Et2N
0.96
6.07
2.00
6.07
2.96
6.04
f1 (ppm)

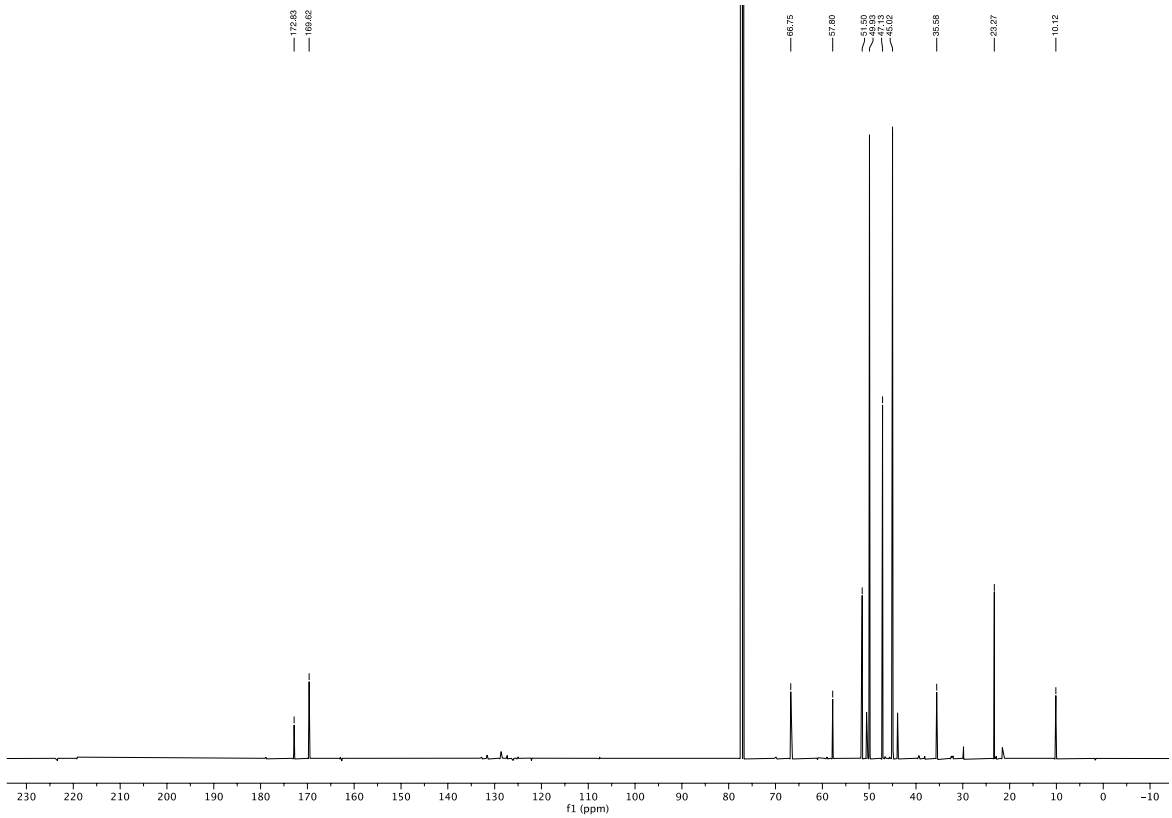
172.83
169.62
66.75
57.80
51.50
49.93
47.13
40.02
35.58
23.27
10.12
f1 (ppm)

12. References

1. Subbaiah, M. A. M. & Meanwell, N. A. Bioisosteres of the Phenyl Ring: Recent Strategic Applications in Lead Optimization and Drug Design. *J. Med. Chem.* **64**, 14046–14128 (2021).
2. Mykhailiuk, P. K. Saturated bioisosteres of benzene: where to go next? *Org. Biomol. Chem.* **17**, 2839–2849 (2019).
3. Stepan, A. F. et al. Application of the Bicyclo[1.1.1]pentane Motif as a Nonclassical Phenyl Ring Bioisostere in the Design of a Potent and Orally Active γ-Secretase Inhibitor. *J. Med. Chem*. **55**, 3414–3424 (2012).
4. Gianatassio, R. et al. Strain-release amination. *Science* **351**, 241–246 (2016).
5. Zhang, X. et al. Copper-mediated synthesis of drug-like bicyclopentanes. *Nature* **580**, 220–226 (2020).
6. Eaton, P. E. Cubanes: Starting Materials for the Chemistry of the 1990s and the New Century. *Angew. Chem. Int. Ed.* **31**, 1421–1436 (1992).
7. Reekie, T. A., Williams, C. M., Rendina, L. M. & Kassiou, M. Cubanes in Medicinal Chemistry. *J. Med. Chem.* **62**, 1078–1095 (2019).
8. Cassar, L. Eaton, P. E. & Halpern, J. Silver(I)- and Palladium(II)-Catalyzed Isomerizations of Cubane. Synthesis and Characterization of Cuneane. *J. Am. Chem. Soc.* **92**, 6366–6368 (1970).
9. Cassar, L., Eaton, P. E. & Halpern, J. Catalysis of Symmetry-Restricted Reactions by Transition Metal Compounds. The Valence Isomerization of Cubane. *J. Am. Chem. Soc.* **92**, 3515–3518 (1970).
10. Plunkett, S., Flanagan, K. J., Twamley, B. & Senge, M. O. Highly Strained Tertiary sp^3 Scaffolds: Synthesis of Functionalized Cubanes and Exploration of Their Reactivity under Pd(II) Catalysis. *Organometallics* **34**, 1408–1414 (2015).
11. Toriyama, F. et al. Redox-Active Esters in Fe-Catalyzed C–C Coupling. *J. Am. Chem. Soc.* **138**, 11132–11135 (2016).
12. Le, C., Chen, T. Q., Liang, T., Zhang, P. & MacMillan, D. W. C. A radical approach to the copper oxidative addition problem: Trifluoromethylation of bromoarenes. *Science* **360**, 1010–1014 (2018).
13. Liang, Y., Zhang, X. & MacMillan, D. W. C. Decarboxylative sp^3 C–N coupling via dual copper and photoredox catalysis. *Nature* **559**, 83–88 (2018).
14. Lovering, F., Bikker, J., Humblet, C. Escape from Flatland: Increasing Saturation as an Approach to Improving Clinical Success. *J. Med. Chem.* **52**, 6752–6756 (2009).
15. Feng, Y., Liu, L., Wang, J.-T., Zhao, S.-W. & Guo, Q.-X. Homolytic C–H and N–H Bond Dissociation Energies of Strained Organic Compounds. *J. Org. Chem.* **69**, 3129–3138 (2004).
16. The number of patents was determined by a scifinder search conducted on January 12 2023 at 1 pm CET. All patents with at least one spectroscopically characterized drug candidate were counted. See SI for details.
17. Levterov, V. V., Panasyuk, Y., Pivnytska, V. O. & Mykhailiuk, P. K. Water-Soluble Non-Classical Benzene Mimetics. *Angew. Chem. Int. Ed.* **59**, 7161–7167 (2020).
18. Denisenko, A., Garbuz, P., Shishkina, S. V., Voloshchuk, N. M. & Mykhailiuk, P. K. Saturated Bioisosteres of *ortho*-Substituted Benzenes. *Angew. Chem. Int. Ed.* **59**, 20515–20521 (2020).
19. Zhao, J.-X. et al. 1,2-Difunctionalized bicyclo[1.1.1]pentanes: Long–sought-after mimetics for *ortho*/*meta*-substituted arenes. *Proc. Natl. Acad. Sci. U. S. A.* **118**, No. e2108881118. (2021).

20. Epplin, R. C. et al. [2]-Ladderanes as isosteres for *meta*-substituted aromatic rings and rigidified cyclohexanes. *Nat. Commun.* **13**, No. 6056 (2022).
21. Iida, T. et al., Practical and Facile Access to Bicyclo[3.1.1]heptanes: Potent Bioisosteres of *meta*-Substituted Benzenes. *J. Am. Chem. Soc.* **144**, 21848–21852 (2022).
22. Kleinmans, R. et al. Intermolecular [2π+2σ]-photocycloaddition enabled by triplet energy transfer. *Nature* **605**, 477–482 (2022).
23. Frank, N. et al. Synthesis of *meta*-substituted arene bioisosteres from [3.1.1]propellane. *Nature* **611**, 721–726 (2022).
24. Rigotti, T. & Bach, T. Bicyclo[2.1.1]hexanes by Visible Light-Driven Intramolecular Crossed [2 + 2] Photocycloadditions. *Org. Lett.* **24**, 8821–8825 (2022).
25. Eaton, P. E. & Cole, T. W. Cubane. *J. Am. Chem. Soc.* **86**, 3157–3158 (1964).
26. Falkiner, M. J., Littler, S. W., McRae, K. J., Savage, G. P. & Tsanaktsidis, J. Pilot-Scale Production of Dimethyl 1,4-Cubanedicarboxylate. *Org. Process Res. Dev.* **17**, 1503–1509 (2013).
27. Biegasiewicz, K. F., Griffiths, J. R., Savage, G. P., Tsanaktsidis, J., Priefer, R. Cubane: 50 Years Later. *Chem. Rev.* **115**, 6719−6745 (2015).
28. Kassiou, M., Coster M. & Gunosewoyo, H. Polycyclic molecular compounds (2008).
29. Wlochal, J., Davies, R. D. M., Burton, J. Cubanes in Medicinal Chemistry: Synthesis of Functionalized Building Blocks. *Org. Lett.* **16**, 4094–4097 (2014).
30. Chalmers, B. A. et al. Validating Eaton's Hypothesis: Cubane as a Benzene Bioisostere. *Angew. Chem. Int. Ed.* **55**, 3580–3585 (2016).
31. Houston, S. D. et al. The cubane paradigm in bioactive molecule discovery: further scope, limitations and the cyclooctatetraene complement. *Org. Biomol. Chem.* **17**, 6790–6798 (2019).
32. Bernhard, S. S. R. et al. Cubane Cross-Coupling and Cubane–Porphyrin Arrays. *Chem. Eur. J.* **24**, 1026–1030 (2018).
33. Okude, R., Mori, G., Yagi, A. & Itami, K. Programmable synthesis of multiply arylated cubanes through C–H metalation and arylation. *Chem. Sci.* **11**, 7672–7675 (2020).
34. Barborak, J. C., Watts, L. & Pettit, R. A Convenient Synthesis of the Cubane System. *J. Am. Chem. Soc.* **88**, 1328–1329 (1966).
35. Brewer, C. R., Sheehan, N. C., Herrera, J., Walker, A. V. & McElwee-White, L. Photochemistry of (η^4-diene)$Ru(CO)_3$ Complexes as Precursor Candidates for Photoassisted Chemical Vapor Deposition. *Organometallics* **41**, 761–775 (2022).
36. Pettit, R. & Henery, J. Cyclobutadieneiron Tricarbonyl. *Org. Synth.* **50**, 57–59 (1970).
37. Masamune, S., Nakamura, N. & Sapadaro, J. 1,2-Bis(β-tosylethoxycarbonyl)diazene. Its Application to the 2,3-Diazabicyclo[2.2.0]hexene System. *J. Am. Chem. Soc.* **97**, 918–919 (1975).
38. Britten, T. K., Akien, G. R., Kemmitt, P. D., Halcovitch, N. R. & Coote, S. C. An efficient preparation of 1,2-dihydropyridazines through a Diels-Alder/palladium-catalysed elimination sequence. *Tetrahedron Lett.* **60**, 1498–1500 (2019).
39. Altman, L. J., Semmelhack, M. F., Hornby, R. B., Vederas, J. C. Photochemical Isomerisation of Dimethyl 1,2-dihydropyridazine-1,2-dicarboxylate. *Chem. Commun.* **1968**, 686–687 (1968).
40. Britten, T. K., Kemmitt, P. D., Halcovitch, N. R. & Coote, S. C. 4-π-Photocyclization of 1,2-Dihydropyridazines: An Approach to Bicyclic 1,2-Diazetidines with Rich Synthetic Potential. *Org. Lett.* **21**, 9232–9235 (2019).

41. Bashir-Hashemi, A. Photochemical Carboxylation of Cubanes, *Angew. Chem. Int. Ed.* **32**, 612–613 (1993).
42. Collin, D. E., Kovacic, K., Light, M. E. & Linclau, B. Synthesis of *Ortho*-Functionalized 1,4-Cubanedicarboxylate Derivatives through Photochemical Chlorocarbonylation. *Org. Lett.* **23**, 5164–5169 (2021).
43. Chan, A. Y. et al. Metallaphotoredox: The Merger of Photoredox and Transition Metal Catalysis. *Chem. Rev.* **122**, 1485–1542 (2022).
44. Rodríguez, N. & Gooßen, L. J. Decarboxylative coupling reactions: a modern strategy for C–C-bond formation. *Chem. Soc. Rev.* **40**, 5030–5048 (2011).
45. Ruiz-Castillo, P. & Buchwald, S. L. Applications of Palladium-Catalyzed C–N Cross-Coupling Reactions. *Chem. Rev.* **116**, 12564–12649 (2016).
46. Hartwig, J. F. Evolution of a Fourth Generation Catalyst for the Amination and Thioetherification of Aryl Halides. *Acc. Chem. Res.* **41**, 1534–1544 (2008).
47. Zhao, W.; Wurz, R. P.; Peters, J. C. & Fu, G. C. Photoinduced, Copper-Catalyzed Decarboxylative C−N Coupling to Generate Protected Amines: An Alternative to the Curtius Rearrangement. *J. Am. Chem. Soc.* **139**, 12153–12156 (2017).
48. Sodano, T. M., Combee, L. A. & Stephenson, C. R. J. Recent Advances and Outlook for the Isosteric Replacement of Anilines. *ACS Med. Chem. Lett.* **11**, 1785−1788 (2020).
49. Sklyarova, A. S., Rodionov V. N., Parsons C. G., Quack G., Schreiner P. R., Fokin A. A. Preparation and testing of homocubyl amines as therapeutic NMDA receptor antagonists. *Med Chem Res* **22**, 360–366 (2013).
50. Sakai, H. A., Liu, W., Le, C. & MacMillan, D. W. C. Cross-Electrophile Coupling of Unactivated Alkyl Chlorides. *J. Am. Chem. Soc.* **142**, 11691–11697 (2020).
51. Pangborn, A. B., Giardello, M. A., Grubbs, R. H., Rosen, R. K. & Timmers, F. J. Safe and Convenient Procedure for Solvent Purification. *Organometallics* **15**, 1518–1520 (1996).
52. Le, C. C. et al. A General Small-Scale Reactor To Enable Standardization and Acceleration of Photocatalytic Reactions. *ACS Cent. Sci.* **3**, 647–653 (2017).
53. Inman, M. & Moody, C. J. Copper(II)-Mediated Synthesis of Indolequinones from Bromoquinones and Enamines. *Eur. J. Org. Chem.* **2013**, 2179–2187 (2013).
54. Sakaitani & M. Ohfune, Y. Syntheses and reactions of silyl carbamates. 1. Chemoselective transformation of amino protecting groups via *tert*-butyldimethylsilyl carbamates. *J. Org. Chem.* **55**, 870–876 (1990).
55. Luh, T.-Y. & Stock, L. M. Preparation of 1,4-dicarboxycubane. *J. Org. Chem.* **37**, 338–339 (1972).
56. Mehta, G. & Reddy S. H. K. Cycloaddition between 2,3-Dibromo-5,6-trinorbornenobenzoquinone and 1,2-Bis(methoxycarbonyI)cyclobutadiene: Intervention of a Fragmentation Reaction during Quest for Annulated, Functionalized Cubanes. *J. Chem. Soc. Perkin Trans. 1* **1994**, 2949–2951 (1994).
57. Unsinn, A. & Knochel, P. Regioselective zincation of indazoles using TMP_2Zn and Negishi cross-coupling with aryl and heteroaryl iodides. *Chem. Commun.* **48**, 2680–2682 (2012).